

Elaboraron;

Argumedo Guerrero Ismael ✓

Jimenez Morales Jesus

Galicia Solis Eduardo

Presion Arterial ✓

Grupo:

Profesor: Martinez Ortis Alfonso

CB1

Ing. Biomedica ✓

1993 ✓

UNIVERSIDAD AUTONOMA METROPOLITANA

TRABAJO DE INVESTIGACION DE
MEDICINA II

" PRESION ARTERIAL "

INTRODUCCION

Al comenzar la exposición señalaremos que las características más importantes de la circulación, que deben tenerse siempre presentes, es que constituyen un cto. En otras palabras; que la sangre fluye continuamente a través del corazón y los vasos una y otra vez. y que si un volumen de sangre es impulsado, por el corazón, este mismo volumen debe atravesar cada una de las partes de la circulación. Además se la sangre se estree de un segmento circulatorio otro segmento de la circulación debera aumentar su capacidad.

En la primera figura (1) se indica el plan general de la circulación, mostrando las subdivisiones importantes; la circulación mayor, y la circulación pulmonar o menor.

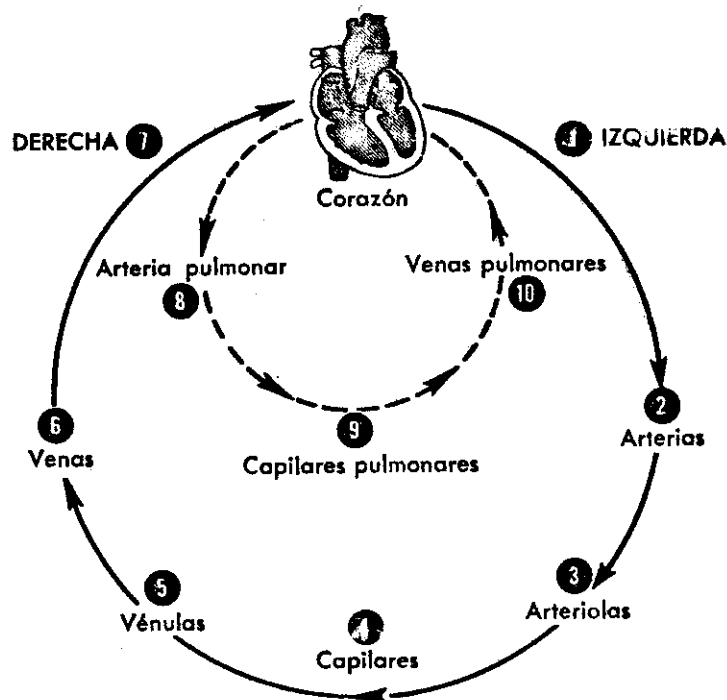


FIG. 13-24. Relación que guardan el circuito mayor y el circuito menor. Según indican los números, la sangre circula de esta manera: hemicardio izquierdo (ventrículo), arterias, arteriolas, capilares, vénulas, venas, hemicardio derecho (desde aurícula hacia ventrículo), pulmones y hemicardio izquierdo, lo cual cierra el circuito. Consúltese este esquema al tratar de estimar el curso de la sangre a cualquier parte del cuerpo.

A su vez cada una de estas divisiones incluye arterias de pequeño calibre, arteriolas, capilares, venulas, venas de pequeño calibre y venas de gran calibre.

La sangre circula fácilmente por todo el sistema excepto por las arteriolas y capilares. En consecuencia, se dice que fuera de los pequeños vasos todos los demás ofrecen muy poca resistencia al paso de la sangre. Para que la sangre pueda atravesar los pequeños vasos "resistencia", el corazón manda hacia las arterias a presión elevada (hasta aproximadamente 120 mm Hg en la sistole para la gran circulación y 26 mm de Hg para la sistole en la circulación pulmonar). A ésta presión nos enfocaremos principalmente y a los órganos que la generan.

CORAZON

ANATOMIA:

El corazón humano es un órgano muscular que posee 4 cavidades y que tiene la forma y el tamaño de tó mano empuñada. Está situado en el mediastino, aproximadamente dos tercera partes de la masa a la izquierda de la línea media del cuerpo y la otra tercera parte a la derecha.

El borde inferior del corazón que forma un ángulo como llamado vértice o punta, está sobre el diafragma y orientado hacia la izquierda. Esto es a la altura del espacio entre la quinta y la sexta costilla (quinto espacio intercostal), el borde superior del corazón o base está inmediatamente por debajo de la segunda costilla. Los límites o el contorno que desde luego indican el volumen del corazón tienen importancia clínica.

En consecuencia, al estudiar trastornos cardiacos el médico anota graficamente el contorno del corazón.

ESTRUCTURA

PARED:

La pared del corazón está formada por tres capas netas de tejido, la parte principal de la pared consiste en tejido muscular especial llamado musculo cardiaco o miocardio el exterior del miocardio está cubierto por la hoja visceral del pericardio

seroso (o epicardio) y se adhiere íntimamente a ella. El interior de la pared miocárdica está revestida de una capa delicada de tejido endotelial llamada endocardio. En la superficie interna el miocardio presenta elevaciones notables, los músculos papilares.

CAVIDADES

El interior del corazón está dividido en 4 cavidades, dos superiores y dos inferiores. Las cavidades superiores se llaman aurículas y las inferiores ventrículos. Los ventrículos son bastantes mayores y de pared más gruesa que las aurículas, por que la acción de bombeo que desempeñan es también mayor. DE manera análoga la pared del ventrículo izquierdo es más gruesa que la del derecho, por que debe impulsar la sangre por todos los vasos del cuerpo, excepto los que van a los pulmones y vuelven de ellos; en cambio, el ventrículo derecho envía solo al circuito menor pulmonar.

Fig. 2

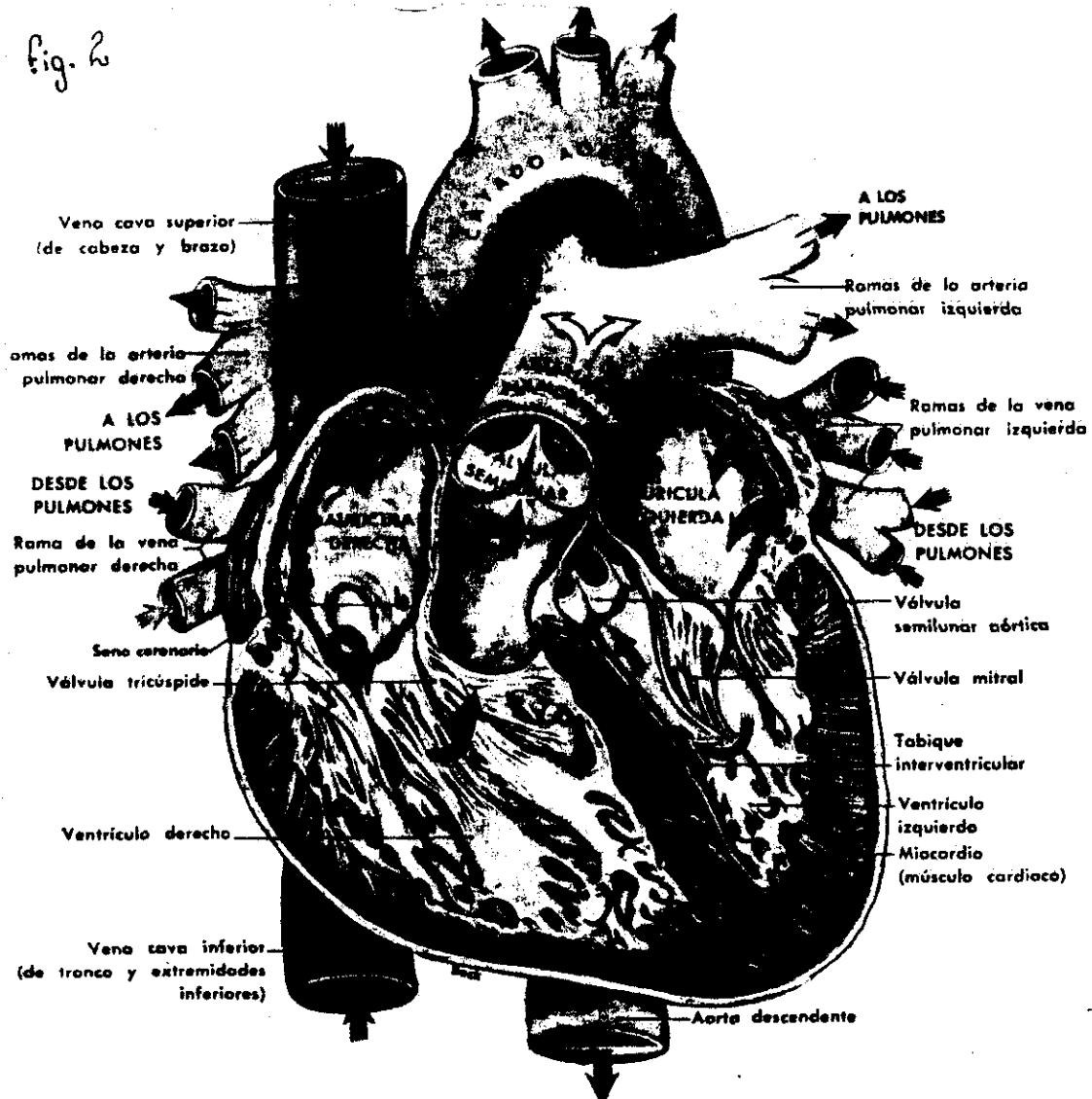


Figura 2. Corte frontal del corazón en el cuál se advierten las cuatro cavidades, las válvulas, los orificios y los vasos principales. Las flechas indican la dirección del flujo sanguíneo. Las dos ramas de la vena pulmonar derecha pasan por detrás del corazón para desembocar en el aurícula izquierda.

VALVULAS Y ORIFICIOS

Las válvulas cardíacas son aditamentos mecánicos que permiten que fluya la sangre protegen los orificios entre los aurículos y los ventrículos la del lado derecho consiste en tres válvulas de endocardio unidas a los músculos papilares del ventrículoderecho por varias estructuras a manera de cordón llamadas cuerdas tendinosas. Dado que esta válvula posee tres hojuelas se llama válvula tricospide y la válvula del lado izquierdo tiene estructura semejante excepto que posee dos hojuelas y en consecuencia se llama válvula bicuspid e o más comúnmente válvula mitral.

Las otras dos válvulas semilunares están, una dentro de la otra arteria pulmonar la cual se llama válvula semilunar o sigmoidea pulmonar y otra dentro de la aorta la cual se llama válvula semilunar o sigmoidea aortica, en el sitio donde se originan los dos ventrículos derecho e izquierdo respectivamente.

FISILOGIA

FUNCION:

La función del corazón es bombear sangre en volumen suficiente para satisfacer las necesidades variables de las células de todo el cuerpo en lo que se refiere a las sustancias que transporta.

CICLO CARDIACO

Ciclo cardiaco significa un látido completo del corazón que consiste en contracción (sistole) y relajación (diastole) de ambas aurículas y además de la contracción y relajación de los ventrículos, las aurículas se contraen simultáneamente; en seguida el presentar relajación, los dos ventrículos se contraen y se relajan, de manera que el corazón no se contrae globalmente como unidad. Las aurículas permanecen relajadas durante la parte de la relajación ventricular y después comienza de nuevo el ciclo.

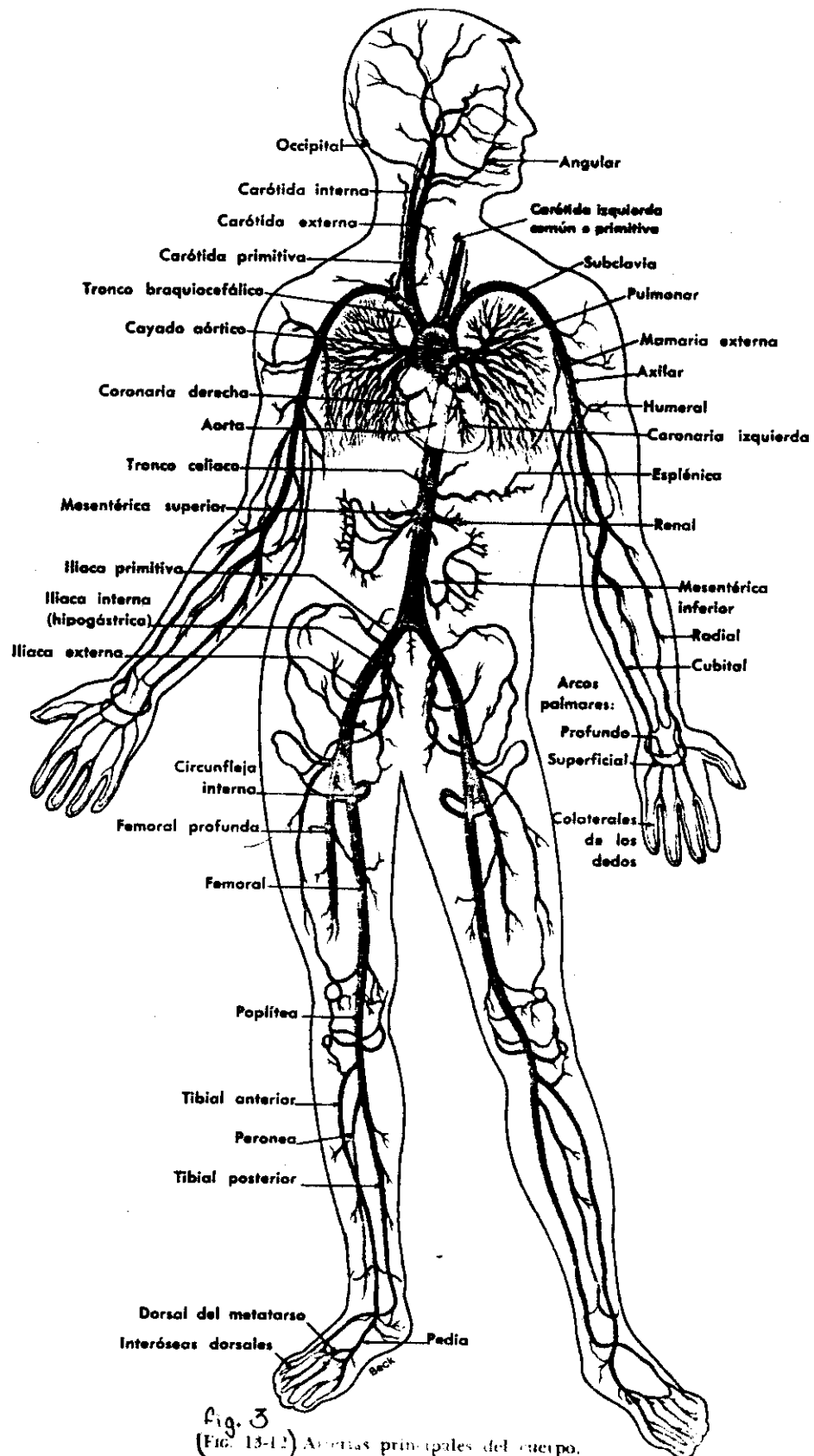
VASOS SANGUINEOS

Hay tres tipos de vasos sanguíneos; a saber; arterias, venas y capilares. Por definición la arteria es un vaso que transporta sangre en dirección centrifuga en cuanto al corazón todas las arterias excepto la pulmonar y sus ramas transportan sangre oxigenada. las arterias de pequeño calibre se llaman arteriolas.

Una vena por otra parte es un vaso que lleva sangre hacia el corazón todas las venas excepto las pulmonares, poseen sangre desoxigenada, las venas de pequeño calibre se llaman venulas, las arterias y las venas son estructuras microscópicas.

Los capilares son vasos microscópicos que conducen sangre de las arterias de pequeño calibre a venas de pequeño calibre esto es : de las arteriolas a las venulas. Fueron el eslabón perdido de la prueba de la circulación durante muchos años, hasta la fecha el microscopio permitió descubrir estos vasos de comunicación entre arterias y venas. Descubrir los capilares fue prueba definitiva de que la sangre fluye del corazón a las arterias arteriolas, capilares, venulas, venas y de nuevo al corazón.

Dado que la función principal de la sangre es transportar materiales indispensables a las células, y extraerlos de las mismas y que la salida y entrada de estas sustancias ocurre en los capilares estos deben considerarse los vasos sanguíneos más importantes desde el punto de vista funcional.



VENAS

Las venas son la prolongación última de los capilares, al igual que los capilares son terminación de las arterias. Las arterias se ramifican en vasos de calibre cada vez menor para formar arteriolas y por último los capilares; en cambio los capilares se unen a vasos de calibre creciente, para formar venulas y por último venas.

Las venas situadas en porciones profundas del cuerpo se llaman venas profundas, a diferencia de las venas superficiales situadas cerca de la superficie y que pueden verse através de la piel.

PRINCIPIO DE CIRCULACION Y PRESIONES EN LOS DIVERSOS VASOS

Un líquido circula a causa que existe un gradiente de presión en los diferentes partes de su lecho. Este principio primario del caudal de líquidos se deriva de la primera y segunda Ley de Newton de los movimientos. En esencia está ley establece los siguientes principios,

- a) Un líquido no circula cuando la presión es la misma en todas sus partes.
- b) Un líquido circula cuando su presión es más alta en una zona que en otra, y lo hace desde su área de presión más baja.

En pocas palabras, por tanto la sangre circula desde el ventrículo izquierdo hacia la aurícula derecha del corazón, por que existe un gradiente de presión sanguínea entre estas dos cavidades.

Conforme el ventrículo izquierdo se contrae y expulsa la sangre hacia la luz de la arteria aorta se crea una presión la cuál como está acción no es constante sino, que es pulsátil, entonces en la aorta la presión es pulsátil. Fluctua entre un valor sistólico de 120 mm Hg y un valor diastólico de 80 mm Hg, con un valor medio de aproximadamente de 100 mm Hg. Estas pulsaciones se extienden a las arterias de grande y pequeño calibre, pero en las arteriolas ya se han amortiguado.

Sistema cardiovascular

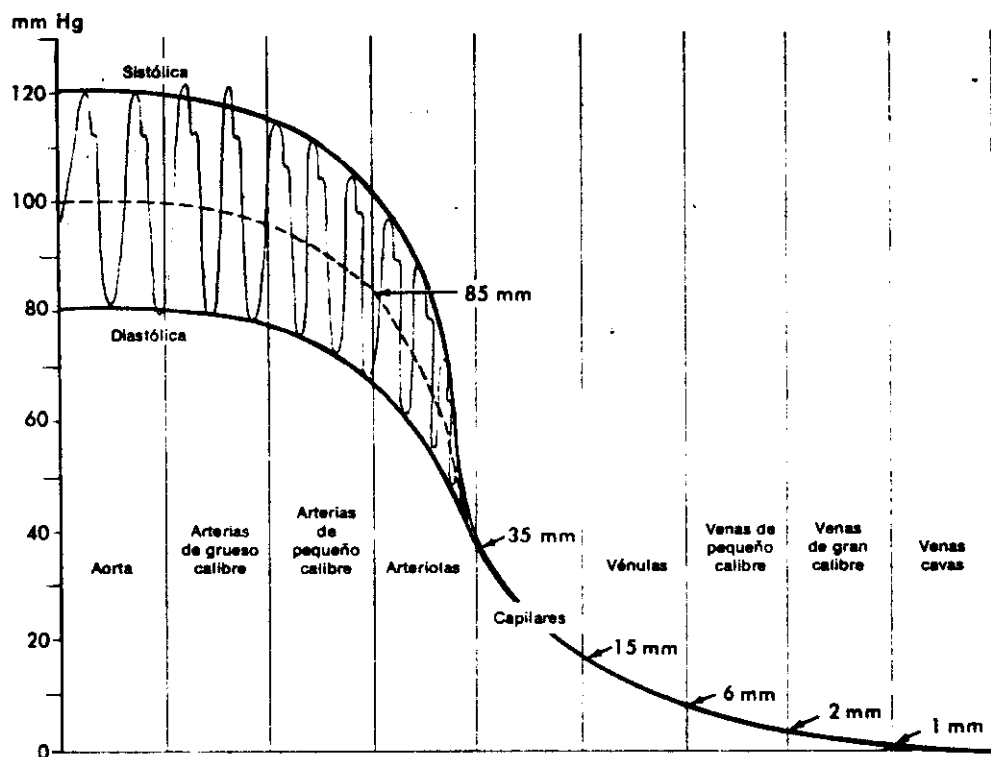


(Fig. 13-25) Gradientes de presión sanguínea; la línea de guiones indica la presión sistólica promedio o media en las arterias.
fig. 4.

La presión arterial media al comienzo de las grandes arterias es casi igual a la que hay en la parte próxima al de la aorta, quizá entre 100 y 99 mm Hg.

La resistencia al curso de la sangre aumenta enormemente en las pequeñas arteriolas, y la presión en el extremo de estos vasos y al principio de las arteriolas es aproximadamente de 85 mm Hg. La caída normal de presión de las arteriolas es aproximadamente de 85 mm Hg al principio hasta 35 mm Hg al final de las mismas. Así pues la mitad aproximadamente de la caída de presión desde el ventrículo izquierdo a la aurícula derecha ocurre normalmente en las arteriolas.

La presión al comienzo de las capilares es normalmente de 35 mmHg, y en el extremo venoso de los capilares se indica en la figura (4), es aproximadamente de 15 mm Hg. La presión media a lo largo de los capilares se halla alrededor de 25 mm Hg en condiciones normales.

Como hay muy poca resistencia al curso de la sangre en el sistema venoso, la presión cae desde 15 mm Hg en el origen de las venulas hasta aproximadamente 6 mmHg en el origen de las pequeñas venas, a 2 mm Hg al principio de las venas de gran calibre a 1 mm Hg al principio de las cavas y finalmente a 0 mm Hg donde las cavas se vacían en la aurícula derecha.

El factor determinante primario de la presión es el volumen de sangre en las arterias. Esto significa que el aumento de sangre arterial tiende a aumentar la presión arterial y, a la inversa, la disminución en el volumen arterial tiende a disminuir la presión arterial.

Hay muchos factores que juntos establecen de manera indirecta la presión arterial por medio de su influencia en el volumen arterial dos de las más importantes son: Gasto cardiaco por minuto y resistencia periférica.

El gasto cardiaco depende tanto de la frecuencia de las contracciones cardiacas por minuto como del volumen de sangre impulsado desde los ventriculos en cada latido.

El volumen de la sangre impulsado por la contracción se conoce como descarga sistólica.

El volumen por contracción refleja la fuerza o poder de la contracción ventricular; cuando más poderosa la contracción mayor el volumen por contracción. El gasto cardiaco por minuto se puede calcular por medio de la siguiente ecuación sencilla,

Volumen por contracción X frecuencia cardiaca = gasto cardiaco por minuto.

Asumase una frecuencia normal de 72 latido por minuto y un volumen normal por contracción de 70 ml.

La resistencia periferica ayuda a establecer la presión arterial. Se entiende por resistencia periferica a la resistencia al caudal sanguíneo impuesto por la fuerza de fricción entre la sangre y las paredes de los vasos, la fricción se desarrolla en parte por las características de la sangre (viscosidad) y en parte por el diámetro pequeño de las arteriolas y los capilares. La resistencia periferica ayuda a determinar la presión arterial al controlar el ritmo de "escape arterial" o cantidad de sangre que corre desde las arterias a las arteriolas.

En resumen la presión arterial depende del volumen de sangre arterial, que es determinado por muchos factores pero especialmente el gasto cardiaco y la resistencia periferica figura (5)

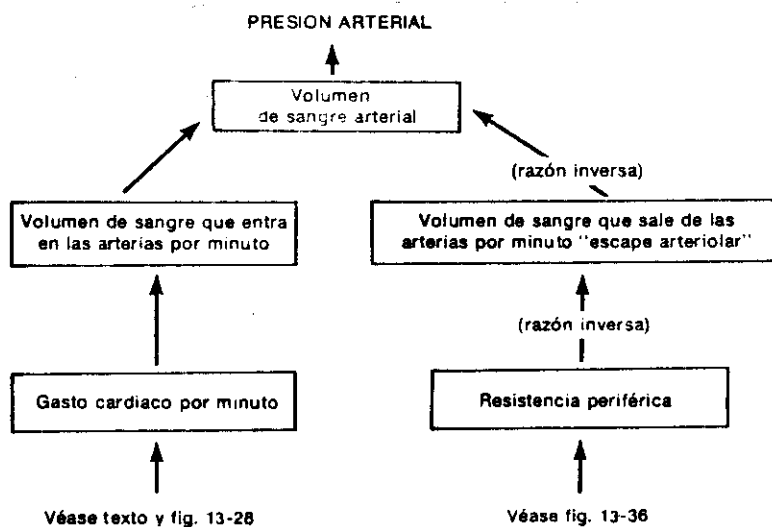


FIG. 13-6. Esquema que muestra la forma en que el gasto cardiaco minuto y la resistencia periférica modifican la presión arterial. Si aumenta el gasto cardiaco por minuto, aumenta el volumen de sangre que llega a las arterias y ello tiende a que sea mayor el volumen de sangre en estos vasos. El aumento resultante del volumen arterial eleva la presión de sangre en las arterias. Si aumenta la resistencia periférica, tiende a disminuir el volumen de sangre que sale de las arterias, lo cual aumenta el volumen de sangre que queda en las arterias, el mayor volumen arterial aumenta la presión arterial.

El factor mecanico que ayuda a determinar el volumen por contracción es la longitud de las fibras miocárdicas al principio de la contracción ventricular.

La ley de Starling del corazón, en esencia dice; dentro de límites cuanto más largas o más estiradas las fibras del corazón en el principio de la contracción, más poderosa será está. La operación de la ley de Starling del corazón garantiza que los mismos volúmenes aumentados de sangre que vuelven al corazón serán expulsados fuera del mismo. Esto ajusta de manera automática el gasto cardíaco al retorno venoso en condiciones ordinarias.

Los reflejos presores constituyen el mecanismo dominante de control de la frecuencia cardíaca aunque también influye en la misma muchos otros factores.

Reflejos presores cardiacos las células sensibles a la presión denominadas baroreceptores (presoreceptores) están localizados en el arco aórtico y el seno carotídeo (el seno carotídeo es una dilatación pequeña situada al principio de la arteria carotida interna, justamente por encima de la bifurcación de la arteria carotida primitiva para formar arterias carotidas interna y externa). Las fibras sensitivas se extienden desde los baroreceptores aórticos del vago para terminar en el bulbo raquídeo y en sus centros, cardíacos y vasomotor.

Si la presión arterial que hay en aorta o seno carotídeo aumenta de manera súbita, estimula a los baroreceptores aórticos o carotídeos. Como se ilustra en la figura (6), esto produce estimulación de los centros cardioinhibidores e inhibición recíproca de los centros aceleradores, los que a su vez envían más impulsos por segundo por las fibras parasimpáticas de los nervios cardioaceleradores que van hacia el corazón. Como resultado, ocurre disminución refleja de la frecuencia cardíaca, e inversamente el proceso aumenta el ritmo cardíaco.

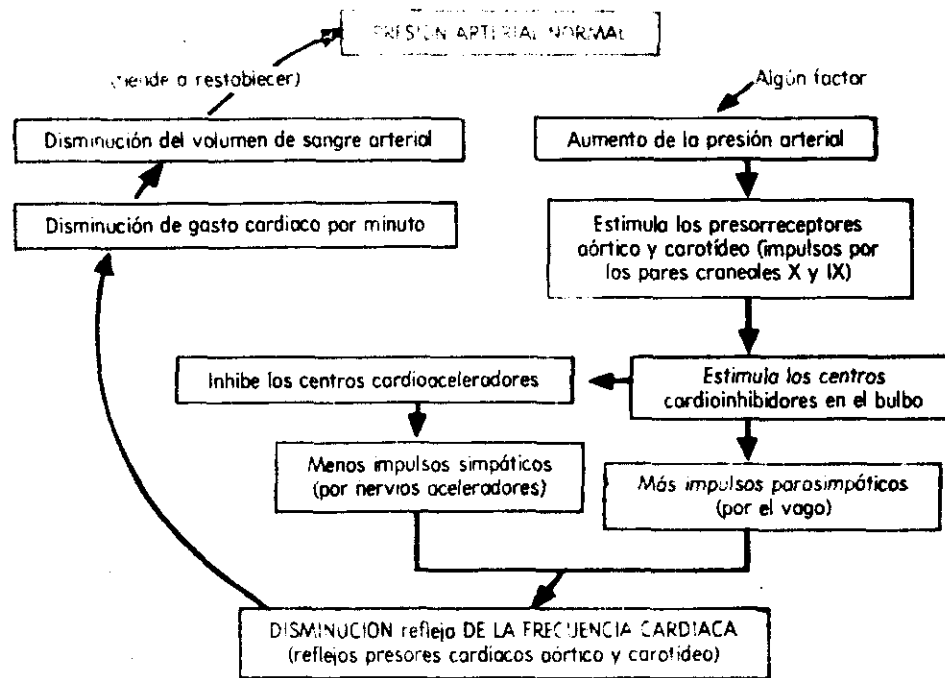


Fig 6
 Fig (13-27) Reflejos presores cardiacos aórtico y carotídeo, son mecanismos que tienden a conservar o restablecer la homeostasia de la presión arterial al regular la frecuencia cardiaca. Adviértase que por este mecanismo el aumento de la presión arterial produce de manera refleja disminución de la frecuencia cardiaca y tiende a disminuir la presión arterial; lo inverso también es valadero. La disminución de la presión arterial produce aumento reflejo de la frecuencia del corazón y tiende a elevar la presión hacia cifras normales.

Factores diversos que influyen en la frecuencia cardiaca incluidos en esta categoría estan los factores importantes como emociones, ejercicio, hormonas, temperatura de la sangre y estimulación de varios exteroceptores.

Ansiedad, miedo e ira tambien hacen a menudo que el corazón lata con mayor rapidez, el ejercicio acelera al corazón en condiciones normales, la estimulación intensa y subita de los receptores del dolor tiende a disminuir la frecuencia cardiaca, en la figura (7).

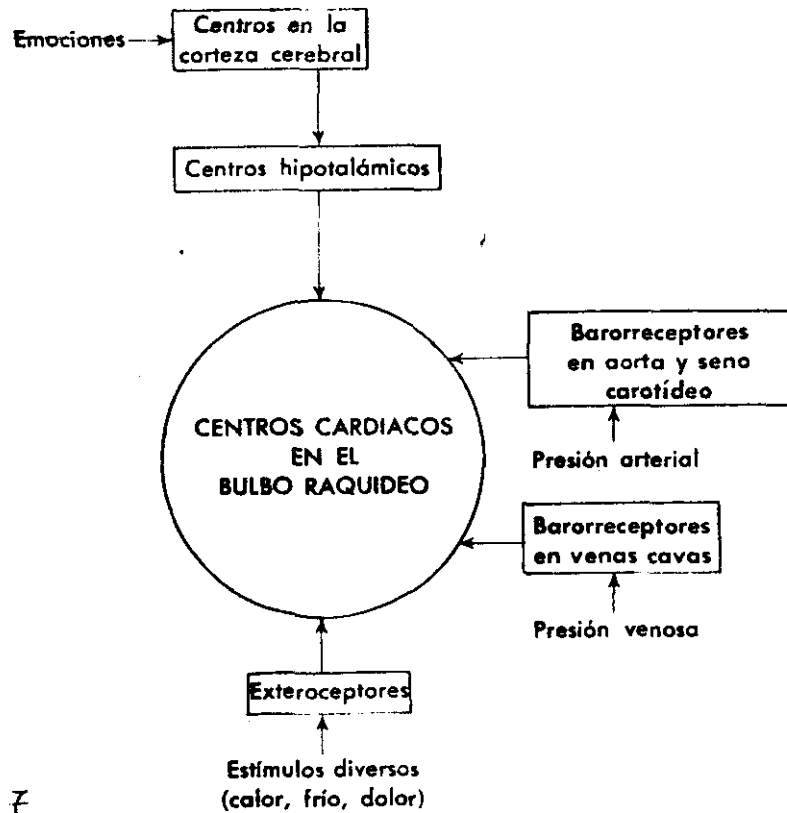


Fig. 7

(Fig. 13-28) Esquema de algunas de las muchas partes del mecanismo que regula la frecuencia cardíaca. Los impulsos de varios receptores son conducidos por fibras sensitivas que terminan en sinapsis con neuronas en los centros cardiacos. Las fibras motoras de los centros telejejan impulsos a neuronas simpáticas y parasimpáticas, que los transmiten al corazón. También llegan a los centros cardiacos impulsos del hipotálamo, posiblemente como parte de la vía por la cual las emociones influyen en la frecuencia cardíaca.

Existe resistencia periférica principalmente a causa de la viscosidad de la sangre y el diámetro pequeño de las arteriolas. La viscosidad sanguínea se debe principalmente a los eritrocitos, pero en parte también a las moléculas proteínicas que existen en la sangre. En circunstancias normales la viscosidad sanguínea cambia muy poco, pero en ciertas anomalías como anemia notable o hemorragia, la disminución de la viscosidad puede ser el factor crucial que disminuya la resistencia periférica y la presión arterial incluso hasta el punto de insuficiencia circulatoria.

Numerosos factores controlan el diámetro de las arteriolas. Podría decirse que constituyen el mecanismo de control vaso motor. Los cambios de presión arterial inician un reflejo vaso motor presor.

Reflejos presores vasomotores Un aumento en la presión arterial estimula los procesos receptores aórticos y caóticos los mismos que inician reflejos cardíacos.

Ellos no solo producen estimulación de los centros cardio-inhibidores, sino también inhibición de los centros vaso constrictores. En consecuencia la frecuencia cardíaca disminuye y las arteriolas y vénulas de los reservorios sanguíneos se dilatan (lo cual se muestra en la figura 8), e inversamente el proceso si la presión arterial baja.

Químico reflejos vasomotores Los químicos receptores situados en los cuerpos aórticos y carotídeos son particularmente susceptibles a la disminución del oxígeno sanguíneo (hipoxia) y algo menos susceptibles al exceso de bióxido de carbono (hipercapnia) y a la disminución del PH arterial. Cuando alguna de estas circunstancias o varias, estimulan a los químicos receptores sus fibras transmiten más impulsos a los centros vasoconstrictores del bulbo y pronto sobreviene vaso constricción de arteriolas y reservorios venosos. Este mecanismo actúan como medio de urgencia cuando ocurren, hipoxia o hipercapnia intensa, esto se muestra en la figura (9)

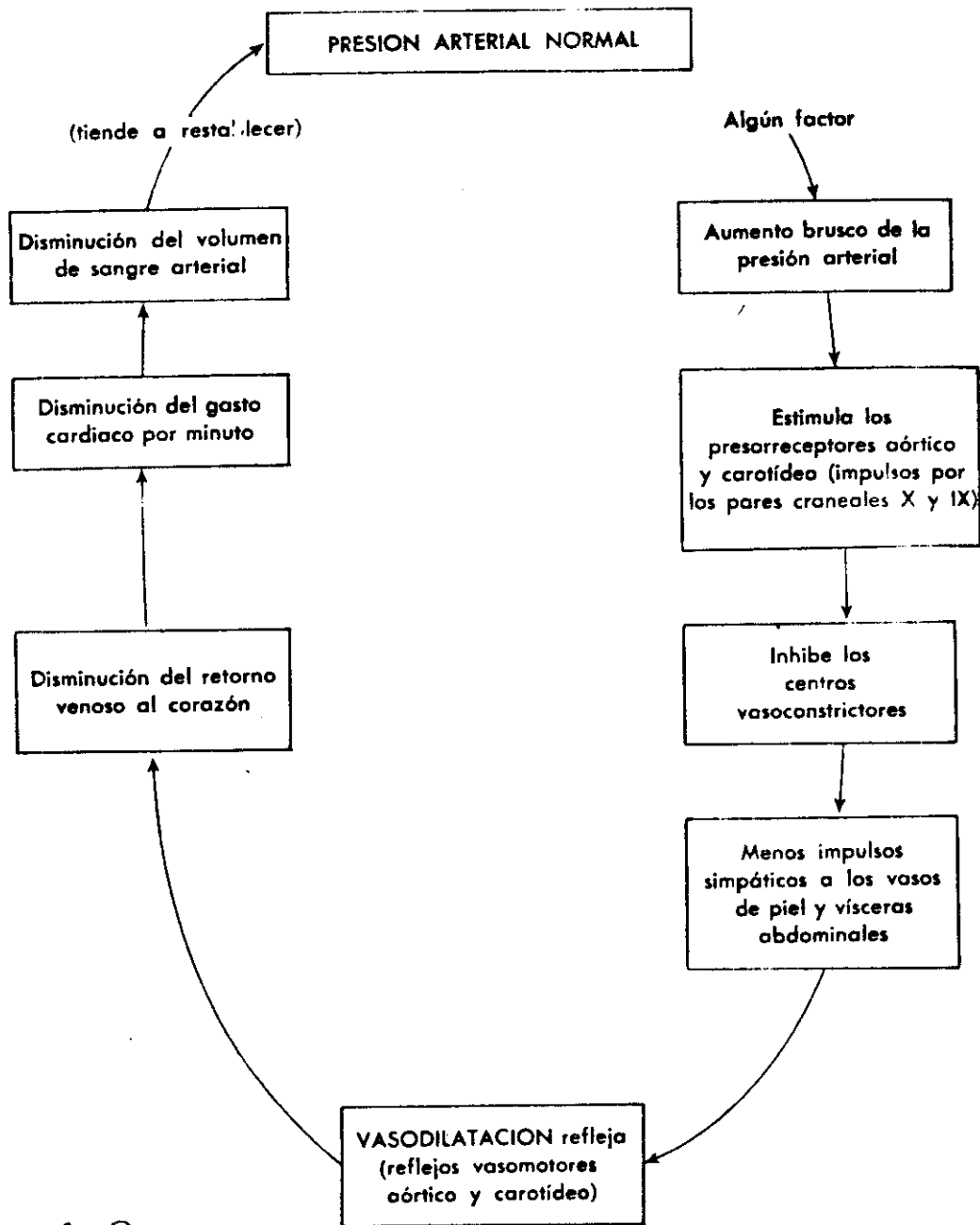


fig. 8
 (FIG. 13-29) El mecanismo reflejo presor vasomotor aórtico y carotídeo que se muestra en el esquema se pone en marcha cuando algún factor causa aumento brusco de la presión arterial. Este mecanismo y los reflejos presores cardíacos aórtico y carotídeo (fig. 13-21) actúan simultáneamente para conservar o restablecer la homeostasia de la presión arterial.

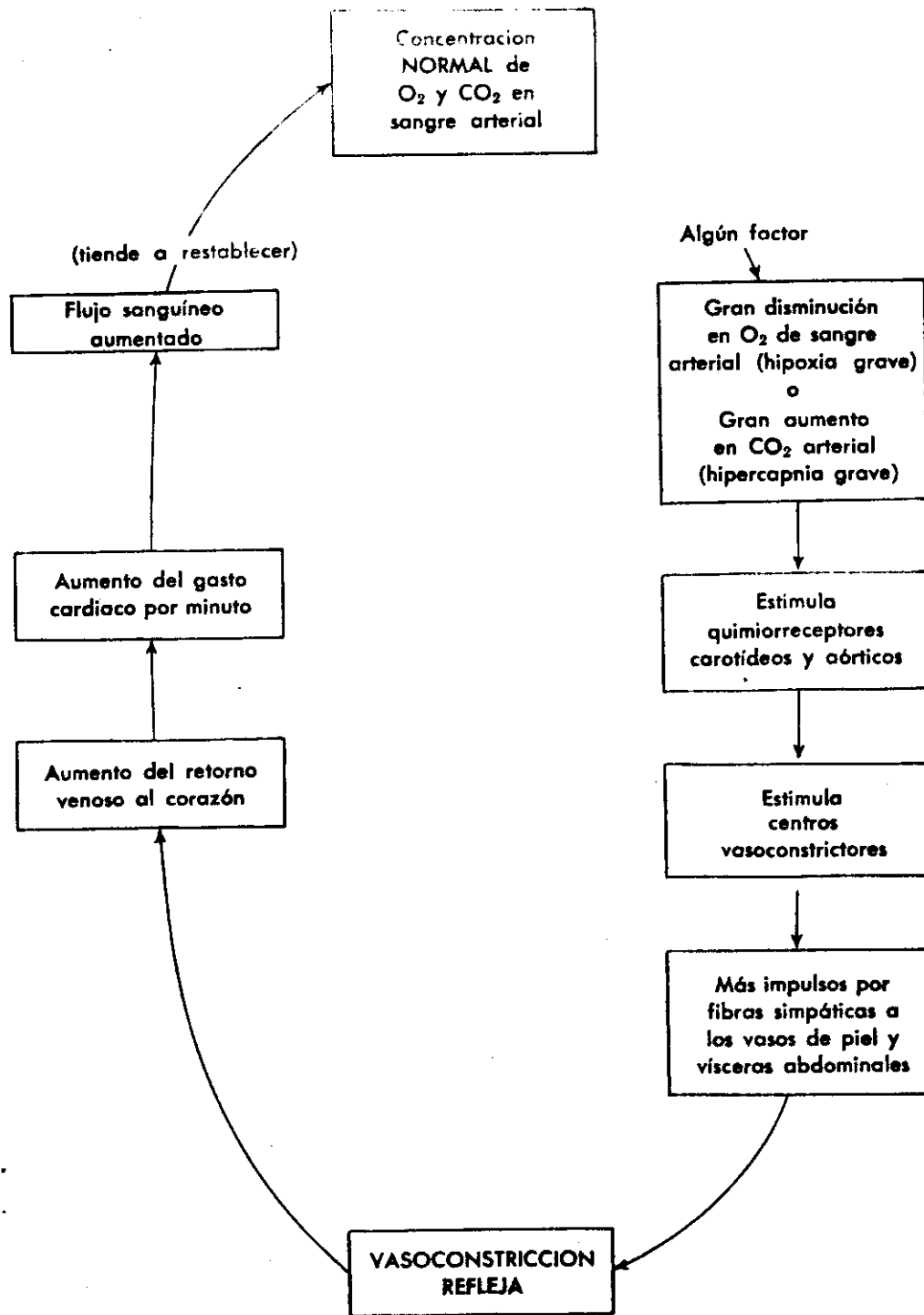


FIG. 13-30. El quimiorreflejo vasomotor que se ilustra aquí no funciona bajo condiciones normales. Opera como respuesta a la reacción general de alarma de hipoxia o hipercapnia graves, y tiende a restablecer las concentraciones sanguíneas normales de O_2 y CO_2 . Como este mecanismo desencadena vasoconstricción refleja, tiende también a aumentar la resistencia periférica y la presión arterial. (Véase también la fig. 13-31.)

MARCO MEDICO PATOLOGICO

Al teraciones de la presión arterial.

VARIABILIDAD DE LA PRESION ARTERIAL GENERAL

Un gran número de factores afectan la presión arterial general ya sea aumentandola o disminuyendola, pero en ambos casos si baja o aumenta de cierto valor normal (120/80) pasa a ser de características anormales y en algunos casos patológicos.

A continuación se citan varios ejemplos que hacen variar la presión arterial, además de las emociones expresadas o no,

Postura. El estar de pie produce reducción transitoria de la presión sistolica y un aumento sostenido de la presión distolica, por lo tanto, se reduce la presión del pulso.

Ejercicio. El ejercicio físico produce aumento de presión sistolica como presión de pulso.

Ingestión de alimentos. Una comida abundante va seguida de un aumento importante de la presión sistolica.

Temperatura. El tiempo caliente (ejemplo, el verano) tiende a disminuir la presión arterial un poco.

Peso. La frecuencia de pacientes de presión sanguínea alta es también mayor en grupos donde el exceso de peso es grande.

Sexo. La presión arterial es más baja en mujeres menores de 40 años y más elevado en las mujeres de 50 años, que en los hombres de la misma edad.

Edad. Tanto la presión sistolica como distolica aumenta en los recién nacidos 90/55, adultos, jóvenes 120/80, vejes 150/90 en promedio.

En vista de lo anterior el valor normal (120/80), sistolica/diastolica, no es una aceveración clara tomando en cuenta los factores anteriores, por lo tanto, se miden intervalos de presión.

(Nota técnica)

Tiempo de llegada del pulso como un metodo para obtener la presión sistolica y diastolica indirecta.

Un nuevo metodo puede describir que se identifique la presión sistolica y diastolica indirectamente, el metodo es basado en ruptura del pulso más alla del puño. Líneas directas arteriales fueron usadas en este estudio para demostrar el principio. El método fue posible aplicarlo usando dos pulsos arteriales, uno tomado justo más alla del puño y el otro en otro sitio conveniente.

Piezoelectrico, fotoelectrico y detección de impedancia del pulso son los candidatos para esta aplicación. (Referencia 9)&

Cuando tenemos que las lecturas de presión son bajas respecto al límite mínimo se dice que es una HIPOTENSION ARTERIAL o PRESION ARTERIAL BAJA. Analogamente, cuando las lecturas son altas respecto al límite máximo se habla de una HIPERTENSION ARTERIAL o PRESION ARTERIAL ALTA y puede ser causada por varios factores -- que a veces se interrelacionan y son :

- a) Fallas en los sistemas reguladores
- b) Por lesiones traumáticas
- c) Enfermedades
- d) Transtornos Psiquiátricos

La Hipertención en sí, se define como el aumento cronico de la presión arterial y representa una de las causas principales de enfermedad y muerte.

No es tan frecuente la Hipotención como enfermedad en comparación con la Hipertención, y podemos controlar estos cambios mediante un control de presión sanginia.

El MMPCACPS, es un modelo multiple de procedimientos de control adaptado, para controlar presión sanguinia, puede ser considerado para un sistema computarizado de retroalimentación con reguladores de rango de infusión de drogas (nitroprusid) para mantener la presión sanguinia.

Ya que los parametros de transferencia funcional son diferentes para cada paciente y más fuertes son las variaciones de tiempo cada uno de los algoritmos se crea para el mantenimiento de ambos estados y las especificaciones del transeunte, para esos efectos la simulación computada puede mostrar que el modelo multiple de procesos de control adaptado puede ser sucesivamente aplicada para el control de presión sanguínea, a pesar del incremento y ~~dele~~ traso de la constante de tiempo y ganancias; el resultado de ambas simulaciones y experimentos animales indica que el modelo multiple de control adaptativo (MMCA) como algoritmo tiene el potencial de controlador automático de toda presión sanguínea mediante un ancho de parámetros, siempre en la presión de representatividad.

La experimentación de Further, con animales sujetos para variación de funcionalidad de transferencias es remodelado para un uso estos estudios comparados con otros adaptadores algorítmicos puede ser interesante. (Referencia 12)

HIPOTENCIÓN

Introducción.

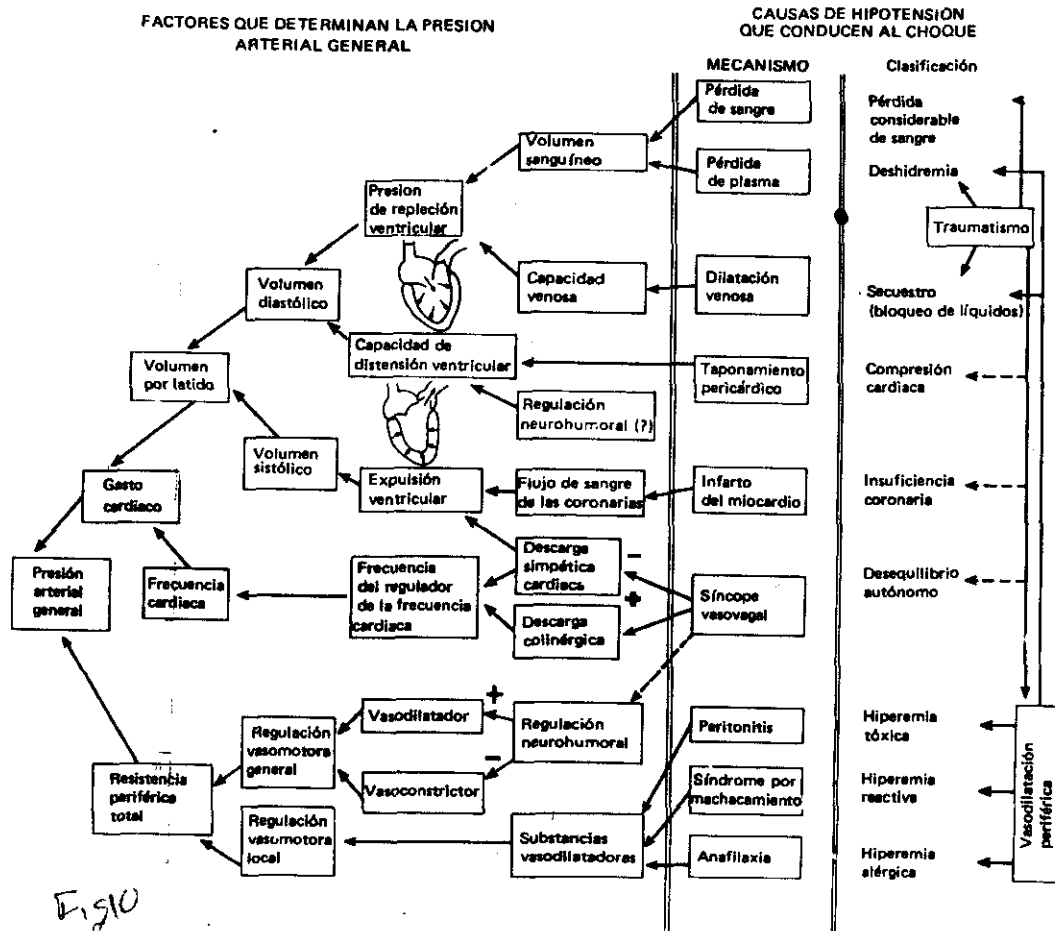
Los mecanismos de regulación que normalmente sostienen la presión arterial general dentro de límites estrechos a pesar de las amplias variaciones de actividad son necesariamente complejas. El fracaso de la regulación que produce la presión arterial baja es un importante problema clínico, la determinación de mecanismos que la involucren y la localizan en lesiones y enfermedades requieren un enfoque acertado y razonado.

A continuación se exponen los mecanismos más significativos bajo los cuales se presenta la Hipotensión Arterial General, las consecuencias debido a está, con depresión física y psíquica subita (choque) sus versiones más comunes y finalmente círculos viciosos de la Hipotensión, además se incluye la figura 11 como una mención de un tipo de hipotensión transitoria, por causa de un fuerte estímulo emocional, en la figura se muestra los mecanismos que

FIGURA 10

MECANISMO DE LA HIPOTENCION ARTERIAL Y DE CHOQUE

Los diversos factores que determinan la presión arterial general pueden ser utilizados como marco para clasificar las causas de la disminución de la presión sanguínea, que conduce al estado llamado "choque", los mecanismos puestos en lista en la columna de lado derecho operan por medio de los mecanismos enumerados se perturban el equilibrio de la presión sanguínea. Las adaptaciones de compensación pueden ocurrir teóricamente en cada punto de ramificación, lo que indica la complejidad de las respuestas aún cuando un solo estímulo aislado o una sola perturbación haya iniciado la disminución de la presión sanguínea.



intervienen desde el estímulo hasta la hipotensión que desemboca en un desvanecimiento.

(Fig. 11)

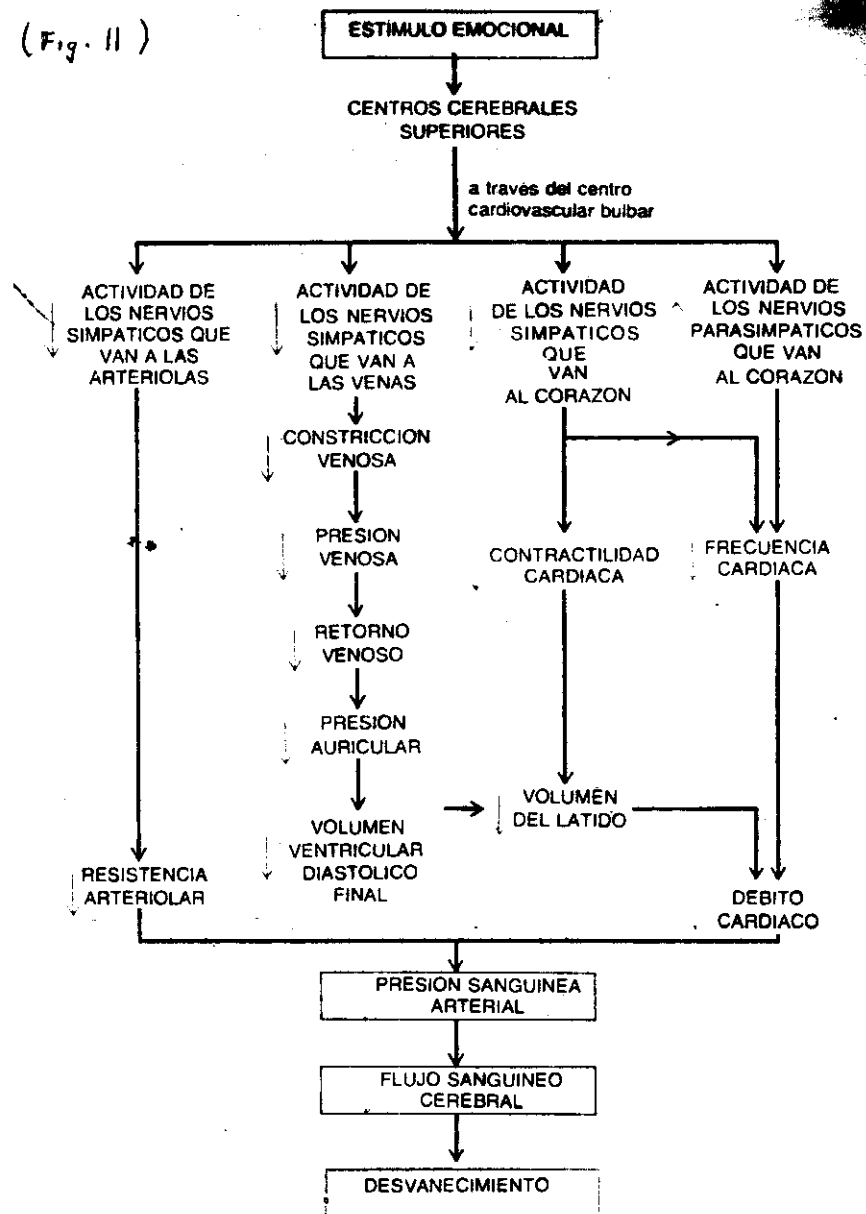


TABLE -2 POSTURAL HYPOTENSION

<p>I. <i>Diminished Cardiac Output</i></p> <p>A. Interference with venous return and cardiac filling at the muscular, venous, or cardiac level:</p> <ol style="list-style-type: none"> 1. Poor muscular pumping mechanism: <ol style="list-style-type: none"> a. Muscular atrophy b. Poor postural adjustment in young asthenic persons standing at strict attention c. Passive tilting 2. Venous disease: <ol style="list-style-type: none"> a. Incompetent valves b. Varicose veins c. Obstruction (e.g., late pregnancy) 3. Cardiac: Tamponade, constrictive pericarditis, atrial myxoma, ball valve thrombus <p>B. Absolute or relative depletion of intravascular volume:</p> <ol style="list-style-type: none"> 1. Relative: Due to dilatation of capacitance vessels by drugs (e.g., nitrites) or disease (e.g., venous angiomatosis) 2. Absolute: <ol style="list-style-type: none"> a. Hemorrhage, internal or external b. Excessive loss of fluid by diuresis, vomiting, diarrhea c. Increased capillary permeability with loss of fluid in interstitial spaces d. Urinary salt wasting due to selective hypoaldosteronism <p>C. Diminished myocardial performance:*</p> <ol style="list-style-type: none"> 1. Myocarditis, severe coronary arterial disease 2. Postural arrhythmias with excessively slow or extremely rapid heart rate 3. Outlet obstruction as in aortic or pulmonary stenosis (usually leads to exercise rather than orthostatic hypotension) 	<ol style="list-style-type: none"> 2. Arteriolar vasodilators as nitrites or nitroprusside <p>B. Neurologic dysfunction:</p> <ol style="list-style-type: none"> 1. Lesion in afferent limb: Tabes dorsalis, rarely in polyneuritis 2. Lesion in central nervous system <ol style="list-style-type: none"> a. Some forms of chronic idiopathic hypotension; possible relationship to Shy-Drager syndrome b. Parkinsonism either isolated or part of a more extensive degenerative disease c. Cerebral arteriosclerosis d. Syringomyelia, various myelopathies, Wernicke's syndrome, tumors e. Drugs (e.g., meprobamate) 3. Lesion in efferent sympathetic limb (parasympathetic may be affected but is not responsible for hypotension) <ol style="list-style-type: none"> a. Some forms of chronic idiopathic hypotension b. Polyneuritis (e.g., diabetes, porphyria) c. Myelopathies d. Iatrogenic: <ol style="list-style-type: none"> (1) Postsympathectomy (2) Neural blocking drugs <ol style="list-style-type: none"> (a) Ganglion blocking agents, adrenergic blockers (b) Monoamine oxidase inhibitors (c) L-dopa
<p>II. <i>Impaired Peripheral Resistance</i></p> <p>A. Arteriolar:</p> <ol style="list-style-type: none"> 1. Disease: Relatively rare (e.g., amyloidosis), and then usually associated with neural involvement as well 	<p>III. <i>Undetermined or Mixed Mechanisms</i></p> <p>A. Adrenocortical insufficiency: Possibly related to cardiac dysfunction and aggravated by fluid loss; reactions of resistance and capacitance vessels said to be normal</p> <p>B. Diabetic acidosis</p> <p>C. Pheochromocytoma (distinctly uncommon)</p>

Mecanismos más significativos que producen hipotensión y llegan a la conducción de choque (depresión física y psíquica súbita):

- a) Pérdida considerable de sangre.
- b) Deshidremia
- c) Secuestro o estancamiento de líquidos
- d) Traumatismos
- e) Compresión cardíaca
- f) Insuficiencia cardíaca
- g) Desequilibrio autónomo
- h) Vasodilatación periférica.

PERDIDA CONSIDERABLE DE SANGRE

El ser humano puede perder algo de 500 ml de sangre sin presentarse modificaciones cardiovasculares de importancia.

Pero si la pérdida de sangre es de tal magnitud que los mecanismos neurales y hormonales fallen para compensar la pérdida por completo, entonces la presión arterial descenderá.

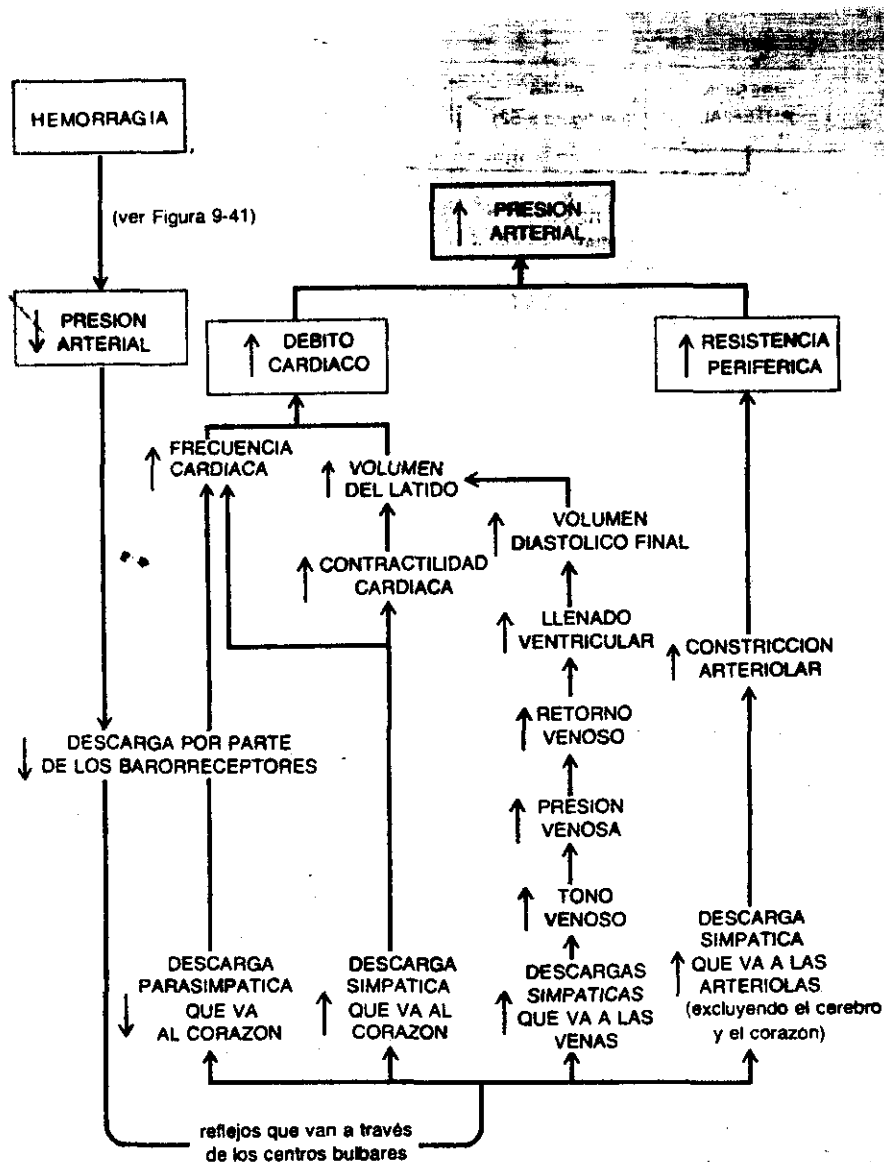
Aunque la simple pérdida de sangre acompañada del descenso de presión sanguínea es suficiente para definir hipotensión por (PCS) porque muchas personas sufren hipotimias (pérdida del conocimiento pasajero con debilidad de la respiración y la circulación). Con solo ver la sangre para decir que existe hipotensión por (PCS) deben comprender pruebas de cada una de las etapas que intervienen en la cadena funcional de eventos que conducen a esta, como son disminución:

- a) específica del volumen de la sangre.
- b) Volumen diastólico.
- c) Débito cardíaco

Pero el cuerpo comienza activarse generalmente y para indicar que los mecanismos de compensación adecuados entran en actividad se presentan:

- a) Vasoconstricción periférica de compensación.
- b) Taquicardia.
- c) Aumento de la expulsión sistólica.

Se presenta en la siguiente figura un esquema de reactivación de la presión sanguínea.



Medición de la constante K de la presión sanguínea sobre un rango de presión en la arteria radial canina.

La evaluación de la constante K de presión sanguínea en la nueva ecuación:

$$M = D - K (S - D)$$

Medida sobre un ancho rango de presión en la arteria radial canina.

Esta ecuación es usada a estimación de valuación de la presión sanguínea media de las valuaciones medidas de las pre-

siones sanguíneas sistólicas y diastólicas. Esto fué fundido en las múltiples variaciones de K, esto se concluye con esta ecuación de una estimación precisa de la presión sanguínea media de las presiones diastólica y sistólica reales.

(Referencia 5).

Estimación del monitor de pulso y presión sanguínea hitachi HME-20.

El funcionamiento de el monitor de pulso y presión sanguínea (PS) hitachi y monitoreo electrocardiográfico es descrito altamente significativa la (P menor que 0.001) con relación fué encontrado entre presiones interarteriales sistólica y diastólica y las presiones registradas por el monitor hitachi. Similarmente la estimación cardíaca electrocardiográficamente computada. Y el dado por el monitor hitachi fueron significativamente correlacionado (P menor que 0.001). La presión sanguínea fué desestimada por una medida de -12 mmHg y tendiendo a ser más erróneo cuando la presión arterial fué mayor 150 mm Hg. Estos resultados son comparables a los más caros monitores de pulso y presión sanguínea.

Concluimos que el instrumento puede reproducir una satisfactoria estimación de la razón-corazón y presión sanguínea.

Y puede ser de uso particular cuando el cambio de presión sanguínea es de importancia primaria, antes que una medición absoluta.

(Referencia 8).

En si los pacientes y animales en experimento pueden sobrevivir muchas horas con una presión arterial media de 40 a 50 mm Hg y responder rápidamente a la restauración del volumen sanguíneo si malos efectos.

En si el tiempo hipotensión por (PCS) como se describio debe reservarse si la presión sanguínea se estabiliza en un nivel muy bajo (es decir por debajo de 60 mm Hg).

Si los sistemas de compensación comienzan a fallar y la presión arterial no se sostiene, llega a producirse un estado patológico de hipotensión llamado "hipotensión con pérdida de sangre con descompensación" y desemboca a un choque hipovolémico (tratado posteriormente).

DESHIDREMIA

La pérdida en grandes cantidades de los líquidos del organismo ya sea debido al cólera, quemaduras, enfermedades de Addison, pérdida de agua etc. conduce a una reducción del volumen de plasma.

La hipotensión deshidremia se caracteriza por aumento de la viscosidad de la sangre, en las cifras hematocrito debido a su concentración de las células y de los elementos sanguíneos.

SECUESTRO O ESTANCAMIENTO DE LIQUIDOS

Casi tres cuartas partes del total del volumen sanguíneo están contenidas normalmente dentro de las venulas conductos venosos y los reservorios venosos. Si una gran parte del sistema venoso aumenta su capacidad repentinamente, gran cantidad de importancia del volumen total de sangre podría ser secuestrado o podría estancarse (Secuestro es empleado para denotar un aumento de sangre en los conductos vasculares en los cuales podría fluir o no la sangre hacia adelante).

El secuestro o estancamiento de sangre probablemente asume mucha importancia en la producción de estados semejantes al del choque por traumatismo, peritonitis o en síndromes de machacamiento.

Aunque también el estar de pie mucho tiempo quieto (formación militar) hace que aumente la acumulación de sangre en los vasos en declive predisponiendo una caída de la presión arterial suficiente para producir hipotimia.

No se tienen métodos adecuados para la determinación de la cantidad de sangre en diferentes partes del organismo.

los datos de la frecuencia que ocurre, la importancia y la contribución de este mecanismo a la hipotensión son completamente insuficientes.

TRAUMATISMOS

Traumatismos (heridas, trastornos causados por estos), es un término no específico y los efectos de las lesiones son tan extensos y variados que ningún mecanismo funcional único puede nombrarse como causa inicial de la hipotensión resultante como se expondrá a seguir. Si hay una herida y la sangre escapa del sistema vascular a los tejidos o hacia afuera del cuerpo produce:

- a) Disminución del volumen de sangre.
- b) El daño a los capilares puede conducir a pérdidas de plasma que se acumula en los tejidos.
- c) Distensión vascular y la hiperemia (es la congestión sanguínea en un órgano) en las partes que han sufrido lesiones que conduce a un secuestro o acumulación de sangre.
- d) El hemopericardio puede producir compresión ventricular en algunos casos.
- e) La regulación autónoma del corazón y los vasos periféricos pueden transformarse por la descarga masiva de los nervios somáticos y viserales aferentes.
- f) Vasodilatación de los tejidos donde se produjo la lesión puede tender a reducir la resistencia periférica, y otros mecanismos pueden contribuir en algo a la hipotensión después de lesiones variadas.

COMPRESION CARDIACA.

La rápida acumulación de sangre o líquido en el saco pericardíaco puede ser considerada como un fenómeno que obstaculiza la distensión ventricular y evita la repleción diastólica ventricular normal.

En teoría la compresión extracardiaca produce:

- a) Disminución del volumen ventricular sistólico y diastólico
- b) Reduce volumen por latido.
- c) Baja el gasto cardiaco a pesar de la taquicardia.

La hipotensión arterial general se presenta cuando la disminución del gasto cardiaco no se ve compensada en forma adecuada por el aumento de resistencia periferica total.

INSUFICIENCIA CORONARIA

El infarto miocardico agudo puede producir grave y un mortal hipertención arterial. Los obstaculos agudos que se presenta a la irrigación en una región importante del miocardico producen:

- a) Reducción de la expulsión ventricular y volumen por látido
- b) Reducción de la eficacia de la parte miocardica no afectada.
- c) Reducción del gasto cardiaco a pesar del aumento del volumen y la taquicardia.

Aparece un cuadro clínico de choque más completo de compensación es activado a la disminución de la presión arterial general.

DESEQUILIBRIO AUTONOMO

El sistema nervioso autónomo del simpatico afecta directamente:

- a) Volumen por látido (actua sobre el miocardio)
- b) Frecuencia cardiaca (actua sobre el regulador)
- c) La resistencia periferica (actua sobre los vasos perifericos)

&. De crecimiento de la presión arterial inducido por descarga del simpatico seguido de la administración del factor nutriuretico, para compensar esta acción nutriuretica.

Ratas consientes SHR yWKY con una infusión durante 7 días con ANF(Arg 102 -Tyr 126)100ng/hr/rata. por mediode una bomba miniosmatica y su presión sanguínea basal (BP). Cambien en la excreción de sodio y catecolaminas urinarias comparadas con los ultimos dias de la infusión. El SHR inicial BPde 181 - 3 mm Hg se declina gradualmente a 137- 5 mm Hg. Cambio no significativo en la presión sanguínea observado en el ANF,infusido en el grupo de WKY. Sin embargo las ratas(WKY) exhibieron un incremento de sodio y la razón dopemina/ norepireprina cuando se compararon ratas con infugión simulada.

(Referencia 15).

En si el desequilibrio autónomo se caracteriza por bradycardia y vasodilatación regional causando la hipotensión.

Si el desequilibrio es transitorio produce pérdida breve de conciencia pero rara vez produce hipotensión prolongada o síntomas típicos de choque.

Si el desequilibrio es grave por ejemplo lesión craneal puede producir estados semejante al choque que se caracteriza por prolongada y por hipotensión arterial general.

VASODILATACION PERIFERICA

La reducción de la resistencia periférica total es la causa principal que produce hipotensión en gran número de estados clínicos (peritonitis, lesiones por machacamiento y anafilaxia) que se caracteriza por gran vasodilatación.

Como actúa el cuerpo en estos casos, es el aumento de gasto cardíaco como en el ejercicio, y la vasoconstricción en otras regiones.

La contribución de las venas, arterias etc, en los cambios de volumen y cambios de resistencia a la sangre por un pulso de impedancia eléctrica.

Un pulso de impedancia, registro no invasivo, tiene contribuciones para ambos cambios en volumen sanguíneo. De las arterias y para el cambio de resistencia otros recursos son seguros para cuantificar la relativa contribución y tiene otra subestimación para estimar la contribución segura que no estimula las condiciones fisiológicas. Nosotros tenemos usado un sistema de fluido circulatorio, para condiciones simuladas fisiológicas y cuantificadas están dos contribuciones; nosotros hallamos que el cambio resistivo contribuye bastante (21.51% en la contribución del cambio de volumen arterial para cambiar a la morfología de un pulso de impedancia. Esto es siempre una diferencia entre fases.

Contribuciones. Esto es el resultado de la contribución de los cambios de resistividad para esos pulsos altos de impedancia que puede ser un 5.5% .

(Referencia 13).

Es decir estos estados clinicos deben ser acompañados por extrema taquicardia y aumento del gasto cardiaco pero la disminución de la resistencia periferica total por vaso dilatación escasa vaso constricción compensadora o un obstaculo con gran aumento del gasto cardiaco hace la reducción sostenida de la presión arterial.

CONSECUENCIAS DE LA HIPOTENSION

Como se menciona, en la hipotensión desciende el gasto cardiaco este disminuye tanto que los tejidos corporales no pueden recibir riego sanguineo suficiente, lo que significa que no se puede alimentar suficientemente ni eliminar adecuadamente los productos de deshecho. Todo estado que puede disminuir el gasto cardiaco a otras muy bajas puede causar choques circulatorio.

El choque cardiaco puede ocurrir por debilidad del corazón o la disminución del retorno venoso y se clasifica en :

- a) Choque cardiaco.
- b) Choque por retorno venoso disminuido.

CHOQUE CARDIACO.

Es una insuficiencia del gasto cardiaco bajo que suele ocurrir inmediatamente después de ataque cardiaco grave, (insuficiencia coronaria , con presión cardiaca), que trae consigo disminución enorme de la capacidad del corazón de emplear sangre.

Con frecuencia el paciente muere antes de que el corazón recomienze a recuperarse.

CHOQUE POR DISMINUCION DE RETORNO VENOSO

Los factores que hacen que disminuya el retorno sanguineo al corazón con resultante choque son:

- a) Disminución del volumen sanguineo (deshidremia, perdida considerable de sangre), que produce choque hipovolemico.
- b) Aumento del lecho vascular es decir vasodilatación periferica que produce choque por extasis venoso (secuestro o estancamiento del líquido, hipermia reactiva, hiperemia toxica, vaso dilatación periferica, traumatismo.

CHOQUE NEUROGENO _____desequilibrio autónomo
CHOQUE ANAFILÁFTICO _____hiperemia alérgica.

En si el choque neurogeno y el anafiláftico se incluye dentro de choque por extasis venosa pero se dividieron para mostrar la clasificación de la causa.

CHOQUE HIPOVOLEMICO

Depende de la pérdida de sangre que hace disminuir el volumen sanguíneo (hemorragia intensa, pérdida de líquidos o síndrome de machacamiento) y el corazón no retorna suficiente volumen sanguíneo, produciendo el descenso de presión y choque.

CHOQUE POR EXTASIS VENOSA

Se suscita si los vasos pierden su tono vasomotor, su diámetro aumenta, la sangre se estanca, el retorno venoso es escaso, baja la presión y se suscita choque.

CHOQUE NEUROGENO

Es causado por la supresión brusca de impulsos simpáticos del sistema nervioso central al vascular periférico pérdida del tono vasomotor, de aumento del retorno venoso y la presión en el aparato circulatorio. El desavenimiento emocional es ejemplo de este tipo de choque.

CHOQUE ANAFILÁFTICO

Es la extasis venosa causada por reacciones alérgicas, si una persona es alérgica a una sustancia, la reacción produce liberación de otras sustancias que desencadenan el estado de choque. Una de estas sustancias es la Hislamina que hace dilatar los vasos sanguíneos causando la extasis venosa y disminución del retorno sanguíneo que conducen rápidamente al choque anafiláftico. En la anafilaxia la rapidez del estancamiento venoso ocurre tan rápido que el paciente muere antes de iniciar el tratamiento.

Cada uno de los anteriores estados de choque presenta diferentes etapas de gravedad .

Las etapas del choque son:

a) Choque compensado.- Es cuando es muy ligero, por lo que los diversos sistemas de compensación pueden mantener la presión sanguínea y el riego de sangre recuperando rápidamente

su estabilidad el paciente.

b) Choque progresivo.- Si es mas intenso continuara empeorando el paciente en este caso de choque.

c) Choque irreversible .- la gravedad es tal que el paciente si es que sigue vivo ningun medio terapeutico podra salvarlo.

Ahora citaremos algunos tratamientos del choque en función de las etapas antes descritas.

TRATAMIENTOS DEL CHOQUE.

Choque cardiaco.- Consiste en aumentar la eficiencia propulsora cardiaca no siendo fecil, muriendo un 85% de las personas.

Una ayuda seria administrar noradrenalina para aumentar la presión arterial mediante vasoconstricción de las arteriolas perifericas que a su vez fomenta mayor flujo de sangre por las coronarias hacia el miocardio.

Choque hipovolemico.- el volumen puede aumentarse por transfusión de sangre, administración de plasma o una solución salina isotonica incluso, si el paciente esta conciente. Puede darsele agua ya que este sufre una sed intensa que lo obliga a beber. De esta manera aumenta la presión que aumenta el retorno venoso y alivia el choque.

Choque neurogeno y anafilactico .- Como la causa principal es la extasis venosa se administraran fármacos de estimulo al sistema nervioso simpatico que causen vasoconstricción con lo que se obliga a la sangre retornar al corazón, aumentando la presión arterial.

VARIACIONES EN LA EVOLUCION Y TERMINACION DE LA HIPOTENCION
En si teoricamente la eliminacion eficaz del factor o factores que iniciaron la hipotención arterial general pueden volver la presión arterial a niveles normales y restaurar la salud normal, sin embargo la experiencia ha demostrado que la mayor parte de los tipos de hipotención pueden ser de suficiente grado y duración que pueden presentarse deterioro y muerte aun despues de la desaparición de los factores iniciales .

Como un ejemplo los pacientes que sufren hipotención por

perdida de sangre prolongada, mejoran transitoriamente despues de la restauración del volumen sanguineo, y despues gradualmente cae a pesar de los esfuerzos por mantener el volumen sanguineo por la resistencia periferica y el gasto cardiaco (choque irreversible).

La rapida administracion de medicamentos pospone la posibilidad de morir por un mecanismo solamente para ser seguido de otro diferente. Volviendo al ejemplo de la hipotención por perdida de sangre pueden aparecer tres causas diferentes de rapida sucesión.

a) Progresiva caída de la presión arterial apesar de la restauración del volumen sanguineo y agentes vasopresores.

b) Paro respiratorio

c) Intensa bradicardia

El paro respiratorio resultaria de una depreción cerebral grave que son manifestaciones de la difucion cerebral y aparecen, la perdida de conciencia, reflejos pupilares.

La bradicardia muy marcada es un proceso relativamente frecuente como fenomeno terminal.

CIRCULOS VICIOSOS EN EL COLAPSO CIRCULATORIO TERMINAL

La reducción del flujo sanguineo es el resultado natural del gran desenso de la presión arterial general, la presión arterial reducida disminuye en forma correspondiente el gradiente de perfución arterovenosa.

El flujo sanguineo cerebral puede verse primordialmente disminuido por este mecanismo. Una de las respuestas compensadoras dela hipotencion es la vasoconstricción generalizada producida por los reflejos baroreceptores debido a esto, el flujo atraves de la red esplendarica (de las vicerias), riñones , los musculos y la piel es notablemente reducida.

La taquicardia compensadora contribuye a la reducción del flujo coronario, en si ningun tejido es totalmente respeta-
docuando dieminuye el flujo sanguineo.

La irrigación sanguinea del sistema nervioso central es adversamente afectada por la reducción de la presión arterial por que la circulación cerebral no responde mucho a la didminución del flujo sanguineo.

Como se menciona la pronunciada reducción de la presión

arterial media debe en consecuencia, producir la correspondiente reducción del flujo sanguíneo cerebral.

El flujo sanguíneo cerebral inadecuado produce insuficiencia de los centros de regulación respiratoria resulta en paro respiratorio.

La autoreinfusión puede desaparecer el tono vasoconstrictor compensatorio, la relajación venosa aumenta la capacidad venosa y entonces disminuye la presión, de llenado ventricular y el gasto cardíaco. La brusca aparición de bradicardia puede indicar muy serio desequilibrio autónomo o causa de la depresión en el sistema nervioso.

La combinación de efectos por la baja de presión mas la taquicardia puede conducir insuficiencia miocárdica con caída posterior del gasto cardíaco y reducción todavía de la presión arterial.

Al no haber regulación neural, se expresa esta como relajación de la construcción compensadora, esta disminuye, esta disminuye directamente la presión arterial sin mayor reducción del gasto cardíaco.

Ahora si la construcción compensadora es muy intensa y prolongada para disminuir drásticamente el flujo a través de muchas redes vasculares ocurre que los vasodilatadores químicos se acumulan y finalmente aumentan lo suficiente para vencer el tono constrictor que se parece al de la hiperemia activa.

Con esto se observo que los fenomenos terminales en los casos mortales en los estados de choque pueden considerarse como un grupo circulo viciosos potenciales aun sin tener conexión evidente con la causa original de la hipotensión arterial general

La figura 12 muestra una ramificación de los ciclos viciosos del colapso circulatorio terminal por causa de la hipotensión grave y prolongada.

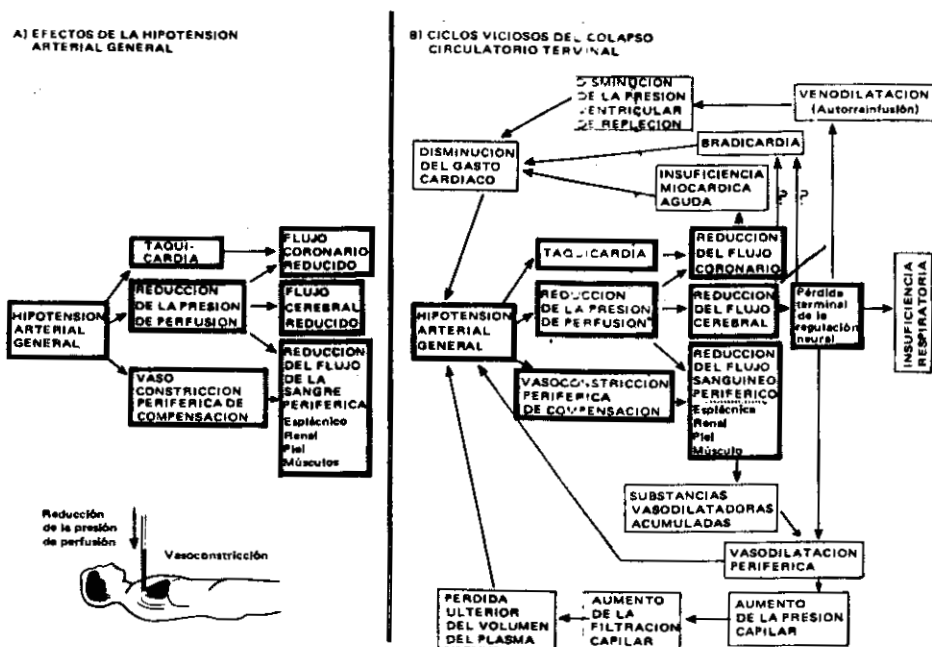


Fig. 12. Hipotensión arterial general con círculo vicioso A, algunos efectos funcionales de compensación a la hipotensión arterial general comprenden la reducción del flujo sanguíneo coronario y cerebral, lo mismo que la reducción del flujo de la sangre periférica por los órganos o vísceras más importantes.

B, la hipotensión grave y prolongada puede producir círculos viciosos que tiendan a deprimir todavía más el gasto cardíaco o a producir vasodilatación que hace la hipotensión progresivamente más imposible de ser tratada.

HIPERTENSION

La hipertensión (alta presión sanguínea), se define como aumento de la presión arterial, el límite superior comunmente aceptado para la presión arterial normal es de 140/90 mm Hg debido a que hay variaciones fisiologicas presiones sistolicas superiores a 140 mmHg no se asocian a hipertensión, sin embargo la presión diastolica es el indicador mas importante de la presión arterial alta (hipertensión).

Como al presión general media, aumenta con la edad el número de personas que tienen cifras altas de presión arterial de un cierto nivel (140/90), es indidublemente muy alto, pero solo un pequeño porcentaje de estas personas, la elevación de la presión arteria va evidentemente asociado a algún estado patológico.

La mayoría de los casos, el desarrollo de la hipertensión no puede ser explicado en la actualidad, en este caso la presión arterial elevada es denominada hipertensión primaria o esencial es decir, sin causa distintiva que haya causado su elevación o que pueda identificarse facilmente.

La presión arterial general no es un estado patológico si no un signo (entre varios) que es común a gran variedad de estados fisiologicos y patológicos. Algunos pacientes pueden ser identificados en los que la presión arterial es el resultado directo de una causa especifica y puede ser aliviada por la supresión de esta causa.

La tabla (3) presenta una dosificación etiologica (causas de las enfermedades) de la hipertensión, a continuación se enlistan las diferentes clases de hipertensión.

- a) Hipertensión esencial.
- b) Hipertensión renal.
- c) Hipertensión endócrina (Hormonal)
- d) Hipertensión neurogena.
- e) Hipertensión cardiovascular.

TABLE 3 AN ETIOLOGIC CLASSIFICATION OF HYPERTENSION

I. Arterial Hypertension (elevation of systolic and diastolic blood pressures)	
A. Essential hypertension	
1. Labile (intermittent)	
2. Established ("fixed")	
B. Renal hypertension	
1. Kidney disease	
a. Glomerulonephritis	
b. Chronic pyelonephritis	
c. Congenital polycystic kidneys	
d. Obstructive uropathy	
e. Diabetic glomerulosclerosis	
f. Interstitial nephritis due to analgesics, gout, hypercalcemia	
g. Connective tissue diseases, periarteritis nodosa, scleroderma, lupus erythematosus	
h. Renal tumor	
i. Renal amyloidosis	
j. Radiation nephritis	
k. Hereditary nephritis	
2. Renal arterial disease	
a. Fibrous dysplasias	
b. Atherosclerotic disease	
c. Embolic obstruction	
d. Traumatic arterial dissection or occlusion	
3. Compression of kidney	
a. Perinephritis	
b. Perirenal hematoma, usually post-traumatic	
C. Endocrine hypertension	
1. Catecholamine excess: pheochromocytoma	
2. "Steroid" hypertension	
a. Mineralocorticoid excess	
(1) Primary aldosteronism	
(2) Functional enzymatic block leading to adrenal hyperplasia (e.g., 11-hydroxylase deficiency in adrenogenital syndrome, 17-hydroxylase deficiency, androgen-induced hydroxylase deficiency in masculinizing tumors)	
(3) Iatrogenic: Excess DOC or fluorinated steroid administration	
b. Glucocorticoid excess - various causes of Cushing syndrome (adrenal, pituitary, ectopic ACTH syndromes, ovarian tumors)	
3. Oral contraceptives	
4. Condition associated with hypertension	
a. Acromegaly	
b. Thyroid disorders	
(1) Myxedema	
(2) Thyrotoxicosis, usually a cause of systolic, not diastolic, hypertension	
D. Neurogenic hypertension	
1. Anxiety states (?)	
2. Intracranial disease	
a. Increased intracranial pressure	
b. Encephalitis	
c. Diencephalic syndrome	
d. Lead encephalopathy	
3. Disturbances in vasomotor center	
a. Bulbar poliomyelitis	
b. Disturbances in vascular supply	
4. Spinal cord and peripheral nerves	
a. Transection of the cord, transverse myelitis	
b. Polyneuritis	
c. Porphyria	
E. Hypertension of coarctation of the aorta	
F. Hypertension of toxemia of pregnancy	
1. Preeclampsia	
2. Eclampsia	
II. Systolic Hypertension	
A. Caused mainly by an increased stroke output of the left ventricle	
1. Complete heart block	
2. Aortic regurgitation	
3. Patent ductus arteriosus	
4. Thyrotoxicosis	
5. Arteriovenous fistula	
6. Paget's disease of bone	
B. Caused mainly by a decreased distensibility of the aorta	
1. Arteriosclerosis of aorta	
2. Coarctation of aorta	

La presión arterial excesiva por causa de la hipertensión puede causar rotura de vasos sanguíneos cerebrales para producir pérdida súbita o total del conocimiento y movimiento (apoplejía), en el riñón produciendo insuficiencia renal y en otras partes para producir ceguera, sordera, ataques cardíacos entre otros males y entorpeciendo sobre carga en el corazón, usando insuficiencia cardíaca.

A continuación se describen los tipos de hipertensión como función anormal de los mecanismos reguladores y otros.

Se hace notar que el 95% de las hipertensiones caen en la llamada hipertensión esencial y el resto en los otros tipos.

HIPERTENSION ESENCIAL

Es un término aplicado a la presión arterial alta que no puede ser atribuida a ninguna lesión específica, como esta se eleva progresivamente con la edad los pacientes que la sufren se encuentran, de las curvas de distribución en el extremo más alto (curvas de frecuencia para cada edad), la herencia, medio ambiente y sexo pueden alterar la magnitud hasta la que llega a la presión arterial. Generalmente entre más elevada sea la presión arterial se acorta la posibilidad de sobrevivir. El dolor de cabeza y el vértigo son síntomas comunes de estos pacientes, y los accidentes vasculares, cerebrales (Trombosis), son complicaciones frecuentes.

La presión arterial general elevada conduce a hipertrofia del ventrículo izquierdo, hasta insuficiencia cardíaca en etapas finales, en la hipertensión benigna, la presión fluctúa más ampliamente de lo normal pero elevándose progresiva y lentamente con los años.

En la hipertensión maligna (no muy frecuente) la presión alta progresa rápidamente los cambios vasculares característicos de la retina (retinopatía hipertensiva) aparece muy temprano en esta fase de la enfermedad y, las funciones renales se hacen rápidamente insuficientes.

La insuficiencia ventricular izquierda o los accidentes vasculares cerebrales pueden causar la muerte antes de que la insuficiencia renal llegue a desarrollarse por completo.

HIPERTENSION ESENCIAL (CAUSAS)

En sí la causa de la hipertensión esencial es comparable por ejemplo a intentar determinar la causa de la fiebre en algún grupo de pacientes antes de que las causas conocidas hayan sido específicamente eliminadas.

Grandes esfuerzos se han hecho para determinar los mecanismos que pueden ser responsables. (Figura 13)

Casos como los siguientes ejemplifican esto:

- a) Hipertensión renal sin enfermedad del riñón.
- b) Hipertensión de origen suprarenal sin distinción de las suprarenales,

c) Hipertensión isomotora en anomalías sin dañar el sistema nervioso central.

d) Hipertensión vascular sin lesión en el aparato circulatorio.

Producen controversias y confusiones semánticas que han arrojado poca luz sobre estos temas.

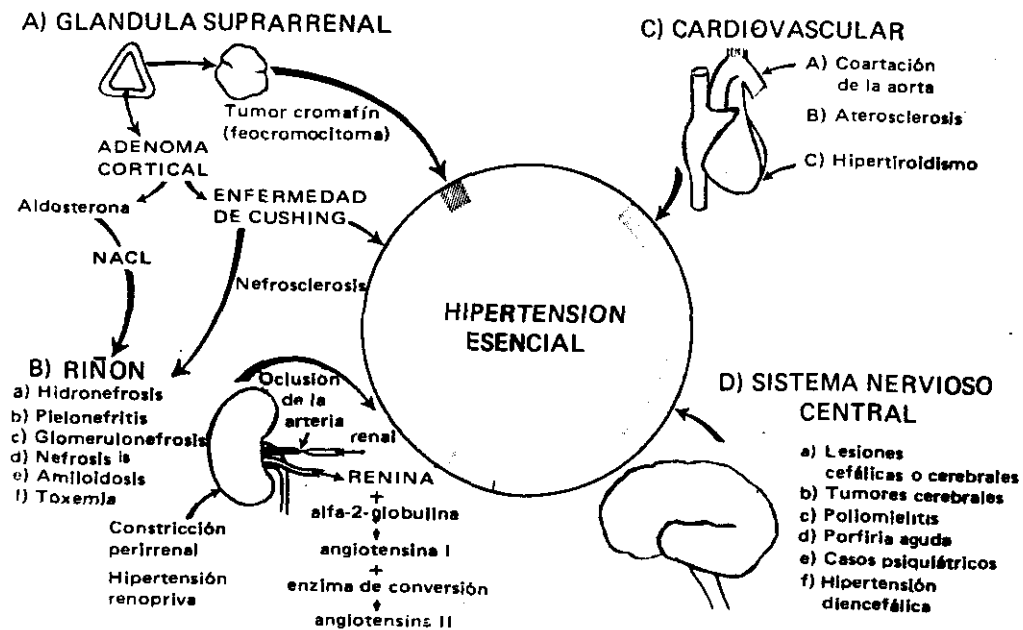


Figura 13. Hipertensión esencial la evaluación de la presión arterial general es una característica común en muchos estados diferentes de procesos patológicos que comprenden las suprarrenales, los riñones, el cerebro y el aparato cardiovascular.

Del número tan elevado de la población que presenta presión arterial general elevada, solo una pequeña porción sufre estos distintos procesos de enfermedad. El resto, que es tan grande es definido como hipertensión esencial, lo que significa que su causa no ha sido determinada.

Exclusión de mecanismos estandar .

En el inicio de la hipertensión esencial de ningún mecanismo de la figura 13, puede demostrarse como fenómeno en operación porque el metabolismo y electrolitos están en su nivel normal el flujo sanguíneo renal y funciones de los riñones son normales la arteriosclerosis no son mayores entre los pacientes y la presencia de lesiones neurales no pueden demostrarse.

La angiotensina puede producir estados espontáneos y experimentales de elevación de presión pero se descarga este mecanismo por lo siguiente en las fases iniciales de la hipertensión moderada en personas de poca edad los riñones parecen normales desde el punto de vista anatómico-funcional y cantidades anormales renina, no se han encontrado constantemente en casos de hipertensión primaria.

Por otro lado en pacientes con insuficiencia cardiaca congestiva pueden tener alto nivel de renina sin tener hipertensión por esto es que se descarta que la renina en concentraciones que no pueden determinarse sea la causa de la hipertensión.

LA hipertensión sigue a la hipertensión

Como los pacientes que sufren hipertensión esencial no muestran causas identificables de ella, su terapéutica se ha dirigido principalmente hacia la reducción de la presión arterial por diversos medios, pero la presión arterial general alta actúa de modo para producir aumentos todavía mayores. Teóricamente la presión arterial general elevada producida por cualquier causa que sea, se convierte en una enfermedad que se sostiene así mismo.

Microprocesador - control de infusión de droga para control automático de presión sanguínea. (Referencia 7)

Un control - microprocesador de infusión de bombeo es descrito por el control automático de hipertensión o antihipertensivo tratado con sodio nitroprusico, el sistema requiere de continuos monitoreos de presión sanguínea como una señal de entrada a el microprocesador, el látido regula la presión sanguínea al nivel deseado, por cambios de peso adecuado de infusión frecuente.

El bombeo de infusión probablemente sea muy valioso para cuidado intensivo y microcirugía bajo hipertensión controlada.

Readaptación del mecanismo presoreceptor

Si se aumenta la presión arterial por medio de estimulación se puede demostrar que los presoreceptores periféricos mismos pueden adaptarse aun aumento sostenido de la presión arterial.

Si se deja de estimular la frecuencia cardiaca se acelera, lo que indica que los mecanismo presereceptores se han establecido a un nivel más alto y actúan para obtener de nuevo estabilidad al nivel más alto de presión sanguínea.

El concepto de readaptación del mecanismo presereceptor no constituye una explicación satisfactoria de la elevación sostenida de la presión arterial por que está tiende a disminuir a cifras normales después de largos períodos de tiempo cuando se suprime el estímulo.

Arteroesclerosis del seno carotideo

La región del seno carotideo es un lugar de predilección para la arteroesclerosis. El engrosamiento patológico y aún la calcificación en esta parte ocurre, cuando en otras porciones del árbol arterial no son afectadas.

Si la pared del seno carotideo se hace rígida por este medio la cantidad de estiramiento de la pared en casos particulares de la presión se reduciría limitando un estiramiento de los presereceptores de deformación de la pared propia del seno. Aún así los nervios podrán responder a la compresión externa y si embargo, mostrar frecuencia reducida de descarga después de cambios de presión externa.

Vaso constricción generalizada

Diversos mecanismos pueden intervenir en una vaso constricción generalizada suficiente para producir hipertensión la elevación del tono vascular se atribuye a una fuerza anormal ejercida por el musculo liso de los vasos que no quedan bajo acción inmediata del sistema nervioso.

La hipertrofia es una característica prominente de los vasos de resistencia en pacientes que sufren hipertensión repetida o continua elevación de la presión interna o por aumentos intermitentes de la actividad constrictora del simpático.

Inchazón vascular

El hinchamiento de la pared arterial fué considerada como una causa potencial de aumento de la resistencia periférica puesto que el 13% de hinchazón de la pared arterial se vio que hacia aumentar la resistencia al flujo en un 54% una causa seria del aumento de la concentración de sodio y agua en las paredes aórticas.

Las dietas bajas en sal podran aliviar la hipertensión reduciendo el contenido de líquidos en las paredes vasculares. Entonces se diria el edema de las paredes vasculares seria de modo general equivalente a una hipertrofia moderada.

Hipertensión renal

Se identifico la relación que existe entre las proteínas de la orina y las alteraciones patológicas del riñon, con hipertrofia del ventriculo izquierdo y se describio imparcialmente el aumento de la resistencia periférica acompañada de alteraciones de las funciones renales.

La presión arterial general se eleva en una gran numero de enfermedades renales (de hecho casi todas) también se indican en la figura 13 algunos transtornos.

La existencia de obstaculos a la irrigación renal o compresión externa del parénquima renal, se pueden asociar a la elevación presión arterial general.

Se tiene obstrucción unilateral de la arteria renal entonces la presión puede ser aumentada, la obstrucción puede ser causada por engrosamiento local (arteroesclerosis) o constricción local, cuando se elimina con éxito la obstrucción o se extirpa el riñon afectado.

En general se esta de acuerdo que cualquier mecanismo que opone obstaculos a la irrigación sanguínea del parénquima puede esperarse que cause elevación de la presión arterial.

El mecanismo opresor renal puede activarse por diferentes enfermedades renales ya que transtornan el flujo sanguíneo renal de un medio u otro. Por citar algunas enfermedades como hidronefritis, la piel o nefritis entre otras. La pielonefritis se asegura que produce obliteración y destrucción de las arterias renales de diámetro pequeño, una oclusión arteriosclerosa de las arterias rena-

les, puede ser o no complicado con pielonefritis por abundar de sus efectos.

Hipertensión hormonal

En ocasiones existe disfunción de la glándula suprarrenal por causa de tumores o estimulación excesiva de los suprarrenales por la hipófisis.

Una rara forma de tumor en la médula suprarrenal es el feocromocitoma. Su causa es por la multiplicación anormal de células que producen un adenoma entonces la d-adrenalina y la noradrenalina que segregan normalmente son liberadas periódicamente produciendo hipertensión ascendente, palpitaciones, dolores de cabeza, ansiedad, temblor, náuseas, vómitos, gran palidez es decir excitaciones directas al simpático. La presión arterial se eleva intermitentemente con signos y síntomas de liberación masiva de sustancia transmisora del simpático en algunos pacientes la presión arterial fluctúa ampliamente pero queda persistentemente elevada. Nos basta decir que la extirpación completa del tumor suprime los ataques sintomáticos, en algunos pacientes en que los ataques han sido eliminados quirúrgicamente su presión permanece elevada después de la eliminación de su causa.

También los cambios de presión arterial son observados constantemente en pacientes con enfermedades que afectan la corteza suprarrenal. La hipertensión se presenta aproximadamente en el 85% de pacientes que sufren el síndrome de Cushing que consiste en secreción excesiva de hormonas adrenocorticales y se observa en precocidad sexual, hermafroditismo, virilismo en mujeres y feminización en hombres y obesidad.

En el momento todavía es imposible identificar la anomalía que se presentan en el metabolismo de esteroides corticales responsable de la hipertensión.

Hipertensión neurologica

La presión arterial alta va acompañada de diversos transtornos histopatológicos y funcionales del sistema nervioso central tales como las lesiones cerebrales, tumores cerebrales y destrucción selectiva de tejido cerebral como en los casos raros (como poliomeilitis) transtornos psiquiátricos, hiperacción cardiovascular ver tabla 3, y figura 13 y pueden ser resultados de daños producidos a partes muy seleccionadas del sistema nervioso central.

Descripción de algunas condiciones:

Aumento de presión intracraneal

Las lesiones encefálicas o tumores cerebrales estratégicamente colocados producen una elevación de la presión del líquido cefalorraquídeo del sistema nervioso central entonces la presión arterial general tiende a aumentar a medida que se eleva la presión del líquido cefalorraquídeo.

La elevación de la presión arterial es debido a la compresión del tallo cerebral de una región bulbar que contiene los centros de regulación cardiovascular.

Lesiones destructivas algunos pacientes que sufren poliomeilitis aguda que comprende el tallo cerebral (parálisis bulbar) presentan intensa hipertensión.

Transtornos psiquiátricos

La admisión muy generalizada del hecho que la excitación y otros factores psicológicos pueden influir generalmente en los niveles de la presión arterial general.

La opinión actual es una actitud conservadora sobre los resultados de la frecuencia de hipertensión en personas neuróticas o con psicosis y se duda con respecto a este mecanismo como causa dominante de la hipertensión crónica.

Medición directa de presión sanguínea; riego evolución tecnológica y problemas comunes.

(Referencia 11)

Síndrome diencefálico

Es causado por estimulación difusa del diencéfalo humano y los signos y síntomas son: hipertensión, parches de enrojecimiento de la cara y parte alta del tórax y extremidades finas y pálidas taquicardia e hiperperistaltismo.

Hipertensión cardiovascular

La presión arterial general puede elevarse como resultado de ulceraciones dentro del aparato cardiovascular mismo.

Trastornos cardiovasculares que provocan elevación de la presión arterial quedan ejemplificados, como coartación de la aorta, la arteriosclerosis generalizada y la pericarditis nudosa (fig,13, y tabla 3).

También llega a presentarse contricción de la aorta tóraxica como defecto de desarrollo. Se caracteriza por reducción de luz de la aorta aún conducto delgado e impide gradualmente el flujo de sangre desde el arco aórtico hasta la aorta dorsal descendiente y desarrollándose conductos colaterales pero a pesar del desarrollo de estos conductos la presión sanguínea usualmente se encuentra muy por encima de las arterias generales y elevándose por arriba del sitio en que se presenta la contricción.

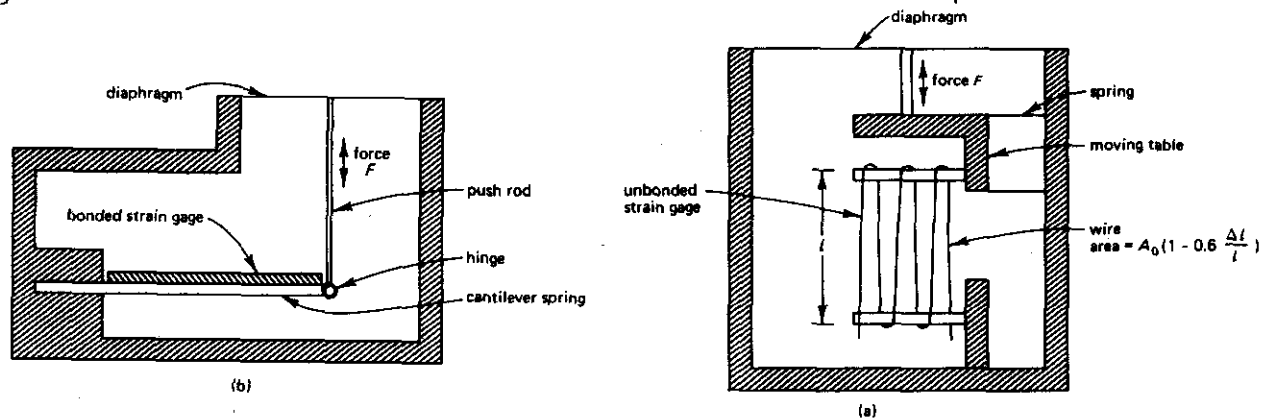
La corrección quirúrgica de la constricción aórtica va seguida de rápido descenso de la presión arterial que vuelve a cifras normales después de unos días.

MARCO INGIENERIL

Instrumentos Calibradores de Fuerza por Alambres i Conexiones

Un largo número de Instrumentos médicos que se usan en la actualidad son los "Transductores" de Fuerzas o de Alambres, por ejemplo: los más usados con cateteres son de éste tipo.

Calibradores de Fuerza en alambres son instrumentos o mecanismos generalmente de pequeñas señales usados con circuitos preamplificadores de puente, un u otro voltaje exitación de corriente directa o corriente alterna pueden ser usados para el puente. La relativa ventaja del uso de corriente alterna o corriente directa, depende sobre la detallada señal y en las condiciones de diseño del circuito; los calibradores de hacer fuerza pueden ser usados en todos los instrumentos en un modelo garantizado y no garantizado en otros modelos



La figura muestra un diseño de un Diagr ma "Calibrador de Presi n" utilizando un calibrador de hacer fuerza no garantizado, la figura **b** muestra un tipo garantizado.

El cambio de resistencia del alambre es causado por tres factores:

- El cambio relativo en la longitud del alambre $\Delta l/l$
- El cambio relativo en el  rea de la secci n de campo $\Delta A/A$
- El cambio relativo en la resistividad del alambre

El cambio en el incremento de resistividad con fuerzas tensiles, es aplicable a un alambre, si la $\Delta p/p$ (c) es positiva, el cambio

El cambio en el area del alambre es relacionada con el cambio en el diámetro $\Delta A / A = 2 \Delta d / d$, y el cambio relativo en el diámetro es relacionando con el cambio relativo de la longitud, esta relación es proporción de Poisson's.

Characteristics of Strain Gage Materials

Material	Temperature coefficient of resistivity, α_R	Temperature coefficient of expansion, $\alpha_E (\times 10^{-6})$	Gage factor, m_f	Tensile strength, Y_p (pascals, $\times 10^6$)	Modulus of elasticity, Y_e (pascals, $\times 10^{10}$)	Maximum $\Delta l/l$	Maximum $\Delta R/R$
Platinum	0.0038	9	6	340	15	0.0023	0.014
Constantan	-0.0002 to +0.0002	14.8	2	410	17	0.0024	0.005
Nichrome	0.0004	13.2	2.5	690	19	0.0036	0.009
Mercury in flexible tube	0.0009	30	2				
Silicon	0.007	5.4	170	620	19	0.0033	0.5

Tabla 3

La característica de varios materiales que son usados en calibradores de alambre son listados en tabla 3 e incluye actualmente varios tipos de materiales; un metal puro (platino) con coeficiente de baja temperatura de aleación resistida con un fluido conductor (mercurio) y un semiconductor cristalino (silicio)

El coeficiente de temperatura y resistividad α_R en la ecuación ;

$$R = R_0 [1 + \alpha_R (T - T_0)]$$

Las fuerzas tensiles Y_p es la fuerza máxima que el material tolera sin de formaciones permanentes, de la definición para la elasticidad en el módulo de Young.

$$\Delta l / l = Y_p / Y_e$$

Transistores piezoresistivos

Muchos instrumentos pueden ser designados usando un contador de líneas de volumen de silicio; sin embargo recientemente, materiales con regiones de impurezas difusas pueden ser sucesivamente aplicados al diseño de instrumentos. Algunos de esos materiales tienen grandes imprevistos y características de ejecución de temperatura y es comparada con los materiales de almacenamiento.

Con la aplicación de la tecnología de la teoría de piezas de resistencia para el diseño de instrumentos médicos (transductores) específicos como un cateter intracardiaco tipo calibrador de presión piezoresistivo puede ser analizado en la figura 15

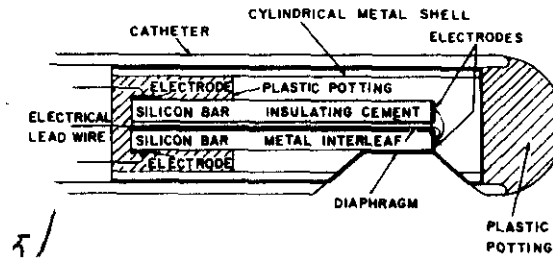
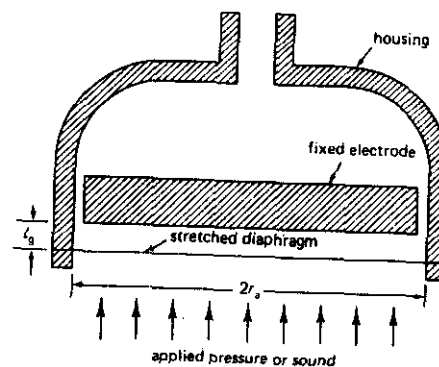


Fig.15.

Considera dos elementos de transductor piezoresistivo en un catete intracardiaco, hay otros tipos de transductores como el respiratorio como un diseño más útil que se caracteriza por su sensibilidad y tiene una frecuencia usual cuando después es limitado por el y es de resonancia mecánica más baja que la frecuencia del instrumento.

Hay transductores de diafragma-estiramiento en términos de aplicaciones medidas, el transductor variable en capacitancia en uso más grande es .

Probablemente el instrumento o diafragma-estiramientos fig. (16)



El diseño geométrico puede ser usado como un transductor de capacitancia de presión o es un micrófono condensado.

Un diseño es un calibrador capacitivo de presión de las cualidades de intereses son las frecuencias resonantes, límites permisibles, el cambio en aplicación de presión de baja capacitancia, al rendimiento de voltaje generado, con un voltaje aplicado y es manejado por vibraciones en cintas. Transductores Balanceo-Fuerza. Consideremos el calibrador de transformación Diferencial de la (Fig. 17)

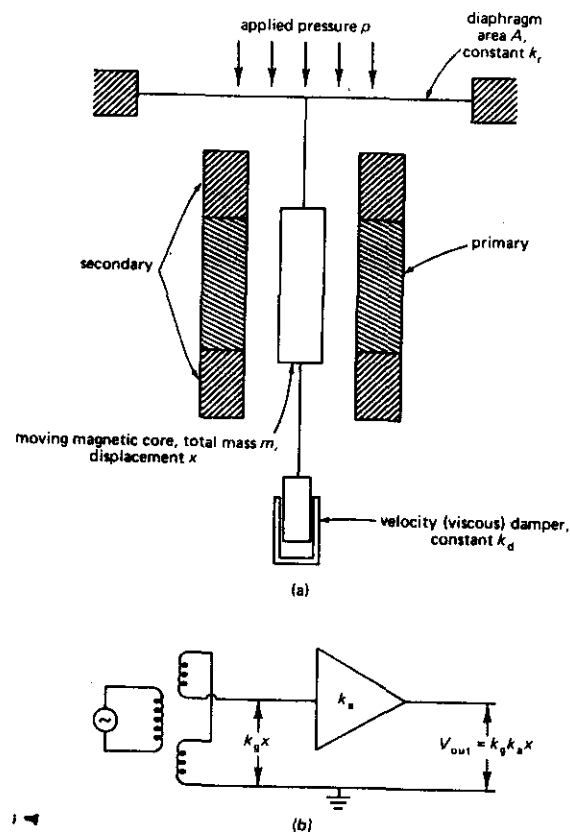


Figura 17.

Cuando la presión es aplicada, el diafragma se desvía y mueve el centro magnético. El amortiguamiento es suministrado por un mecanismo en el cual la viscosidad del aceite determina la proporcionalidad de la velocidad. El cambio de posición del centro producen un voltaje de rendimiento diferencial y es modulada a una frecuencia portadora.

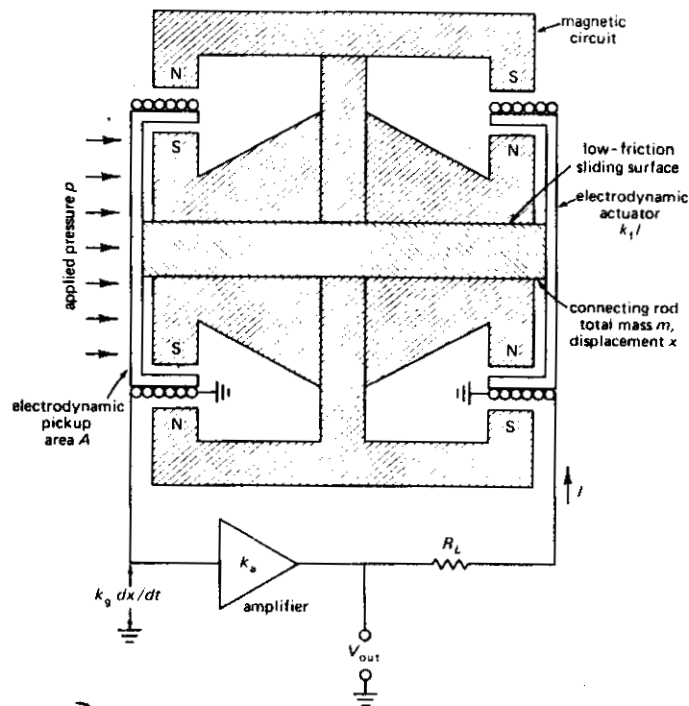
Es un instrumento el cual tiene algunos defectos:

1.- Cuando se aplican diferentes presiones la desviación varía del diafragma, desde que el diafragma no salta correctamente, esa puede ser alguna señal no lineal de rendimiento causada por el diafragma no linealmente.

2.-Bajo condiciones variadas del medio ambiente quien da las características de no linealidad puede cambiar la posición adicional no linealizadas puede cambiar adicionales en la lectura del instrumento.

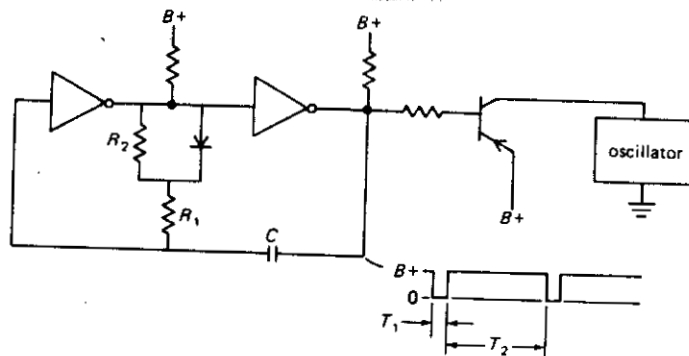
3.-Finalmente las variaciones mecánicas y en los componentes (diagrama, centro, espirales) con variaciones en la temperatura puede producir errores en la temperatura.

Calibrador de presión con velocidad de captación y fuerza electrodinámica que actúa. Un interés ante microfono de valance de fuerzas flexibles propio para medición de presión dinámica y utilizando un deflector de velocidad de movimiento en lugar del desplazamiento dicho instrumento se muestra en la fig. 18,



Unidad pulsátil de frecuencia modulada

Una unidad de implante para la telemetría de lentas variaciones y datos de temperatura y presión, tal circuito se muestra en la figura 19.



Para obtener modulación en frecuencia del rango de repetición, la variable existente puede causar un cambio en RyC .

Muchos de estos transductores existentes son: de resistencia variable y capacitancia variable y son por eso sus aplicaciones con estas características.

Medición de la presión arterial

La medición de la presión arterial comprende tanto la determinación de la presión sistólica como de la diastólica esto representa la amplitud del pulso en el punto de medición. de los

Esfigmomanometria

Como las ondas del pulso se extienden rápidamente por todo el sistema arterial y son modificadas en grado variable, la presión arterial en cualquier momento varía en cualquier parte del árbol arterial. Los registros más exactos de la presión arterial se obtienen por medio de agujas intraarteriales conectadas con sistemas de registro de la presión, el registro general se obtiene en papel que corre con relativa lentitud y las ondas de pulso se comprimen en tiempo. (fig. 20)

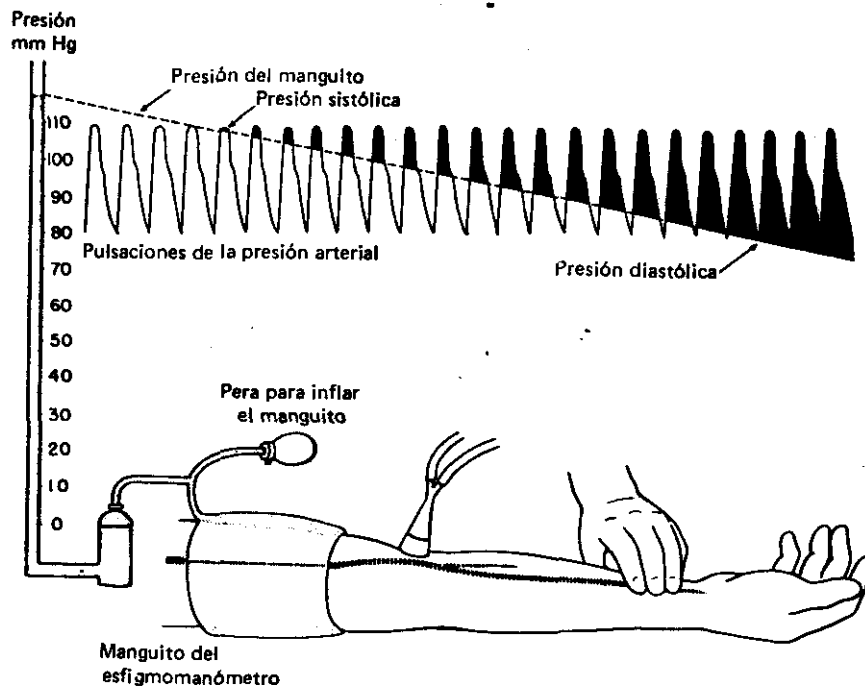


FIG. 20. Esfigmomanometria. Cuando la presión que existe dentro del manguito del esfigmomanómetro aumenta por encima de la presión de la sangre arterial, las arterias que se encuentran bajo el manguito son obstruidas, y no puede palpase el pulso en la articulación del puño. A medida que la presión del manguito se afloja gradualmente, el máximo sistólico de la presión finalmente llega a exceder de la presión que existe dentro del manguito de la presión, y la sangre penetra en forma de chorro en las arterias situadas por debajo del manguito, y produce pulsaciones palpables en la articulación del puño. La repentina aceleración de la sangre por debajo del manguito produce vibraciones que son audibles por medio de un estetoscopio. La presión en el manómetro mercurial en el momento en que se escucha el pulso o se siente al palpar la radial, indica la presión sistólica. A medida que la presión del manguito disminuye todavía más, los sonidos aumentan de intensidad y entonces de un modo repentino se amortiguan a la altura de la presión diastólica, a la que las arterias permanecen abiertas durante toda la onda completa del pulso. A presiones todavía menores, los sonidos desaparecen por completo cuando se restablece el flujo laminar.

La presión arterial generalmente es medida por medio de un esfignomanómetro que consiste en un manguito no elástico que contiene una bolsa de caucho inflable y esta conectada por medio de un tubo de caucho a una pera de caucho y con un instrumento que registra continuamente la presión dentro del manguito cuando queda bien ajustada al brazo la inflación de la bolsa de caucho comprime a los tejidos por debajo del manguito si la presión de la bolsa excede una presión al máximo de la presión arterial, la arteria permanece (oprimida oprimada) y no se palpa ninguna onda de pulso en la arteria. Si la presión alcanzara un punto en el cual el apogeo de la onda de pulso si excede la presión de los tejidos que lo rodean la arteria permanecerá colapsada.

Ruidos de Korotkoff

En la arteria braquial a medida que se reduce la presión que se encuentra colocado bajo el codo, se escucha por medio del estetoscopio los soplos de compresión sistólica los cuales son dos: los primeros son "tonos cortos" que aparecen al pasar parte de la onda del bajo del manguito.

El análisis experimental del mecanismo de producción de estos sonidos indica que los primeros tonos cortos o sonidos de golpe son debido a aceleración transitoria por la distensión brusca de la pared arterial. El sonido de compresión parece originarse en el chorro de turbulencia que se forma en situación diastólica al segmento arterial comprimido.

Fuentes de error en la medición de la presión arterial

Una indebida selección o aplicación de los manguitos de los esfignomanómetros.

La presión que existen en la bolsa de caucho es transmitida a mayor profundidad en el centro del manguito, y si es suficientemente amplio el manguito debidamente ajustado, la presión indicada por el manómetro se extiende a los tejidos que rodean inmediatamente la arteria (fig. 21 A); pero si el miembro es demasiado grueso en relación al ancho del manguito, la presión que se ejerce al alrededor de la arteria es significativamente menor que la registrada en la bolsa de caucho y el manómetro (fig. 21B). Por lo tanto la lectura de la presión por lo tanto la lectura-

de la presión sistólica y diastólica puede ser demasiada elevada si el manguito al aplicarlo queda flojo (fig. 21 C).

Presión sanguínea arterial media

La presión sanguínea fluctúa durante cada ciclo cardiaco con frecuencia se usa la presión arterial media en los informes clínicos y experimentales puede ser determinada amortiguando el pulso o integrando la onda de pulso arterial en registros exactos.

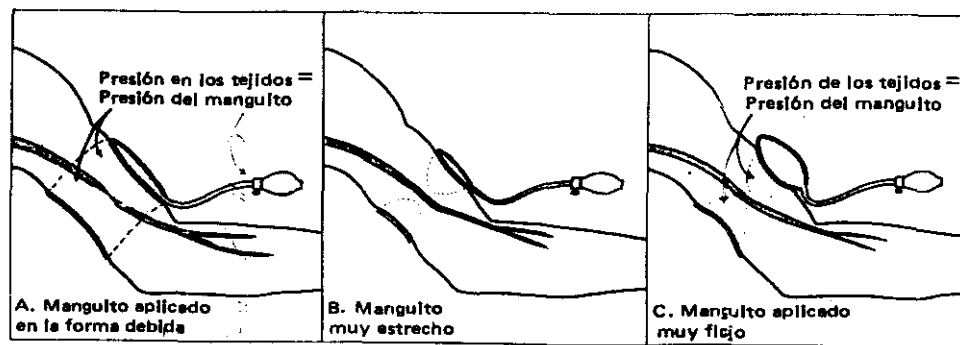


FIG. 21. Transmisión de las presiones del manguito a los tejidos del brazo. A, Cuando el manguito de un esfigmomanómetro de suficiente ancho en relación con el diámetro del vaso es aplicado en la forma debida, la presión en los tejidos alrededor de la arteria por debajo del manguito iguala a la presión del manguito; sin embargo, la presión por abajo del extremo del manguito no penetra tan profundamente como en el centro del propio manguito.

B, Un manguito que es demasiado estrecho en relación con el diámetro del miembro no transmite su presión al centro del miembro. En estas condiciones, la presión del manguito debe exceder grandemente a la presión arterial para producir la oclusión total de la arteria y entonces se hará una lectura errónea tanto de la parte alta de la presión sistólica como de la presión diastólica, al guiarse por el manómetro de mercurio.

C, Si se aplica muy flojo un manguito de suficiente amplitud, este manguito se hace redondeado antes de ejercer presión sobre los tejidos y produce la misma clase de error que un manguito muy estrecho.

Y por este metodo se encuentra posco más o menos a un tercio de la distancia que existe entre la presión sistólica y la diastólica a la configuración de la onda de pulso (fig. 22)

DETERMINACION DE LA PRESIÓN ARTERIAL MEDIA

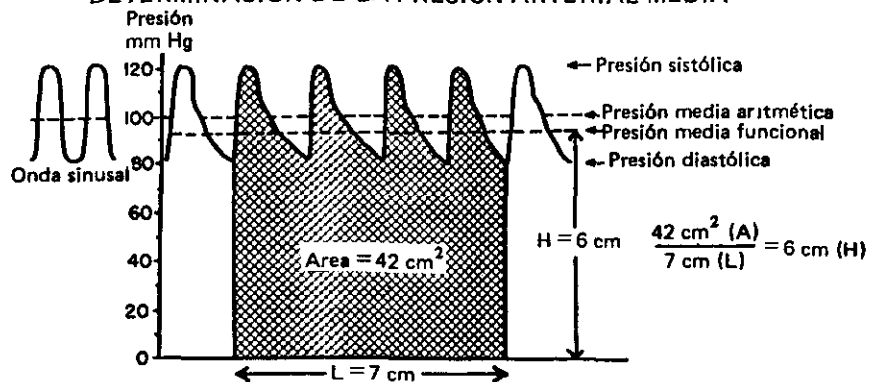


FIG. 22 Presión arterial media. Si la presión sistólica es de 120 mm Hg y la presión diastólica de 80 mm Hg, la presión media aritmética es de 100 mm Hg. Si la onda del pulso arterial fuera simétrica (onda sinusal), esta cifra representaría la presión media de perfusión; sin embargo, el intervalo durante el cual la presión arterial es menor de 100 mm Hg es más largo que durante aquel en que se eleva por encima de esta cifra, de manera que la presión funcional media es menor de 100 mm Hg. La presión funcional media es determinada dividiendo el área de la región sombreada (área = 42 cm²) por la dimensión horizontal (L = 7 cm) para determinar la altura de un rectángulo que tiene la misma área (H = 6 cm). La presión funcional media tiende a ser más elevada que la presión diastólica aproximadamente en un tercio de la presión del pulso, pero este cálculo no se aplica a las ondas del pulso que tienen diferentes contornos, es decir, con cambios de la frecuencia cardíaca.

Registro continuo de la presión arterial

A medición de la presión arterial ha desempeñado durante largo tiempo papel muy importante en la investigación cardiovascular. Los datos recientes han creado gran interés para registrar con toda exactitud, tanto la presión pulmonar como la presión general. Los transductores de presión apropiados para registrar las rápidas fluctuaciones en las presiones arteriales e intraventricular un manómetro mercurial resulta inadecuado para registrar la presión que fluctúa amplia y rápidamente. La inercia del líquido y la resistencia a su paso por el manómetro evitan que el nivel del líquido siga cambios tan rápidos como los de la presión arterial.

El manómetro, indudablemente no indica ni la magnitud de la presión sistólica ni diastólica.

Las presiones que presentan rápidas fluctuaciones pueden ser registradas solo por medio de aparatos de frecuencia adecuada. La respuesta de frecuencia es una medida de la velocidad con que un sistema de registro responde a cambios de presión repentina.

Transductores mecánicos de presión

El transductor común para la medición de la presión consiste en un tambor provisto de una membrana de caucho acoplada a una palanca escribiente. Si la membrana de caucho es muy flácida (fig. 23) la inercia del líquido y la palanca se opone a una respuesta rápida a los cambios de presión en la membrana o proporciona una fuerza relativamente débil.

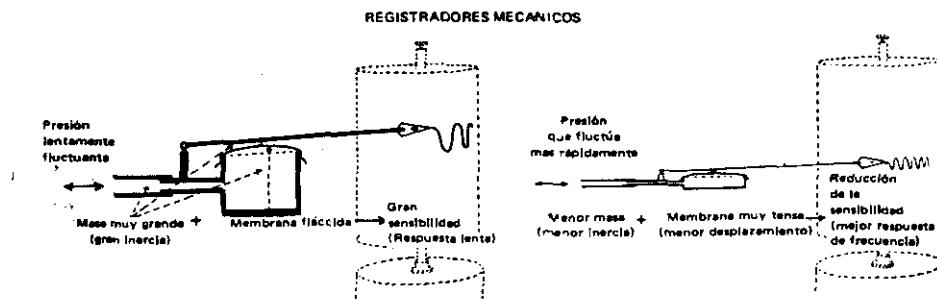


FIG. 23 Registradores mecánicos de la presión. El registro de la presión ordinariamente comprende el desplazamiento de algún tipo de membrana elástica. Para desplazar la membrana, el líquido debe moverse dentro de la cápsula de registro. La inercia del líquido, la membrana y el mecanismo de registro tienden a resistir el desplazamiento. Cuando la masa que está en movimiento es grande y la membrana es flácida, el sistema de registro puede ser muy sensible a las presiones que fluctúan lentamente, pero no responderán a los cambios rápidos de presión. Reduciendo la masa en movimiento y utilizando membranas rígidas, se disminuye la sensibilidad, pero no se mejora la respuesta de la frecuencia.

Un sistema de esta índole no puede responder con la suficiente rapidez para seguir la presión arterial.

La frecuencia natural de un transductor puede ser considerada según la masa que queda suspendida en un resorte o muelle, mientras más pequeñas es la masa y más rígido el resorte más rígida será la oscilación.

Cuando la masa del líquido y la palanca son grandes en relación con la tensión de la membrana las oscilaciones son lentas si la membrana es muy tensa la frecuencia aumenta, pero la sensibilidad se reduce.

Transductores electricos de presión

En los movimientos ligeros de las membranas más rígidas pueden ser usadas para estudiar corrientes de voltaje que pueden ser amplificadas por medio de amplificadores electrónicos y los movimientos de membrana producen:

- a) La resistencia
- b) La capacitancia
- c) La inductancia.

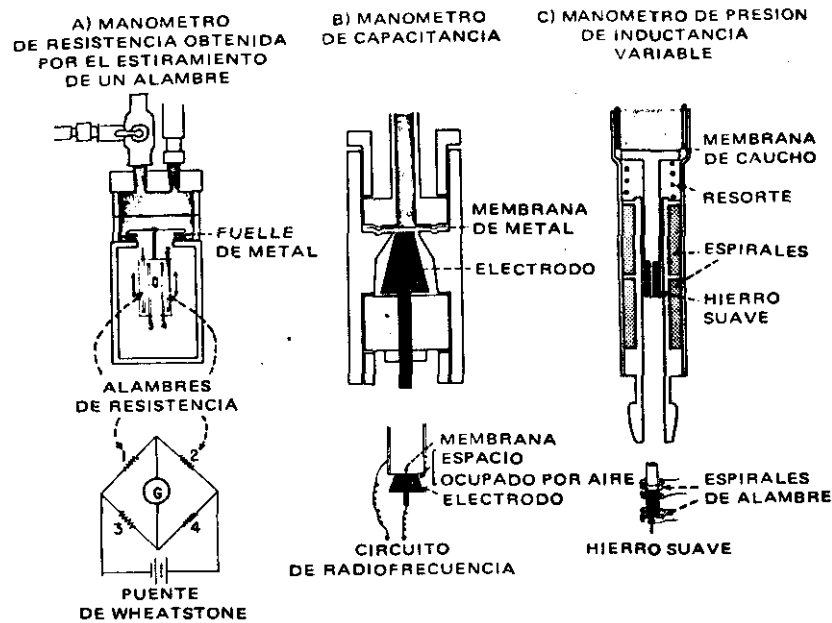


FIG. 24 Transductores eléctricos de presión. A, El manómetro de alambre a tensión, de resistencia no limitada (manómetro de Statham), consiste en un fuelle de metal que es comprimido por el aumento de presión dentro de la cámara. El desplazamiento del fuelle hacia abajo es transmitido a una corredera de metal soportada por cuatro juegos de alambres sensitivos a la tensión y enrollados a tensión y unidos para formar un puente de Wheatstone. El desplazamiento de la corredera de metal hace que se estiren dos juegos de alambre y que los otros dos se relajen. Estos cambios de la resistencia desequilibran el puente en proporción a la presión aplicada. El gasto resultante del voltaje que proviene del puente, es amplificado y registrado por diversos medios.

B, El manómetro de diafragma de capacitancia eléctrica es un condensador formado por un electrodo (teñido en negro) separado de una membrana de metal rígida por un espacio de aire cuidadosamente ajustado. El desplazamiento de la membrana hace que cambie el grueso del espacio de aire. Esto da como resultado un cambio en la capacitancia que es registrado por un circuito de frecuencia de radio. (Tomado de Lilly.¹¹)

C, Las variaciones del flujo magnético en armaduras de alambre pueden ser producidas por movimiento de una corredera de hierro colocada dentro de la armadura. En un transductor de presión de transformador diferencial, la corredera de hierro queda unida al centro de una membrana elástica, de tal manera que los cambios de presión producen cambios del flujo magnético. (Tomado de Gauer y Gienapp, *Science*, 112:404, 1950.)

En cada caso, las membranas rígidas con escaso desalojamiento de líquido de respuesta relativamente altos de frecuencia pueden ser usadas para las señales del gasto cardíaco siendo amplificadas.

REFERENCIAS

Disposable Blood Pressure Transducer System

EDWARD L. SPOTTS, B.S., M.S.

Cobe Laboratories
Lakewood, CO

THOMAS P. FRANK, B.S.

Ametek Controls Division
Feasterville, PA

A unique **disposable invasive hemodynamic blood pressure transducer system** has been developed. The system consists of a disposable piezoresistive flow-through transducer with twelve-inch pigtail, a reusable extension cable, an electronic interface module and a custom interconnect cable to attach to most monitors. The transducer has Linden Luer fittings and replaces the dome and reusable transducer in monitoring systems. The cost of the transducer is kept low so that it can be disposable through efficient modern, high-volume semiconductor technology and the fact that additional electrical isolation is accomplished in the interface module. Besides providing electrical isolation, the **interface module provides a universal output which will accommodate all common AC, DC, and pulsed excitation signals from monitors.**

INTRODUCTION

An **invasive** blood pressure transducer is a device for **continuous** measurement of patient's blood pressure. It is connected to a fluid-filled tube in a blood vessel that transmits the pressure signal. The transducers currently available are reusable devices which cost \$500 to \$600 (1982). They have a disposable dome which isolates the sterile fluid pathway from the reusable device. Present transducers must be tested for calibration regularly by the user and must be handled carefully as they are fragile. Additionally, it is considered necessary that the transducer be routinely sterilized to reduce risk of infection.

SIGNIFICANT PHILOSOPHY

When the disposable transducer system was being designed, many parameters had to be considered. To be successful, the transducer had to solve some of the problems with existing devices. Regular calibration could be eliminated by factory pre-calibration. Sterilization of each device would eliminate the need for a dome. Easier set up and debubbling procedures were necessary. Small size and rugged design would

allow versatility in mounting. Small volume displacement would give excellent frequency response.

In addition, the system had to meet all of the tough standards which users have come to expect of existing devices. Patient electrical safety and over-pressure protection were essential. The system had to be compatible with a wide variety of patient monitors.

THE TRANSDUCER

The heart of the blood pressure transducer utilizes a **piezoresistive-type silicon strain gauge**. This silicon sensor is positioned to interface directly with the fluid media being monitored. Therefore, it is mandatory that the sensor be resistant to performance degradation due to contact with foreign substances. Certain contaminants in the fluid media can affect the piezoresistors' operating characteristics. The technique of isolating the piezoresistors by using conformal coatings at the sensor-fluid interface cannot be used because the coatings contribute to a significant performance degradation. Allowing the piezoresistors to be buried beneath the surface of the sensor diaphragm through diffusion or ion implantation provides adequate isolation. (See Figure 1.)

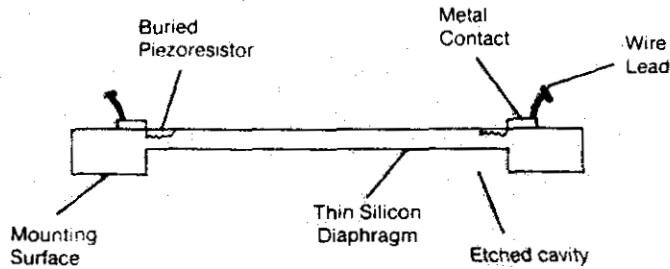


Figure 1

Sensor cross-section illustrating buried piezoresistors.

There are several major advantages that silicon strain gauges display over conventional strain gauges. Applied pressure at the diaphragm of the silicon sensor strains the crystalline structure. This strain causes a large change in value of the piezoresistors, resulting in an extremely high sensitivity.

Most strain gauges bonded to dissimilar materials are inherently unstable. The bonding of the pressure-sensing elements to dissimilar materials results in

... "There are several major advantages that silicon strain gauges display over conventional strain gauges." ...

thermo-elastic strain. The pressure sensing elements of the new pressure sensor are ion-implanted into the silicon's crystalline structure, providing a totally integrated pressure-sensing element.

The inherent crystalline structure of silicon provides another important feature. The elasticity permits the diaphragm to be flexed over a specified pressure range. After the applied pressure or rated over pressure is removed, the diaphragm will return to its original null voltage condition. Conversely, other types of strain gauges are made of materials which creep, and may require re-zeroing of the monitoring system.

The final major advantage is that the silicon sensors can be fabricated using common *integrated circuit processing* technology. The finished product is an inexpensive chip of silicon that accomplishes both pressure sensing and electrical output. This technique allows the pressure sensor to be interfaced directly with the total system.

At the sensor-fluid interface, the sensor is molecularly bonded to a flat area ground onto the outer wall of a tube. The preferred approach is to bond the sensor to a tube which has a coefficient of expansion similar to silicon. The effect is diminished thermal stress and excellent mechanical stability.

A hole which penetrates that wall of the tube provides the fluid pathway between the monitored media and the passive side of the sensor (See Figure 2).

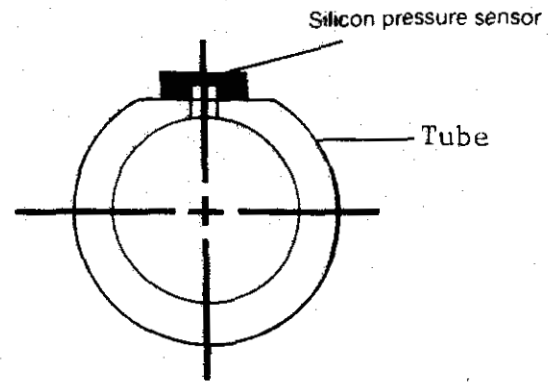


Figure 2

Cross section of sensor bonded to tube.

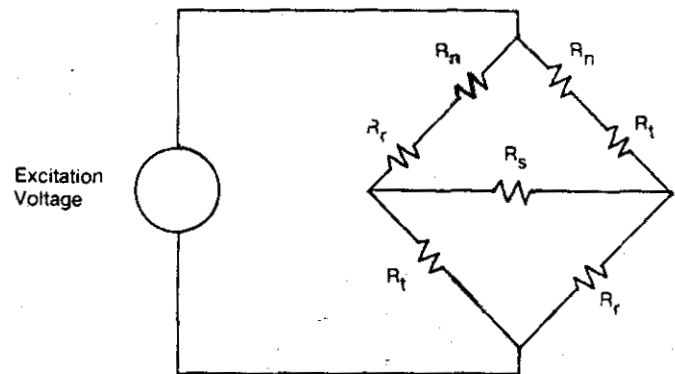


Figure 3

Schematic for thick film resistors placement.

When monitoring liquid dynamic pressure, it is essential that air bubbles not be trapped in the fluid line. Consequently, the final criterion is a package design which minimizes the chance of bubble entrapment.

FABRICATION TECHNIQUES

The fabrication of the pressure sensor does not yield four piezoresistors with identical values. The resultant is an initial null offset voltage. This offset is cancelled through the use of a laser-trimmed thick film network (TFN). The TFN is printed onto a ceramic substrate and connected to the sensor via gold wire bonds. Both the pressure sensor and the TFN use gold termination pads to eliminate problems with dissimilar metal interfaces.

The inherent sensitivity of the silicon sensor varies because of manufacturing tolerances on the diaphragm thickness and diameter. This variation in sensitivity also is overcome by a precision laser trimmed TFN. At this point, the transducers become completely interchangeable (See Figure 3).

Because of the need to monitor pressures precisely over a varied temperature, a thick-film thermistor network is used again, to optimize sensitivity compensation. The pressure sensor bonded to the tube and the thick film support circuitry are assembled into a main housing made of medical grade polycarbonate.

Ports are then assembled to the main housing and are sealed. Upon completion of the cover assembly, the transducer is sealed from environmental effects, including moisture. A vent hole is incorporated in the twelve-inch pigtail, allowing the necessary atmosphere reference to be extended to a remote location (See Figure 4).



Figure 4
Disposable blood pressure transducer.

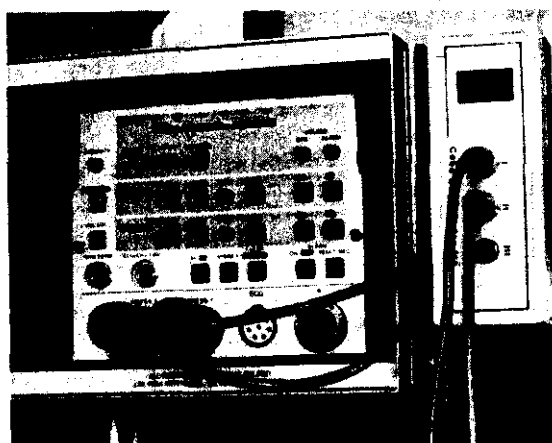


Figure 5
Illustration of electrical isolation system and monitor.

NEED FOR AN INTERFACE MODULE

To take advantage of low-cost, rugged semiconductor technology, an interface module was designed that makes the transducer compatible with existing monitors. The transducer's built-in electrical isolation is supplemented in the interface module (See Figure 5).

The interface module can be used with all popular brands of monitors. The module has up to three pressure channels and is powered by 115 volts AC or is available with battery option.

The module will accommodate up to three disposable transducers simultaneously. Each channel consists of five basic circuit blocks. These blocks are:

- Excitation voltage regulator
- Gain stage
- Isolation stage
- Scaling stage
- Output stage.

Power for all three channels is provided by a single $\pm 15V$ power supply in the module (See Figure 6).

The isolation stage provides 8 KV of isolation between the patient and the monitor, incorporating a Burr-Brown 3656 isolation amplifier. Leakage current is less than 5 microamperes. This stage also provides the power for the isolated gain stage and the transducer excitation. The transducer excitation voltage is precisely regulated to +10.00 V in the voltage regulator stage.

The output of the transducer is amplified to a usable level by the isolated gain stage. This stage also helps attenuate electromagnetic interference. The amplified signal is then fed into the isolation stage, which electrically isolates the patient from the monitor. The scaling stage multiplies this "pressure signal" by the excitation voltage of the patient monitor. This excitation voltage can be DC to 5 kHz, 1.5 to 15 Vrms.

The output stage produces a nominal 350 ohm impedance level and assures that the sensitivity of the Disposable Transducer system is 5 microV/V/mm Hg, both industry standard values.

CONCLUSION

By using the disposable transducer in preconnected packs, a great deal of convenience and patient safety can be realized. Dome attachment may be obsolete. Sterility concerns are virtually eliminated. Hospital personnel no longer must be concerned with broken or lost reusable transducers. Debubbling is quick and easy. With the universal interface module, the same transducer can follow the patient through different areas of the hospital. With the high accuracy and ruggedness of the transducer, calibration need not be performed.

Each hospital will have to perform a cost/benefit analysis to evaluate the potential of this new technology.

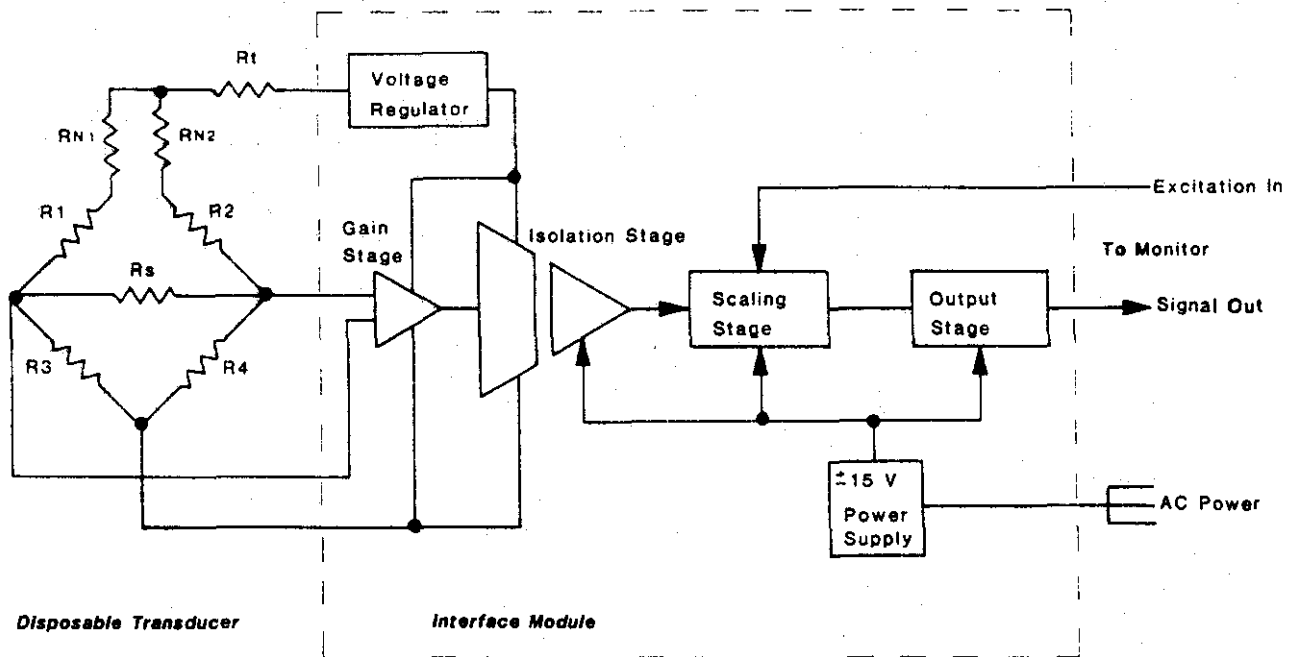


Figure 6
Block diagram of electrical isolation interface.

BIOGRAPHIES

EDWARD L. SPOTTS, B.S., M.S.

Ed Spotts is the manager of Monitoring Research and Development at Cobe Laboratories, Lakewood, Colorado. He received his B.S. in Mechanical Engineering at the University of Wyoming in 1969, and his M.S. in Engineering Management and Mechanical Engineering at the University of Alaska in 1974. He served in the U.S. Navy from 1969 to 1972. From 1974 until 1979 he held various positions at Storage Technology Corporation working on high performance computer storage systems.

THOMAS P. FRANK, B.S.

Thomas P. Frank was a New Product Development Engineer at Honeywell's MicroSwitch division from 1980 to 1982. At MicroSwitch, he was involved in the development and design of piezoresistive type pressure transducers for medical applications. A native of Neenah, WI, Thomas graduated in 1977 from Fox Valley Technical Institute, Appleton, WI, and in 1980 from the Biomedical Program at Milwaukee School of Engineering, Milwaukee, WI. Thomas is now Product Manager, Silicon Pressure Transducers for Ametek Controls Division, Feasterville, PA. Thomas is an active member of the Association for the Advancement of Medical Instrumentation and of the IEEE's Engineering in Medicine and Biology Society.

2nd ANNUAL NORTHEAST REGIONAL SYMPOSIUM ON TECHNOLOGY IN MEDICINE

November 10-12, 1982 - Windsor Locks, CT

The New England Society of Clinical Engineers will co-sponsor the *2nd Annual Northeast Regional Symposium on Technology in Medicine* to be held on November 10, 11 and 12, 1982, at the Bradley Ramada Inn, Bradley International Airport, in Windsor Locks, Connecticut. A multitude of major and minor sessions ranging from "Applications of Digital Imaging Techniques" to "Current Trends in Electrosurgery" will be presented. Numerous exhibitors and manufacturers' representatives will make presentations and display clinical and non-clinical electronic equipment.

SPONSORED BY:

The New England Society of Clinical Engineers; The Hartford Center For Clinical Engineering Education; The Medical Device Society; Iroquois Biomedical Society; and, as a cooperating society, The Northern New England Society of Biomedical Technology.

For registration and additional information:

New England Society of Clinical Engineers, c/o Robert Pisacane, Ph.D., Director of Clinical Engineering/Information Services, Providence Hospital, 1233 Main St., Holyoke, MA 01040; (413) 536-5111, ext. 2313.

Manual Determination

For manual blood pressure determination by the auscultatory method, a stethoscope is placed over the brachial artery in the standard position under the Dinamap blood pressure cuff. In addition, two front panel switches on the Dinamap must be operated. First, the MODE switch is changed from the AUTO to the CAL position. Then, the momentary contact SELECT FUNCTION switch is pushed to the MANUAL READ position and released. This procedure, ordinarily used as a calibration check, causes the pressure in the cuff plus a zero offset value to appear in the mean pressure display window. The CAL number is identified by the fact that three decimal points always appear along with it, an indication that the number is not to be read as a mean pressure. When in the calibrate mode, an internal solenoid in the Dinamap occludes one of the air ports connecting to the cuff. The cuff can now be inflated and deflated with the bulb, and pressure can be read on the aneroid manometer. The mean pressure display on the Dinamap will read a number equal to the zero offset plus the cuff pressure. This summation might be somewhat confusing, so the digital reading is best ignored. It is easy to remember to disregard this number, as the three decimal points are also displayed.

Results

The time limit of operation in the CAL mode for manual blood pressure determination is three minutes. After this time, the alarm will sound even if the ALARM switch has been turned OFF. If the alarm does sound, and it is desired to continue taking blood pressure measurements by the auscultatory method, turn the POWER switch OFF for 3 seconds, and then back ON. Then momentarily depress the SELECT FUNCTION switch to the MANUAL READ position, and the CAL number will appear again. The cuff is now back to the manual inflation/deflation control mode.

The additional connecting tubing and aneroid manometer increases the volume that the automatic instrument's pump must fill. In addition, these added components have compliance which could conceivably affect the instrument's performance. In practice, however, these additions are small in comparison to the basic blood pressure cuff and connecting tubing of the instrument. In clinical use of the Dinamap, we have seen no change in performance with this modification.

CONCLUSIONS

After the operator has learned to switch between automatic and manual modes, it becomes a simple matter to do this routinely. In the automatic mode, observing the cuff pressure on the analog meter

gives some assurance that the automatic instrument is functioning properly. Manual determination of blood pressure is useful under special conditions and as a teaching exercise. We have found that this analog/manual modification is helpful and convenient to use in the operating room. It would perhaps be easier if manual operation could be realized by simply shutting off power to the instrument; also providing for backup operation in case of power failure. The principle of this type of manual/analog adaptation may also be useful when applied to a variety of automatic non-invasive blood pressure monitors.

REFERENCES

- Apple, H.P., (1980), Automatic noninvasive blood pressure monitors: what is available. In: Gravenstein, J.S., Newbower, R.S., Ream, A.K., Smith, N.T. (Eds). *Essential Noninvasive Monitoring in Anesthesia*. Grune & Stratton, New York, pp 7-23.
- Ramsey, M., (1979), Noninvasive automatic determination of mean arterial pressure. *Med. Biol. Eng. Comput.* 17:11-18.
- Ramsey, M., (1980), Noninvasive blood pressure monitoring methods and validation. In: Gravenstein, J.S., et al, (Eds). *Essential Noninvasive Monitoring in Anesthesia*. Grune & Stratton, New York, pp 37-51.
- Yelderman, M., Ream, A.K., (1979), Indirect measurement of mean blood pressure in the anesthetized patient, *Anesthesiology* 50:253-256.

BIOGRAPHIES

ALVIN WALD

Alvin Wald holds a bachelor's degree in electrical engineering from The Cooper Union, a master's degree from Polytechnic Institute of Brooklyn, and the Ph.D. in biomedical engineering from New York University. He is also a certified clinical engineer. At present he is Technical Director of the Biomedical Engineering Service of the Department of Anesthesiology at Columbia University College of Physicians and Surgeons and the Presbyterian Hospital. He is active in local and national biomedical engineering groups, and is the representative of the Institute of Electrical and Electronics Engineers, Engineering in Medicine and Biology Society to the American National Standards Institute Medical Devices Standards Management Board and the Committee on Medical Electronics.

JOHN T. NEIDZWSKI

John T. Neidzowski is presently part of the technical team of the Department of Anesthesiology at Columbia Presbyterian Medical Center. He joined the Department of Anesthesia team at Columbia Presbyterian in September of 1979 after completing the Penn State BMET Internship at Miami Heart Institute, Miami Beach, FL. In 1977 he earned a Bachelor of Science degree in biology from King's College, Wilkes-Barre, PA, and in December of 1974, an Associate of Science Degree (cum laude) from Luzern County Community College, Nanticoke, PA.

Automatic Noninvasive Blood Pressure Monitors: Analog/Manual Adaptation Of Dinamap(TM)

Ref. (2)

ALVIN WALD, Ph.D., C.C.E.

JOHN T. NEIDZWSKI, B.S.

Department of Anesthesiology
Columbia-Presbyterian Medical Center
New York, NY

This paper describes some of the features and limitations of the newly-developed, automatic, noninvasive blood pressure monitors. In particular, an analog/manual modification is presented which can be adapted to a variety of such devices. The manual/automatic adaptation of the Critikon Dinamap(TM) blood pressure monitor is specifically described. This modification provides continuous observation of cuff pressure and permits the option of manual cuff inflation and deflation. The analog/manual adaptation is useful in special patient conditions and as a teaching aid.

Key Words: Blood Pressure Monitor, Automatic; Blood pressure, analog/manual; Critikon Dinamap(TM); Dinamap, Critikon.

INTRODUCTION

Microprocessor technology is now being used to operate and control a wide variety of instrumentation. In the medical field, a number of automated, noninvasive blood pressure monitors are presently available, and new models are being continually introduced. These instruments will periodically inflate and deflate the cuff and measure and display blood pressure, all completely automatically. The parameters which can be displayed include: systolic, diastolic, mean and pulse pressure, and heart rate. The automatic operation is a great convenience to busy physicians and nurses when caring for seriously ill patients.

Microprocessor control allows a wide choice of operating features in automatic blood pressure monitors. One approach is to limit external controls to as great an extent as possible. This choice makes the device relatively simple to operate, but the user has no control over the modes of operation. A different approach is to allow the user to program the unit so as to select various operating conditions. In clinical practice, this freedom of choice can sometimes be excessive and result in confusion to the inexperienced user. Most instruments are a combination of both machine and user programmability, the emphasis being on one or the other.

A more subtle disquietude arises from the microprocessor control of the instrument operation and digital display. Traditionally, an analog mercury or

aneroid manometer is used for noninvasive monitoring of blood pressure. The physician or nurse controls the cuff pressure and the inflation and deflation rates; arterial pulsations are heard with a stethoscope and seen on the sphygmomanometer. An automated blood pressure monitor presents the user with the proverbial "black box," over which he has limited control and practically no knowledge of what goes on within.

Perhaps the most critical decision of the instrument design philosophy is the method used to detect arterial blood pulsations. Different manufacturers use different techniques which result in various advantages and disadvantages. The Automated Screening Device, Inc., Sentry(R) and the Critikon, Inc., Dinamap(TM) use the oscillometric principle. This principle might not yet be fully recognized, but it has the advantage of not requiring a transducer under the cuff. Vita-Stat Medical Service, Inc., manufactures the Vita-Stat(R) and Abbott Medical Electronics Co. manufactures the Sphygie(R) automatic blood pressure monitors which employ the technique of electronic amplification of Korotkoff sounds. This technique is well accepted, but it is subject to external noise. The Roche Medical Electronics Arteriosonde(R) 1225 uses an active ultrasonic transducer, while the Sphygometrics Inc., Infrasonde(R) D4000 uses a passive piezoelectric transducer to detect arterial wall pulsations. Other manufacturers also use these techniques.

It is not a simple matter to compare and evaluate the different commercially available automatic blood pressure monitors. Patient conditions such as profound shock or cardiac arrhythmias may confound a completely automatic device. In any case, the user should be fully aware of the limitations of any automated instrument. Apple (1980) has shown some of the considerations necessary for evaluating the different methods of blood pressure determination. There is no single method which will always give true blood pressure; each technique is fraught with peril. Meticulous care and attention to detail is required when calibrating an instrument and recording blood pressure in any comparative study. What is generally considered to be the "true blood pressure" is that measured via an intra-arterial catheter connected to a pressure transducer. Even with this method, compliance of the arterial wall or of the catheter and transducer can distort the waveform. Ramsey (1980) describes some of the precautions which must be taken when validating blood pressure measurements.

DINAMAP(TM) 845: AUTOMATIC/MANUAL MODIFICATION

For over a year, we have been using the Critikon, Inc., Dinamap(TM) Model 845 to monitor pressure and heart rate during surgery. There are separate digital displays for mean, systolic and diastolic pressures, and for heart rate. The use of the Dinamap to determine mean arterial pressure has been previously described and evaluated (Ramsey, 1979; Yelderian, 1979). In general, we have been well served by this instrument, but as with any instrument, there are limitations.

It must be anticipated that special conditions might arise when the pre-programmed algorithm of the Dinamap, or any other automatic blood pressure monitor, does not obtain pressures satisfactorily. The manufacturer specifies that the Dinamap will not work properly on patients with atrial fibrillation, with heart rate below 40 or above 160 beats per minute, and with systolic pressure higher than 225 mmHg or mean pressure lower than 26 to 29 mmHg. Some patient conditions require rapid continual blood pressure determinations, which are not possible to obtain with the Dinamap. From 30 to 40 seconds are needed for a typical blood pressure determination with this instrument. If the need for manual blood pressure determination develops suddenly, it may not readily be possible to disconnect the cuff from the Dinamap and connect it to a manual bulb and aneroid manometer.

PROPOSED ADAPTATION OF AUTOMATIC BLOOD PRESSURE MONITORS

We have devised a system to help mitigate some of the limitations of automatic blood pressure monitors in general, and the Dinamap in particular. An analog/

manual adaptation has been implemented to provide some assurance to the user that the instrument is functioning properly, and to permit rapid manual auscultatory measurements of blood pressure when faced with unanticipated patient or instrument conditions. This system involves interconnection between the instrument and an aneroid manometer with blood pressure bulb. A diagram of the arrangement is shown in Figure 1.

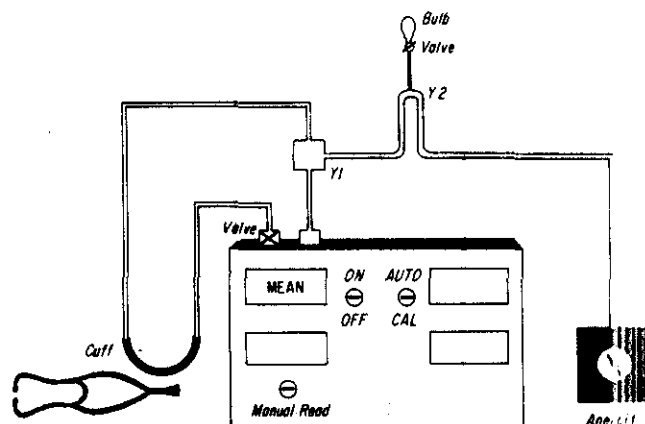


Figure 1
Schematic of analog/manual adaptation for automatic blood pressure monitor.

The Dinamap cuff differs from a standard cuff in having separate connectors for air inlet and outlet. In regular use, a dual-lumen air hose connects the cuff to two ports on the Dinamap. To implement the analog-manual modification, one of the hoses is disconnected from its port. A test-block T-piece (Y1), a standard Dinamap accessory, is connected to the port, to the cuff, and, with a short piece of rubber hose, to one leg of an ordinary stethoscope Y-piece (Y2). The parallel leg of the Y-piece is connected to an aneroid manometer, and the third leg to a blood pressure bulb.

In the automatic mode, all that is required is that the blood pressure bulb valve be closed for the instrument to operate normally. If the bulb valve is inadvertently left open, the cuff will not inflate and no cuff pressure will be displayed. In the automatic mode, cuff pressure can be read on the aneroid manometer, as well as on the automatic instrument. The Dinamap pressure deflates in steps which are clearly visible on the aneroid scale. Pressure oscillations can also be seen during the pulsatile arterial phase. These analog observations give the anesthesiologist some assurance that the automatic instrument is operating properly. If an air leak develops in the internal or external tubing, the stepwise deflation of the cuff is compromised, a condition which can easily be seen on the aneroid manometer.

Evaluation of blood-pressure transducers

Ref. (3)

This article summarizes the report of the evaluation of some pressure transducers, which was published in July 1982 in 'Health Equipment Information' 105.

The report, the second in a series covering a number of blood-pressure transducers, is an evaluation of three conventional transducers, two wrist-watch style transducers and three miniature transducers. *Catheter-tip devices are not included.* The evaluation was carried out by Dr R. H. Smallwood of the Department of Medical Physics and Clinical Engineering, Royal Hallamshire Hospital, Sheffield, UK. The report commences with an overall comparison of the transducers, which covers the type of dome, the method of cleaning, the method of excitation and comments on the durability of the transducers. This is followed by a table showing the specification of the transducers, as claimed by the manufacturers. The specifications have been converted to a common system of units to allow a direct comparison to be made. The next section gives an individual report on each transducer, headed by a photograph of the transducer on a grid scale, and followed by the manufacturer's comments. A table showing the results of the evaluation is followed by an appendix outlining the philosophy behind the standards which have been used, and giving details of the test methods. The appendix is reprinted, with minor alterations, from R. H. Smallwood (1978) The technical evaluation of blood pressure transducers. 'Engineering in Medicine', 7, 4, pp. 211-215.

The overall comparison of the transducers, together with the tables showing the claimed specification and the results of the evaluation, is reprinted here. The Editors are grateful to the DHSS for permission to use crown copyright material.

Introduction

The transducers reported here are:

Conventional transducers

*Bell & Howell	4-3271
*Elcomatic	EM 751 (and 751A)
*Statham	P23 ID

Wrist-watch transducers

AME (Akers)	AE 840
*Hewlett-Packard	1290A

Miniature transducers

Cambridge	Titran
Gaeltec	Luer Fitting Transducer
Statham	P50A.

Measurements of transducers marked with an asterisk are new to this report. Others are taken from the first evaluation report (STB 9/77), the transducers still being available. For the sake of completeness all the information needed to compare the transducers has been repeated in this report.

The basis for inclusion in the evaluation was that the transducer was of UK manufacture, or offered features of particular interest, or commanded a significant part of the UK market. One example of each transducer was assessed and the conclusions are based on the assumption that the units tested were representative of their type.

The transducers were subjected to laboratory assessment, the tests reflecting aspects of importance in clinical practice.

Standards

There is no British Standard nor is there an internationally recognized standard for the safety and performance requirements of blood-pressure transducers. It was, therefore, necessary to devise a specification, the details of which, together with the test methods used, are given in the Appendix to this report.

Units of blood-pressure measurement

Most people in the health professions will be familiar with 'mmHg' as the unit of measurement for blood pressure. However, manufacturers quote the specification for their trans-

ducers not only in the familiar mmHg but also in pascals (Pa) and millibars (mbar). In an attempt to standardize pressure measurement the pascal has now been accepted as the international unit of pressure measurement but the bar, with its smaller subdivision—the millibar—is also an acceptable international unit. It was decided for this report to express measurements of pressure in millibars; manufacturers' quoted pressure ranges have all been translated into this unit.

The relationship between the various units are:

$$1 \text{ mbar} = 0.1 \text{ kPa} = 0.75 \text{ mmHg.}$$

Thus

80 mbar	=	8 kPa	=	60 mmHg
120 mbar	=	12 kPa	=	90 mmHg
160 mbar	=	16 kPa	=	120 mmHg
200 mbar	=	20 kPa	=	150 mmHg
400 mbar	=	40 kPa	=	300 mmHg.

Overall comparison

There are various factors to be considered before deciding which transducer best suits your requirements. As with most things, there is no definite right or wrong transducer; the one you choose will depend on your own local circumstances and on the use you intend for it.

You should remember that transducers are available with a range of connectors to suit different monitoring systems. At the time of ordering you should state with which system you intend to use the transducer.

Below are some general points you should bear in mind.

Style of transducer

The transducers in this evaluation fall into three basic styles:

Conventional:	Bell & Howell	4-3271
	Elcomatic	EM 751 and 751A
	Statham	P23 ID
Wrist-watch:	AME (Akers)	AE 840
	Hewlett-Packard	1290A
Miniature:	Cambridge	Titran
	Gaeltec	Luer fitting transducer
	Statham	P50A.

One another. use can be if you need to use the the patient is now p lightweight transducer: they obvi freedom of ducers are less likely over pres tubing.

Reusable

With the ca a male Luc capability with integr using dispo infection in which may because the subjected to accidental d could reduce the transduc

Manufacturer supp

Country of origin
Cost of transducer

Type and cost of di

Supply voltage ac

Pressure range (mba)
Volume displacement

Zero pressure offset
Sensitivity (mV/ltra)
Non-linearity & hys

Zero drift (mbar/c)
Sensitivity drift (%/c)

Main leakage curre
(a) From circuit b

(b) From screen to

Maximum safe volta

Maximum safe press
Temperature range
Method of steriliz
Reusable domes

Notes

1. Disposable dom
2. Specification
3. Bridge operatio

One style does not have performance advantages over another, but the size and positioning of the transducer whilst in use can confer advantages in particular situations. For example, if you need to take frequent blood samples it is more convenient to use the conventional-bodied transducer which is mounted at the patient's bedside and is, therefore, very accessible. Recent technical advances have meant that auto-zeroing of a transducer is now possible; this has led to advantages for the smaller lightweight transducers in certain situations. The miniature transducers, for instance, are useful in long-term monitoring as they obviate the need for extension tubes and allow greater freedom of movement for the patient. The wrist-watch transducers are strapped directly on to the patient and are, therefore, less likely to be knocked and damaged, or suffer damage from over pressurizing the diaphragm by pinching the extension tubing.

Reusable or disposable domes

With the exception of the Gaeltec transducer, which is built into a male Luer connector, all the transducers evaluated had the capability of using either reusable domes, or disposable ones with integral diaphragms. The most important advantage of using disposable domes is that they reduce the risk of cross-infection in comparison with transducers with reusable domes, which may not always have been properly sterilized. Further, because the transducer does not need to be sterilized it is not subjected to so much handling and consequently not so liable to accidental damage. Theoretically, the use of disposable domes could reduce the total number of transducers required because the transducer bodies themselves are always kept on the wards.

However, as with all good things there are disadvantages, the major one being an apparent increase in revenue costs; disposable domes tend to cost about half the amount of reusable ones (see table 1).

Method of cleaning

The use of sterile disposable domes, which have integral diaphragms, gets round the tricky problem of properly sterilizing transducers between use. However, with the exception of the two wrist-watch style transducers for which the manufacturers supply only disposable domes, all the transducers in this evaluation may need to be sterilized: manufacturers recommend chemical sterilization, usually by ethylene oxide, though few hospitals have an approved facility for this type of sterilization. Other chemical procedures are merely methods of disinfection. One manufacturer, Elcomatic, at one time claimed their EM 751A could be autoclaved and, in fact, during the first evaluation it was subjected to 10 autoclave cycles with less than 1% change in calibration. However, the manufacturer found that hospitals were not sealing the electrical socket properly before autoclaving, allowing water vapour to get in and causing the transducer to fail. This is no longer a method of sterilization recommended by the manufacturer.

Method of excitation

Most of the transducers can be used with either an a.c. or d.c. excitation amplifier. The Gaeltec Luer fitting transducer is intended for a.c. excitation only and should be used with an a.c. amplifier if long-term stability is important. However, if d.c. excitation is required the manufacturer can supply an a.c./d.c.

Table 1. Claimed specifications taken from the manufacturers' literature.

	AME AE 840	Bell & Howell 4-3271	Cambridge Titan	EM 751 751A	Gaeltec Luer fitting transducer	Hewlett-Packard 1290A	Statham P23 1D	Statham P50A
Manufacturer/supplier	Simonsen & Weel Ltd	Bell & Howell Ltd	Gaeltec Ltd	Elcomatic Ltd	Gaeltec Ltd	Hewlett-Packard Ltd	Gould Ltd	Gould Ltd
Country of origin	Norway	USA	UK	UK	UK	USA	USA	USA
Cost of transducer	£308	£371.45	£280	£202 (751), £222 (751A)	£260	£475	£275	£299
Type and cost of domes	Disposable only, £2.45	Disposable £3.50 Reusable £5.35	Reusable only, £5.00	Disposable, £3.55 Reusable £9.20	None	Disposable only, £3.86	Disposable £3.50 Reusable £5.30	Disposable £5.50 £3.50 Reusable £3.50
Supply voltage a.c./d.c.	15V d.c. or a.c. max	7.5V d.c. (112V d.c. max)	5V d.c. or a.c. (10V max)	10V d.c. or a.c. max	2 to 6V a.c. r.m.s. (d.c. not specified)	3.5 to 5V r.m.s. at 2400 Hz ± 5%	7.5V d.c. or a.c. (10V max)	See note 3
Pressure range (mbar)	-27 to 400	0 to 530	-40 to 400	±400	-40 to 400	-40 to 530	-67 to 100	-67 to 400
Volume displacement (mm ³ /100 mbar)	0.022	Not specified	Not specified	<0.15	Not specified	0.15	0.03	Not specified
Zero pressure offset (mbar)	-max 8	12	40	53	Not specified	Not applicable	20	20
Sensitivity (mV/100 mbar/1)	1.50	0.375 ± 1%	>0.26	0.375 ± 1%	0.375	3.00 ± 2%	0.375	0.375
Non-linearity & hysteresis (mbar)	-max 2	2	4	0.22	4	% of reading + 1 mmHg (i.e. 3 at 200 mbar)	3	2
Zero drift (mbar/°C)	-max 0.2	0.17	0.26	0.13	0.26	Not specified	0.26	Not specified
Sensitivity drift (%/°C)	-max 0.15	Not specified	0.2	0.02	0.2	Not specified	0.02 ²	Not specified
Mains leakage current								
(a) From circuit to saline (µA)	1.5 at 250V, 50 Hz	<2 µA at 260V r.m.s., 50-60 Hz	Not specified	Not specified	Not specified	5 at 120V r.m.s., 60 Hz	<2 at 115V r.m.s., 60 Hz	5 at 220V, 50 Hz
(b) From screen to saline (µA)	Not applicable	Not specified	5	Not specified	Not specified	Not applicable	Not specified	Not specified
Maximum safe voltage	750V d.c.	2.5 kV a.c. rms	2 kV d.c.	2 kV d.c.	1 kV d.c.	10 kV defibrillator pulse	10 kV d.c.	10 kV d.c.
Maximum safe pressure (mbar)	6000	-930 to 5300	6700	6700	6700	8000	6700	13 300
Temperature range (°C)	-20 to 100	18 to 38	15 to 40	10 to 40	15 to 40	10 to 40	-55 to 80	Not specified
Method of sterilization of reusable domes	Not applicable	Chemical, ethylene oxide	Chemical, not specified	Chemical, ethylene oxide	Chemical, not specified	Not applicable ¹	Chemical, ethylene oxide	Chemical, ethylene oxide

Notes

1. Disposable domes only, but manufacturer states that transducer body may be sterilized with ethylene oxide.
2. Specification unclear - sensitivity drift quoted as 0.045 mmHg/°F.
3. Bridge-operating voltage is 0.75V d.c. or a.c. rms. Operating voltage of transducer is determined by resistors in the user-specified connector.

Table 2. Some of the results of the technical evaluation.

	AME AE 840	Bell & Howell 4-3271	Cambridge Titan	EM 751 751A	Gaeltec Luer fitting	Hewlett-Packard 1290A	Statham P23 ID	Statham P50A
Excitation voltage (V)	5.0 d.c.	7.5 d.c.	5.0 d.c.	5.0 d.c.	5.0 d.c.	3.5V a.c. rms at 2400 Hz ¹⁴	5.0 d.c.	5.0 d.c.
Zero pressure offset (mbar)	14.3	16.5 ⁴	48.3	7.2	15.7	Not applicable	7.3	16.0
Change in offset with dome tightening (mbar)	Not applicable	3.2	0.3	0.25	Not applicable no dome	Not applicable bayonet connection ¹⁵	2.51 ⁷	1.5
Sensitivity (mV/100 mbar V)	1.49	0.379	0.325	0.375	0.245 ¹²	3.04	0.376	0.381
Non-linearity hysteresis (mbar)	2.6	0.2	0.55	0.12	1.43	2	0.18	0.5
Zero drift (mbar, C)	0.1	0.02 ⁵	0.04	0.16	0.13	0.4	0.29	0.13
Sensitivity drift (%/C)	0.27	0.01	0.02	0.01	0.06	<0.02	0.06	<0.001
Maximum rated pressure test	Pass ¹	Pass	Pass	Pass ⁸	Pass	Pass	Pass	Pass
Mains leakage current								
(a) From circuit to saline (µA)	1.0	1.7	0.6	2.5 ⁹	1.5	1.7	0.8	0.6
(b) From screen to saline (µA)	Not applicable	0.4	0.7	2.5	1.6	Not applicable	0.4	Not measured
Maximum rated voltage test	Fail ²	Pass ⁶	Pass ⁷	Pass ¹⁰	Fail ¹³	Pass ¹⁶	Pass	Pass
Drop test	Pass	Pass	Pass	Fail ¹¹	Pass	Pass	Pass	Fail ¹¹
Cable test	Pass ³	Pass	Pass ³	Pass	Pass ³	Pass	Pass	Pass ³

Notes

1. Tested at 2000 mbar—manufacturer now rates it at 6000 mbar.
2. Rated maximum voltage only 750V so test to 2 kV not performed.
3. 5 kg steady pull.
4. Zero pressure offset is a non-linear function of supply voltage—only within manufacturer's specification at or close to 7.5V d.c.
5. First sample had excessive drift and was replaced by manufacturer.
6. 3.5 kV d.c. applied.
7. Offset increased to 112 mbar.
8. Tested at 5300 mbar—manufacturer now rates it at 6700 mbar.
9. Results for EM 751 only; EM 751A sample failed due to faulty assembly.
10. EM 751 tested at 2 kV d.c.
11. Following drop test mains leakage current was approximately 100 µA but manufacturer has now improved construction.
12. Sample tested did not have standardized output.
13. Withstood only 1 kV d.c. for 15s.
14. Also tested at 3.5V d.c. rms 5000 Hz—result not significantly different.
15. Up to 23 mbar change with pressure on dome or Luer connectors.
16. 10 kV d.c. applied.
17. Change of 51 mbar with disposable dome—probably due to excess fluid between dome and transducer diaphragm—not present with reusable dome.
18. Following drop test, calibration unchanged up to 330 mbar. 10% reduction in output at 400 mbar.

interface at no extra charge. Hewlett-Packard specify their 1290A should be used with an a.c. amplifier only, and, more specifically, only with their monitors that have an excitation frequency of 2400 Hz. We tested our sample at a frequency of 5000 Hz and found the performance was still within the manufacturer's specification. We therefore believe that the Hewlett-Packard 1290A has a more general application than the manufacturer claims. The Bell & Howell 4-3271 is specified for use with a d.c. amplifier only.

Durability

Some of the factors which impinge on the life of the transducer have already been discussed, for instance the style of the transducer, the necessity of sterilization, but there are other factors to be taken into consideration.

The major abuses transducers are subjected to are excessive pressure to the diaphragm, being dropped on the floor, or the application of tension to the cable. On this latter point, the stiffness of the cable and its strength must be carefully balanced. If the cable is too stiff, the likelihood of damage to the transducer from a 'whiplash' effect will be increased. This is particularly important with the small, lightweight miniature and wrist-watch transducers. Nevertheless, the cable must be strong enough to withstand strain and flexing. Gaeltec have told us that they have improved the flexibility of the cable on their Luer fitting transducer which used to be fairly stiff. Transducers with detachable cables (Bell & Howell and EM 751A) have the advantage that the cable can be more flexible, and perhaps less durable, as it is an easy matter to attach a new cable.

One of the commonest ways of over-pressurizing a transducer is to flush it through with a small volume syringe. It is easy to apply a high pressure to the transducer—2.5

kilogram-force (kgf) applied to a 1 ml disposable syringe will give a pressure of 14.6 bar (11 000 mmHg), which is above the rated overload pressure of any transducers tested. In contrast, the same force applied to a 20 ml disposable syringe gives a pressure of 800 mbar (600 mmHg). The recommended layout for flushing transducer and catheter is shown in figure 1. It will be seen that the transducer and catheter can be flushed separately, and a very high pressure can be applied to flush narrow-bore catheters without damaging the transducer. The smaller transducers do not have a dome with two arms. The dome should be filled without the transducer connected, and the transducer should then be attached without any force being applied to the syringe. Other causes of over-pressurization are stepping on, or wheeling trolleys over, the catheter, and using motor-driven infusion systems without a safety cut-out. The remedies are obvious! All the transducers evaluated, with the exception of the AME AE 840, were able to withstand the 5000 mbar pressure test: the AE 840 had a maximum pressure rating of 2000 mbar, which it passed, but the manufacturer now assures us that it can withstand a maximum pressure of 6000 mbar.

An easy way to damage a delicate transducer is to store it unprotected—in a drawer or on a shelf for example. The manufacturer always supplies the transducer in a rigid, often plastic, box. These should be retained and when the transducer is not in use, it should be stored in the original box.

Recommendations

(All prices quoted are those current at the end of April 1982.)

Looking at the four conventional transducers

Bell & Howell	4-3271 (£371.45)
Elcomatic	EM 751 (£202) and EM 751A (£222)
Statham	P23 ID (£275)

Flush tr

Catheter —

Measure

Catheter —

Flush ca

Catheter —

Figure 1 transduce is used to at least 2 between the trans and will flush low position: air bubble should be injected

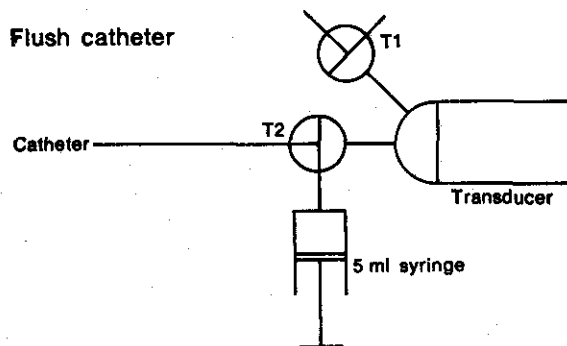
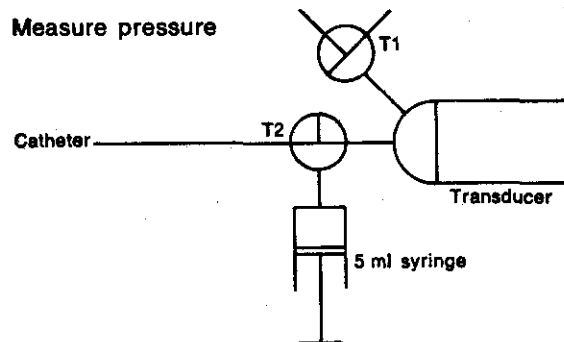
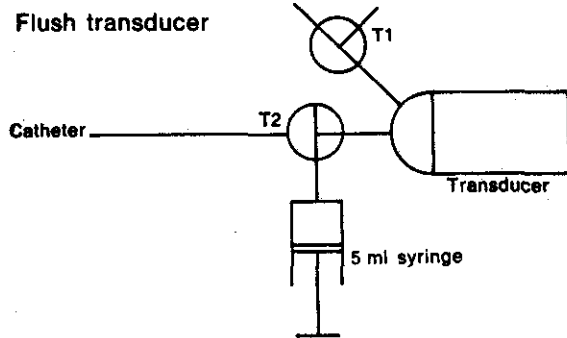


Figure 1. The recommended procedure for flushing the transducer and catheter, T1 and T2 are three-way taps. T1 is used to vent the transducer to atmosphere, and a syringe of at least 5 ml capacity is attached to T2, which is placed between the transducer and the catheter. With this layout, the transducer is isolated when the catheter is being flushed, and will not be subjected to the high pressures necessary to flush long, small-bore catheters. The transducer should be positioned with T1 uppermost, to facilitate the removal of air bubbles from the dome, and the plunger of the syringe should be above the nozzle, so that air bubbles are not injected into the system.

The zero pressure output of the Statham varied with excitation voltage and perhaps more disconcertingly with transducer orientation. Further, its thermal drift was such that we suggest this transducer is suitable for arterial pressure measurement only. Though the Bell & Howell is considerably more expensive than the two Elcomatics, the thermal drift of the replacement 4-3271 indicates that this is a good general-purpose transducer suitable for either arterial or venous pressure measurement, whereas the Elcomatics are best considered for arterial use only. One doubt with the Bell & Howell transducer is that the zero pressure output is not accurate with all transducer amplifiers, only those with an excitation frequency at or near the manufacturer's rated supply voltage of 7.5 V d.c. For those who use reusable domes, it is worth noting that both the 4-3271 and the EM 751A have the advantage of a detachable cable allowing the transducer to be completely immersed during sterilization.

Copies of *Health Equipment Information* are free to NHS staff (through the Administrator); otherwise they can be bought: (£3.00 each) from the DHSS Leaflets Unit, PO Box 21, Stanmore, Middlesex HA7 1A7, UK.

Seminar announcement

Biomaterials in Artificial Organs

This is the fifth in the series of Strathclyde Bioengineering Seminars and will be held on 12 and 13 September 1983; it is being organized by the Strathclyde Bioengineering Unit in association with the International Society for Artificial Organs. Four sessions are planned: blood purification procedures (to be chaired by Professor P. C. Farrel, Australia); metabolic assist (with Professor R. E. Sparks, USA, in the chair); interaction of biomaterials with tissue and blood (chairman Dr R. M. Lindsay, Canada); and a fourth consisting of workshops on the three plenary sessions.

The proceedings of the seminar are to be published by the Macmillan Press Ltd (at c. £26.00) and abstracts of the papers presented will appear, for the meeting, in *Artificial Organs*. The registration fee, which covers the set of abstracts, tea, coffee and a reception is £90.00.

Details from Dr J. D. S. Gaylor, University of Strathclyde, Bioengineering Unit, Wolfson Centre, 106 Rottenrow, Glasgow G4 0NW, UK.

A lo que se refiere

Sweep-Frequency Marker Generator For Blood Pressure Transducer Testing

ARNOLD ST. J. LEE, P.E.
Principal Consultant
Information Transfer Corporation
2008 Cotner Avenue
Los Angeles, California

Ref. (4)

A circuit which places accurate frequency calibrations on swept-frequency recordings is presented. This circuit is useful in the calibration of direct blood pressure transducers and will have applications in the testing of other biological transducers as well. The design range of 1 Hz to $128\sqrt{2}$ Hz is suitable for testing a broad range of biological transducers and systems. The circuit basically measures the periods between successive zero crossings. Pulses are generated that may be recorded on a swept-frequency strip chart record of an individual transducer. A series of sixteen marker pulses indicates 1 Hz, $\sqrt{2}$ Hz, 2 Hz, $2\sqrt{2}$ Hz, up to $128\sqrt{2}$ Hz. A special wide pulse at 16 Hz distinguishes the marker pulses.

Index Under: Blood Pressure Transducer Testing; Pressure Transducer Testing; Transducer Testing; Transducer Frequency Response; Sweep-Frequency Marker; Testing, Blood Pressure Transducers.

INTRODUCTION

A common method of testing direct blood pressure transducer systems (in addition to observing their response to a square wave of pressure) is to record the system output with a swept-frequency, constant-amplitude sine wave of pressure input. At the low frequencies of interest (1-180 Hz), it is inconvenient to employ resonance phenomena to generate frequency markers. Accurate measurement of the frequency on a swept-frequency strip chart record is difficult, if not impossible. While mechanical methods have been used to synchronize a strip chart to a swept-frequency oscillator, such methods are cumbersome. The circuit presented here enables convenient calibration of blood pressure system swept-frequency tests and will have other applications with a broad range of biological transducers.

APPLICATION

Figure 1 shows a typical application of the sweep-frequency marker generator in blood pressure transducer testing. Figure 1 (top) shows a "brand X"

transducer at the end of an arterial line with an air bubble present. A resonance is present along with attenuation of high frequencies. A simultaneous test of a Millar catheter tip transducer is shown below the "brand X" recording for reference purposes.

The output of the sweep-frequency marker circuit is shown in the middle of the record. The initial stroke of the wide pulse marks 16 Hz. The other marker pulses are at 1 Hz, $\sqrt{2}$ Hz, 2 Hz, $2\sqrt{2}$ Hz, 4 Hz, $4\sqrt{2}$ Hz, and so on, up to a last frequency mark of $90.5 (64\sqrt{2})$ Hz. The sweep-frequency marks may be conveniently used to determine transducer frequency characteristics.

DESCRIPTION OF CIRCUIT

The circuit shown in Figure 2 measures the period between successive zero crossings of a swept-frequency voltage, and outputs a pulse to a recorder event-marker each time the period becomes shorter than $\frac{1}{f_m}$ seconds for the required f_m , mark frequency, of each mark. Because logarithmic sweeps are often used, marks at equal log spacing were chosen. It seemed adequate to have one mark between each octave (double the frequency) marker. The circuit responds to a swept fre-

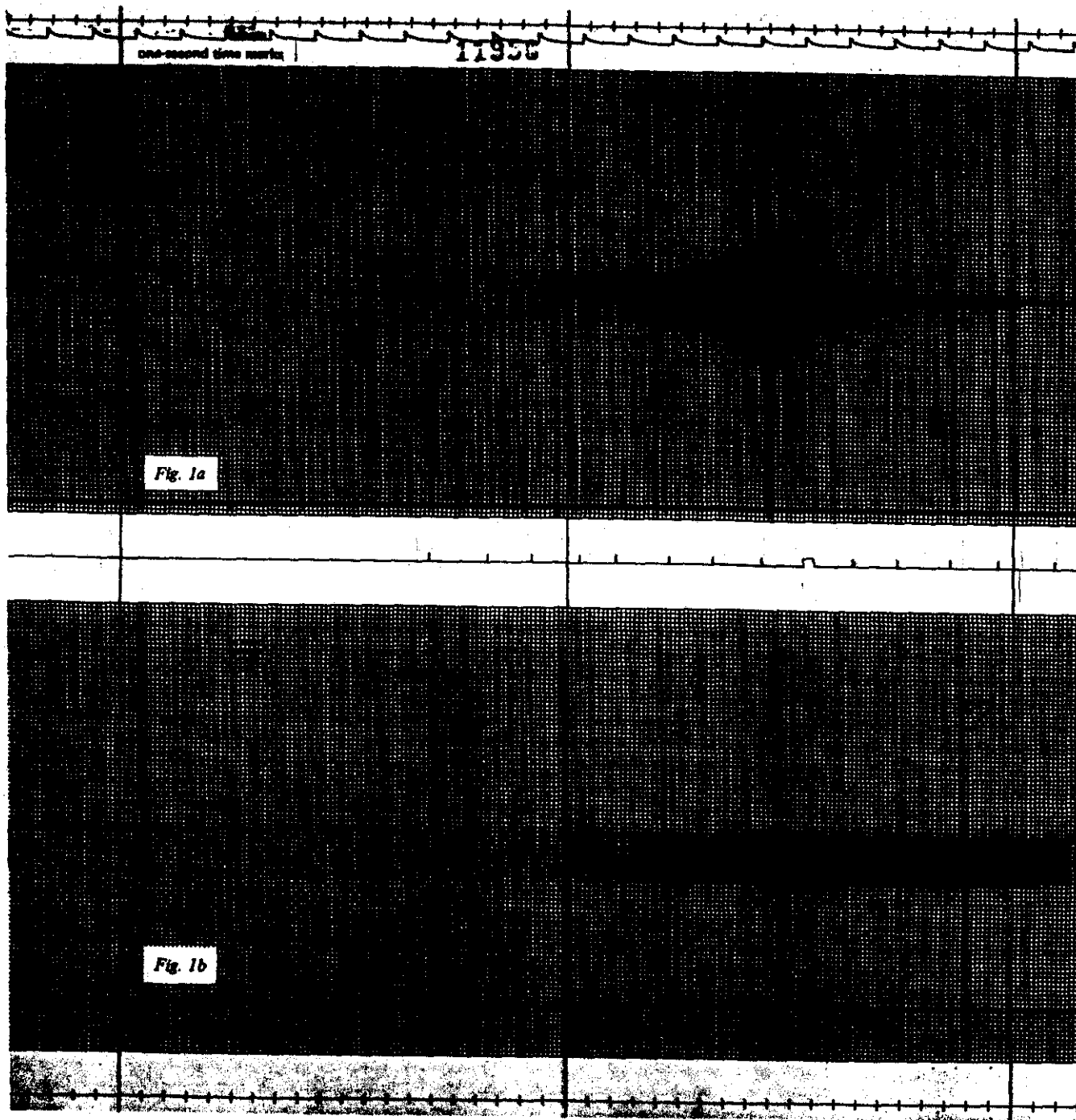


Figure 1

Typical Use of Swept-Frequency Marker Generator in Testing Blood Pressure Transducers
 Sweep-frequency markers are shown here between two recordings. The "Brand X" transducer (top) at the end of an arterial line with an air bubble shows resonant response and attenuated high frequency response. The Millar Catheter Tip Transducer (bottom) is shown for reference. In these calibrations, 20 vertical lines equal 10 torr. The last frequency mark is at 90.5 (64J 2) Hz.

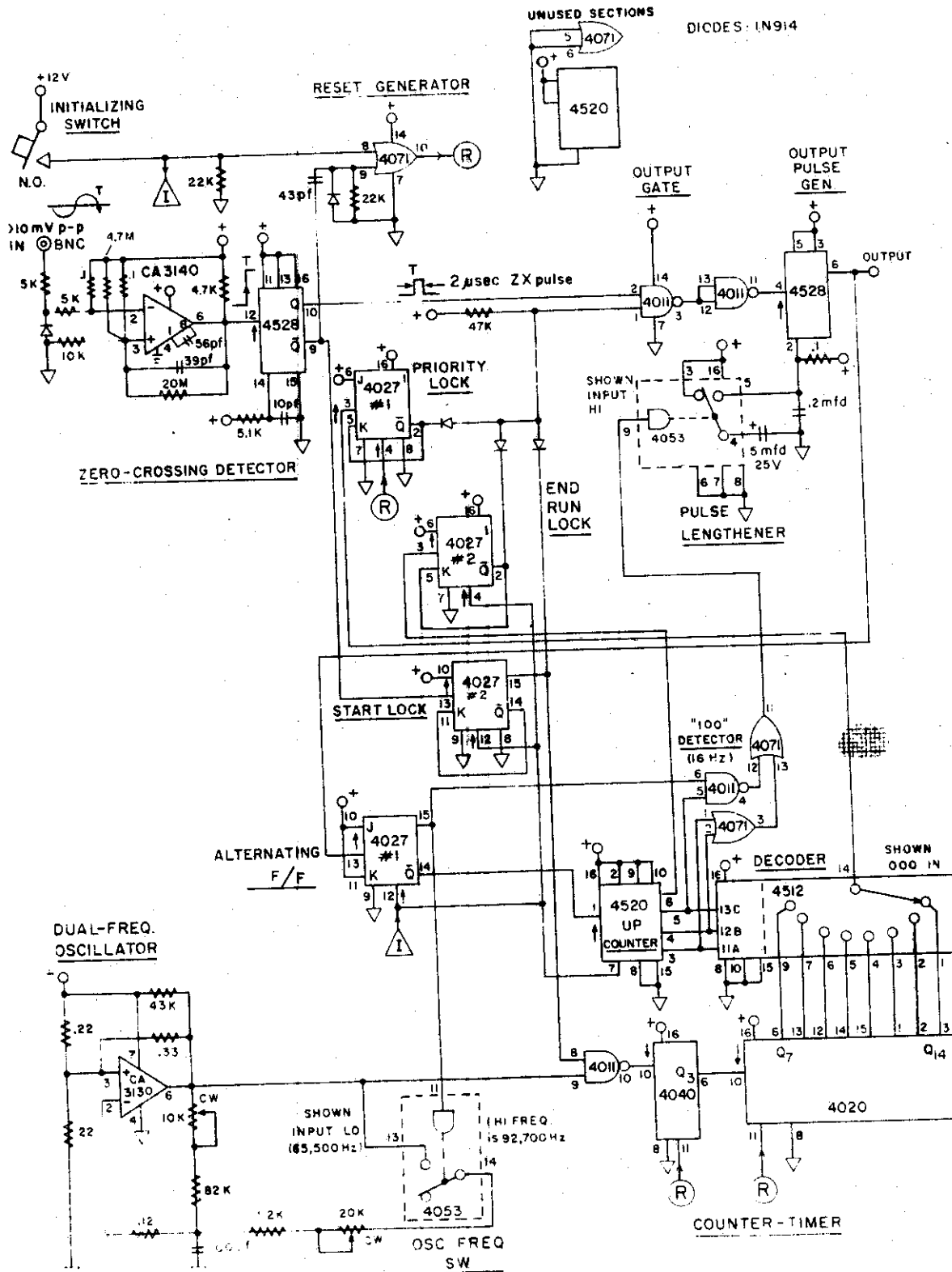


Figure 2
Sweep-Frequency Marker Generator Schematic

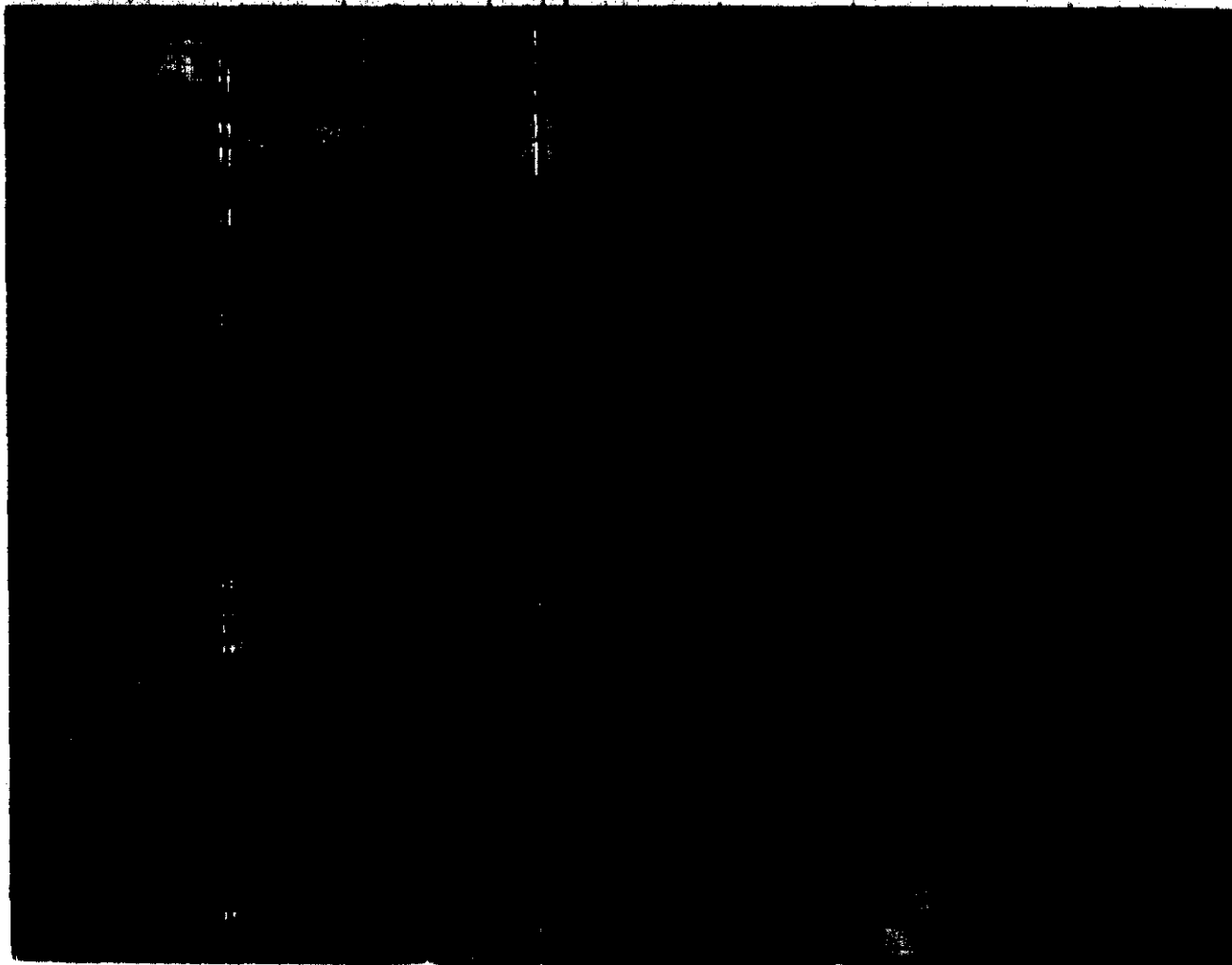


Figure 3
Breadboard of Sweep-Frequency Marker Generator

quency starting below 1 Hz by outputting a series of 16 pulses at 1 Hz, at $\sqrt{2}$ Hz, 2, $2\sqrt{2}$, 4, $4\sqrt{2}$, etc., up to $128\sqrt{2}$ Hz. The problem of "marking the marker" (indicating the frequency of the marker) was solved by making the 16 Hz pulse substantially longer in duration than the usual 20 msec. Even though a given test sequence might not include the whole range, it would always be practicable to include 16 Hz. If the circuit is initialized with the sweep frequency greater than 1 Hz, a mark would be generated at each zero crossing until the circuit "catches up" with the frequency generator, after which it operates normally.

The input signal (which must be greater than 10 mV peak) is applied to a zero crossing detector which outputs 2 μ sec "zero-crossing" pulses (ZX pulses) from both Q and \bar{Q} at every negative-going crossing. The 2 μ sec ZX pulse proceeds through the output gate (if it can), and triggers the output pulse generator, whose duration is controlled by the pulse lengthener switch to be either 20 or 520 msec.

The output gate may prevent the ZX pulse from reaching the output pulse generator by three different mechanisms:

- 1) the start lock is in reset position (unlocked, Q low);
- 2) the priority lock is locked (\bar{Q} low); or
- 3) the end-run lock is locked (\bar{Q} low).

The initializing switch directly resets the start lock and the end-run lock, and indirectly (through the reset generator) resets the priority lock. Thus, immediately after initializing, the ZX pulse is blocked by start lock low. However, the first ZX Q pulse, on returning high, flips the start lock into the locked state.

The next ZX pulse can thus go through the output gate, provided that the priority lock is not flipped first. The priority lock is clocked from the decoded output of a selectable-modulus counter-timer, which counts clock pulses from the dual-frequency oscillator (either 65,540 Hz or 92,670 Hz). In the initialized state, the

priority lock will be flipped on the (8192 x 8)th clock, or 1.000 second. If the *priority lock* is flipped before the next negative-going zero crossing (this means that the input signal frequency is still lower than 1 Hz), the ZX pulse will be blocked by the *output gate*. However, at the end of each ZX pulse the *priority lock* is reset, repeating the process until a negative-going zero crossing occurs before one second has passed.

When this happens, the *output pulse generator* output flips the *alternating F/F* so that the clock pulses being counted now are at the higher frequency ($\times\sqrt{2}$, or 92,670 Hz). Now the *priority lock* is locked (*output gate* disabled) at $\frac{1}{\sqrt{2}}$ seconds, and no output pulse is generated until the input signal frequency is greater than $\sqrt{2}$ Hz. When this occurs, the output pulse again flips the *alternating F/F*, whose \bar{Q} output goes high, triggering the 4520 UP counter, which, along with reverting the clock to 65,540 Hz, changes the address of the *decoder* from 000 to 001. This now flips the *priority lock* on the (4096 x 8)th clock pulse (0.5 seconds; 2 Hz). The sequence is repeated until the *decoder* address reaches 100 (recognizing 16 Hz), when the "100" detector output to the pulse lengthener adds an additional 5 μ fd to the *output pulse generator* timing circuit, causing the output pulse length to change from approximately 20 to approximately 520 msec. The *end-run lock* is locked (flipped) when the 4520 UP counter reaches 1000, putting an end to the circuit operation. Figure 3 shows the constructed and operational breadboard of this circuit. Table I lists the circuit components.

TABLE I
CIRCUIT COMPONENTS

12 volt power supply	1
Toggle switch DPDT, momentary	1
CA 3130 OP AMP	1
CA 3140 OP AMP	1
4011 QUAD NAND GATE	1
4027 J-K F/F	2
4040 12-Stage Counter	1
4053 Analog Electronic Switch	1
4071 QUAD OR GATE	1
4512 8-Channel Data Selector	1
4520 Dual 4-Stage UP Counter	1
4528 Dual Monostable Multivibrator	1
Resistors ($\frac{1}{4}$ W):	
22K	2
5.1K	2
10K	1
.1M	3
4.7M	1
4.7	1
20M	1

47K	1
112K	1
12M	1
82K	1
.22M	2
4.3K	1
.33M	1

Capacitors:

100 pf	1
43 pf	1
39 pf	1
56 pf	1
10 pf	1
.2 μ fd 50V	1
5 μ fd 25V	1

Diodes:

IN914, or similar	5
-------------------	---

Trim pots:

100K	1
20K	1
10K	1

CONCLUSIONS

A useful circuit has been designed that produces calibration marker pulses during swept-frequency testing of transducers. The output of this circuit may be recorded on a strip chart event marker. This circuit is useful in testing a broad range of physiological transducers where swept-frequency testing is used.

ARNOLD ST. J. LEE, B.A., P.E.

Arnold St. J. Lee attended Temple University (Science), Lehigh University (M.E.) and University of Pennsylvania (E.E. and Physics), while working at the Temple University Medical School, initially as a laboratory technician, and finally as physicist to the Physiology Department. He then worked as E.E., M.E., physicist and Project Engineer at Electronic Associates, Inc., Boeing Airplane Co. and Birkkan Corp. (now Litton's Pot. Div.). He started and did most of the engineering at Invengineering, Inc., an independent product R&D laboratory. As Assistant Professor of Anesthesiology, he directed the Milstein Laboratory of Medical Instrumentation at Columbia University. He spent two years at Varian Associates as Senior Scientist and is now Principal Consultant for Information Transfer Corporation, while also a member of UCLA's Anesthesiology Department with the title of Associate Clinical Professor of Anesthesiology.

Assessment of Hitachi HME-20 pulse and blood-pressure monitor

Robin J. Northcote, Joseph O'Donoghue and David Ballantyne

The Victoria Infirmary, Glasgow G42 9TY, UK

The performance of the Hitachi HME-20 pulse and blood-pressure (BP) monitor in comparison with direct intra-arterial BP recording and electrocardiographic monitoring is described. Highly significant ($p < 0.001$) correlations were found between intra-arterial systolic and diastolic pressures and pressures recorded by the Hitachi monitor. Similarly, the electrocardiographically computed heart-rate, and that given by the Hitachi monitor were significantly correlated ($p < 0.001$). Systolic blood-pressure was underestimated by a mean of -12 mmHg and tended to become more erroneous when intra-arterial pressure was >150 mmHg. These results are comparable to more expensive pulse and blood pressure monitors. We conclude that the instrument can reproduce a satisfactory estimate of heart-rate and blood-pressure and may be of particular use when a change of blood-pressure is of prime importance, rather than an absolute measurement.

KEY WORDS: BLOOD PRESSURE, HITACHI HME-20 MONITOR.

Introduction

In recent years, increasing reliance has been placed on automated or semi-automated devices to measure blood-pressure (BP) indirectly. These measurements are believed to be free of observer error, and thus provide a more reliable estimate of BP when compared to the traditional mercury column sphygmomanometer. Reports on the conventional sphygmomanometer show that as many as half of those used in hospital are inaccurate [1] and that hospitals usually have no policy for maintaining sphygmomanometers. For these reasons a number of new techniques for measurement of BP have been developed [2 and 3]. In addition, by providing a device permitting self-recording of blood-pressure, BP can be measured by the patient at home, thereby minimizing error induced by the anxiety of a hospital visit. These BP recordings may be more representative [4 and 5]. Serial measurement of BP in this way also allows for the assessment of new antihypertensive or vasoactive agents outside a hospital.

Despite their widespread use, however, the performance characteristics of such devices are often poorly documented. It is important, if these machines are to be used in screening programmes or in population studies, to determine the accuracy and variability of the recordings obtained. A number of automatic instruments have been developed. Some have depended on the application of ultrasound reflectance for the detection of arterial blood flow. Others depend on detection of Korotkoff sounds. Some of these devices have the facility of automatic control of over inflation and deflation [6 and 7].

The Hitachi HME-20 blood-pressure and pulse monitor is one of the more recently introduced devices based on Korotkoff sound detection. This is a low-cost device which has been used for research purposes, in intensive-care units and in rural general practice. We are not aware of any critical assessment of the device in the medical literature.

Materials and methods

The Hitachi HME-20 pulse and blood-pressure monitor is a fully automatic unit which can operate from mains or battery. An electronic microphone, shielded from extraneous noise in the pressure cuff, is employed to detect Korotkoff sounds. Phase V of the Korotkoff sounds is taken as the diastolic end-point. Automatic inflation and deflation is performed and results are displayed on a fluorescent digital display. The measuring range is from 0-300 mm Hg and 30-200 beats per minute. In operation, the cuff is positioned so that the microphone overlies the maximal pulsation of the brachial artery. If an inadequate signal is detected, the instrument fails to produce a result and indicates an error on the display screen, thus minimizing possible error when used by an unskilled individual.

Supine blood-pressure was recorded from the left arm and the results compared with simultaneously recorded intra-arterial measurements. The procedure was performed towards the end of left heart catheterization for coronary arteriography in eight subjects; all of whom consented to the study. In each case the catheter tip was positioned in the arch of the aorta to approximate to the innominate artery. Thereafter, 10 successive simultaneous measurements of blood-pressure were recorded. Catheter patency was maintained between readings by continuous flushing with a normal saline and heparin mixture. Intra-arterial pressure was charted continuously and calculated as a mean of 15 complexes immediately prior to cuff inflation and heart-rate was calculated from a simultaneous electrocardiogram, using the mean of five R-R intervals preceding cuff inflation.

Intra-arterial BP was measured using a Bentley Trantec Physiological Pressure Transducer (Model 800) and a Siemens electromanometer with a Mingograph 81 six-channel recorder, calibration being carried out prior to each procedure with a mercury manometer. Direct calibration of the system was carried out before each recording against a mercury column, 100 mmHg being equivalent to a 5 cm deflection on the recording paper. 150 cm long manometer connecting lines were used, manufactured by Portex. Zero reference level was taken as mid-thorax in the supine position. Although this technique has been accepted by others to provide an

adequate statistical system may be applied to the recommended intra-arterial of the cuff rea

Statistical analysis

Comparisons were made using Armitage's test and regression between measurements in recordings.

Results

In general, the pressure, both of diastolic ($p < 0.001$) systolic and diastolic heart-rate (estimated by an underestimate) a systolic pressure the device underestimates the difference between the two methods each parameter in the table between-measurements (3 and 4), only mmHg of the readings are in the region of 10% also fell within \pm the electrocardiogram not significant when compared (0.1). However, variability of

Table 1. Hitachi HME-20 using Student's

Systolic
Intra-arterial
Cuff
Diastolic
Intra-arterial
Cuff
EKG
Heart-rate

adequate standard [3], the authors appreciate that such a system may have a tendency to over-estimate true arterial systolic blood-pressure. The blood-pressure cuff was applied to the left arm, and American Heart Association recommendations for the cuff size were fulfilled [9]. Intra-arterial pressures were read by one of us, unaware of the cuff readings.

Statistical analysis

Comparisons between direct and indirect readings were made using Student's paired t-test (two tailed) and Armitage's test for trend [10]. Correlation coefficients and regression lines were calculated, together with a between-method frequency histogram for the difference in recordings.

Results

In general, the device underestimated systolic blood-pressure, but reproduced an accurate assessment of diastolic pressure. There was a highly significant ($p < 0.001$) correlation with direct readings for both systolic and diastolic recordings (see figure 1) and also for heart-rate (figure 2). Systolic pressure was underestimated by a mean of -12 mmHg ($p < 0.001$). Gross underestimation of systolic pressure tended to occur with a systolic pressure over 180 mmHg, where in two patients the device underestimated by more than 30 mmHg on a number of occasions. Table 1 shows that no significant difference could be demonstrated between the mean values for diastolic BP, or the mean heart-rate between the two methods. The mean and standard deviation of each parameter and results of paired t-tests is also shown in the table. For each comparison, a histogram of between-method difference has been constructed (figures 3 and 4), only 31% of systolic recordings fell within ± 10 mmHg of the intra-arterial readings, although 62% of the readings are within 10 mmHg of the line of identity in the region of 100–150 mmHg. 80% of diastolic recordings also fell in this range. 63.9% of heart-rate measurements fell within ± 5 beats per minute of those calculated from the electrocardiogram. Variability of measurements was not significantly different for systolic blood-pressure when comparing IA against the Hitachi monitor ($p > 0.1$). However, there was a significant difference in variability for diastolic pressure ($0.02 > p > 0.01$).

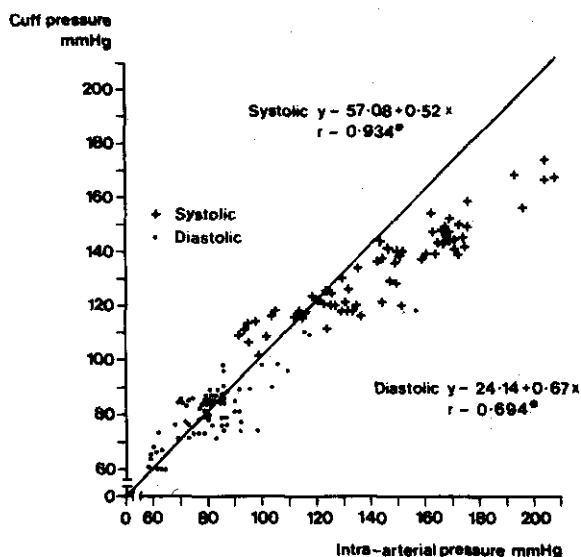


Figure 1. Scatter plot of intra-arterial blood-pressure versus cuff-recorded pressures. Line shown is line of identity. ($*p < 0.001$.)

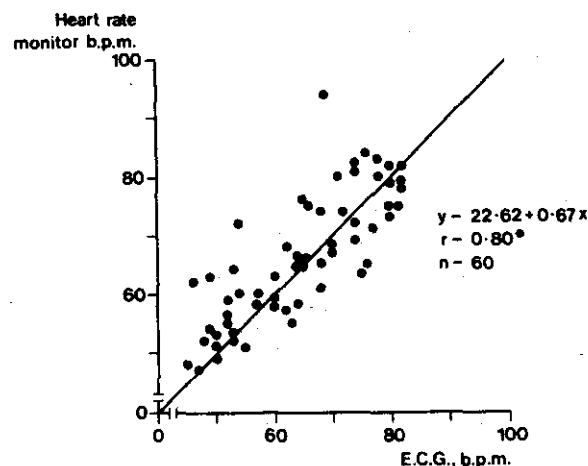


Figure 2. Scatter plot of heart-rate obtained from electrocardiogram and simultaneously recorded by Hitachi HME-20. ($*p < 0.001$; b.p.m. = beats per minute; ECG = electrocardiogram.)

Table 1. Hitachi HME-20 (cuff) recorded blood-pressure compared with simultaneous intra-arterial blood-pressure (pressures in mmHg), using Student's paired t-test (two-tailed).

	Mean	S.D.	No.	Mean differences between values	S.D. of differences	t	p
<i>Systolic</i>							
Intra-arterial	115	30	71	-13	15.6	7.02	<0.001
Cuff	133	17					
<i>Diastolic</i>							
Intra-arterial	81	13	71	-0.2	7.9	0.21	>0.9
Cuff	80	10					
E.C.G.	65	11	60	1.6	7.31	1.69	>0.05
Heart-rate cuff	66	11					

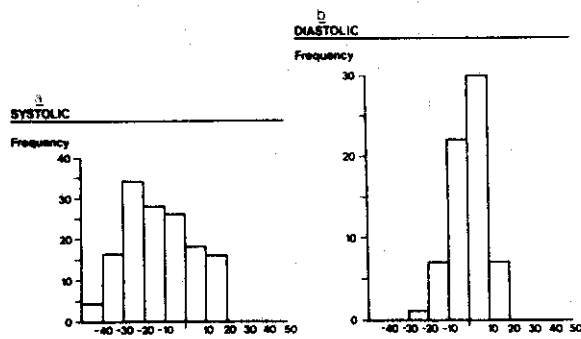


Figure 3. (a). Frequency histogram of between method difference for systolic pressure. 31% of monitor readings within ± 10 mmHg of intra-arterial pressure, 62% within ± 20 mmHg. (b). Frequency histogram of between-method difference for diastolic pressure. 80% of monitor readings within ± 10 mmHg of intra-arterial pressure.

Heart-rate measurement variability did not differ significantly ($p > 0.1$) when compared to the ECG recordings. The scatter diagrams for systolic and diastolic blood-pressure indicate a trend away from the line of identity. To determine if this trend is significant for a given range of blood-pressures a Chi-squared value was calculated for successive ranges of blood pressures (viz. for systolic BP: <100 , $100-109$, $110-119$, ≥ 120 mmHg). Thus χ^2 can be split into a component due to linear regression (i.e. trend) and a component due to departures from linear regression. The procedure is as detailed by Armitage [10]. The results for systolic blood-pressure are shown in table 2, which shows a highly significant trend which results in erroneous measurement as the blood-pressure increases. Similar results (overall $\chi^2 < 0.001$) are apparent for diastolic blood-pressure. When heart-rate is subjected to this analysis, no significant trend was demonstrated, and thus it can be accepted that the relationship between

Table 2. Armitage's test for trend, applied to ranges of systolic blood pressure, indicating a highly significant trend.

Group	<100	100-109	110-119	≥ 120	Total
Success	7	3	4	2	16
Failure	0	0	1	54	55
Total	7	3	5	56	71
Expected success	1.58	0.68	1.13	12.62	
Expected failure	5.42	2.32	3.87	43.38	
Score	-2	-1	0	1	

Overall (1) $\chi^2 = 55.2$; three degrees of freedom ($p < 0.001$).
 (2) χ^2 due to linear regression = 49.4; one degree of freedom ($p < 0.001$).
 (3) χ^2 due to departures from linear regression = $\chi^2 - \chi^2 = 5.8$ with two degrees of freedom ($p > 0.05$).

ECG and Hitachi HME-20 recorded heart-rate follows the line of identity.

We assessed the value of this device in a number of situations. It was of particular use for home and ambulant BP recording. The machine is light (2.6 kg with batteries) and portable, and requires little maintenance.

HEART RATE

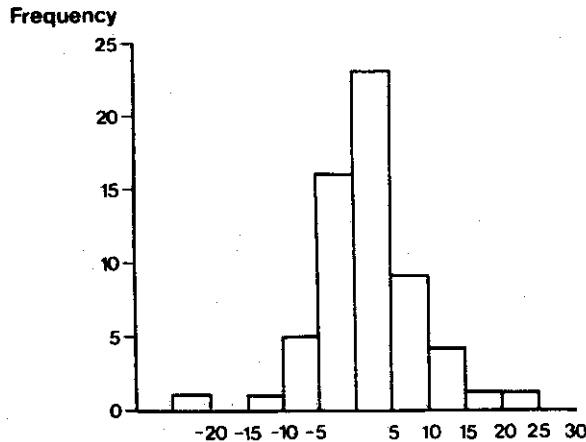


Figure 4. Frequency histogram of between-method difference for heart-rate. 63.9% of monitor readings within ± 5 beats per minute (b.p.m.) of electrocardiographically recorded rate. 86.8% of readings within ± 10 b.p.m.

Patient operation is simple and the cuff is designed so that it is easy to apply. In addition, very little time is required for patient education, unlike the conventional sphygmomanometer [8]. Unfortunately, the device is not suitable for recording blood-pressure during patient movement, for example exercise electrocardiography, as even slight additional noise created by movement is detected by the microphone and results in erroneous measurement.

Discussion

In general, the Hitachi HME-20 pulse and BP monitor provides a satisfactory estimate of diastolic pressure and heart-rate. There is a tendency to underestimate systolic pressure, however, and this is most marked when intra-arterial pressure is more than 150 mmHg (see figure 1); recordings in this range account for the skewed distribution of differences in figure 3(a), which indicates that only 31% of measurements were within ± 10 mmHg of IA recordings. There is an acceptable standard of measurement, however, between 100 and 150 mmHg. Highly significant correlation coefficients for heart-rate and both systolic and diastolic BP indicate that, when changes in a parameter are of prime importance (for example when evaluating anti-hypertensive medication), the device will reproduce an accurate record of these changes. Because of the additional noise created by exercise, which is detected by the cuff microphone, we did not find the instrument valuable as a means of assessing BP during exercise.

Systolic pressure was underestimated by a mean of -12 mmHg. This is comparable with the standard sphygmomanometer, which has been shown to underestimate systolic pressure by -10 mmHg [3], and also the random zero sphygmomanometer which records clinic blood-pressures significantly lower than simultaneous IA pressures (mean -13/-1 mmHg) [8]. In a previous study evaluating BP recorders [3], all seven devices assessed gave significantly different values compared to IA recordings for systolic BP and in five cases signifi-

cantly (and alternative laboratory indirect measurement differences) considerable variability taken in this

Thus, the ECG currently available for measuring heart rate is underestimated by other devices for individual patients (>150 mmHg) patients commonly estimate with this measurement pressure, we gross differences. However, we identity for addition, the extended period excellent. The number measuring 15 and 16] a position posing engineering which, because prove attractive many more

Acknowledgements

We wish to thank throughout also due to statistics. Mrs M. U

References

1. CONCEPTS Defects

MEDE 24-25.1

A show previous maint. which account

Firm

cantly underestimated diastolic BP. None of these alternative recorders are capable of measuring heart-rate. Labarthe *et al.* [2] evaluated seven instruments, but used indirect means only. We considered that an intra-arterial standard was necessary for our evaluation of this more recent device. Many workers have found a wide range of differences when comparing IA and indirect cuff BP measurements [11 and 12]. Indirect BP is subject to considerable variability [13], and to minimize the effect of this variability, serial simultaneous measurements were taken in this study.

Thus, the Hitachi HME-20 compared favourably with currently available devices, and may be superior when measuring diastolic pressure. Its main shortcoming is underestimation of systolic BP, and this failing is shared by other devices of this sort [3]. While occasional large individual differences in systolic pressure did occur (>150 mmHg), the mean recordings from eight patients compared favourably, suggesting that a satisfactory estimate of blood-pressure patterns can be obtained with this instrument. Although our intra-arterial measurement may itself overestimate systolic blood-pressure, we do not feel that this could account for the gross differences in systolic pressure outlined above. However, we demonstrated a trend away from the line of identity for both systolic and diastolic blood-pressure. In addition, the technical reliability of the device over extended periods of operation has been found to be excellent, both during hospital and domestic use. The number of innovations in techniques and devices for measuring blood-pressure is surprisingly small [2, 3, 14, 15 and 16] and the reports are often lacking in detail. This position possibly reflects the gap between medical and engineering interests. We have evaluated a monitor, which, because of its low price and ease of operation, may prove attractive to both the clinician and patient and can be relied upon to provide a comparable performance to many more expensive devices.

Acknowledgements

We wish to thank Miss Rita Smith for her co-operation throughout the course of this investigation. Thanks are also due to Miss E. A. Strevans, Department of Mathematics, Strathclyde University, for statistical advice and Mrs M. Utley for secretarial help.

References

1. CONCEJCOE, S., WARD, M. K. and KERR, D. N. S. (1976) Defects on sphygmomanometers: an important source of

- error in blood pressure recordings. *British Medical Journal*, **1**, pp. 886-888.
2. LABARTHE, D. R., HAWKINS, C. M. and REMINGTON, R. D. (1973) Evaluation of performance of selected devices for measuring blood pressure. *American Journal of Cardiology*, **32**, pp. 546-553.
3. HUNYOR, S. N., FLYNN, J. M. and COCHINEAS, C. (1978) Comparison of performance of various sphygmomanometers with intra-arterial blood pressure readings. *British Medical Journal*, **2**, pp. 159-162.
4. AYMAN, D., and GOLDSHINE, A. D. (1940) Blood pressure determinations by patients with essential hypertension: difference between clinic and home readings before treatment. *American Journal of Medical Science*, **200**, pp. 465-471.
5. JULIS, S., MCGINN, N. F., and HARBURG, E. (1964) Comparison of various clinical measurements of blood pressure with the self-determination technique in normotensive college males. *Journal of Chronic Disorders*, **17**, pp. 391-396.
6. DOYLE, J. T., HOOBLER, S. W. and FOX, S. M. (1966) *Proceedings of Symposium on Objective Recording of Blood Pressure*. (American Heart Association, New York).
7. ROCHMIS, P. G. (1969) *Proceedings of the 2nd Annual Conference on Automated Indirect Blood Pressure* (Roche Medical Electronics Division, Hoffman-La Roche, Inc., Cranbury, New Jersey, USA).
8. GOULD, B. A., KIESO, H. A., HORNUNG, R. and ALTMAN, D. G. (1982) Assessment of the accuracy and role of self-recorded blood pressures in the management of hypertension. *British Medical Journal*, **285**, pp. 1691-1694.
9. KIRKENDALL, W. M., BURTON, A. C., EPSTEIN, F. H. and FREIS, E. D. (1967) Recommendations for human blood pressure determination by sphygmomanometers. *Circulation*, **36**, pp. 980-988.
10. ARMITAGE, P. (1972) *Principles of Medical Statistics* (Blackwell, Oxford), pp. 362-365.
11. RAFTERY, E. B. and WARD, A. P. (1968) The indirect method of recording blood pressure. *Cardiovascular Research*, **2**, pp. 210-218.
12. ROBERTS, L. N., SMILEY, J. R. and MANNING, G. W. (1953) Comparison of direct and indirect blood pressure determinations. *Circulation*, **8**, pp. 232-242.
13. ARMITAGE, P., FOX, W. and ROSE, G. A. (1966) The variability of measurements of causal blood pressure. II Laboratory study. *Clinical Science*, **30**, pp. 325-335.
14. RAFTERY, E. B. (1978) The methodology of blood pressure recording. *British Journal of Clinical Pharmacology*, **6**, pp. 193-201.
15. GEORGE, C. F., LEWIS, P. J. and PETRIE, A. (1975) Clinical experience with use of ultrasound sphygmomanometer. *British Heart Journal*, **37**, pp. 804-807.
16. PERLOFF, D. and SOKOLOV, M. (1978) The representative blood pressure: Usefulness of office, basal, home and ambulatory readings. *Cardiovascular Medicine*, **3**, pp. 655-668.

MEDEQUIP 85

24-25 April 1985: American Embassy, London

A show of the latest US Medical Equipment arranged by the United States International Marketing Center. (A previous Medequip [1983] resulted in \$54 million worth of orders.) Participation is open to American manufacturers, their UK subsidiaries or representatives, and to British firms marketing products in these areas which are at least 51% of American origin. US new-to-market firms are particularly welcome. The USIMC will accommodate a select group of 18-20 firms, who have specialized in developing medical equipment.

Firms or persons interested in participating or attending should contact Mary Russell on 01 629 4304.

A solid state recorder for ambulatory monitoring of pulmonary-artery pressure

S. G. Perry*, A. W. Nathant, T. Cochran†, P. T. Gosling* and A. J. Camm†

St. Bartholomew's Hospital, West Smithfield, London EC1A 7BE

A compact, portable recording system has been developed to record pulmonary-artery pressure in ambulatory patients. A transducer mounted on the tip of a conventional cardiac catheter is inserted percutaneously and positioned in the main pulmonary artery. Analogue circuitry, including peak and trough detectors, pre-processes the pressure/voltage waveform to yield sampled values for the systolic and diastolic pressures. Systolic and diastolic values sampled every 30 s are digitized and stored in CMOS semiconductor memory. Data acquired over a prolonged period is transferred to a microcomputer for permanent storage and subsequent analysis. Five patients were each successfully monitored for at least 24 h. The zero-level drift was less than 1% and gain stability was also better than 1% over 48 h. This device allows practical, safe, reliable and prolonged pressure recording and has wide-ranging clinical potential.

Introduction

Left-heart failure is a common clinical manifestation of coronary artery disease, hypertension, aortic or mitral valve disease and of various cardiomyopathies. In haemodynamic terms it is characterized and may be quantified by a rise in the left ventricular end-diastolic pressure. This may be measured directly for short periods of time and usually requires arterial puncture. However, in the absence of mitral stenosis, the mean pulmonary-artery wedge pressure and the pulmonary-artery diastolic pressure are both similar [1] and approximate to the left ventricular end-diastolic pressure. These pressures are easily measured using simple and safe venous catheterization and such measurements facilitate the diagnosis and effective treatment of patients with both acute and chronic heart-failure, as well as pulmonary hypertension. Progress of disease can also be followed. Haemodynamic profiles of drugs designed to treat heart-failure may be determined.

Bedside pulmonary-pressure monitoring has been used for many years [2 and 3] both for diagnosis and also for assessing the response to therapy. However, changes in cardiac output and in peripheral volume in the ambulant subject may have considerable effect on systemic and pulmonary haemodynamics [4]. Evaluation of these changes has hitherto been limited. In particular, the assessment of exertional dyspnoea and the design of ideal treatment regimens is restricted by the sole use of bedside monitoring.

Normal pulmonary-artery pressure is in the region of 25/8 mmHg but may vary, for example from 10 to 100 mmHg systolic. Currently, available technology does not allow accurate, prolonged recording of such pressures and to overcome the problems associated with this type of monitoring we have adopted a new approach.

System design

The system design can be considered in four stages: (1) transducer, (2) pre-amplifier and data processing, (3) data storage, (4) data retrieval and presentation.

Transducer

A miniature strain-gauge transducer (Gaeltec Ltd, Dunvegan, Isle of Skye, UK), measuring 10 mm in length by 1.6 mm in

diameter, mounted onto a 2 mm diameter polyurethane catheter, is used to directly measure the pressure in the pulmonary artery (figure 1). The strain-gauge elements are vacuum deposited onto the diaphragm, as are the connections to the lead wires. The catheter has a fine central bore to allow atmospheric pressure to be used as the reference pressure for the transducer. The diaphragm is covered with a thin layer of silicone rubber to protect it from body fluids. The transducer is equilibrated by soaking in sterile saline for at least 5 h prior to insertion; the catheter may then be inserted percutaneously through the venous system and positioned in the main pulmonary artery.

Pre-amplifier and data processing

A standard unit provides the excitation signal for the transducer and also some initial amplification and demodulation to produce the desired signal. After further amplification and filtering to give an output of 10 mV per mmHg applied pressure with a frequency response from 0 to 20 Hz (3dB), the pressure signal is then passed to two analogue peak detectors which follow the systolic and diastolic pressure waveforms. 'Bleed' resistors are incorporated to allow slowly varying systolic and diastolic levels to be followed. The two output signals are then passed through a low-pass filter with a time constant of 30 s to smooth out variations due to respiration.

Data storage

The two signals proportional to systolic and diastolic peak pressures are sampled every 30 s and then multiplexed into an 8



2 mm



Figure 1. The transducer tipped catheter.

* Department of Medical Electronics.

† Department of Cardiology.

bit analogue-to-digital converter (ADC) having a conversion time of 1 ms. The full-scale range of the system is -10 mmHg to $+100$ mmHg, giving a resolution of ± 0.43 mmHg. After conversion, the 8 bit data bytes are written into semiconductor memory in the order: systolic, diastolic, systolic, diastolic etc. After each diastolic datum has been stored the memory address counter is incremented by one. Memory capacity for each parameter is 4096 bytes, which gives a total continuous recording time of up to 33 h. To ensure that only valid data are brought out of memory on replay, the last memory address is stored on latches and during replay the stored address is compared with the current address. When the two are equal an 'end-of-data' flag is set.

The master clock which controls the timing of the system has two frequencies; one for use in record mode set at 1 Hz and the other for use in playback mode set at 2 kHz. Record and playback are selected by means of a front-panel mounted key switch, which also has a 'hold' position to allow the recorder to be transported between patient and data-retrieval system without either loss of valid data or recording of false data. A block diagram of the complete unit is shown in figure 2.

To reduce current drain the recorder was constructed using CMOS semiconductor technology. Using a supply voltage of ± 5 V, the current consumption was approximately 14 mA. Power was supplied by two 9 V (PP9 size) rechargeable batteries each with a capacity of 1.2 Ah. The complete unit measures 230 mm \times 220 mm \times 95 mm and weighs approximately 1.5 kg.

For ambulatory use the recorder is carried by means of a shoulder strap. A photograph of the unit is shown in figure 3.

Data retrieval and presentation

Data is transferred from the recorder via a standard digital input/output interface to a Data General MP100 Micro-Nova mini-computer (Data General, Adelaide House, London EC4). Eleven lines were required to effect the transfer: the eight data lines, a data-available line to strobe input data into the computer's data-input register, an end-of-data line and the earth line. The transfer rate was controlled by the internal clock in the recorder; a complete transfer of 24 h of data taking approximately 1 min.

On receipt of the end-of-data flag, the data may be validated by displaying on a visual display screen before being converted to mmHg and written to an 8 in floppy disc for storage. Each side of a disc can hold 25 full 24 h recordings. Line-printer copy of the data is also available (figure 4). Data stored on floppy disc is plotted off-line using a Data General 3/12 computer system supporting a Tektronix 4010 graphics terminal and a Bryans 26000, A3 plotter. The data may be plotted as a full 24 h recording or in an expanded form at up to hourly intervals.

Results

Five patients have been successfully monitored for up to four consecutive 24 h periods. Mean pressures ranged from

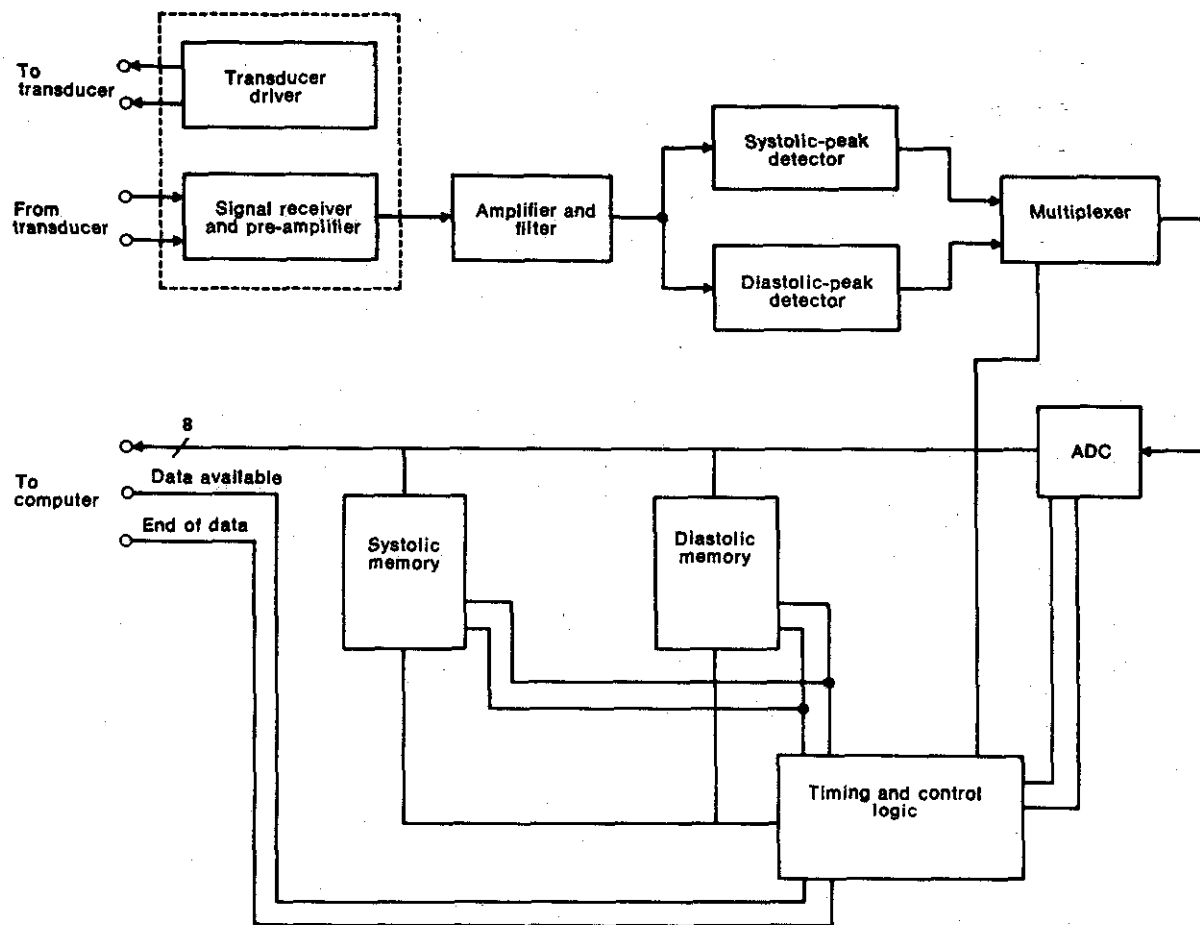


Figure 2. Block diagram of the recorder system.

Figure 3.

PATIENT
STUDY DI
CATHETE!

5768
1 *
2 *
3 *
4 *
5 *
6 *
7 *
8 *
9 *
10 *
11 *
12 *
13 *
14 *
15 *
16 *
17 *
18 *
19 *
20 *

Figure 4. L values. The correlative s

means of a
an in figure 3.

anda digital
Micro-Nova
London EC4).
the night data
data into the
line and the
internal clock
of data taking

by be validated
being converted
range. Each side
inter copy of the
floppy disc is
computer system
and a Bryans
as a full 24h
early intervals.

for to four
ranged from



Figure 3. A subject with the recorder attached.

17/3 mmHg to 70/30 mmHg. The transducer was calibrated immediately prior to insertion and again on removal. Over the period of recording, the zero-level drift and gain stability of the transducer were less than 1% of full scale.

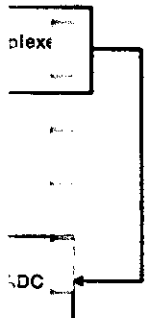
Figure 5 shows a typical 24 h plot of systolic and diastolic pulmonary-artery pressures. The numbered arrows correlate with symptoms noted in the patient's diary. Several points can be noted from this figure. The mean systolic/diastolic ratio was 17/3 mmHg. There were, however, considerable excursions from these mean levels; the systolic pressure ranged from as low as 5 mmHg up to 33 mmHg, while the diastolic values ranged from -6 mmHg to 9 mmHg. As might be expected, the pressure variations were least marked during sleep.

Figure 6 illustrates the effectiveness of the system for monitoring the progress of drug treatment in an ambulatory patient. The figure shows the systolic and diastolic pressure variations over a 24 h period in which vasodilator therapy was introduced. The patient's pressure fell gradually from 70/30 to 50/19 mmHg.

Discussion

Two major factors which determined the design of this ambulatory pressure recorder were the choice of pressure transducer and the method of data storage.

Ambulatory systemic arterial pressures may be monitored using the Oxford continuous blood-pressure recorder [5]. This system uses an external pressure transducer connected to the patient via a fluid-filled catheter which is flushed continuously to prevent blockage. The analogue pressure signal is recorded onto magnetic cassette-tape for off-line analysis. The technical



PATIENT NAME : NUMBER : 604122 DATE : 9 10 81
 STUDY DESCRIPTOR : COMP STUDY 6
 CATHETER CALIBRATED TO 100 mm Hg (FULL SCALE) STUDY START TIME = 10:58

5768	DATA VALUES											
1 *	23	9	22	8	22	9	22	9	22	9	22	9
2 *	22	9	22	100	100	100	100	9	21	9	21	9
3 *	22	7	22	6	19	6	18	6	17	6	16	6
4 *	17	6	18	6	18	6	17	6	17	5	17	6
5 *	17	5	17	6	19	6	18	6	18	5	17	5
6 *	18	5	18	5	18	6	18	6	18	6	18	6
7 *	18	6	18	6	18	6	18	6	18	6	18	6
8 *	18	6	18	5	18	5	18	6	18	6	18	6
9 *	18	6	19	6	18	6	18	6	19	6	22	7
10 *	21	6	19	6	20	6	20	6	19	6	18	6
11 *	18	6	18	6	19	6	19	7	20	7	20	6
12 *	19	7	19	7	19	7	19	6	18	6	19	6
13 *	19	6	19	6	19	6	20	6	20	6	21	6
14 *	21	6	21	6	19	6	19	6	18	6	21	6
15 *	20	6	19	6	18	6	18	6	19	6	19	6
16 *	22	5	23	6	24	6	24	6	25	6	23	6
17 *	21	6	20	6	20	6	20	6	39	6	30	6
18 *	29	6	24	6	22	6	20	6	19	6	19	6
19 *	19	6	19	6	19	6	19	6	19	6	19	6
20 *	37	6	26	6	21	6	19	6	19	6	19	6

Figure 4. Line-printer output showing typical pressure values. Each line represents 3 min of alternate systolic and diastolic values. The values of 100 recorded on line 2 correspond to the pressing of a time-marker button to allow comparative/correlative studies to be synchronized.

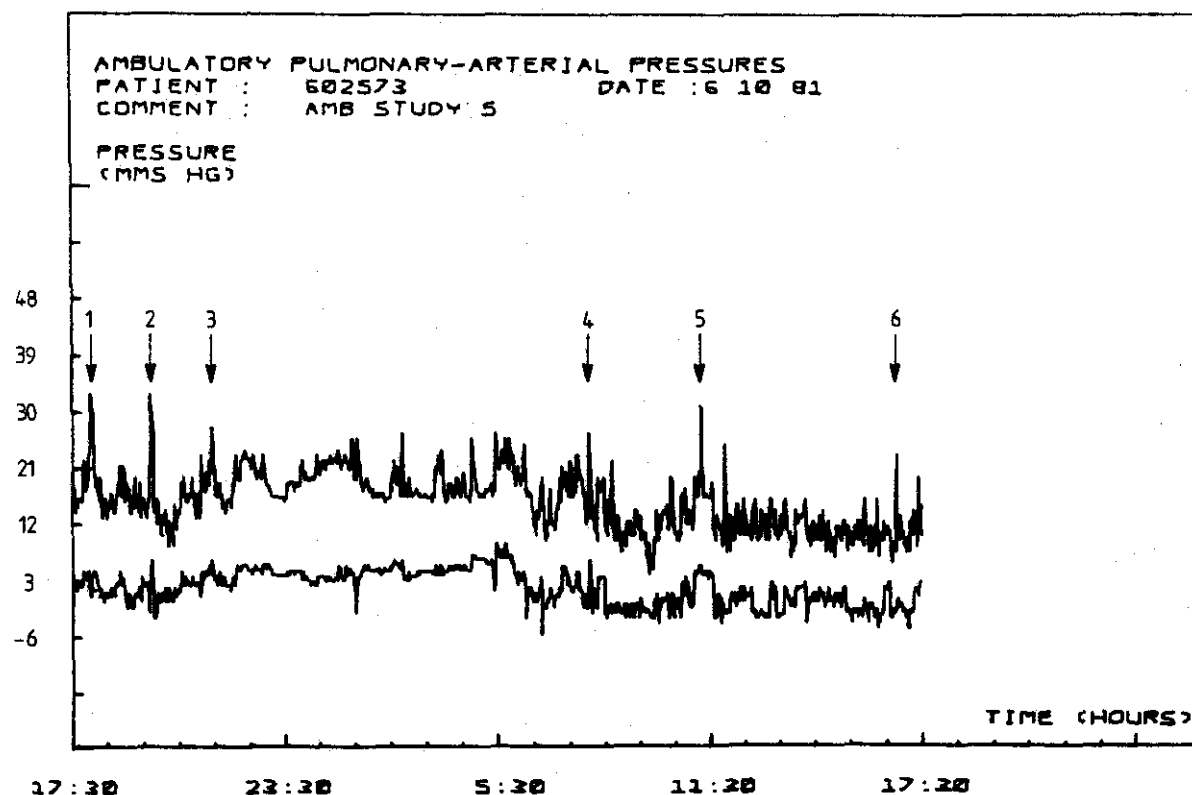


Figure 5. A typical 24 h plot of systolic and diastolic pulmonary-artery pressures. The numbered arrows correlate with the symptoms noted in the patient's diary as follows: (1) exercise test; (2) slight chest pain; (3) period of bad chest pain; (4) dull chest pain; (5) feeling sick; (6) climbing stairs.

evaluation of Millar-Craig *et al.* [6] shows that errors inherent in tape-recorder systems would be too great to allow such small changes in pulmonary-artery pressure to be monitored accurately.

Use of a transducer tipped catheter overcame many of the problems associated with external transducers [7]. In particular, hydrostatic pressure changes due to alteration in transducer position relative to the pulmonary artery are eliminated [7]. The need for constant flushing devices to prevent catheter blockage is also obviated.

However, use of this type of indwelling transducer does present its own problems. Once inserted, it cannot be recalibrated without removal, which means that it must have stable zero-offset and gain characteristics. To ensure zero-offset stability, equilibration of the transducer in saline for several hours is essential because the silicone rubber membrane over the diaphragm absorbs fluid and deforms, applying an effective zero-offset pressure. However, once equilibrated the zero drift on the transducer did not exceed ± 1 mmHg. The use of AC excitation helps reduce electrolytic corrosion of the transducer strain-gauge elements. Its small size and the sensitivity required for accurate monitoring dictate that the transducer membrane be rather delicate. Care is needed in the initial handling and insertion stages to prevent damage. But once successfully inserted this type of pressure-monitoring catheter is both stable and reliable [8].

Semiconductor memory was chosen for data storage to overcome the noise, drift and linearity problems associated with cassette-tape recorder systems or radiotelemetry systems previously used for ambulatory pressure monitoring [6 and 9]. This, however, imposes limits on the amount of data that may be

stored in a conveniently sized unit. There is inevitably a compromise between storage capacity, physical size and battery power consumption. In order to compress the data to be stored into the 8 kbytes of available memory systolic and diastolic pressures were sampled every 30 s for the present study. Even in this compressed form, the data recorded is of clinical value for both the primary diagnosis of pathological haemodynamic disorders and for monitoring therapy in a wide range of cardiac conditions.

Future developments

The prototype described in this paper has shown that it is feasible to record pulmonary-artery pressure in ambulatory patients over a lengthy period. It has limited memory capacity and is inflexible to the extent that a change of the recorded parameters requires a completely new system. Incorporating a microprocessor to analyse the incoming signal directly would reduce both of these drawbacks; the need for much of the analogue pre-processing circuitry would be removed, as would the present timing and control logic. With reduced component numbers, memory capacity could be increased to at least 64 kbytes, allowing storage of a greater number of parameters including, for instance, the heart-rate. Shorter sampling intervals would also be possible. In addition, a microprocessor-based system would provide greater power and greater flexibility. If different physiological parameters were to be measured, only the controlling software need be altered. This suggests the possibility of a recording system capable of monitoring most physiological parameters where only the transducer or its interface need be changed.



Figure 6. A myocardial infarction. The sharp increase in pressure is observed.

Conclusion

A portable device for ambulatory pulmonary-artery pressure recording has been developed. It is accurate, safe and reliable for both the assessment of cardiac failure and with

Acknowledgements

Dr Nathan is a research fellow of the Research Board.

References

1. SCHEINMAN, R. S. Relation of pulmonary-artery pressure and left ventricular pressure.

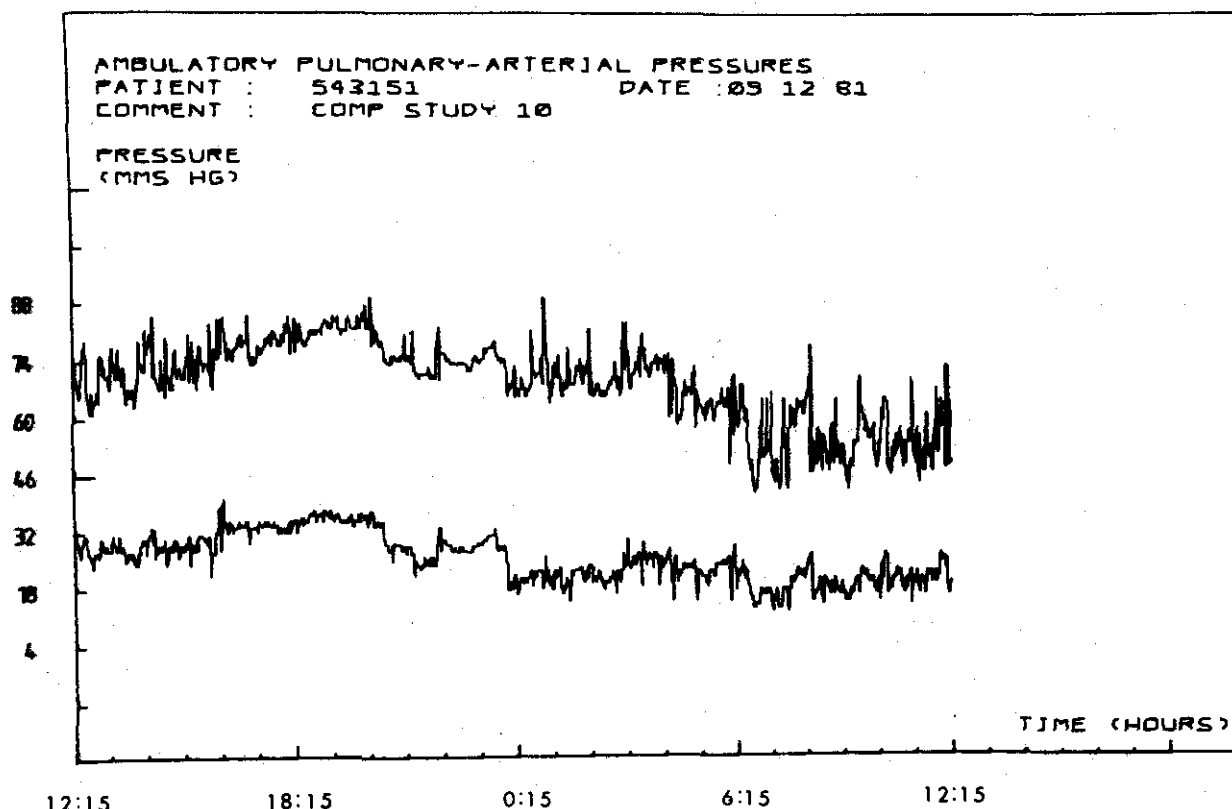


Figure 6. A plot showing the effect of vasodilator therapy in a patient with left-ventricular dysfunction following myocardial infarction. Treatment was started at approximately 18:00 hours. The subsequent fall in pulmonary-artery pressure can be observed.

Conclusion

A portable device has been developed to measure and store sampled pulmonary-artery pressure values in ambulatory subjects. Used in a clinical setting it has been shown to be accurate, safe and reliable and has wide-ranging potential for both the assessment and monitoring of patients with heart-failure and with pulmonary hypertension.

Acknowledgements

Dr Nathan is the recipient of a British Heart Foundation research fellowship and Dr Cochrane is supported by the Joint Research Board of St. Bartholomew's Hospital.

References

1. SCHEINMAN, M., EVANS, G. T., WEISS, A. and RAPAPORT, E. (1973) Relationship between pulmonary artery end-diastolic pressure and left ventricular filling pressure in patients in shock. *Circulation*, **47**, pp. 317-324.

2. RATSHIN, R. A., RACKLEY, C. E. and RUSSELL, R. O. (1972) Hemodynamic evaluation of left ventricular function in shock complicating myocardial infarction. *Circulation*, **45**, pp. 127-139.
3. DALEN, J. E. (1979) Bedside hemodynamic monitoring. *New England Journal of Medicine*, **301**, pp. 1176-1178.
4. VEREL, D. and GRAINGER, R. G. (1978) *Cardiac Catheterization and Angiography* (Churchill Livingstone, London), pp. 14-15.
5. LITTLE, W. A., HONOUR, A. J., SLEIGHT, P. and STOTT, F. D. (1972) Continuous recording of direct arterial pressure and electrocardiogram in unrestricted man. *British Medical Journal*, **iii**, pp. 76-78.
6. MILLAR-CRAIG, M. W., MANN, S., CASHMAN, P. M. M. and RAFTERY, E. B. (1981) Continuous tape-recording of ambulatory blood pressure. Technical considerations. *Biotelemetry and Patient Monitoring*, **8**, pp. 56-66.
7. POOLE-WILSON, P. A. (1978) Interpretation of haemodynamic measurements. *British Journal of Hospital Medicine*, **20**, pp. 371-382.
8. GROSSMAN, W. (1974) Pressure measurement. In *Cardiac Catheterization and Angiography*, edited by Grossman, W. et al. (Philadelphia), pp. 81-82.
9. BACHMANN, K. and ZERZAWY, R. (1981) Radiotelemetry of direct blood pressure measurements in the arterial and pulmonary circulation. *Biotelemetry and Patient Monitoring*, **8**, pp. 15-27.

Ref. (4)
Siete.

Microprocessor-control of drug infusion for automatic blood-pressure control

L. M. Auer H. Rodler

Universitätsklinik für Neurochirurgie in Graz, Landestrankenhaus, A-8036 Graz, West Germany

Abstract—A microprocessor-controlled infusion pump is described for the automatic control of hypotension or antihypertensive treatment with sodium nitroprussid. The system requires the continuous monitoring of blood pressure as an input signal to the microprocessor, the latter regulating blood pressure to the desired level by stepwise changes in infusion rate. The infusion pump proved valuable for intensive care and neurosurgery under controlled hypotension.

Keywords—Blood-pressure control, Infusion pump, Microprocessors

1 Introduction

HYPOTENSIVE and antihypertensive therapy is a routine measure in clinical medicine. Sodium-nitroprusside has turned out to be an especially effective drug both for precise blood-pressure regulation during surgery under controlled hypotension and for hypertensive emergencies (AUER, 1978*a*, 1978*b*; BECKER and BENOWITZ, 1979; SHEPPARD, 1980). Its direct action on vascular smooth muscle explains the rapid action within the first minute of infusion. One problem arising from such a therapy is the need for continuous control of infusion rate, adapting it to the continuously monitored blood pressure. For this an additional nurse is necessary during the drug's administration in intensive care, and an additional task for the anaesthetist during hypotensive surgery.

Therefore, a device was developed to control antihypertensive and hypotensive treatment automatically and keep blood pressure on a desired level with the aid of a microprocessor.

2 Technical elements and computer program

Blood pressure is monitored continuously via a catheter in the radial artery, a Stratham P23dB transducer and a Hellige electromanometer. This signal enters a microprocessor-regulated infusion pump. Fig. 1 demonstrates the automatic infusion device with its display of infusion rate and operating levers. One knob allows the choice of a desired blood pressure value (mean pressure); a second element allows the selection of time interval for automatic

dosage-rate changes. The microprocessor regulates the infusion rate necessary to bring blood pressure from its current value to the desired level, and to keep it at this level $\pm 5\%$.

This system is hence especially appropriate for automatic control of blood pressure in patients with short-lasting hypertensive crises, when the infusion pump immediately delivers a certain amount of drug if the blood pressure exceeds the 5% level above the desired pressure. Additionally, the trigger level above and below the chosen pressure level is freely adjustable.

For microprocessor control of the peristaltic infusion pump, an Intel microprocessor type 8085A, an e.p.r.o.m. type 8755A16K, a REM type 81552K and an a.d. transducer type 8708 6-channel 8-bit are used. The microcomputer records the blood pressure signal arriving via the a.d. transducer (Fig. 2).

As safety features, an air alarm and a 'critical low pressure' alarm are included in the system.

A rubber section of the infusion line is squeezed sinusoidally by a pacemaker-driver camshaft with flaps. The motor itself has a 4-phase-frequency drive generated by the microprocessor.

The microcomputer program is based on clinical experience of the standard way of infusing sodium nitroprussid for blood-pressure control in more than 100 patients in the intensive-care unit and in the operating theatre. One regulatory principle of such systems with a biological feedback, blood-pressure response in the present case, is the observation of a latency period. The interval between infusion of the drug and response of blood pressure is around 30 s. Therefore, the optimal time interval for such regulatory steps of the microprocessor pump was found to be around 45 s. This value can be selected by knob 3 as shown on Fig. 1. Every 45 s, the infusion rate

First received 4th February and in final form 18th May 1980
0140-0118/81/020171-04\$01.50/0
© FMBE 1980

is increased in steps of 10 ml/h of a 5% solution of sodium nitroprusside. M.A.P. values are recorded every 20 ms. A mean value from every 5 s period is calculated. Infusion rate is changed according to the mean value of m.a.p. from the last 5 s period before the end of the 45 s interval (or any other chosen interval). This system regulates automatically upwards and downwards, until the blood pressure enters a range of $\pm 5\%$ around the desired level. It likewise generates an unchanged quantity of drug infusion as long as blood pressure remains within this range of $\pm 5\%$. As soon as blood pressure exceeds the 5% range or falls below it, the infusion rate is increased or decreased by one step, and the procedure of stepwise increase or decrease of infusion is started again, until pressure is again within

the range or exactly at the desired level. Here, again, the reference value of m.a.p. is the mean value of the last 5 s period before m.a.p. touched one of the thresholds above or below the desired level of m.a.p. At 10% below the desired pressure level the infusion rate is reduced to half. A 'critically low level' at 15% below the desired level stops the infusion pump, until it starts again above the upper 5% level.

The maximum dosage is 300 ml/h of the 5% solution of sodium nitroprusside.

The described microprocessor regulation did not induce low-frequency oscillations of m.a.p. as might have been expected from m.a.p. alternately touching the thresholds above and below the wanted level. Spontaneous oscillations of m.a.p. such as Traube-Hering-Meyer waves occurred as usual (Figs. 3b and 5a), however, they mostly remained uninfluenced by the therapy, except when sudden changes of m.a.p. were induced.

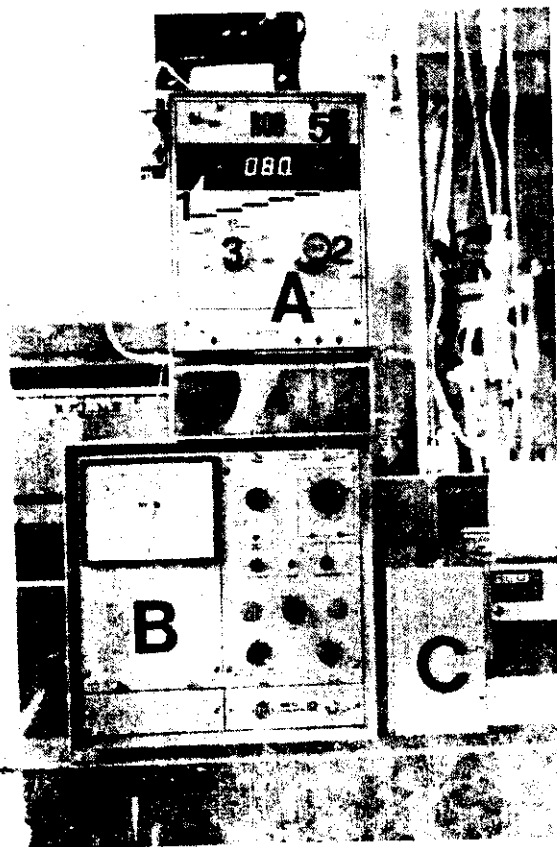


Fig. 1 (A) Microprocessor-infusion pump
(B) Electromanometer for continuous blood-pressure monitoring
(C) 2-channel writer
1 Display of infusion rate in ml/h
2 Selection knob for desired blood-pressure level
3 Selector for desired time interval between single steps of dosage rate changes
4 Pump engine
5 Alarm indicators for air bubbles in the infusion drip and critical low pressure, respectively; both alarm also function acoustically

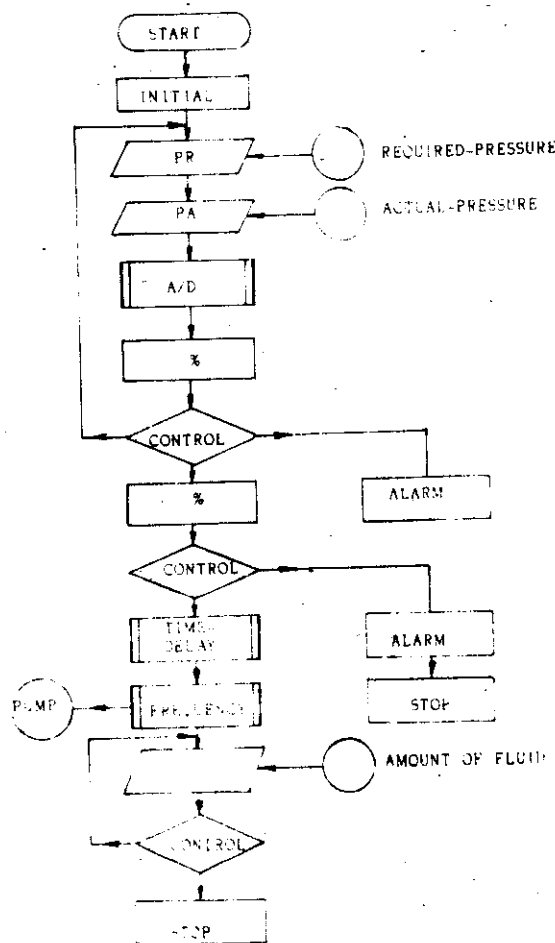


Fig. 2 Flow chart of automatic blood-pressure control device

Fig. 3 Control of the system



Fig. 3 Re (a)

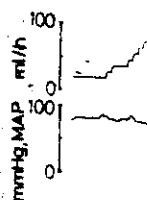


Fig. 4 Control (a) C

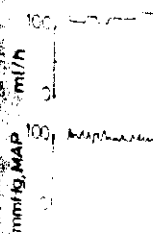


Fig. 5 Control (a) H

Clinical experience

The system described has been used in intensive-care patients, especially patients with severe head

injury and following cerebrovascular or brain tumour surgery. During neurosurgical operations the pump was used for controlled hypotension, and intraoperative hypertension. Fig. 3 demonstrates regulation to a mean arterial pressure of 100 mmHg on intensive care patients. Fig. 4 shows an example of controlled hypotension. In Fig. 5, the special

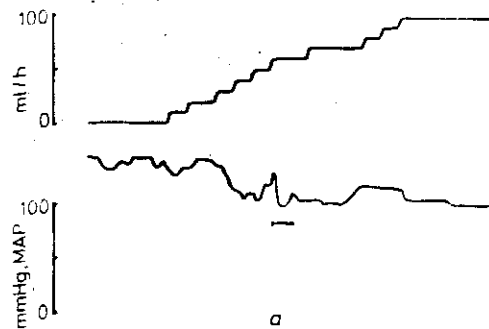
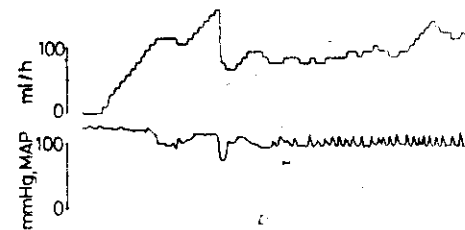


Fig. 3 Regulation of m.a.p. in intensive-care patients
(a) Example of antihypertensive treatment in an intensive care patient. M.A.P. is automatically lowered from 150 mmHg to 100 mmHg. The infusion rate (upper curve) is increased stepwise until an adequate rate in ml/h is reached. Bar = 1 min



(b) Antihypertensive control to a desired level of 100 mmHg. The hypertensive crisis is not visible any more on the blood-pressure curve, but on the dosage rate curve which increases for short periods of blocked antihypertensive crisis. The blood-pressure finally shows a typical circulatory rhythm. Bar = 1 min

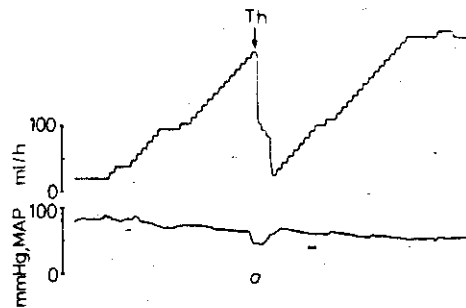
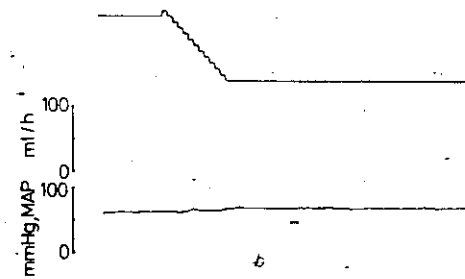


Fig. 4 Controlled hypotension
(a) Controlled hypotension during surgery. M.A.P. had slowly been brought to 80 mmHg and is then lowered down to 55 mmHg for clipping of an aneurysm. Th = administration of intravenous anaesthetic drug supporting hypotension for a short while. The dosage rate is therefore lowered



intermittently, thereafter rising again to bring about a continuous m.a.p. decreased to the desired level of 55 mmHg. Bar = 1 min
(b) Blood pressure is kept at this level during the phase of preparation and clipping of the aneurysm. The dosage rate stabilises at a rate of about 120 ml/h. Bar = 1 min.

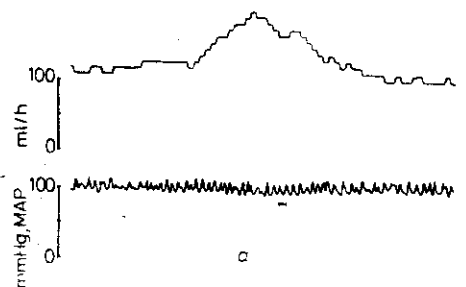
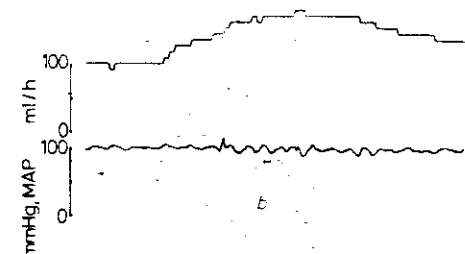


Fig. 5 Examples of 'automatic antihypertensive control'. Hypertensive episodes are blocked by immediate



reaction of the infusion-pump system that increases dosage rate so as to keep m.a.p. on the chosen level

advantage of the system for shortlasting and rapid hypertensive crises becomes evident, showing the

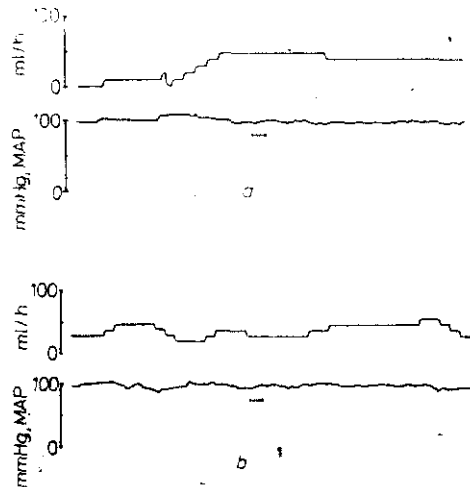


Fig. 6 During intervals between hypertensive episodes, m.a.p. is observed and the 'automatic antihypertensive control' is in a 'waiting position', the pump distributing no drug at all or very low doses between 10 and 50 ml/h

quick reaction of infusion rate that inhibits blood pressure from rising, before a nurse could have noticed the pressure rise and reacted by giving an antihypertensive drug. Between such pressure peaks, the pump remains in a 'waiting position', administering a low dosage for preservation of the desired pressure level (Fig. 6). Sometimes, a potential rise in m.a.p. could not even be noticed on the blood-pressure curve (see Figs. 3b, 5a and b), since counteraction by an increase in dosage rate came

promptly. In other instances, especially accompanying a sudden fall of m.a.p., a clear correlation between m.a.p. change and dosage rate could be observed as in Figs. 3b and 4a. A sudden decrease of m.a.p. led to an equally rapid reduction of infusion rate. Similar steps have been tried either with the aid of big computers (SHEPPARD *et al.*, 1975, 1980) or using microprocessors without time-intervals and step-by-step dosage-rate regulation.

The present device proved very accurate in the maintenance of a desired level of blood pressure with only small deviations.

Acknowledgments—This work was supported by the 'Österreichischer Fonds der gewerblichen Wirtschaft'.

References

- AUER, L. M. (1978a) The action of sodium-nitroprusside on the pial vessels. Experimental study in cats. *Acta Neurochir.*, **43**, 297-306.
- AUER, L. M. (1978b) The use of sodium-nitroprusside as a hypotensive and antihypertensive agent in neurosurgical patients. *Neurosurg. Rev.*, **1**, 139-145.
- BECKER, C. E. and BENOWITZ, N. L. (1979) Hypertensive emergencies. *Med. Clin. North Am.*, **63**, 127-140.
- SHEPPARD, L. C., KOUCHOUKOS, N. T., SHOTTS, J. F. and WALLACE, F. D. (1975) Regulation of mean arterial pressure by computer control of vasoactive agents in postoperative patients. In: *Computers in Cardiology*. Rotterdam, The Netherlands, October 2-4, 91-94.
- SHEPPARD, L. C., SHOTTS, J. F., ROBERSON, N. F., WALLACE, F. D. and KOUCHOUKOS, N. T. (1980a) Computer controlled infusion of vasoactive drugs in post cardiac surgical patients. IEEE Conference, EMBS Denver, October 6-7, in press.
- SHEPPARD, L. C. (1980b) Computer control of the infusion of blood and drugs in the intensive care unit. *Proc. Tübinger Symp. Rechnergestützte Intensivpflege*, in press.

Helio

M. Singh
Biomedical E

A

Key

1 Introduction

LASER app
importance
measureme
vessels, carc
dermatology
and POWEL
and WHITEI
1978; KIMU
applications
characteristi
exposure lev
for example, fo
determine th
wall so that i
plate could l
In this pag
determination
various parts
made betwe
body shape.

2 Method

The total
contribution
the layers be
Since these t
GOLDMAN a
cosine law, th
integrating sp
The assembl
reflectance is
20 mW heli
Physics, USA
focussed by a
index 1-544

First received 3/10/81
0140-0118/81/0000-0000
© IEMBE 1981

Noninvasive Determination of Central Blood Pressure by Impedance Plethysmography

FARRY HERSCOVICI, SENIOR MEMBER, IEEE, AND DEAN H. ROLLER

Abstract—A new algorithm based on impedance plethysmography provides reliable determinations, on an experimental basis, of arterial blood pressure. Signals over the brachial artery are picked up by four Van Slyke type electrodes attached to the skinward side of a regular blood pressure cuff. Mathematical formulas are used to define those impedance pulses that correspond to systolic, diastolic, and mean arterial blood pressure values. The envelope of the impedance pulses recorded during cuff deflation can be defined by linear regressions, function of just one normalized independent variable, which is the ratio between the amplitude of the pulse with maximum amplitude and of the amplitude of the pulses with constant amplitude. These linear regressions are assumed to be universally applicable, the influence of individual anatomic variations having been eliminated by the use of a normalized variable. The results of this study prove that the variable pulse amplitude obtained during a cuff deflation is a quantifiable reaction of the circulatory system to arterial constriction.

INTRODUCTION

The oscillometric technique, one of the oldest techniques for arterial blood pressure determination [1], is based on the well-known but insufficiently explained physiological phenomenon: i.e., where a pneumatic cuff bandaged over the arm is deflated from a starting pressure well over the subject's systolic pressure, the arterial wall pulsates due to the pulsatory blood circulation. The pulsations modulate the pressure in the cuff and these oscillations are sensed by a pressure transducer. Typical pressure oscillations are shown in Fig. 1. It is assumed that information directly related to blood pressure is contained in their envelope [3]–[11].

Below the diastolic pressure the oscillometric pulse amplitudes are never constant. There is no externally imposed arterial constriction below diastolic pressure; hence, circulation should be unaffected while the cuff pressure is decreasing below this value. But there is a relationship (Fig. 1) between cuff pressure and the corresponding pulse amplitude in normal circulation: if the pressure in the cuff is either low or absent, then the pulsations are poorly transmitted to the transducer [12]. There is no marker in the oscillometric envelope at the instant when normal locomotion returns and this prevents the development of an algorithm that is related to normal unrestricted circulation.

Distal impedance plethysmography overcomes this

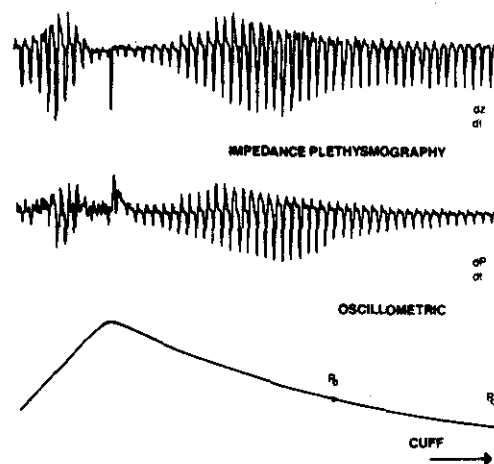


Fig. 1. Simultaneous recordings during cuff deflation of impedance plethysmographic signals and oscillometric signals.

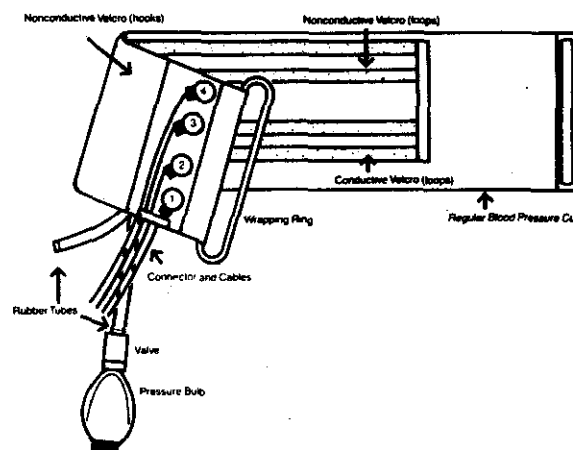


Fig. 2. The blood pressure cuff with four electrodes as used in this study.

drawback, being able to represent blood circulation even without a constriction applied around the limb.

In our studies, we applied a special set of four electrodes to the skinward side of a regular blood-pressure cuff (Fig. 2). When the cuff is either inflating or deflating, a similar phenomenon of modulated pulsations occurs as described for the oscillometric technique. The train of electrical impedance pulses as a function of cuff pressure (P_C) (Fig. 1) is very similar to the simultaneous oscillometric record, with the very important difference that when P_C is below diastolic pressure (P_D), the amplitudes (negative) of the impedance pulses are constant all the

Manuscript received April 19, 1985.
 Herscovici is with the University of Miami, Coral Gables, FL 33124.
 Roller is with Research Corporation, Miami, FL 33102.
 Roller is with South Miami Hospital, Miami, FL 33143.
 IEEE Log Number: 86-8031.

way to almost zero cuff pressure, consequently marking the unrestricted arterial blood circulation in the arm.

Several attempts were made in the past to use impedance plethysmography for blood pressure measurements [13]–[17]. These attempts were based on empirical algorithms similar to those used for oscillometric measurements. The first pulse during cuff deflation was considered representative of the systolic pressure P_S ; diastolic pressure P_D was assumed to be marked by the inflection in the vanishing envelope. A cuff-pressure with two electrodes together with another two pasted electrodes placed on the limb, far from the cuff, were used to form a four-electrode impedance plethysmography system [14], [15].

In the publications cited, no attempts were made to determine the mean arterial pressure (P_m) by impedance plethysmography. The maximum pulse amplitude is assumed to signify mean brachial pressure in the oscillometric measurements [3], [4]. All our experiments have proven that with both impedance plethysmography and oscillometric techniques the maximum of the negative pulse envelope occurs at the same cuff pressure.

In the literature concerned with impedance plethysmography, the pulses produced by the pulsating blood are called $\Delta Z(t)$ pulses. For baseline stability reasons most of the investigators prefer to use the differential of these pulses called dZ/dt pulses.

Fig. 1 shows an example of the dZ/dt pulses sensed with the system described above. The amplitude (negative) of these pulses is very different from person to person, as is the ratio between the maximum amplitude and the amplitude of the constant amplitude pulses. The dZ/dt pulse amplitude, therefore, should be a function of such anatomic factors as: thickness of the arterial wall, elasticity of the surrounding tissue, ratio between artery and limb diameters, artery position inside the limb, blood resistivity, etc.

Up to the diastolic pressure, or at least up to around 40–50 mmHg cuff pressure, the negative pulse is constant and the above physical characteristics will determine the pulse amplitude for a particular subject. In other words, the negative amplitude of the constant-amplitude dZ/dt pulses (A_0) is mainly a function of the static (anatomic) characteristics of the body.

At a certain cuff pressure P_M , the dZ/dt pulse amplitude reaches a maximum, A_M . This maximum pulse amplitude should be a function of some dynamic characteristics of the body, as for example: the ability of the circulatory system to develop passive hyperemia or to increase the arterial compliance, the cardiac output, the blood pressure, the limit of linear expansion of the arterial wall, the limit of linear compression of the tissue, etc.

It is obvious, then, that the maximum pulse amplitude, A_M , is a function of dynamic (physiologic) characteristics of the body, as well as of the previously mentioned static ones.

We can obtain a dimensionless indicator of the body's dynamic characteristics by dividing the maximum amplitude, A_M , by the constant amplitude, A_0 . Using the ratio

A_M/A_0 as an independent mathematical variable, we assumed that we can establish some rules governing the envelope of the electrical impedance pulses and identify the amplitude of those pulses that signify systolic, mean arterial, and diastolic pressures.

The theoretical development of these rules is not the goal of this paper; consequently, the three hypothesized linear functions were determined and tested experimentally.

DETERMINATION OF THE RELATIONSHIPS GOVERNING THE ENVELOPE OF THE IMPEDANCE PULSES

Method

Four strips of HI-MEG conductive Velcro are attached to the skinward side of a regular blood pressure cuff (Fig. 2) and connected to an impedance plethysmograph.

The instrument, shown in a block diagram form (Fig. 3), delivers a constant alternating current (10 kHz) to the outer two cuff electrodes. A differential amplifier with high input impedance senses the impedance variations $\Delta Z(t)$ produced between the two inner cuff electrodes by the pulsating blood. The instrument also contains a demodulator and a loop for the compensation of the dc component of the electrical impedance signal (in fact, the mean limb impedance Z_0), and a differentiating amplifier (time constant $RC = 50 \cdot 10^{-3}$ s) for the generation of the first derivative of $\Delta Z(t)$, the so-called dZ/dt pulse.

The cuff is inflated or deflated by a system composed of an air pump (pressure/vacuum), a pressure transducer, an amplifier, an electronic switch, and a set of electromagnetic air valves (Fig. 4).

Blood pressure is measured during cuff deflation. Between the systolic and the diastolic pressures the rate of deflation was self-adjusted between 2.5 mmHg and 5 mmHg per heartbeat (depending on the subject's arm size). The deflation is linear within 5.5 percent, referring the deviation to the pressure domain (systolic–diastolic) for that particular patient. The whole blood pressure determination takes about 45 s. The rate of deflation was set manually but in the future it can be controlled as a function of the patient's heart rate.

A significant number of human impedance plethysmography measurements were made simultaneously with direct blood pressure measurements in the aorta and later processed. Aortic blood pressure measurements were made using a Hewlett-Packard Catheter System Model 8890 α with a Pressure Conditioner Model 8816 (max. frequency 200 Hz) and a Fluid-Filled Transducer Model 1280C (max. frequency 300 Hz).

Samples of the simultaneous recordings are shown in Fig. 5. The middle trace is the direct blood pressure in the aorta: the top peak of each pulse is P_S , the bottom peak is P_D , the flat portion of the trace is P_m .

A group of 26 patients were involved in the first experiments. Each had cardiac problems but none had clinically apparent peripheral vascular disease. There were 23 males and 3 females ranging in age from 35 to 81 years

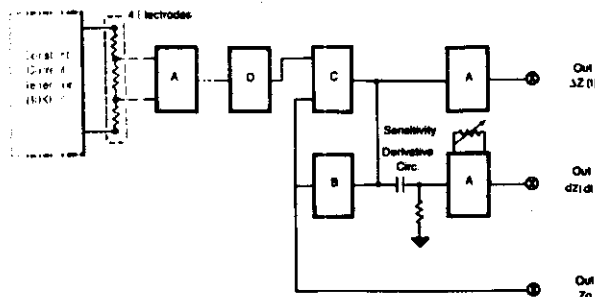


Fig. 3. Block schematic of the impedance plethysmograph used in this study. A—amplifiers, D—demodulator, C—comparator, B—automatic impedance control.

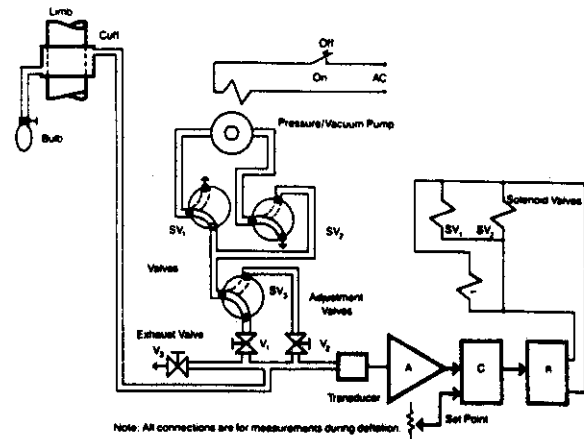


Fig. 4. Block diagram of the inflator-deflator. A—amplifier, C—comparator, R—relay.

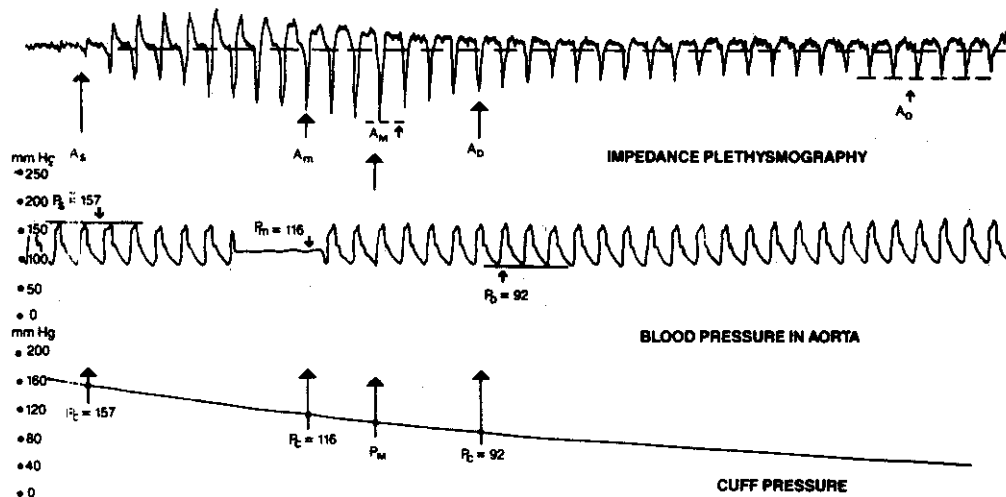


Fig. 5. Simultaneous recordings of the central catheter line and of the impedance plethysmograph during a cycle of cuff deflation.

(mean, 63). The recordings of two of these patients could not be processed because these patients had large arms, unsuited for the "adult" size (12.4 × 25.9 cm) of our pressure cuff; another one was not processed because of unreliable information from the catheter line (very irregular rhythm and pressure). The cardiac catheterization procedure was performed after mild sedation with Diazepam and local anesthesia in the inguinal area using the standard Seldinger technique.

While the pressure catheter was maintained in the aorta, 3-10 successive complete deflation cycles of impedance measurements were done on each patient.

The following method was used to find functional relationships among different impedance pulse amplitude and the independent variable A_M/A_0 .

a) For each recording cycle the values A_M and the average of t_0 between cuff pressure of 40 and 50 mmHg were measured and then the ratios A_M/A_0 were calculated and averaged for each patient.

b) The pressure values measured by the catheter line for each of the three significant blood pressures were marked on the cuff pressure curve.

c) These points were vertically projected to the dZ/dt recordings.

d) The negative amplitude of the nearest pulse or the interpolated value of the neighboring pulses was marked down.

e) These amplitudes of dZ/dt were normalized and averaged for each patient, then plotted as functions of A_M/A_0 for that particular patient in graphs representing all the patients.

The baseline for each recording was the residual level of dZ/dt for $P_C > P_S$. All the amplitudes were measured from the strip chart.

Results

A small number of the recordings were partially or totally unprocessable because of technical problems, such as missing catheter P_m value, patient movement, loss of calibration in the catheter line, a patient with $P_S > 200$ mmHg (this is the maximum value processable by our present equipment but there is no technical or physical limitation to going beyond 200 mmHg), etc. A total of

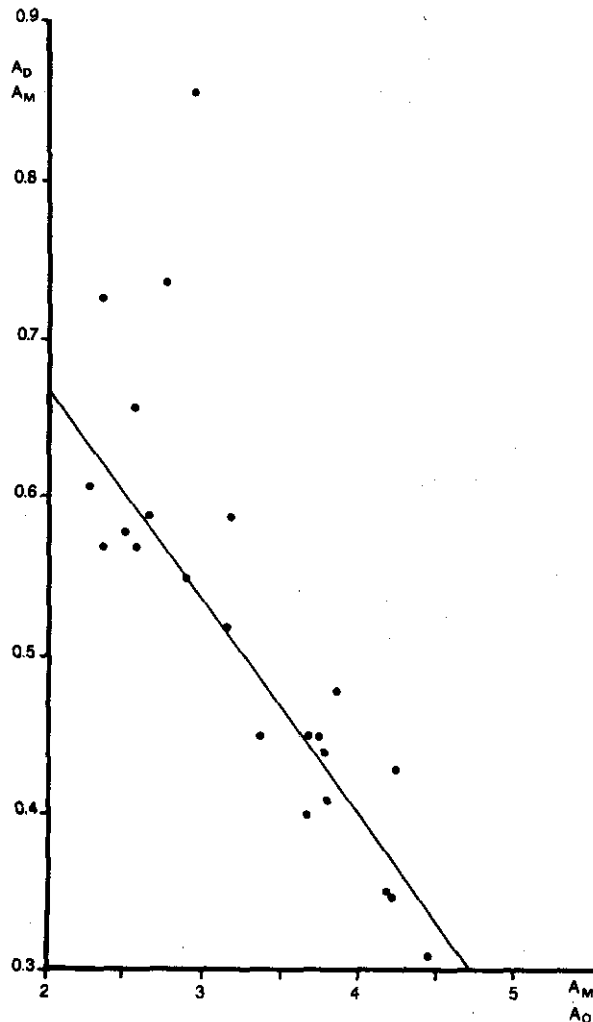


Fig. 6. A_D/A_M as a function of the independent variable, A_M/A_0 . $N = 26$, $r = 0.79$, $p = 0.08$; $N = 24$, $r = 0.92$, $p = 0.04$.

133-142 recordings were processed for each of the three characteristic blood pressure values (P_D , P_S , P_m) (almost 6 recordings/patient/characteristic pressure value).

The results of these measurements are presented in Figs. 6, 7, and 8. Statistical calculations show good linear correlations for each group of data. The regression lines calculated for each group of data lead us to define three equations:

$$\frac{A_D}{A_M} = 0.965 - 0.141 \frac{A_M}{A_0} \quad (1)$$

$$\frac{A_S}{A_0} = 0.596 \frac{A_M}{A_0} - 1.07 \quad (2)$$

$$\frac{A_m}{A_D} = 0.632 \frac{A_M}{A_0} - 0.221 \quad (3)$$

where A_D is the dZ/dt pulse amplitude at the moment the cuff pressure is equal to the diastolic pressure P_D ; A_S is the dZ/dt pulse amplitude at the moment the cuff pressure is equal to the systolic pressure P_S ; A_m is the dZ/dt pulse amplitude at the moment the cuff pressure is equal to the mean pressure P_m .

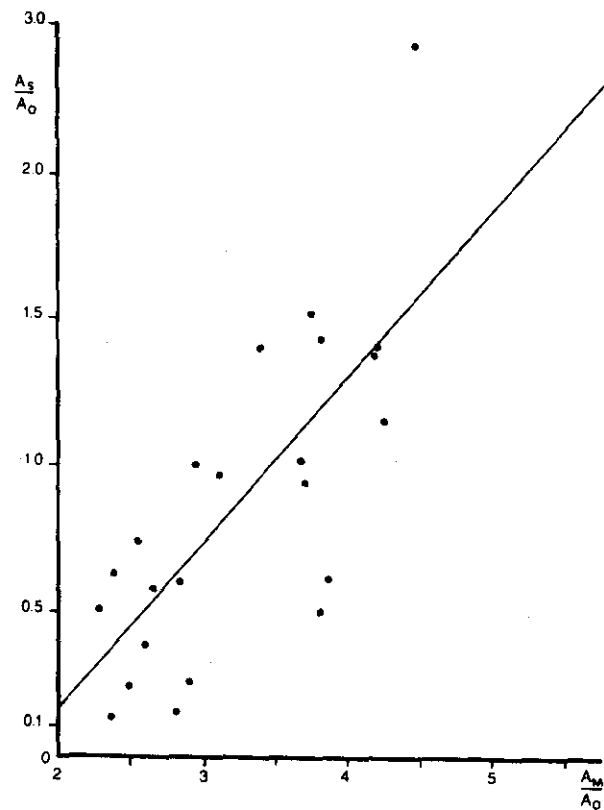


Fig. 7. A_S/A_0 as a function of the independent variable, A_M/A_0 . $r = 0.76$, $p = 0.36$.

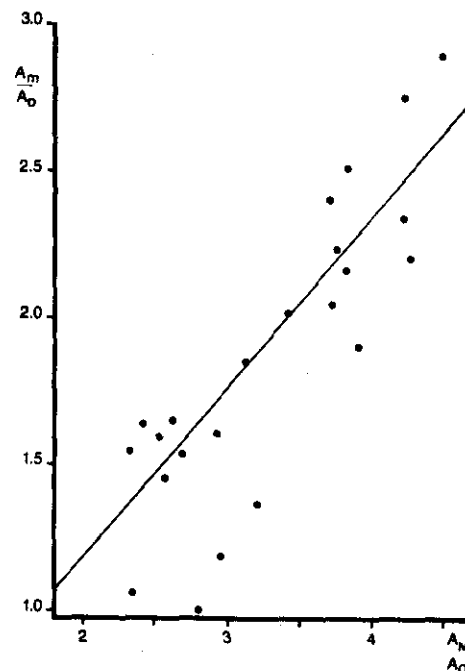


Fig. 8. A_m/A_D as a function of the independent variable, A_M/A_0 . $r = 0.87$, $p = 0.26$.

Equations (1), (2), and (3) prove that the phenomenon, previously described as just a qualitative reaction of the circulatory system to arterial constriction, is now quantifiable. These equations are assumed to be universally applicable: the anatomic differences of each individual are

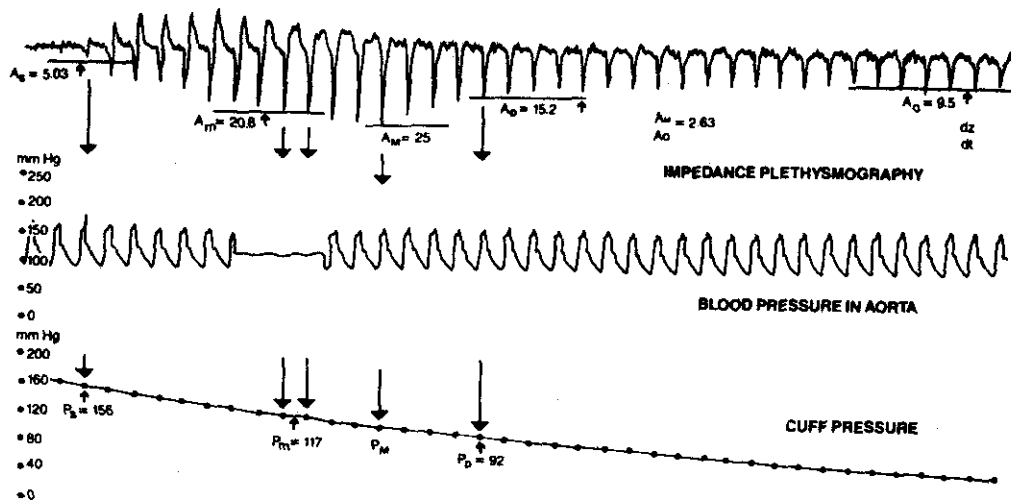


Fig. 9. Method of finding the significant pressure values from the electrical impedance recording.

eliminated by the normalized independent variable, A_M/A_0 .

BLOOD PRESSURE DETERMINATION

Method

Figs. 9 and 10 illustrate how the previous equations (1), (2), and (3) can be utilized. We assume that during a cuff deflation cycle we have stored a train of pulses as in Fig. 9.

The amplitudes of the pulses are averaged in the cuff pressure range of 40–50 mmHg, and A_0 is found. It appears experimentally that the average of 6–8 pulses is sufficient. However, on occasions when the respiratory artifact is very strong, A_0 should be averaged over a full respiratory cycle.

The maximum pulse (A_M) is found and identified and the independent variable A_M/A_0 is calculated. It is only a matter of computation to find A_D from (1) and A_S from (2). Electrically, these values of A_D and A_S represent two thresholds. The pulses closest to these thresholds correspond to P_D and P_S , respectively. The actual pressure is read from the cuff pressure trace by vertically projecting the pulses significant for P_D and P_S (Fig. 9). If the threshold is between two pulses, then the pressure is obtained as the average of the two.

Once the pulse amplitude A_D is computed, (3) will yield A_m . The same procedure as described above will lead to the determination of the actual mean arterial pressure P_m .

As a general rule [4], $P_D < P_m$ and $P_m > P_M$ where P_M is the cuff pressure which corresponds to the appearance of the pulse with maximum amplitude A_M (Figs. 5 and 9).

Results

The first application of the above algorithm was the retrospective determination of blood pressure by impedance plethysmography for the 26 patients involved in the above-mentioned study (Group I). The values determined by

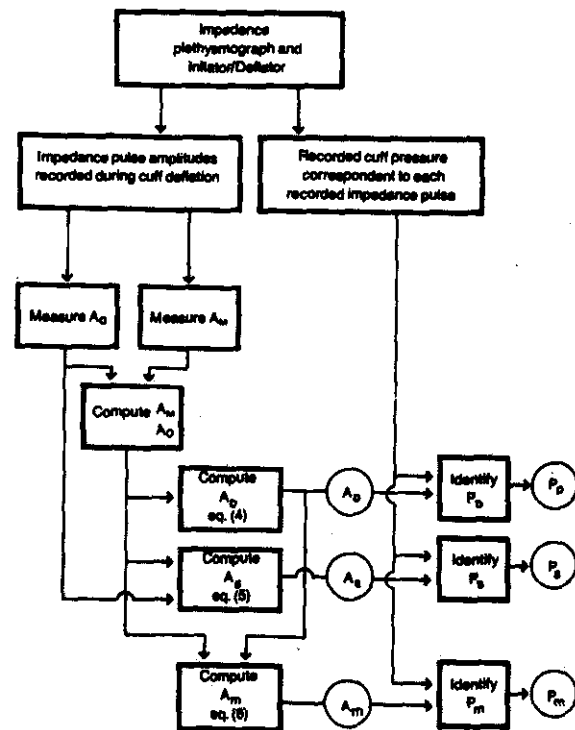
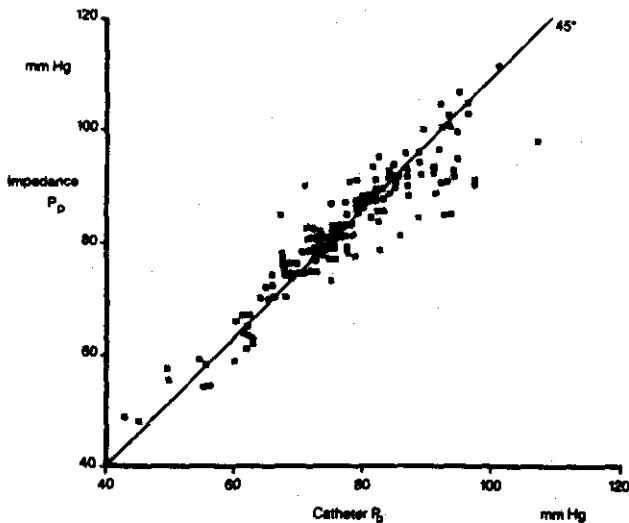
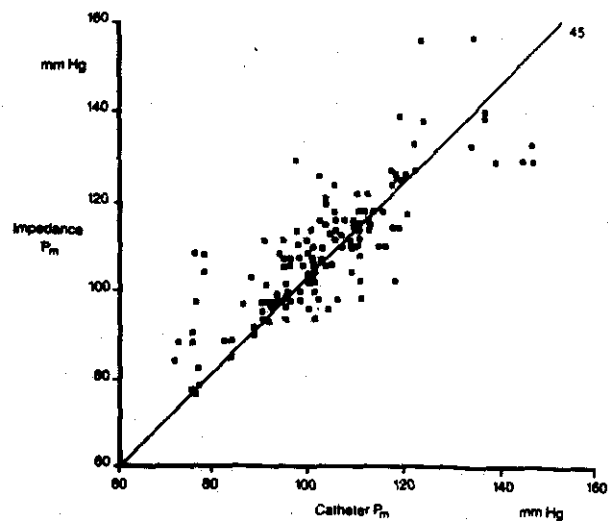
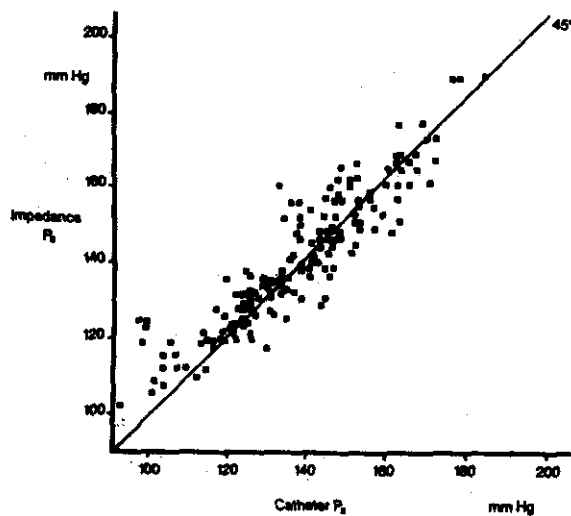


Fig. 10. Flow chart of the methodology of blood pressure determination by impedance plethysmography.

impedance plethysmography were compared with the values obtained by direct measurement of intraaortic pressure.

Meanwhile, a second group of 19 patients was submitted to the same data-collecting procedure as previously described. They consisted of 13 males and 6 females who ranged in age from 42 to 70 years (mean, 60). They were all suffering from cardiac illnesses; none had clinically apparent peripheral vascular disease. During the procedure they were sedated and anesthetized in the same condition as Group I.

Five of these patients had to be eliminated from the

Fig. 11. P_D by impedance versus P_D by catheter.Fig. 13. P_m by impedance versus P_m by catheter.Fig. 12. P_S by impedance versus P_S by catheter.

study because of some technical problems, e.g., inaccurate instrument manipulation, catheter movement, etc.

The recordings obtained from these new experiments (Group II) were also processed as in Fig. 9 using (1)–(3).

The blood pressure values obtained from the two groups of patients using the impedance plethysmographic (IPG) procedure described above, as compared with the equivalent values obtained by direct intraaortic recording catheter (CATH), are presented in Figs. 11, 12, and 13. The statistical calculations are summarized in Table I for Group II and for Groups I and II pooled together. In this table the error was calculated by dividing the deviation of each sample to the catheter pressure value of that sample, catheter value being considered as the true determination:

$$\epsilon^{\%} = \frac{P_{IPG} - P_{CATH}}{P_{CATH}} \cdot 100. \quad (4)$$

We did statistical calculations for the whole determinations as well as for the determinations averaged per pa-

tient. A good correlation between the values of each blood pressure value measured by impedance plethysmography and by direct aortic line, and a normal Gauss distribution of the errors introduced by the impedance technique were found. The results of these calculations are presented in Table I and Figs. 14, 15, and 16. Standard deviation, skewness, kurtosis, and the distribution of errors were all based on the error of determination as defined by relation (4).

The relatively larger error for P_m (Fig. 16) is not attributed to the algorithm (3) but to the methodology used to determine the pulse with the amplitude obtained from (3). While normally the pulse significant for P_m was found in the portion of the recordings with higher pressure values than P_M , in 11.6 percent of the cases (18 out of the 155 strips), the catheter P_m was of smaller value than P_M . The algorithm for P_m [see (3)] was found and applied, considering as a rule that the pulse significant for P_m must be looked for at the recording portion with $P_m > P_M$ [4]. We do not yet have the explanation of this situation nor an algorithm for detecting this anomaly. Further studies are planned to determine if these are normal events or if they are due to errors in the equipment calibration.

Even so, if all these results are compared with the results of Bruner *et al.* [12, pp. 184–188], one can see that this new technique is able to provide a tremendous improvement in accuracy compared with the auscultatory or the oscillometric techniques.

DISCUSSION AND CONCLUSION

The above results show that the hypothesis that three linear equations can accurately state as an algorithm for blood pressure determination is fairly well proven to be valid and that this is a good way to extract P_D , P_S , and P_m from impedance plethysmographic measurements.

Based on the algorithm and the methodology described above, a practical clinical monitoring instrument can be envisioned using a simple computing scheme for gener-

TABLE I
P_{IPG} VERSUS P_{CATH}

Variable	N Patients Groups I & II/II	M Determinations Groups I & II/II	Statistics	Determinations Averaged per Patient (All Patients)		All Determinations	
				Groups I & II	Group II Only	Groups I & II	Group II Only
P _D	38/14	196/49	Correlation Coefficient	0.94	0.94	0.91	0.90
			Level of Significance	0.0001	0.0001	0.0001	0.0001
			Standard Deviation	4.80	6.15	5.48	7.26
			Skewness	0.01	0.69	0.29	0.33
			Kurtosis	3.17	1.28	1.85	0.39
P _S	37/13	182/46	Correlation Coefficient	0.92	0.90	0.92	0.87
			Level of Significance	0.0001	0.0001	0.0001	0.0001
			Standard Deviation	6.19	8.48	6.04	8.80
			Skewness	1.58	1.42	1.37	0.99
			Kurtosis	5.15	2.29	4.29	0.94
P _M	36/13	153/43	Correlation Coefficient	0.84	0.83	0.81	0.79
			Level of Significance	0.0001	0.0001	0.0001	0.0001
			Standard Deviation	8.64	11.32	8.82	11.80
			Skewness	1.76	0.87	1.10	0.75
			Kurtosis	3.31	0.66	3.00	0.60

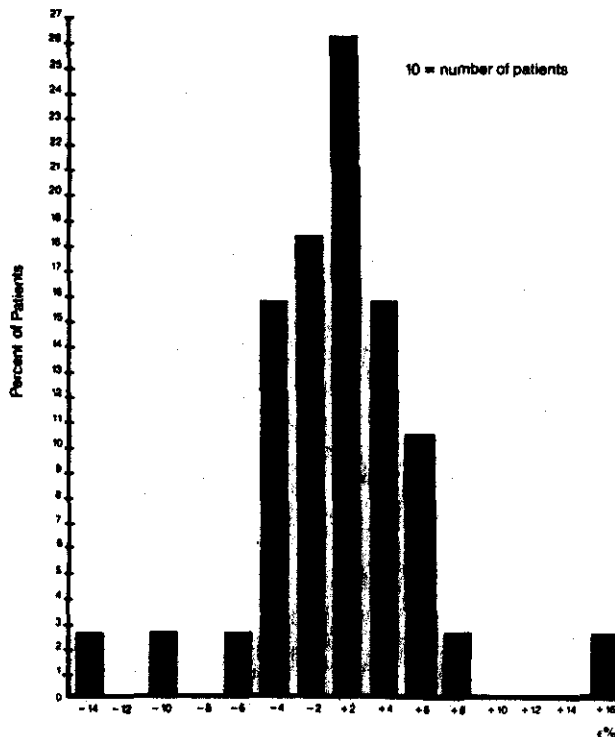


Fig. 14. Distribution of errors for P_D.

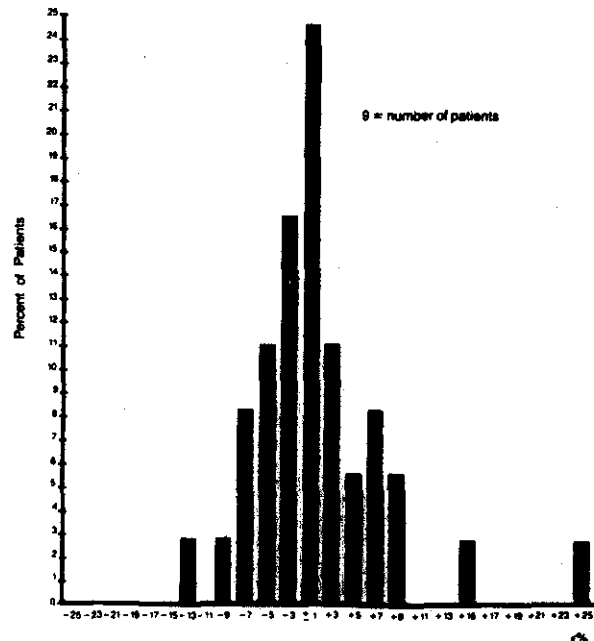


Fig. 15. Distribution of errors for P_S.

ating the three blood pressure values in real time, noninvasively. The advantages of such an instrument are:

- the shape of $(-dZ/dt)$ pulses is not important; only the peak value of each pulse is needed;

- only the steady value, A_0 , and the largest amplitude pulse, A_M , are needed for setting the thresholds for pressure readings;

- the accuracy of the amplitude determination is not important; all calculations are in normalized form;

- it is only necessary to know the cuff pressure that coincides with the peak of each pulse.

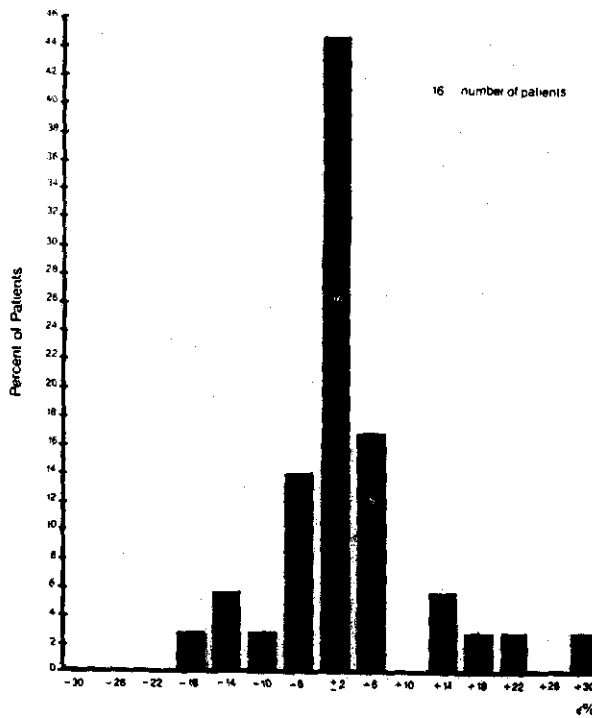


Fig. 16. Distribution of errors for P_m .

The phenomenon on which this new technique is based is mathematically described. The blood pressure values are derived from a mathematical model that can be tested and refined by increasing the number of subjects involved in its validation.

The superiority of the technique presented here as compared with other techniques for blood-pressure determination is the fact that it is the first one by which all three of the important blood pressures values can be measured noninvasively and almost simultaneously. The auscultatory, oscillometric, and ultrasonic techniques measure only two values and calculate the third.

It is well known that blood pressure measured directly from the aorta differs significantly from that obtained from the arm [18]–[21]. The present algorithm provides central blood pressure values which are the most important clinically [21] but, we assume that it is feasible to express the results in terms of brachial pressure if correction factors for the relationships between central and brachial pressure, as identified in other studies, are taken into account. This assumption is based on the facts that: i) the shape of the impedance pulse has no contribution to the measurement and ii) the change in pulse amplitude is not important, the computation being based on the ratio of two amplitudes (A_M and A_0).

It is presumed that this technique (as well as all techniques using inflating cuffs) may not be useful for patients with local upper extremity vascular disease. We must mention also that the sensitivity to motion artifact may not improve as compared with other noninvasive techniques.

The simplicity of the technique, using a regular blood pressure cuff with four conductive Velcro electrodes attached to the skinward side of the cuff, makes the tech-

nique attractive for use in the physician's office and in hospitals. The attachment of all four electrodes to the skinward side of a regular blood pressure cuff is original in our approach. It allows the operator to have a single item applied on the patient's arm and it provides measurements in a relatively narrow limb segment directly over the arterial obstruction when the cuff is pressurized. The application of the cuff completes preparations for the measurements. The technique is able to comply with the proposed AAMI standard for electronic blood-pressure measurement without restrictions.

As many studies were done about comparisons between other noninvasive techniques for blood-pressure determination and the direct line technique, the authors did not consider of priority interest to relate the present technique to any one of these. Good correlation with the direct line technique is decisive for any new technique.

ACKNOWLEDGMENT

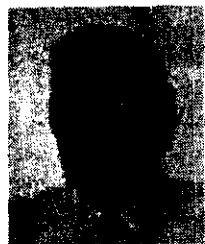
The authors would like to thank the nurses and technicians of the South Miami Hospital Cardiovascular Laboratory for their technical assistance. Thanks also are extended to J. Parker, who collected most of the data processed in this paper, and to Dr. M. Terris, who helped with the statistical calculations. We are especially grateful to Dr. P. P. Tarjan, Chief Scientist at Cordis Research Corporation for discussion and criticism of the manuscript, as well as for his great support of this work. B. C. Tillery, Cordis Research Corporation, provided editorial assistance and D. Lee, clerical help.

REFERENCES

- [1] M. B. Rappaport and A. A. Luisada, "Indirect sphygmomanometry, a physical and physiologic analysis and a new procedure for the estimation of blood pressure," *J. Lab. Clin. Med.*, vol. 29, p. 638, 1944.
- [2] "Blood pressure measurement: A comparison of techniques," AAMI-Medical Instrumentation Series 103, 1981.
- [3] M. Ramsey III, "Noninvasive automatic determination of mean arterial pressure," *Med. Biol. Eng. Comput.*, vol. 17, p. 11, 1979.
- [4] G. W. Manck, C. R. Smith, L. A. Geddes, and J. D. Bourland, "The meaning of the point of maximum oscillations in cuff pressure in the indirect measurement of blood-pressure. Part II," *J. Biomed. Eng. (ASME)*, vol. 102, pp. 28–33, 1980.
- [5] J. Looney, Jr., "Blood pressure by oscillometry," *Med. Electron.*, vol. 9, p. 57, 1978.
- [6] M. E. Croslin, "Method and apparatus for performing noninvasive blood pressure and pulse rate measurements," U.S. Patent 4 271 844, June 9, 1981, Assignee Medtek Corp., Princeton, NJ.
- [7] G. J. Flynn, "Method and apparatus for diastolic pressure measurement," U.S. Patent 4 271 843, June 9, 1981.
- [8] W. D. Jansen, J. D. Haney, C. C. Day, and S. A. Schneberger, "Systolic pressure determining apparatus and process using integration to determine pulse amplitude," U.S. Patent 4 137 907, Feb. 6, 1979, Assignee American Optical Corp., Southbridge, MA.
- [9] W. D. Jansen and J. D. Haney, "Systolic pressure determining apparatus and process using integration to determine pulse amplitude," U.S. Patent 4 140 110, Feb. 20, 1979, Assignee American Optical Corp., Southbridge, MA.
- [10] W. J. Williams, "Method and apparatus for blood pressure measurements," U.S. Patent 4 117 835, Oct. 3, 1978, Assignee Weisman & Allen, Madison Heights, MI.
- [11] L. A. Geddes, *Cardiovascular Devices and Their Applications*. New York: Wiley, 1984, pp. 67–72.
- [12] J. K. Raines, M. Y. Jaffrin, and S. Rao, "A noninvasive pressure-pulse recorder: Development and rationale," *Med. Instrum.*, vol. 7, p. 245, 1973.

[13] P. S. H. [14] L. b. P. [15] L. at M. [16] S. t. [17] I. Y. [18] H. S. [19] N. F. V. [20] R. fe. A. [21] V. c. W. M. [22] J. E. &

- [13] F. J. Jaussen, "The rheographic determination of systolic and diastolic blood pressure," in *Dig. 7th Int. Conf. Med. Biol. Eng.*, Stockholm, Sweden, 1976.
- [14] D. K. Swanson, and J. G. Webster, "Detecting systolic and diastolic blood pressure under a cuff using impedance plethysmography," in *Proc. Annu. Conf. Eng. Med. Biol.*, vol. 17, 1973, p. 118.
- [15] D. K. Swanson, "Measurement errors and origin of electrical impedance changes in the limb," Ph.D. dissertation, Univ. Wisconsin, Madison, pp. 114-137, 1976.
- [16] S. N. Mohapatra, "Noninvasive cardiovascular monitoring by electrical impedance technique," Pitman Medical, 1981, p. 222.
- [17] P. Rolfe, *Noninvasive Physiological Measurements*, Vol. 1. New York: Academic, 1979, p. 109.
- [18] H. Van Bergen, "Comparison of indirect and direct methods of measuring arterial blood pressure," *Circulation*, vol. X, p. 481, 1954.
- [19] M. Voelz, "Measurement of the blood pressure constant K , over a pressure range in the canine radial artery," *Med. Biol. Eng. Comput.*, vol. 19, p. 535, 1981.
- [20] R. M. Gardner, H. C. Wong, D. M. Sorenson, and J. Parker, "Differences between central and peripheral arterial pressure," in *Proc. AAMI 17th Annu. Meet.*, San Francisco, CA, 1982, p. 40.
- [21] W. Mathewson, J. Jarrard, and E. Jeveli, "A statistical comparison of electronic acoustic and oscillometric blood pressure measurements with conventional auscultation method," in *Proc. AAMI 17th Annu. Meet.*, San Francisco, CA, 1982, p. 77.
- [22] J. S. Gravenstein, R. S. Newbower, A. K. Ream, and N. T. Smith, *Essential Noninvasive Monitoring in Anesthesia*. New York: Grune & Stratton, 1980, p. 63.



Harry Herscovici (SM'79) was born in Romania in 1928. He received the B.S. and M.S. degrees in electronics engineering from the Polytechnical Institute of Bucharest, Bucharest, Romania, in 1952 and the Ph.D. degree in electronics engineering from the Polytechnical Institute of Iassy, Romania, in 1973.

From 1951 to 1963 he was with the Institute for Research in Electrical Engineering, Bucharest, as the Head of the Research Department in Electronic Industrial Instruments and from 1963

to 1977 with the Institute for Research and Design in Automation, Bucharest, where he headed the Research Department in Process Control Instrumentation. Since 1978 he has been with Cordis Corporation, Miami, FL, where he holds the position of Principal Research Engineer in the affiliate Cordis Research Corporation. In 1985 he was appointed Adjunct Associate Professor in the Department of Biomedical Engineering, University of Miami, Coral Gables, FL. He is the author of several books, several patents and about 30 technical papers in the field of applied electronics. His main interest at the present time are cardiac pacemakers with special features and noninvasive instrumentation for the assessment of the circulatory system.



Dean H. Roller was born in New York City in 1949. He received the B.S. degree in biological sciences from the Massachusetts Institute of Technology, Cambridge, in 1970 and the M.D. degree from the University of Pennsylvania, Philadelphia, in 1974. His cardiovascular fellowship training was obtained at Yale University, New Haven, CT.

Since 1979 he has been Associate Director of the Cardiovascular Laboratory at South Miami Hospital, Miami, FL.

Dr. Roller is a Fellow of the American College of Cardiology and Fellow on the Clinical Council of Cardiology of the American Heart Association, as well as a member of numerous other professional societies.

Ref. (9)

Technical note

Pulse arrival time as a method of obtaining systolic and diastolic blood pressure indirectly

Keywords—Blood pressure, Pulse-arrival-time method

1 Introduction

If the peripheral arterial pulse is easily detected and with the standard cuff method, it permits determination of systolic pressure, i.e. cuff pressure for pulse appearance during cuff deflation. To date, it has not been possible to obtain diastolic pressure using the peripheral pulse by seeking a transition in waveform or amplitude. However, if attention is focused on the instant in the cardiac cycle when the pulse appears, it is possible to obtain diastolic pressure. This short technical note describes the principal and typical results using normo-

hyper- and hypotensive dogs.

The principle underlying the pulse-arrival time (p.a.t.) method is illustrated in Fig. 1a using a sine wave to simulate blood pressure and a line with a negative slope to simulate decreasing cuff pressure. Note that as cuff pressure falls from above systolic pressure the distal pulse appears earlier and earlier in the cardiac cycle ($\Delta T_1, \Delta T_2$). Finally, when cuff pressure falls below diastolic pressure (at ΔT_n), the pulse no longer appears any earlier in the cardiac cycle. Therefore, a plot of cuff pressure against pulse arrival time (ΔT) provides transitions which identify both systolic and diastolic pressures as shown in Fig. 1b.

Implementation of the p.a.t. method requires the availability of a constant time reference in the cardiac cycle; two such references exist: the R wave of the e.c.g. or an arterial pulse detected at any convenient site. To illustrate the potential of the p.a.t. method to indicate systolic and diastolic pressures, studies were carried out using five dogs with both timing references.

Anesthetised dogs were used and a disposable infant blood-pressure cuff (4.3 x 11 cm) was applied to the forelimb. The ipsilateral and contralateral radial arteries were cannulated for recording pressure. Cuff pressure and the e.c.g. (lead II) were also recorded on a high-speed strip-chart recorder (Gould, Inc., Cleveland, Ohio, USA). The records were measured with a time resolution of about 2 ms. The point of positive slope, i.e. the beginning of pulse upstroke, was used for measurement as shown in Figs. 2 and 3.

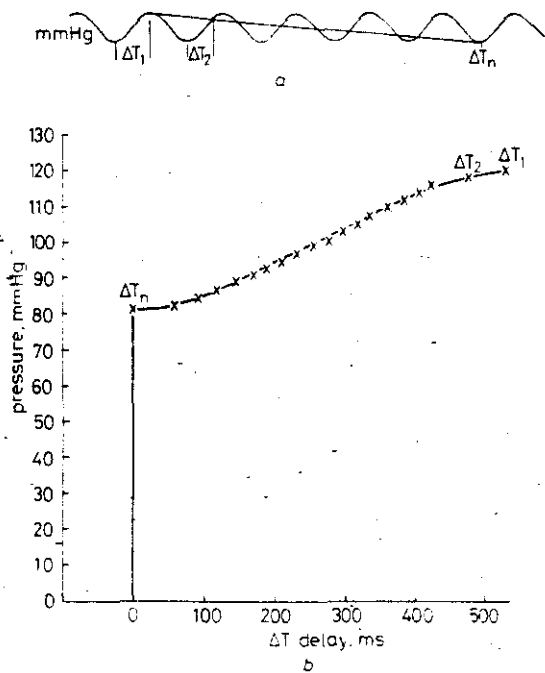


Fig. 1 Principle employed in the pulse-arrival time (p.a.t.) method for measuring blood pressure indirectly. (a) illustrates a sine wave used to simulate blood pressure and the line with the negative slope simulates cuff pressure. As soon as the cuff pressure falls below systolic pressure the pulse breaks through at a time T . As cuff pressure falls, the pulse breaks through earlier and earlier in the cardiac cycle ($\Delta T_2 - \Delta T_n$). A plot (b) of cuff pressure against delay (ΔT) allows identification of systolic and diastolic pressures which correspond to ΔT_1 and ΔT_n .

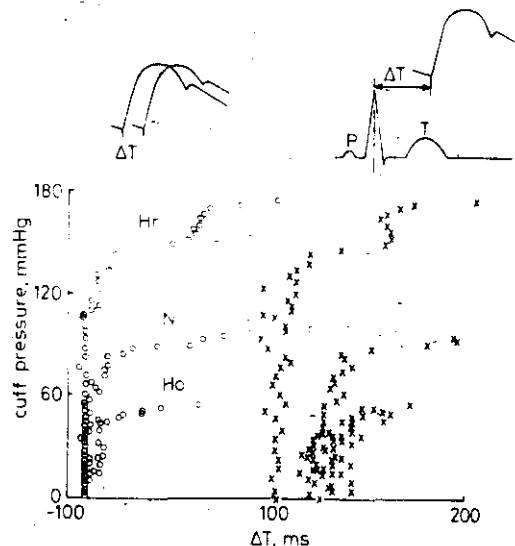


Fig. 2 Relationship between cuff pressure and pulse-arrival delay time (ΔT) using an arterial pulse (left) and the R wave of the e.c.g. (right) as timing references in a normotensive dog.

First received 18th September 1980 and in final form 17th March 1981
0140-0118/81/050671-02\$01.50/0
© IFMBE 1981

The protocol involved consisted of quickly inflating the cuff well above suspected systolic pressure, then cuff pressure was decreased slowly, e.g. 1 mm Hg/heart beat. Pulse arrival time was measured using the R wave of the electrocardiogram as timing references. Blood pressure was measured by noninvasive, direct, intra-arterial, and by a cuff technique.

Typical results of cuff pressure against pulse arrival time in the normotensive dog using the R wave and contralateral pulse as timing references are shown in Fig. 2. Note that the use of either timing reference provides identification of systolic and diastolic pressures. Fig. 3 presents results in a

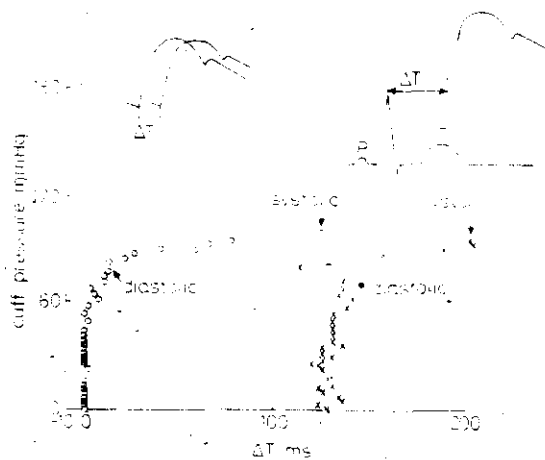


Fig. 3 Relationship between cuff pressure and pulse-arrival time (ΔT) in a normo (N), hyper (H), and hypotensive (Ho) dog using the arterial pulse (left) and the R wave of the e.c.g. as timing references

typical normo-, hyper- and hypotensive dog. The results indicate the use of the R wave of the e.c.g. as a timing signal provides data with much more scatter than is obtained when using an arterial pulse for timing.

The fact that use of the e.c.g. as a timing reference provides data with considerable scatter is not surprising when one considers the time interval which consists of a portion of the time required for the spread of excitation over the ventricles, the period of isovolumic contraction, and the pulse-transit time from the aortic valve to the artery under the blood pressure cuff. Of these times, the isovolumic period is the most variable. Use of the contralateral pulse as a timing reference eliminates this variable, as well as any change due to pulse-wave velocity, which is known to increase with increasing blood pressure. Thus, the method of using a pulse wave for timing should be designated the differential pulse-arrival time method.

2 Conclusion

A new method has been described which permits identifying systolic and diastolic pressures indirectly. The method is based on the breakthrough time of the pulse beyond the cuff. Direct arterial lines were used in this study to demonstrate the principle. The method can be possibly applied using two arterial pulse pickups, one located just beyond the cuff and the other at any other convenient site. Piezoelectric, photoelectric or impedance pulse detection are all candidates for this application. A second paper will show how accurate the method is with two skin-surface transducers.

L. A. GEDDIS
M. VOLZ
S. JAMES
D. REISER

Biomedical Engineering Centre
Purdue University
West Lafayette, IN 47907 USA

Ref.(10)

M. Yamakoshi, A. Hasegawa, T. Kawanishi, Y. Koshi

Department of Applied Informatics, Faculty of Engineering, Kansai University, Suita, Osaka, Japan
565-0871

H. Shimizu, H. Ito

Department of Biology, Faculty of Education, Kansai University, Suita, Osaka, Japan
565-0871

Abstract A microprocessor-based instrument designed with a view to the long-term ambulatory monitoring of indirect arterial pressure in the upper extremities was developed using a volume-oscillometric technique. For the purpose of the study, features such as (1) program-controlled cuff pressure, (2) detection of the systolic end-point and the point of maximum amplitude of arterial volume pulsations, (3) reading of the cuff pressures corresponding to those two points, (4) integration, and (5) recording of the systolic and mean pressure together with heart rate on a digital memory-integrated circuit were performed automatically. A validation study, which was first, performed and analysed by a conventional person, and then, by the instrument, and ambulatory monitoring were carried out. With this instrument non-invasive and accurate monitoring of arterial pressure could be made in unrestricted subjects during daily activities.

Keywords: Microprocessor-based portable instrument, Noninvasive, Long-term monitoring, Systolic and mean arterial pressure, Volume-oscillometric method

Med. & Biol. Eng. & Comput., 1995, 23, 469-485

1 Introduction

MEASUREMENTS of arterial blood pressure are influenced by numerous factors such as

- (a) position
- (b) environmental conditions
- (c) body position
- (d) physical and mental activities

and it may fluctuate considerably. In addition, there exists a circadian rhythm. Much effort, therefore, has been made to devise a technique which allows ambulatory monitoring of blood arterial pressure in unrestricted subjects during daily activity and work (BACHMANN and KEMMICH, 1981). For this purpose, there is a need to design a very compact and handy instrument.

We have previously proposed a new volume-oscillometric method for the indirect measurement of systolic and mean arterial pressure, and demonstrated its accuracy and validity through *in vitro* and *in vivo* studies using excised arterial segments and human fingers (YAMAKOSHI *et al.*, 1982a,b). This method, unlike other conventional cuff-oscillometric methods (GIBSON, 1970; RAMSEY, 1979; YILDIZ, 1980 and BACHMANN, 1981), designed to measure arterial pressure by detecting the arterial volume pulsations using a

photoplethysmograph which is placed just below the cuffing cuff. From the considerations of its practical use (YAMAKOSHI *et al.*, 1982b), it has been suggested that it is possible to construct an instrument based on this method more simply and compactly compared with a conventional commercially available arm-cuffing cuff sphygmometers.

The present paper describes a microprocessor-based instrument equipped with a microprocessor, which was designed for long-term ambulatory monitoring of indirect arterial pressure using this method. The operation and evaluation of the instrument and examples of ambulatory monitoring are also presented.

2 Materials and methods

2.1 Description of the instrument

In this instrument for the long-term ambulatory monitoring of systolic and mean arterial pressure in the upper extremities together with heart rate at a defined interval, all the necessary procedures are carried out automatically. The procedures are

- (a) control of cuff pressure
- (b) detection of the systolic end-point and the point of maximum amplitude of arterial volume pulsations
- (c) reading of the cuff pressure corresponding to those two points
- (d) processing
- (e) recording of the data

Correspondence should be addressed to Dr. Yamakoshi.

- (b) a microprocessor-based central processing and recording (CPVS) unit with microcomputer for sequential control and data storage
- (c) a data reproducing and analysing (DRA) unit using a conventional personal computer.

The former two units are carried by a subject during the measurement. The details of each unit are described below.

2.2.1 CPVS unit This unit is for controlling the cuff pressure and for detecting the vascular volume pulsation, comprising

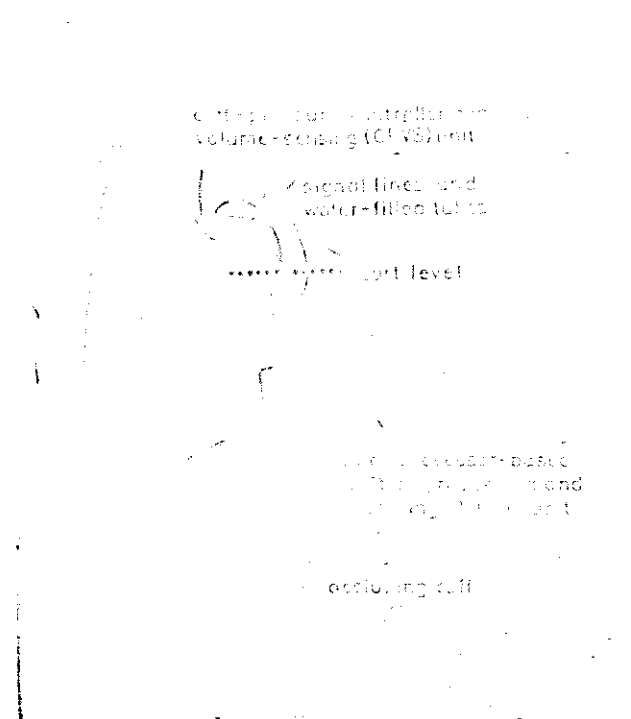


Fig. 1 Photograph of the portable instrument for the long-term ambulatory monitoring of indirect arterial pressure carried by a subject

divided into three parts: the pressure controller, the photoplethysmograph for detecting the pulsating vascular volume and the vascular volume pulsation.

The cuff is composed of a thin-walled cylinder (24 mm inner diameter, 120 mm long and 1.5 mm thin-walled (0.1 mm) rubber tube, tripping valve, inner diameter and 120 mm long) which is fixed on the cylinder and its flange is firmly fixed at both ends of the cylinder by a pair of acrylic caps so as not to deform the cylinder during the application of the cuff pressure. The bottom of the cylinder and the tube is filled with water. The tube is filled with water by applying counterpressure hydraulically. The flange through the cuff which is firmly fixed by an aluminium ring to reduce artefacts due to finger movements.

Two side connections are placed on the cylinder for controlling the cuff pressure. The cuff pressure is controlled by a micro-roller pump (total diameter and 50 mm long; flow rate 0.8 ml/min) driven by a miniature DC motor and measured by a pressure transducer (linearity, 0-300 mm Hg to within 0.5 per cent scale) connected to the cuff through a water-filled chloride tube (0.5 mm inner diameter).

This unit containing the pressure transducer is carried in a breast pocket of the subject which is fixed at heart level. The change in hydrostatic pressure due to the difference in height between the measuring site and the heart level is corrected to obtain the indirect arterial pressure at heart level.

The photoelectric plethysmograph comprises three parallel-connected infra-red light-emitting diodes (LEDs) as a light source and two parallel-connected phototransistors as a photodetector. The arrangements and dimensions of the LEDs and PTs are shown in Fig. 2. They are placed on the dorsal and palmar side of the basal phalanx, respectively, and fixed directly on the skin using pieces of adhesive tape. It was taken not to overlap the finger segment with the tape. The output signal from PT is led to an AC amp (time constant 1 s, cutoff frequency 10 Hz) to obtain the pulsatile component of the photoplethysmograph (PPG).

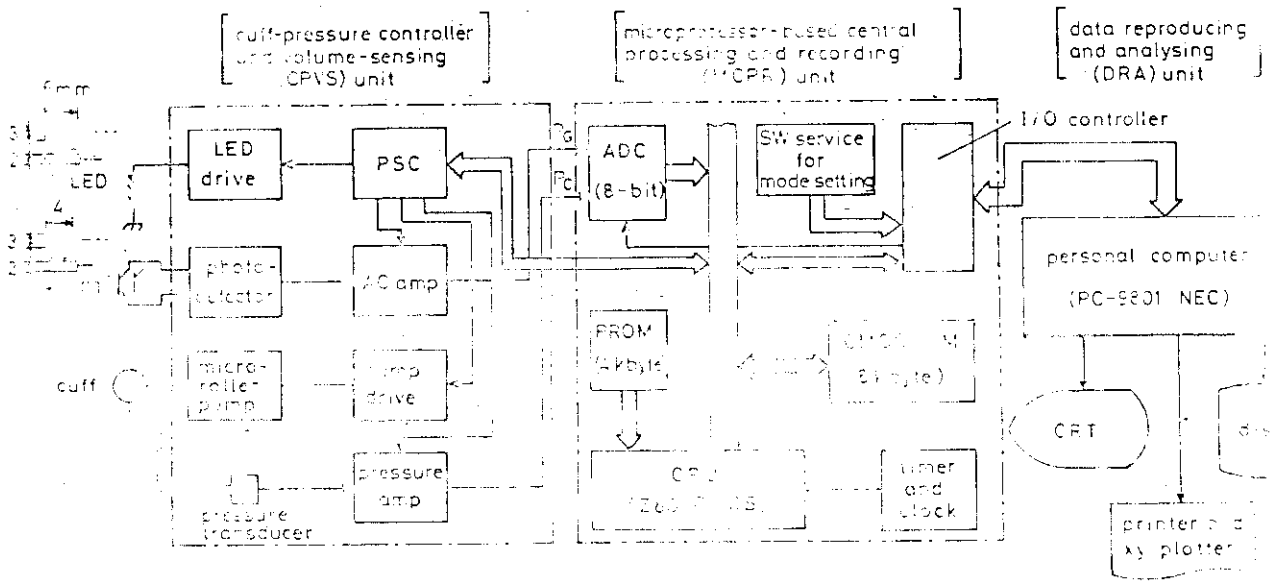


Fig. 2 Diagram of the instrument. The cuff pressure is controlled by a micro-roller pump driven by a miniature DC motor. The output signal from the photoelectric plethysmograph (PEP) is led to an AC amp (time constant 1 s, cutoff frequency 10 Hz) to obtain the pulsatile component of the photoplethysmograph (PPG).

- (c) detection of the systolic end-point (P_{cs}) and the point showing the maximum value of PG_p (PG_{pmax})
- (d) processing of the systolic (P_{cs}) and mean pressure (P_{cm}) corresponding to the respective two points and heart rate (HR) in the memory (RAM, 8 kbyte CMOS).

Interactive software for these procedures using a central processing unit (CPU, Z80 CMOS) and a programmable read-only-memory element (PROM, 4 kbyte) is provided in this unit.

The sequence of operation of this system is illustrated by the timing chart shown in Fig. 3. Following a start signal, voltage is sequentially supplied to each part of the two units from a power supply controller (PSC), then the cuff pressure (P_c) is raised from a preset lower pressure level ($P_{cmin} = 20$ or 40 mm Hg) to a preset upper pressure level ($P_{cmax} = 160$, 200 or 250 mm Hg). When PG_p is detected at the preset upper level, P_c is both raised and PG_p disappears. After P_{cmin} the upper level or the disappearance of PG_p is confirmed, P_c is decreased rapidly until PG_p appears again (a-b mode operation). Then P_c is gradually raised for 2 s to confirm again the disappearance of PG_p (b-c mode operation). The successive two (a-b and b-c) operations are necessary to ascertain whether the PG_p signals detected are effective to determine the systolic pressure or not.

After the b-c mode operation, P_c is decreased gradually at a rate of 2-4 mm Hg per heart beat. During this stage the first appearance of PG_p ($PG_{p(1)}$ in Fig. 3) is detected to serve as the systolic end point (SEP). The indirect systolic pressure P_{cs}

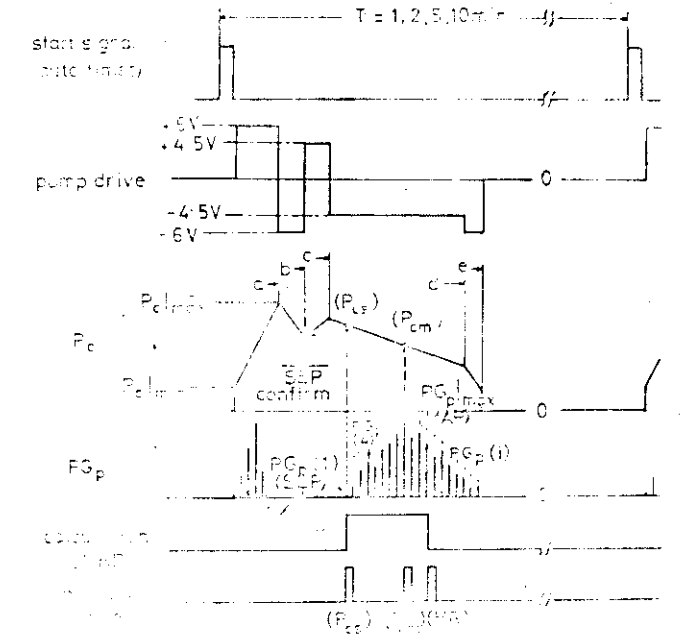


Fig. 3. Sequence of operations for the indirect systolic pressure measurement.

is determined by the first appearance of PG_p ($PG_{p(1)}$ in Fig. 3). The indirect diastolic pressure P_{cd} is determined by the last appearance of PG_p ($PG_{p(i)}$ in Fig. 3). The indirect mean pressure P_{cm} is determined by the point showing the maximum value of PG_p (PG_{pmax} in Fig. 3). The indirect heart rate (HR) is determined by the number of heart beats during the measurement interval T (min) by the equation $HR = n/T \times 60$ (beats/min).

The values of P_{cs} , P_{cm} and HR are stored in the memory in the order to store the data element. After the end of these three data, P_c is decreased gradually to the lower pressure level (P_{cmin}) (c-d mode operation).

Less than 30 s are required for each measurement interval T can be selected by the measurement interval at 1, 2, 5, or 10 min. The size of this unit is $170 \times 70 \times 30$ mm. Its weight is approximately 250 g. It is made of three modules which provide measurement 30 h at 1.5 h interval.

2.2.3 DR 1-ml. This unit is for reproducing and storing the data stored in the RAM element within the microcomputer unit. The MCPR is connected to a personal computer via an appropriate interface provided to perform data retrieval from the memory. The values of each set of stored data are transferred to the computer, and then processed to obtain the histograms of P_{cs} , P_{cm} and HR . The maximum, minimum and mean values of these data together with variance are also computed. Certain additional statistical data are also available. At the end of the run, these results can be shown on a cathode-ray tube display together with a histogram using an xy plotter before being stored on an 8 in floppy

2.3 Evaluation: subjects and methods

More than 24 h of continuous recording of indirect systolic pressure and HR by this instrument has been successfully performed in 25 subjects (20 males, 20-45 years of age, females, 28-38 years old). Mostly the left fourth intercostal space was used as a measuring site. The subjects lived their normal life.

First, the reliability and accuracy of the stored data were evaluated through the simultaneous comparison of the respective values (P_{cs} , P_{cm} and HR) determined from the raw signals of the photoplethysmography with the direct and end pressure. The experiment was conducted in two intensively and three hypotensive subjects. The experiment of the indirect arterial pressure measurement in hypertensive subjects was also made in two normotensive subjects using an indirect method. The indirect arterial pressure was also made in two normotensive subjects using a two-channel portable cassette cassette recorder (channels 1 and 2 DC).

The main aim is to detect the relationship between the indirect systolic pressure (P_{cs}) and the indirect diastolic pressure (P_{cd}) and the indirect mean pressure (P_{cm}).

$$P_{cs} = P_{cd} + 1.33(P_{cm} - P_{cd})$$

The indirect systolic pressure (P_{cs}) and the indirect diastolic pressure (P_{cd}) are related to the indirect mean pressure (P_{cm}) by the equation:

$$P_{cs} = P_{cm} + 1.33(P_{cm} - P_{cd})$$

The cuff signal was also simultaneously recorded in order to confirm whether the PG signal was recorded as an artefact or not. The subject carried both the CPVS and MCPR units together with the data recorder in the experiment. Average recording time and the measurement interval in each subject were 2 h and 5 min, respectively. After the measurements the recorded raw signals in the data recorder were reproduced by a playback system. From the playback recordings the cuff pressures corresponding to the systolic end-point (P'_{cs}) and to the point of the maximum amplitude (P'_{cm}) of the PG signal were manually determined together with the heart rate (HR') read from the ECG signal. These values (P'_{cs} , P'_{cm} and HR') were compared with the respective stored digital values (P_{cs} , P_{cm} and HR) calculated by the MCPR unit.

For the comparison with the direct measurement, a catheter was inserted into the left brachial artery at the medial side of the cubital fossa (the catheter tip in the artery was placed 3.5 cm proximal to the insertion point) and connected to a Statham P-37 pressure transducer. The direct brachial arterial pressure P_a was recorded in the data recorder via a pressure amplifier. The catheter and transducer were fixed with a bandage to the left arm using a pad. The subject was allowed to walk around the ward. At least 25 simultaneous measurements were made for each subject. A trend display against time showing the simultaneous data of the indirect systolic (P'_{cs}) and mean (P'_{cm}) pressures determined manually from the raw signals and the corresponding direct systolic (P_{as}) and mean (P_{am}) pressures was obtained from three subjects after the measurements.

The performance, practicability and convenience in use for

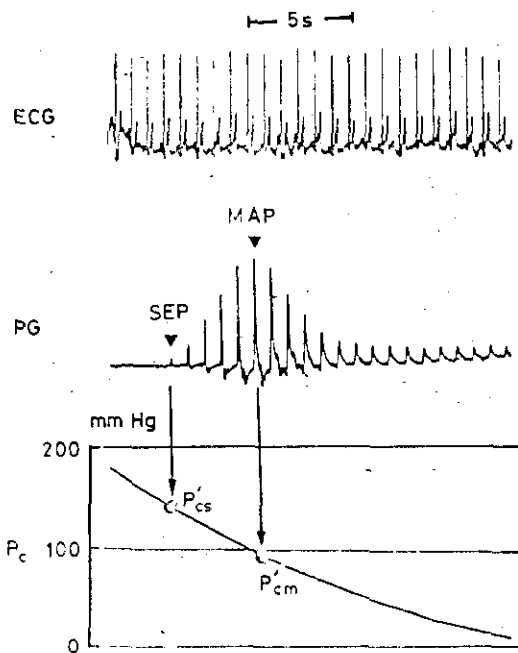


Fig. 4 Playback writout of a single recording showing ECG, photoplethysmographic pulsating signal PG and cuff pressure P_c obtained from the left fourth finger of a healthy subject and recorded in a cassette data recorder. SEP and MAP indicate the systolic end-point and the point of maximum amplitude of the PG signal, respectively. Indirect systolic (P'_{cs}) and mean pressure (P'_{cm}), which were manually determined from the values of cuff pressure, correspond to the P_{cs} and P_{cm} , respectively. The R-R interval of the ECG is the same as that of the heart-beat peak point of PG. The P_{cs} and P_{cm} are the values of cuff pressure corresponding to the

point of the maximum amplitude of the PG signal.

Fig. 5 shows typical playback recordings of simultaneous measurements showing the simultaneous recordings of ECG, photoplethysmographic pulsations PG and cuff pressure P_c obtained from the left fourth finger in a healthy subject. Both the systolic end-point (SEP) and the point of the maximum amplitude (MAP) of the PG signal were obtained, and the values of the cuff pressure corresponding to these two points (P'_{cs} and P'_{cm}) were determined manually.

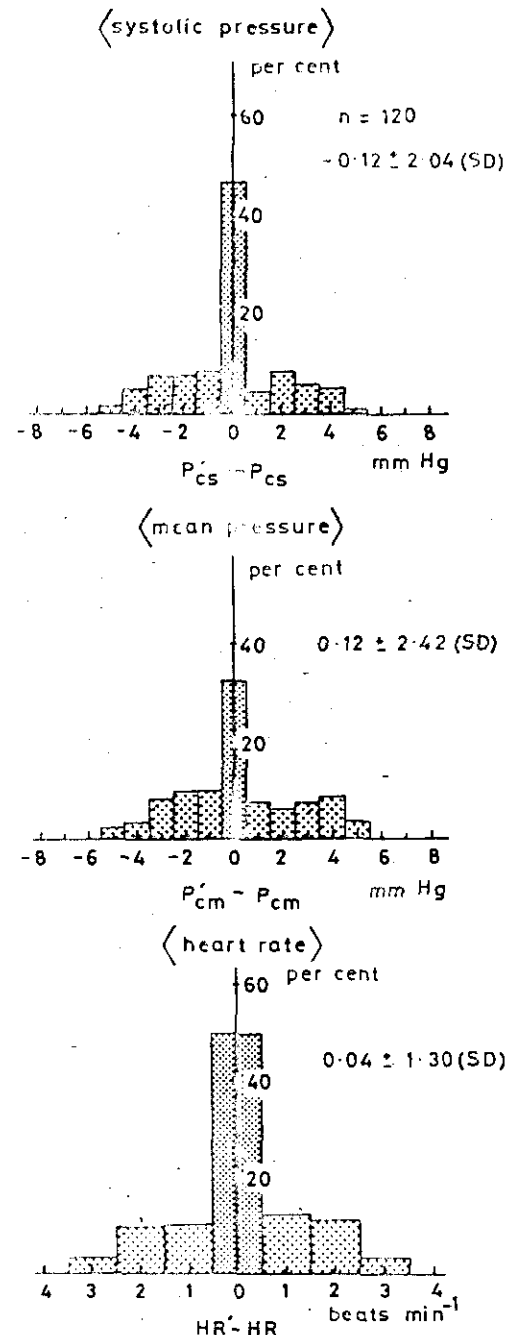


Fig. 5 Error histograms of the differences of systolic and mean pressure (middle part) and heart rate (bottom part) between the values determined manually (P'_{cs} , P'_{cm} and HR') and the values of systolic and mean pressure and heart rate, respectively, determined from the raw signals of photoplethysmographic pulsations and ECG recordings. The data were obtained from 120 measurements of P'_{cs} , P'_{cm} and HR' from three subjects. The P_{cs} , P_{cm} and HR are the values of cuff pressure and heart rate, respectively, calculated by the instrument.

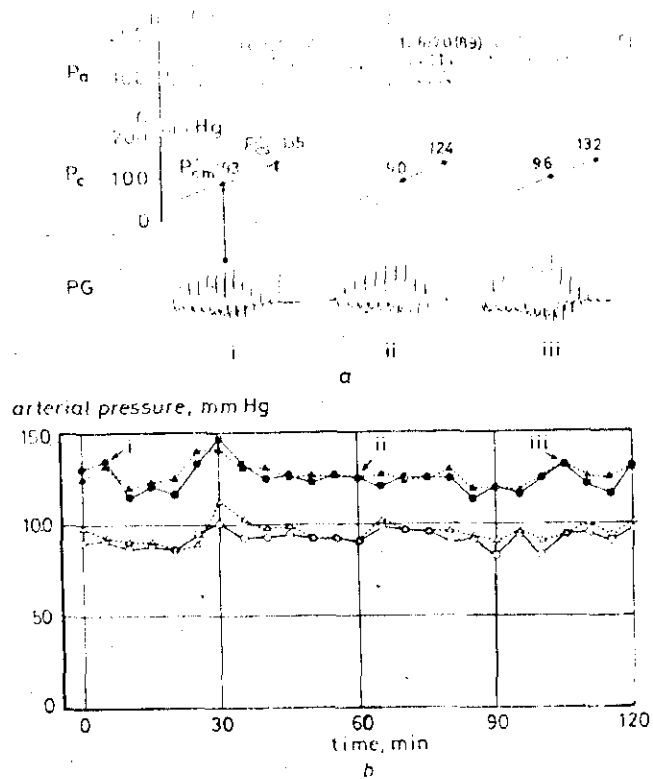


Fig. 6 (a) Three representative playback recordings of left brachial direct arterial pressure P_a , cuff pressure P_c and photoplethysmographic pulsations PG obtained from the left fourth finger of a catheterised subject. (b) The values of indirect systolic (P'_{cs} , ●) and mean pressure (P'_{cm} , ○) determined manually and corresponding direct (P'_{as} , ▲) and mean pressure (P'_{am} , △) at the respective times are plotted against time, showing the volume-oscillometric method used in this instrument to permit accurate tracking of arterial pressure. The data plots indicated by i, ii and iii in this graph correspond to the respective pressure values obtained from the recordings presented in (a)

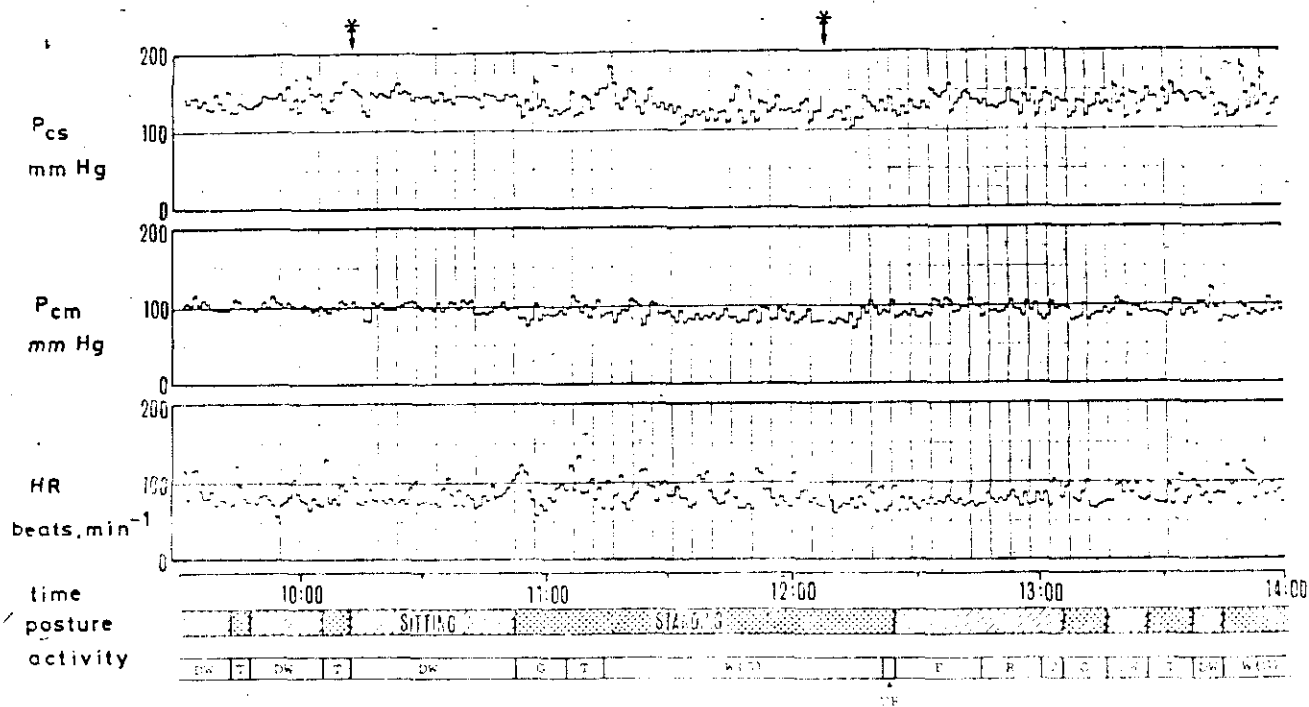


Fig. 7 Part of the ambulatory monitoring of indirect systolic P'_{cs} and mean pressure P'_{cm} and heart rate HR . This monitoring was carried out for 4.5 h (9.30 a.m.–2.00 p.m.) at 1-min intervals. The subject's postures and activities are shown in the lower part of the figure. The two asterisks at the top indicate the times of a telephone call and a cigarette. DR: driving; DW: drinking; G: walking; I: telephoning; L: eating; R: resting; U: walking

correlation coefficients between P'_{cs} and P'_{as} , P'_{cm} and P'_{am} were 0.997 and 0.994, respectively, obtained from the correlation coefficient between the values of P'_{cs} , P'_{cm} and HR range from 1.00 to 1.00. The mean \pm SD of P'_{cs} and P'_{cm} were 133 ± 27 mm Hg (mean \pm SD) and 101 ± 20 mm Hg (mean \pm SD) and from 55 to 140 min^{-1} (79 ± 20 beats min^{-1}) respectively. The mean values of the difference between these paired values ($P'_{cs} - P'_{as}$, $P'_{cm} - P'_{am}$ and $HR - HR'$) were -0.17 ± 0.27 (SD) mm Hg, 0.12 ± 0.42 (SD) mm Hg and 0.04 ± 1.17 (SD) beats min^{-1} , respectively. The linear regression equations and correlation coefficients (r) between these were $P'_{as} = 0.987 P'_{cs} + 1.70$ ($r = 0.997$), $P'_{am} = 1.01 P'_{cm} - 0.17$ ($r = 0.994$) and $HR = 0.993 HR' + 0.48$ ($r = 0.991$). The paired values determined manually and automatically agreed well within 5 mm Hg in systolic and mean pressures and within 3 beats min^{-1} in heart rate.

Fig. 6a shows three examples of the playback recordings of the left brachial direct arterial pressure P_a , cuff pressure P_c and photoplethysmographic pulsations PG obtained from the left fourth finger of a subject. In Fig. 6b the results of indirect systolic (P'_{cs} , ●) and mean pressure (P'_{cm} , ○) determined manually and corresponding direct systolic (P'_{as} , ▲) and mean pressure (P'_{am} , △) at respective times are plotted. These data plots, indicated by i, ii and iii in Fig. 6b, correspond to the respective pressure values obtained from the recordings (i, ii and iii) presented in Fig. 6a.

For all three subjects in whom catheterisation was performed, a good agreement between the indirect finger and the direct brachial arterial pressures was observed although there are differences in pressures of approximately 5–7 mm Hg, which is presumably due to the difference in the recording sites and/or the hydraulic obstruction produced by the insertion of the catheter (YAMAKOSHI *et al.*, 1982; 1982b).

3.2 Examples of long-term monitoring

Two examples of the long-term monitoring by this

comparative measurements. The effect of the normal daily life and work during the measurement. In the lower part of this figure the postures and activities of the subject are also indicated. The two asterisks in the upper part of the unmeasurable data caused by the failure to discriminate the systolic end point and of the maximum amplitude of PG_p . The changes in these three variables following posture changes, the various conditions of physical activities, and mental stresses are well recorded.

Fig. 8a shows a trend chart of a 24 h monitoring (5 min intervals) of P_{cs} , P_{cm} and HR obtained from the left fourth finger of another healthy subject. The histograms of these three variables throughout the period of the measurement are also shown in the lower panel (Fig. 8b). The unmeasurable data are given by the asterisks and the subject's posture and activity are shown in the lower part of the trend chart. It also demonstrates that the changes in these three variables following the changes in the subject's behaviours are well recorded. Their circadian rhythms are also clearly observed: during awakening, the values of P_{cs} , P_{cm} and HR showed considerable fluctuations at high levels ranging from

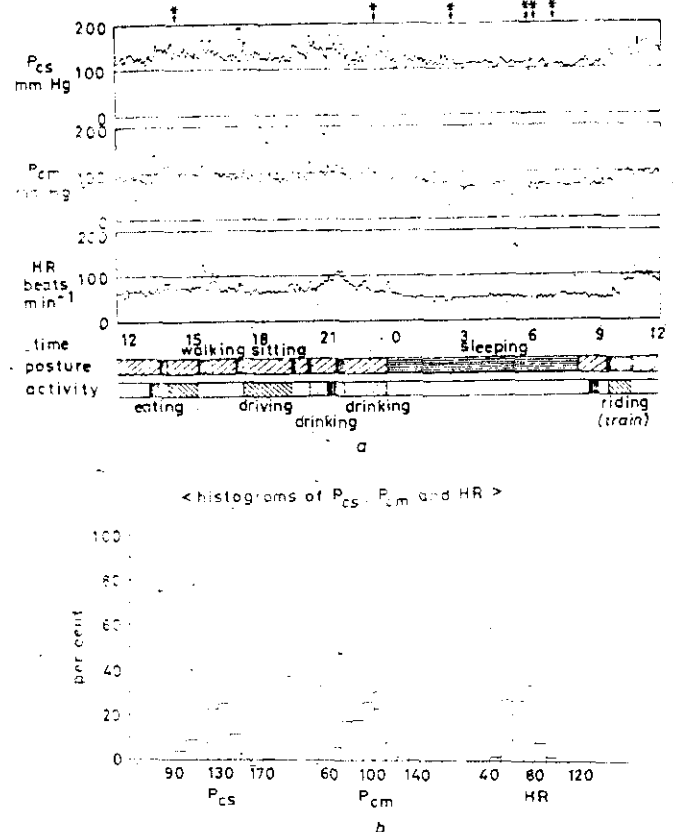


Fig. 8 (a) Trend chart of a 24h monitoring (5 min intervals) of indirect systolic pressure P_{cs} and mean pressure P_{cm} and heart rate HR obtained from the left fourth finger of another healthy subject, and (b) the histograms of these three variables throughout the period of measurement. The unmeasurable data points are indicated by the asterisks, and the subject's behaviour is given in the lower part of the trend chart. See text for further explanation.

	P_{cs}	P_{cm}	HR
Maximum	172	133	126
Minimum	93	63	42
Mean	125	92	66
Standard deviation	30	20	14

Validity of the present method

The results obtained in the present study demonstrate the present instrument is able to measure the indirect arterial pressure in the finger arteries with accuracy and stability comparable to the standard method of daily activity and work.

In daily clinics, blood pressure is generally measured at the brachial artery by the auscultation method. In this study we tentatively adopted the finger artery as the measuring site for the long-term monitoring of blood pressure. The measurements could probably be performed with the subjects' being scarcely affected by the discomfort which has been reported during long-term monitoring using an arm-occluding cuff instrument.

In addition, as the digital-memory integrated circuit was used to store the data, a conventional personal computer could be used to reproduce the data and perform necessary data analyses promptly. In this sense the instrument seems to be more practicable and advantageous than another method for monitoring arterial pressure.

The important points relating to the accurate measurement of arterial pressure by this instrument are summarized as follows.

- (i) proper location of the photoplethysmographic transducer
- (ii) appropriate size of the occluding cuff
- (iii) exact determination of the point of maximum amplitude and the systolic end-point of the photoplethysmographic pulsation.

Inappropriate cuff size with improper location of the transducer will make it impossible to obtain the characteristic change in the amplitude of the pulsations following the gradual change in the cuff pressure. Thus the point of maximum amplitude and/or the systolic end-point cannot be clearly discriminated, causing a large measurement error (YAMAKOSHI *et al.*, 1982b). The present study was carried out carefully avoiding error due to the location of the transducer (YAMAKOSHI *et al.*, 1982b; see the discussion in YAMAKOSHI *et al.*, 1983) the transducer was located just at the middle part of the cuff. Another factor causing measurement error is the cuff width (YAMAKOSHI *et al.*, 1982b). We used a cuff width ranging from 1.3 to 1.5 times the diameters of the finger segments. Therefore the clear characteristic change in the amplitude of the pulsations was obtained to discriminate both the point of maximum amplitude and the systolic end-point.

There are unmeasurable states which are mainly caused by shaking the hand vigorously during the measurement. This results in an uncertainty in distinguishing the photoplethysmographic pulsating signal markings. Although this occasionally appeared as shown in the examples of Figs. 7 and 8, it was not very disadvantageous in practical long-term monitoring.

The change in vasoconstrictive tone in the finger arteries during the measurement may be another causative factor of measurement error (YAMAKOSHI *et al.*, 1980; 1982b). This should be minimal, in so far as the detected photoplethysmographic signal is produced mainly by the blood volume pulsations in such finger arteries. Although we have not assessed this problem through this study, the factor would be less effective considering the experimental conditions. In fact, there is a remarkably good correlation between the indirect arterial pressures measured by this method and the

brachial arterial pressures. It may also be supported by the fact that the present results were successfully obtained under various conditions which would change the vasoconstrictive tone.

Several instruments similar to this have recently been developed using the auscultation method in the upper arm. One was proposed by HINMAN *et al.* (1962), and it was technically improved by SCHNEIDER (1968) and SCHNEIDER *et al.* (1974). This consists of a conventional arm-occluding cuff with a microphone for detecting Korotkoff sound, compressed-air source for supplying cuff pressure, a portable tape-recorder for the sound and cuff pressure and a sequential controller for the measurement. Although this is one of the useful methods of ambulatory monitoring of the indirect arterial pressure, there remain serious practical problems such as

- (i) considerable discomfort produced by long-term measurement using the upper arm as a measuring site
- (ii) the need for a large-capacity air source and electric power
- (iii) cumbersome procedures for playback processing to obtain the results
- (iv) large size and heavy weight.

The instrument described here was designed to overcome these drawbacks.

In conclusion, this instrument for the long-term ambulatory monitoring of indirect arterial pressure appears to have good operating characteristics and to be one of the most helpful and useful means of measuring momentary variations of arterial pressure.

Acknowledgment -The authors wish to thank Mr. S. Onuma, President, M.E. Commercial Corp., Tokyo, Japan, for their assistance in constructing the instrument, Professor K. Tsuchiya, Department of Mechanical Engineering, Waseda University, and Professor T. Togawa, Institute for Medical & Dental Engineering, Tokyo Medical & Dental University, for their valuable criticism.

References

- BACHMANN, K. and KIMMICH, H. P. (1981) (Eds.) Ambulatory monitoring of blood pressure. In *Biotelemetry Patient Monitoring*, 8, 1-120.
- GEDDES, L. A. (1970) *The direct and indirect measurement of blood pressure*. Year Book Medical Publishers, Chicago, 196.
- HINMAN, A. T., ENGEL, B. T. and BICKFORD, A. F. (1962) Portable blood pressure recorder: accuracy and preliminary use in evaluating intradaily variations in pressure. *Am. Heart J.*, 63, 663-668.
- RAMSEY, M. III (1979) Noninvasive automatic determination of mean arterial pressure. *Med. & Biol. Eng. & Comput.*, 17, 11-18.
- SCHNEIDER, R. A. (1968) A full automatic portable blood pressure recorder. *J. Appl. Physiol.*, 24, 115-118.
- SCHNEIDER, R. A., KIMMELL, G. O. and VAN METER, R. P. Jr. (1974) An improved fully automatic portable blood pressure recorder. *Ibid.*, 37, 776-779.
- YAMAKOSHI, K., SHIMAZU, H. and TOGAWA, T. (1980) Indirect measurement of instantaneous arterial blood pressure in the human finger by the vascular unloading technique. *IEEE Trans., BME-27*, 150-155.
- YAMAKOSHI, K., SHIMAZU, H., SHIBATA, M. and KAMIYA, A. (1982a) New oscillometric method for indirect measurement of systolic and mean arterial pressure in the human finger. Part I: model experiment. *Med. & Biol. Eng. & Comput.*, 20, 307-313.
- YAMAKOSHI, K., SHIMAZU, H., SHIBATA, M. and KAMIYA, A. (1982b) New oscillometric method for indirect measurement of systolic and mean arterial pressure in the human finger. Part 2: correlation study. *Ibid.*, 20, 314-318.
- YAMAKOSHI, K., KAMIYA, A., SHIMAZU, H., ITO, H. and TOGAWA, T. (1983) A new noninvasive method for the measurement of arterial blood pressure using the vascular unloading technique. *Ibid.*, 21, 557-565.

arterial blood pressure using the vascular unloading technique. *Ibid.*, 21, 557-565.

YEEDERMAN, M. and REAM, A. (1979) Indirect measurement of mean blood pressure in the anesthetized patient. *Anesthesiol.*, 50, 253-256.

Authors' biographies



Ken-ichi Yamakoshi is Associate Professor in the Research Institute of Applied Electricity, Hokkaido University, Sapporo. He received the B.Sc. and M.Sc. degrees in Mechanical Engineering from Waseda University, Tokyo, in 1970 and 1972, and Ph.D. degrees from Tokyo Medical & Dental University and Waseda University, Tokyo, in 1979 and 1981, respectively. His current research interests include cardiovascular analysis, noninvasive and ambulatory measurement of physiological information and biomedical transducers.



Hideaki Shimazu received the B.Sc. degree in Mechanical Engineering from Waseda University, Tokyo, in 1973. After graduating he studied biomedical engineering for one year as a student in the Institute for Medical & Dental Engineering, Tokyo. He is currently an assistant professor at the Department of Physiology, Kyorin University School of Medicine, Tokyo. His research interests include bioinstrumentation systems, noninvasive and ambulatory measurement of physiological information.



Atsashi Kawarada was born in Kagawa, Japan, on the 11th May 1958. He received a B.S. degree in Electrical Engineering and an M.S. degree in Biomedical Engineering from Hokkaido University, Sapporo, Japan, in 1981 and 1983, respectively. Since 1983 he has been with the Research Institute of Applied Electricity, Hokkaido University, as a postgraduate student working for a Ph.D. in Biomedical Engineering. His current interests include noninvasive and ambulatory measurement of physiological parameters.



Akira Kamiya was born in Tokyo, Japan, on the 14th May 1938. He received an M.D. degree in Medical Science from the University of Tokyo, Japan, in 1965. From 1965 to 1969, from 1969 to 1971, and from 1971 to 1980 he was a research assistant, an assistant Professor, and an associate Professor, respectively, at the Institute for Medical & Dental Engineering, Tokyo, Japan. Since 1980 he has been with the Research Institute of Applied Electricity, Hokkaido University, Sapporo, Japan, where he is a Professor. His current interests include physiological analyses on cardiovascular system and physiological measurement and analyses on material exchange in microcirculation.



Hiroshi Ito is Professor of the Department of Physiology, Kyorin University School of Medicine. He graduated from Keio University Medical School, Tokyo, with the M.D. degree in 1960. After a one-year internship at the Tokyo 2nd National Hospital, he was a postgraduate student at the Department of Physiology, Keio University Medical School and received the Ph.D. degree in 1965. From 1966 to 1968 he was a postdoctoral research fellow at the Department of Neurology, School of Medicine, University of Utah, USA. His research interests include the noninvasive measurement of arterial blood pressure by the vascular unloading technique and the noninvasive measurement of arterial blood pressure by the impedance method.

Direct blood-pressure measurements: risks, technological evolution and some current problems

Ref. (11)

M. O. Toll

Faculty of Engineering & Applied Science, Memorial University of Newfoundland, St. John's, Newfoundland A1B 3X5, Canada

Abstract—The direct measurement of blood pressure has found widespread use in intensive care units, operating rooms, and in emergency departments. Infection, air embolism and thrombosis are some of the risks to patients associated with both the cannulation procedure and with the apparatus used in the blood-pressure measuring process. Although there is constant revision in an attempt to reduce these risks, they cannot be completely eliminated. The need for direct blood-pressure measurements and the physiological effects of air embolism and thrombosis are reviewed. Infection and problems related to the techniques used to insert the catheters are not discussed.

Keywords—Air embolism, Blood-pressure measurement, Cannulation, Catheterisation, Invasive techniques, Patient monitoring, Thrombosis

Med. & Biol. Eng. & Comput., 1984, 22, 2-5

Vol 22 January 84

#1

Yip...
a/Hough...
1984

for...
general

1 The need for direct blood-pressure measurements

THE direct measurement of blood pressure allows a better assessment of the cardiovascular system through direct quantitative measurements. With this monitoring technique the development of dangerous haemodynamic events can be observed and corrected before they develop into cardiac arrests (KAPLAN, 1979).

To achieve direct blood-pressure measurements it is necessary to insert a catheter directly into the cardiovascular system. This invasive technique has certain risks associated with it, and these must be weighed against the benefits that can be obtained. In many patients with cardiac disease the benefits do outweigh the risks (KAPLAN, 1979).

Blood pressure can be measured from both the venous and the arterial side of the circulatory system. Measurements from each side yield important but different cardiovascular parameters.

Central venous pressure (CVP) reflects the patient's blood volume, venous tone, and right arterial and ventricular pressures. For these pressures to be measured accurately it is necessary to have the catheter in a major vein within the thorax or directly in the right side of the heart (KAPLAN, 1979).

CVP values fluctuate about atmospheric pressure (FLANAGAN *et al.*, 1969), and the level of the right heart is usually taken as the zero reference point from which other pressures are measured.

The CVP indicates right heart and not left heart performance. Therefore it is necessary to monitor left arterial pressure directly with a catheter in the left atrium, or indirectly with a Swan-Ganz catheter in the pulmonary

artery using the pulmonary capillary wedge pressure as an approximation of left arterial pressure (KAPLAN, 1979).

2 Patient risks

Probably the two most important risks associated with patient treatment requiring vascular cannulation and direct pressure monitoring are air embolism and thrombosis.

2.1 Air embolism

Air embolism is the introduction of air into the circulatory system. This can occur as a direct result of diagnostic or therapeutic air insufflation (DURANT *et al.*, 1947; GOTTLIEB *et al.*, 1965), during surgery (MICHENFELDER, 1968), as the indirect result of blood transfusion (RUESCH *et al.*, 1960; YEAKEL, 1968), during drug or nutritional infusion (GRACE, 1977; FLANAGAN *et al.*, 1969) and during direct blood-pressure monitoring (ROSS *et al.*, 1979; ORDWAY, 1974).

Vascular air embolism can occur in both the venous and the arterial portion of the cardiovascular system, but each type has its own characteristic effect on the patient.

Venous air embolism may reduce or stop the flow of blood through the right heart (DURANT *et al.*, 1947) or it may cause neurological complications (GRACE, 1977). The exact amount of venous air which is fatal to humans is not known exactly, but the review paper of GOTTLIEB *et al.* (1965) indicated that it may vary between 300-1600 ml. YEAKEL (1968) described an incident where 200 ml of air admitted to the central venous system during an interval of only a few seconds caused the death of the patient. Animal experiments indicate that the rate of air injection is also important in determining the amount of air that proves lethal (DURANT *et al.*, 1947). The lethal dose of intravenous air for humans is estimated by ORDWAY (1974) to be approximately 200 ml when delivered at a rate of 70-105 ml s⁻¹.

Received 13th June 1983

© IFMBE: 1984

Arterial air embolism achieves its effects through a different mechanism. Air entering the pulmonary vein passes through the left side of the heart into the aorta. Then, depending upon the position of the patient, and hence the aorta, it is possible for the air to rise into the coronary and/or cerebral arteries (BAGDONAS *et al.*, 1960). Air entering these vessels could then obstruct the flow of blood to areas supplied by the vessels. CHASE (1934) showed that air emboli can produce vasoconstriction of the artery, and this can compound the effect of the mechanical obstruction of the smaller vessels caused by the presence of air. Animal experiments have also indicated that air emboli could be better tolerated if it entered into the right common carotid artery (1.0 cm³ per kilogram body weight) than if it entered the innominate artery (0.1 cm³ per kilogram body weight) (GOMES *et al.*, 1973). However, in these studies the rate of air injection was not discussed.

Occlusion of the coronary circulation by an air emboli causes ischaemia and ventricular fibrillation. In dogs, small amounts of air (0.05–1.0 ml) injected into the coronary circulation have been shown to be fatal (DURANT *et al.*, 1949). DURANT *et al.* (1949) also described the neurological characteristics of cerebral air emboli.

2.2 Thrombosis

Thrombosis is the formation of a blood clot in the blood vessel. This can be caused by the presence of the catheter itself and is a common complication of radial artery cannulation (BEDFORD and WOLLMAN, 1973). Non-Teflon catheters appear to be more thrombogenic than Teflon catheters (BEDFORD, 1975), and nontapered 20-gauge Teflon catheters have had the lowest incidence of thrombosis (KIN *et al.*, 1975) in radial artery cannulation.

Any solid particle such as a thrombus or foreign material such as a piece of plastic or glass entering the bloodstream could have similar physiological effects to that of a cerebral or coronary air embolus.

3 Technological evolution of vascular cannulation methods

Technological developments in vascular cannulation methods have been influenced to a large extent by accidents which have occurred during cannulation.

In earlier years blood transfusions used gravity as the driving force for infusing blood into the vein of a patient. However, if the bottle became empty and the infusion tube was not clamped, air could enter the venous circulation (DOYLE and FRODSHAM, 1949). Similar incidents of air embolism caused by containers running dry have been reported for CVP catheters (ORDWAY, 1974), infusion sets (PEDERSEN and HESSOV, 1978) and for intravenous infusion with the aid of a mechanical pump (ABERNATHY and DICKINSON, 1979).

Gravity infusion rates are slow, and under certain conditions the blood must be transferred at a rate faster than that produced by gravity alone. Faster infusion rates can be obtained by pumping air under pressure into the transfusion bottle. However, because of the higher pressures and faster infusion rates, even more vigilance is required to prevent air from entering the circulatory system (RUESCH *et al.*, 1960).

To prevent an intravenous line from becoming full of air RUESCH *et al.* (1960) advocated the insertion of a float valve between the fluid container and the patient. In addition, the authors promoted the use of flexible plastic bags for the storage of blood to prevent any air from entering the infusion system.

With the plastic blood bag, a pressure cuff applied around the bag could be inflated to apply additional pressure to the bag and hence increase the infusion rate. This system was thought to be safe from air emboli since the bag was sealed and no air was injected directly into the bag. When empty, the bag would collapse and no more fluid or air could pass into the patient. However, a case was reported (YEAKEL, 1968) in which air did enter the flexible blood bag and a fatal embolism did occur.

As a safety precaution against air emboli in pressurised systems an air detector attached to the high-pressure infusion line was developed (FELLOWS *et al.*, 1966). However, even with such a system, massive air emboli could occur, and ABERNATHY and DICKINSON (1979) indicated that the placement of the air detector was critical.

Air emboli could also occur during the catheterisation procedure (FLANAGAN *et al.*, 1969; COLOUHOUN, 1977; 1979), by the accidental disconnection of the intravenous catheter at the hub (GRACE, 1977; COLQUHOUN, 1977; 1979) or by the accidental removal of the catheter (ROSS *et al.*, 1979).

To prevent accidental catheter disconnection, a simple retaining fixture was developed (COLQUHOUN, 1977). ROSS *et al.* (1979) developed Luer lock hubs with locking rings to prevent separation of the introducer cannula, the catheter, and the infusion system. However, even the Luer lock hubs with locking rings were not failsafe, and a case was reported where the Luer lock failed to engage the hub of the catheter and the two components fell apart (METCALF *et al.*, 1979).

Depending upon the position of the patient, it is possible that small amounts of air constantly infused, in themselves insufficient to cause complications, might accumulate in either the proximal aorta or major branches. This trapped air might then be released into the cerebral circulation as a large bubble when either a sufficient amount has accumulated or when the position of the patient is changed (BAGDONAS *et al.*, 1960).

In addition to being a hazard to the patient, air in a blood-pressure measuring system can also degrade the quality of the monitored pressure waveform (CARR and BROWN, 1981).

Embolisation due to clots formed in a catheter and being flushed retrograde into the central arterial circulation have been discussed by LOWENSTEIN *et al.* (1971). In their paper the authors indicated that the volume of flush solution required to cause retrograde flow through a radial artery cannulation ranged from 3 to 12 ml. EDMONDS *et al.* (1980) repeated these studies with children and found that the volume of flush solution necessary to produce retrograde flow into the central circulation ranged from 0.3–5.0 ml. They also showed an exponential relationship between the flush volume and the patient height.

To minimise thrombus formation and to prolong the usefulness of the catheter LOWENSTEIN *et al.* (1971), and DOWNS *et al.* (1974) indicated that a constant slow infusion of flush solution rather than a large intermittent injection of the flush solution was the preferred method of keeping the catheter patent (open).

To have a constant and slow infusion rate of flush solution it is necessary to pressurise the fluid reservoir, and to place a flow resistance inline with the infusion line.

One of the earliest constant-flow systems reported in the literature was developed by JOHNSON and ITO (1969). This system used a flexible plastic bag and pressure cuff to pressurise the fluid reservoir to 400 mm Hg (this is the same type of system as was described for pressurised blood transfusions), the inline resistance comprising a length of small-bore marine glass tubing. This resistance converted

(0.22 μm pore size) upstream from the glass tubing prevented clogging of the fine-bore resistance.

GARDNER *et al.* (1970), working in co-operation with Sorenson Research Co., further refined the system of JOHNSON and ITO (1969). They developed the Intraflo device currently marketed by Sorenson Research Co.

Although the Intraflo continuous flush system was claimed to be failsafe and was incapable of infusing air into the patient (GARDNER *et al.*, 1970) problems have been reported.

The Intraflo device contained a rubber valve. Under normal operating conditions this valve restricted fluid flow through the catheter to 2–4 ml h^{-1} . However, to fill the blood-pressure transducer dome with fluid, or to purge the system of air, the valve stem could be pulled to open the valve and increase the flow to about 60 ml h^{-1} . The valve was designed to automatically close when the valve stem was released.

SCHWARTZ *et al.* (1977) reported that the valve could remain open after the valve stem was released, with the resulting problems of erroneous pressure readings and possible fluid overload in the patient due to the increased infusion rates. Similar problems with other users prompted ECRI (1978) to issue a hazard warning on the use of the Intraflo device. Subsequently Sorensen redesigned the Intraflo to prevent the valve from remaining open.

4—Current problems with continuous-flush systems

Small bubbles have been observed in the tubing of constant-infusion systems by KAYSER (1975), HARBORT and DALGETTY (1978), and have been measured by GARDNER *et al.* (1977).

Based on theoretical considerations, KAYSER (1975) estimated that an Intraflo constant-infusion system, filled with saline equilibrated with air at 21°C and a pressure of 1060 mm Hg (absolute), could deliver as much as 34.5 $\text{mm}^3 \text{h}^{-1}$ of air to the patient side of the Intraflo when the pressure was decreased to 760 mm Hg and the temperature raised to 35°C. This latter condition represents the arterial pressure and body temperature of the patient.

The measurements of GARDNER *et al.* (1977) showed that in a pressurised system (1060 mm Hg) containing air in both the saline bag and the drip chamber the average rate of gas formation on the patient side of the Intraflo was 0.54 $\text{mm}^3 \text{h}^{-1}$. If air was completely removed from the system the average amount of gas formation decreased to 0.44 $\text{mm}^3 \text{h}^{-1}$.

Although HARBORT and DALGETTY (1978) did not undertake any quantitative measurements, they confirmed the findings of GARDNER *et al.* (1977), which indicated that a system containing air in the drip chamber could generate small bubbles in the monitoring lines after a fast flush. These bubbles were thought to be due to the entrainment of air in the drip chambers during a fast flush, and the greatest number of bubbles occurred in systems which used a microdrip chamber (GARDNER *et al.*, 1977).

HARBORT and DALGETTY (1978) also indicated that large bubbles could form on the low-pressure side of the Intraflo whenever air was contained in the saline bag. These bubbles were thought to appear due to the supersaturation of the saline solution caused by the pressure drop across the Intraflo.

Removal of air from the saline bag would remove some of the source of air bubbles (HARBORT and DALGETTY, 1978) and removal of air from the drip chamber would eliminate the remaining bubbles (GARDNER *et al.*, 1977; HARBORT and

fluid to remove the air defeats the flow-monitoring function of the drip chamber (GARDNER, 1978).

GARDNER (1978) recommended the use of a microdrip chamber to permit monitoring of the fluid flow to indicate a faulty Intraflo valve. Yet an earlier paper (GARDNER *et al.*, 1977) showed that the use of a microdrip chamber and fast flushing were the major determinants for air bubbles in the system.

In addition, it was noted that over a period of time the drip chamber filled with fluid as a result of air being displaced and transmitted throughout the flush system. Once filled with fluid, the drip chamber loses its monitoring function.

Consequently, in the present configuration of the constant-infusion system, there is a trade-off between having a drip chamber to observe flow, with the resulting possibility of air bubble generation during a fast flush, and of relinquishing the flow-monitoring feature to eliminate the generation of air bubbles during a fast flush.

As another alternative, a drip chamber could be used and fast flushing of the left arterial line could be banned. However, in this case there is always the possibility that the system could be flushed accidentally and an air embolus could result.

Inline hydrophilic membrane filters could possibly be used to trap any air in the system (MEEKER *et al.*, 1976). GARDNER *et al.* (1977) mention the use of the screen filter Medlon system to trap bubbles generated during the fast flush. However, no information was provided as to filter placement and what effect—if any—the presence of the filter had on the measurement of blood pressure.

An extensive evaluation of inline fluid filters was conducted by ECRI (1979). This report, along with that of RUSMIN *et al.* (1979), indicates that these filters require special care in implementation and they are also subject to failure.

5 Conclusions

The development and availability of reliable electronic pressure monitoring equipment has made continuous direct monitoring of blood pressure commonplace in the intensive care unit. Recent years have seen a marked increase in the application of direct blood-pressure measurements for long-term monitoring.

Patients undergoing vascular cannulation are exposed to the dangers of thrombosis and air embolism. Patient complications due to these hazards can be reduced by using a pressurised continuous-flush system such as the Intraflo system, eliminating all air from the pressurised continuous-flush system, using a 20-gauge nontapered Teflon catheter, and by careful nursing care and vigilance.

Although every effort has been made to eliminate the hazards of thrombus and air embolism both by developing new or refined equipment and new techniques, these dangers have only been reduced and not eliminated. Consequently vascular cannulation has associated with it a certain degree of risk, but these risks are outweighed by the medical advantages gained from direct blood-pressure measurements.

Acknowledgment—The preparation of this review was supported by the General Hospital Corporation, St. John's, Newfoundland.

References

- ABERNATHY, C. M. and DICKINSON, T. C. (1979) Massive air emboli from intravenous infusion pump: etiology and prevention. *Am. J. Surg.*, 137, 274–275.

- BAGDONAS, A. A., STUCKEY, J. H., DENNIS, C., PIERA, J., AMER, N. S., DOMINGO, R. T. and CAPPELLETTI, R. R. (1960) The role of position in the development of cerebral air embolism following air injection at the base of the aorta. *Surg. Forum*, **10**, 653.
- BEDFORD, R. F. (1975) Percutaneous radial artery cannulation, increased safety using Teflon catheters. *Anesthesiol.*, **42**, 219-222.
- BEDFORD, R. F. and WOLLMAN, H. (1973) Complications of radial artery cannulation. *Ibid.*, **38**, 228-236.
- CARR, J. J. and BROWN, J. M. (1981) *Introduction to biomedical equipment technology*, Wiley, New York NY, 105-110.
- CHASE, W. H. (1934) Anatomical and experimental observations on air embolism. *Surg. Gynec. & Obst.*, **59**, 569.
- COLQUHOUN, B. P. D. (1977) Simple device to prevent disruption of centrally placed intravenous catheters. *Can. J. Surg.*, **20**, 565-566.
- COLQUHOUN, B. P. D. (1979) Air embolism and intravenous catheters. *Letter Br. Med. J.*, **1**, 1489.
- DOWNES, J. B., CHAPMAN, R. L. and HAWKINS, I. F. (1974) Prolonged radial artery catheterization. *Arch. Surg.*, **108**, 671-673.
- DOYLE, L. B. and FRODSHAM, P. (1949) Fatal air embolism during blood transfusion. *Lancet*, **1**, 735.
- DURANT, T. M., LONG, J. and OPPENHEIMER, M. J. (1947) Pulmonary (venous) air embolism. *Am. Heart J.*, **33**, 269-281.
- DURANT, T. M., OPPENHEIMER, M. J., WEBSTER, M. R. and LONG, J. (1949) Arterial air embolism. *Ibid.*, **38**, 481-500.
- ECRI (1978) Sorenson CFS intraflow. *Health Devices*, **7**, 263.
- ECRI (1979) IV Filters 0.2-Micron. *Health Devices*, **9**, 27-47.
- EDMONDS, J. F., BARKER, G. A. and CONN, A. W. (1980) Current concepts in cardiovascular monitoring in children. *Crit. Care Med.*, **8**, 548-553.
- FELLOWS, J. L., GOODRICH, R. G., RITTER, D. G. and RAHIMTOOLA, S. H. (1966) Air detector and safety control for a high-pressure flushing system. *Mayo Clinic Proc.*, **41**, 668-671.
- FLANAGAN, J. P., GRADISAR, I. A., GROSS, R. J. and KELLY, T. R. (1969) Air embolism—a lethal complication of subclavian venipuncture. *N. Engl. J. Med.*, **281**, 488-489.
- GARDNER, R. M. (1978) Recommendations for the use of the Intraflo flush valve. *Letter Crit. Care Med.*, **6**, 392.
- GARDNER, R. M., BOND, E. L. and CLARK, J. S. (1977) Safety and efficacy of continuous flush systems for arterial and pulmonary artery catheters. *Ann. Thorac. Surg.*, **23**, 534-538.
- GARDNER, R. M., WARNER, H. R., TORONTO, A. F. and GAISFORD, W. D. (1970) Catheter-flush system for continuous monitoring of central arterial pulse waveform. *J. Appl. Physiol.*, **29**, 911-913.
- GOMES, O. M., PERREIRA, S. N., CASTAGNA, R. C., BITTENCOURT, D., AMARAL, R. V. G. and ZERBINI, E. J. (1973) The importance of different sites of air injection in the tolerance of arterial air embolism. *J. Thorac Cardiovasc. Surg.*, **65**, 563-568.
- GOTTLIEB, J. D., ERICSSON, J. A. and SWEET, R. B. (1965) Air embolism—review. *Anesth. & Analg.*, **44**, 773-779.
- GRACE, D. M. (1977) Air embolism with neurologic complications: a potential hazard of central venous catheters. *Can. J. Surg.*, **20**, 51-53.
- HARBORT, R. A. and DALGETTY, R. G. (1978) Bubble formation in flush systems. Correspondence *Ann. Thorac. Surg.*, **25**, 179-180.
- JOHNSON, D. G. and ITO, T. (1969) Continuous flush of arterial pressure-recording catheter: a safe and inexpensive system. *J. Thorac. Cardiovasc. Surg.*, **57**, 675-678.
- KAPLAN, J. A. (1979) *Hemodynamic monitoring in cardiac anesthesia*. KAPLAN, J. A., (Ed.) Grune & Stratton Inc., New York NY, 71-115.
- KAYSER, K. L. (1975) A possible hazard with the use of pressurized constant-infusion systems. *Ann. Thorac. Surg.*, **20**, 343.
- KIN, J. M., ARAKAWA, K. and BLISS, J. (1975) Arterial cannulation: factors in the development of occlusion. *Anesth. & Analg.*, **54**, 836-840.
- LOWENSTEIN, E., LITTLE, J. W. and LO, H. H. (1971) Prevention of cerebral embolization from flushing radial-artery cannulas. *N. Engl. J. Med.*, **285**, 1414-1415.
- MEEKER, W. R., RAPP, R. P., DELUCA, P. P. and BIVINS, B. A. (1976) Membrane filters. Additional safety for intra-arterial infusions. *Arch. Surg.*, **111**, 201.
- METCALFE, E., GRIFFITHS, D., PETERS, J. L. and GREENWOOD, N. M. (1979) Air embolism and intravenous catheters. *Letter Br. Med. J.*, **1**, 1630.
- MICHENFELDER, J. D. (1968) Multiple episodes of air emboli: report of a case. *Anesth. & Analg.*, **47**, 355-356.
- ORDWAY, C. B. (1974) Air embolus via CVP catheter without positive pressure. *Ann. Surg.*, **179**, 479-481.
- PEDERSEN, N. T. and HESSOV, I. (1978) Venous air embolism through infusion sets. Theoretical considerations, model experiments and prevention. *Acta. Anaesth. Scand.*, **22**, 117-122.
- ROSS, S. M., FREEDMAN, P. S. and FARMAN, J. V. (1979) Air Embolism after accidental removal of intravenous catheter. *Br. Med. J.*, **1**, 987.
- RUESCH, M., MIYATAKE, S. and BALLINGER, C. M. (1960) Continuing hazard of air embolism during pressure transfusions. *J.A.M.A.*, **172**, 1476-1482.
- RUSMIN, S., RAPP, R. P., BIVINS, B. A. and DELUCA, P. P. (1979) Conditions permitting air flow through an air-venting inline filter. *Am. J. Hosp. Pharm.*, **36**, 749-753.
- SCHWARTZ, A. J., STONER, B. B. and JOBES, D. R. (1977) A hazard of the intraflo continuous flush system. *Crit. Care Med.*, **5**, 115-116.
- YEAKEL, A. E. (1968) Lethal air embolism from plastic blood-storage container. *J.A.M.A.*, **204**, 267-269.

Multiple Model Adaptive Control Procedure for Blood Pressure Control (Ref. 12)

W. G. HE, HOWARD KAUFMAN, SENIOR MEMBER, IEEE, AND ROB ROY, SENIOR MEMBER, IEEE

Abstract—Multiple model adaptive control procedures have been considered for a computer-based feedback system which regulates the infusion rate of a drug (nitroprusside) in order to maintain desired blood pressure. Because the transfer function parameters are different for each patient, and furthermore are time variant, such an algorithm is desirable for maintaining both steady-state and transient specifications. To this effect, computer simulation has shown that multiple model adaptive control procedures might be successfully applied to the control of blood pressure despite the uncertainty in the delays, time constant, and gains. Additional efforts concerned with the actual demonstration of these concepts on dogs have further supported the role of adaptive control for blood pressure regulation.

I. INTRODUCTION

An automated drug (nitroprusside) infusion system for blood pressure control should produce good response characteristics, such as pressure undershoot (i.e., maximum excursion below commanded level) less than 10 mmHg, 20 percent settling time of 5–10 min, steady-state error within ± 5 mmHg, and also satisfy the following clinical conditions [1].

- Drug infusion rate should be limited by

$$U_M \leq 60 W_p i_m C_s^{-1} \text{ (ml/hr)} \quad (1)$$

where

- U_M = maximum infusion rate (ml/hr)
- W_p = patient weight (kg)
- i_m = maximum recommended dose ($10 \mu\text{g} \cdot \text{kg}^{-1} \text{ min}^{-1}$)
- C_s = drug concentration ($\mu\text{g/ml}$).

- For patient safety, the infusion rate should be reduced under hypotension, i.e., when there is a drop in excess of 20 mmHg from the setpoint.

- The reduction rate of blood pressure should be lim-

Manuscript received January 7, 1985; revised June 24, 1985. This work was supported by the National Science Foundation under Grant ECS80-16255. Any opinions, findings, and conclusions or recommendations expressed in this paper are those of the authors and do not necessarily reflect the views of the NSF.

W. G. He is with the Department of Electrical, Computer, and Systems Engineering, Rensselaer Polytechnic Institute, Troy, NY, on leave from the Chengdu Institute of Computer Application, Academia Sinica, Chengdu, China.

H. Kaufman is with the Department of Electrical, Computer, and Systems Engineering, Rensselaer Polytechnic Institute, Troy, NY 12180-3590.

R. Roy is with the Department of Biomedical Engineering, Rensselaer Polytechnic Institute, Troy, NY 12180-3590.

IEEE Log Number 8406102.

ited to 5–10 mmHg/10 s in order to prevent undesired secondary effects, for instance, diminished blood flows.

The idea of multiple model adaptive control (MMAC) was proposed and discussed by Lainiotis in [2] and [3]. A multiple model-type adaptive algorithm for self-organizing control was also proposed by Saridis *et al.* in [4]. From the viewpoint of stochastic control, an MMAC system for the F-8 aircraft was developed by Athans *et al.* in [5].

Because MMAC is a robust procedure, that has not to date been extensively used for biomedical applications, a study has been made for a suitable PI controller-based MMAC system for blood pressure control. In particular, it focused on the partition of plant parameters, design of the controller bank, model bank, and the algorithm itself. An MMAC system, with 8 models, was then designed, and its performance was evaluated both by computer simulation and with dogs. Results indicate the MMAC algorithm to be very effective for controlling blood pressure despite the effects of plant parameter variations and background noise.

II. PLANT CHARACTERISTICS

Based upon the results by Slate and Sheppard [6], the following model will be used for design purposes:

$$F(s) = \frac{Y(s)}{U(s)} = \frac{Ge^{-T_i s}(1 + \alpha e^{-T_c s})}{1 + \tau s} \quad (2)$$

$$P(s) = Y(s) + P_n(s) + P_o \quad (3)$$

where

- $Y(s)$ is the change in blood pressure from its initial value P_o due to the drug,
- $U(s)$ is the drug infusion rate,
- $P_n(s)$ is the plant background noise,
- $P(s)$ is the actual blood pressure.

The parameters in (2) were chosen as [1]: $G = -0.25$ to -9 (nominal = -1), $\tau = 30$ – 60 s (nominal = 40), $T_i = 20$ – 60 s (nominal = 40) [7], $T_c = 30$ – 75 s (nominal = 45), $\alpha = 0$ – 0.4 . P_o is usually 115–140 mmHg, $P_n(t)$ is typically 2–5 mmHg (for low noise levels) or 15–25 mmHg (for high noise levels).

III. MMAC METHOD

The MMAC procedure shown in Fig. 1 is based upon the assumption that the plant can be represented by one of a finite number of models and that for each such model a

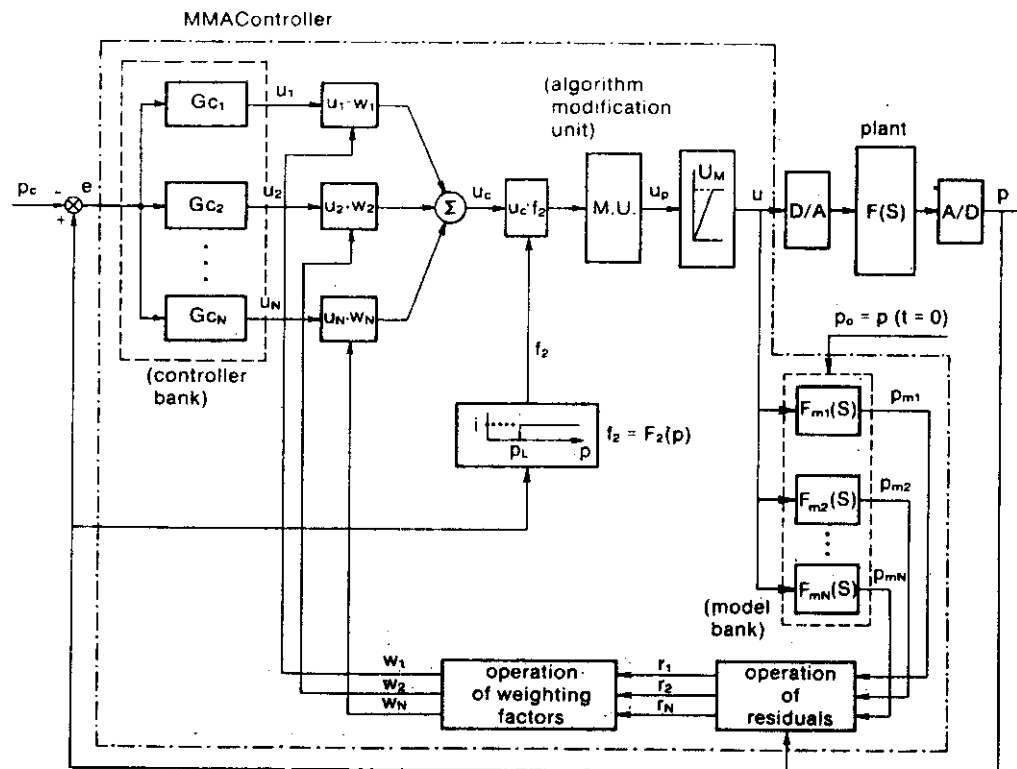


Fig. 1. MMAC system structure.

controller can be *a priori* designed. All of these controllers together then constitute a controller bank. An adaptive mechanism is then needed for deciding which controller should be dominant for a given plant. One procedure for solving this problem is to form a weighted-sum of all the controller outputs, where the weighting factors are determined by the relative residuals between the plant response and the model responses.

In Fig. 1, since the plant gain is negative, the system error is expressed as

$$e(K) = p(K) - p_c \quad (4)$$

where K is the sampling time and p_c is the commanded or set-point pressure level.

For patient safety, two nonlinear units are built into the system. The nonlinear unit limiting infusion rate is given as

$$u = F_1(u_D) = \begin{cases} u_D & \text{for } u_D \leq U_M \\ U_M & \text{for } u_D > U_M \end{cases} \quad (5)$$

where U_M is the allowed maximum infusion rate calculated from (1).

The other nonlinear unit is used to turn off the infusion if and when hypotension occurs [1]. Its expression is given by

$$F_2[p(K)] = \begin{cases} 1 & \text{for } p(K) \geq p_L \\ 0 & \text{for } p(K) < p_L \end{cases} \quad (6)$$

where p_L is defined as

$$p_L = p_c - 20 \quad (7)$$

and p_c is the commanded pressure setpoint.

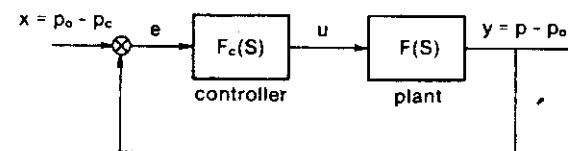


Fig. 2. An equivalent continuous system.

With respect to the MMAC development, Section III-A describes the design of the controller bank, Section III-B discusses the model selection procedure, and finally, Section III-C presents the actual control computation.

A. Controller Bank Design

A controller that is sufficiently robust over a given subset of process models will now be developed. To simplify this procedure, it will be assumed that the weighting factors have converged and that the sampling period is less than $\frac{1}{8} \sim \frac{1}{3}$ of the plant time constant so that the basic control loop of Fig. 1 can be modeled by the continuous system shown in Fig. 2. In this figure, the system input and output are, respectively, the desirable and actual drops in pressure, and the negative plant gain is replaced by its absolute value.

In terms of the closed-loop transfer function $T(s)$, the controller transfer function is

$$F_c(s) = \frac{1}{F(s)} \frac{T(s)}{1 - T(s)} \quad (8)$$

where $F(s)$ is as defined by (2). Generally, $T(s)$ for satisfactory response should have a first-order exponential response with time delay and satisfy the following conditions:

- the controller $F_c(s)$ must have no predictor element
- the closed-loop system should respond to a step input with zero steady-state error.

In a manner similar to that of [8], $T(s)$ might then be chosen as

$$T(s) = \frac{1}{1 + \alpha} \frac{e^{-T_i s} (1 + \alpha e^{-T_c s})}{\frac{\lambda}{1 + \alpha} s + 1} \quad (9)$$

where λ is a tuning parameter related to the time constant of the closed-loop system, and T_i , T_c , and α are the plant parameters in (2).

Substituting (2) and (9) into (8), and using (as in [8]) the first-order Taylor series approximation of $\exp(-T_i s)$ and $\exp[-(T_i + T_c) s]$, gives the following $P-I$ compensator:

$$F_c(s) = G_c \left(1 + \frac{1}{\tau_c s} \right) \quad (10)$$

where

$$\tau_c = \tau \quad (11)$$

and

$$G_c = \frac{\tau}{G[\lambda + (1 + \alpha) T_i + \alpha T_c]} \quad (12)$$

The tuning parameter λ in (12) can be computed to satisfy specifications in the settling time t_s of the closed-loop system defined by (9). This settling time t_s is defined as follows:

$$\left| \frac{y(t)}{x} \right|_{t \geq t_s} \geq C \quad (13)$$

where $y(t)$ and x are, as shown in Fig. 2, the actual and desired pressure drops, and C is a constant less than 1.

Using (9), it can then be shown that

$$C = \frac{y(t_s)}{x} \frac{1}{1 + \alpha} \left\{ (1 + \alpha) - \exp[-(1 + \alpha/\lambda)(t_s - T_i)] (1 + \alpha \exp[(1 + \alpha/\lambda) T_c]) \right\}. \quad (14)$$

If $\lambda \gg T_c$, then

$$\exp\left(\frac{(1 + \alpha)}{\lambda} T_c\right) \cong 1$$

and λ becomes

$$\lambda \cong -\frac{(1 + \alpha)(t_s - T_i)}{n(1 - C)} \quad (15)$$

In order to compute the controller parameters τ_c and G_c , the ranges of plant parameters in each subspace also need to be determined. From simulation results, it was observed that changes in the plant parameters, except for plant gain (and to a lesser extent, the plant delay time T_i), did not adversely affect the undershoot and the settling time. Therefore, the plant gain was divided into several

intervals and the other plant parameters were frozen. The values of the frozen parameters were denoted as τ_o , T_{io} , T_{co} , and α_o ; these typically were nominal or maximum values of the plant parameters. The procedures for such selection are now explained.

Let G_j and G_{j+1} denote the lower and upper limit plant gains for the j th interval and assume that G_1 the minimum possible gain is *a priori* available. A recursive approach for generating the controller gains G_{c_j} and plant gains will now be developed. G_{c_j} will be determined from G_j , and G_{j+1} will then be found from robustness considerations. To this effect, substitute λ , G_j , and the frozen plant parameters τ_o , T_{io} , T_{co} , and α_o into (12) to find the controller gain as

$$G_{c_j} = \frac{\tau_o}{G_j[\lambda + (1 + \alpha_o) T_{io} + \alpha_o T_{co}]} \quad (16)$$

Then, estimate G_{j+1} so that the undershoot and/or phase margin PM is satisfactory over the plant gain subinterval. To do this, recall from [9] that PM (in degrees) $\cong 100 \times$ (damping factor). If τ is frozen as τ_o , and $T_{co} = 0$, the open-loop transfer function in Fig. 2 can be derived from (2), (10), and (11) as

$$F_c(s) F(s) \cong \frac{G_{c_j} G (1 + \alpha) e^{-T_i s}}{\tau_o s} \quad (17)$$

The minimum phase margin of this open-loop system can then be computed as

$$\text{MIN}[PM] \cong \frac{\pi}{2} - \frac{(1 + \alpha) G_{c_j} T_i \text{MAX}[G_{j+1}]}{\tau_o} \quad (j = 1, \dots, N). \quad (18)$$

From (18) and (16),

$$\begin{aligned} \frac{G_{j+1}}{G_j} &= \frac{(0.5\pi - \text{MIN}[PM])[\lambda + (1 + \alpha_o) T_{io} + \alpha_o T_{co}]}{T_i(1 + \alpha)} \\ &= A. \end{aligned} \quad (19)$$

For the worst possible case, T_i and α in (19) should be at their maximum values. Therefore,

$$G_{N+1} = A^N G_1 \quad (20)$$

where N , the number of subspaces, is the smallest integer N such that G_{N+1} is greater or equal to the maximum process gain. G_1 would then be the lowest anticipated plant gain.

B. Model Bank Design

The model bank in Fig. 1 consists of a number of models with constant parameters characterizing the individual plant subspace. Since these models should have the same structure as the plant, they will be described by the following transfer functions:

$$F_{m_j}(s) = \frac{y_{m_j}(s)}{U(s)} = \frac{G_{m_j} e^{-T_{mj}s} (1 + \alpha_{mj} e^{-T_{mcj}s})}{1 + \tau_{mj}s} \quad (j = 1, \dots, N) \quad (21)$$

where the output pressure from model j is

$$P_{mj}(s) = y_{mj}(s) + P_o \quad (j = 1, \dots, N) \quad (22)$$

and

$y_{mj}(s)$ is the change in the j th model output,

$U(s)$ is the model input,

P_o is the initial value of each model's output, which equals the initial plant output.

The relative residual $R_j^2(K)$ will be defined as the normalized squared error between plant and model, i.e.,

$$R_j^2(K) \triangleq \{[p_{mj}(K) - p(K)]/(P_o - P_c)\}^2 \quad (j = 1, \dots, N). \quad (23)$$

Using (3) and (22) and eliminating the plant noise $p_n(t)$, (23) can be transformed into

$$R_j^2(K) = \{[y_{mj}(K) - y(K)]/(P_o - P_c)\}^2 \quad (j = 1, \dots, N). \quad (24)$$

At each sample time K , the model that has the smallest residual is defined as the matching model, which is then used to represent the plant characteristics.

Selection of the model parameters should consider both the optimal match between the characteristics of plant and models, and the system dynamics. Since the plant parameters τ , T_c , and α can be frozen, the model parameters τ_{mj} , T_{mcj} , and α_{mj} were selected as $\tau_{mj} = \tau_o$, $T_{mcj} = T_{co}$ and $\alpha_{mj} = \alpha_o$ (for $j = 1, \dots, N$).

Selection of the model delay time T_{mj} must be made taking into account the undershoot specification. In effect, simulation results that will be shown in Figs. 6 and 7 indicate that different model delay times significantly affect undershoot, especially when the plant gain is high. For a blood pressure control system, large undershoot is not allowed, so that the model delay time should be chosen as the maximum expected plant delay time.

Appropriate model gains are required for the MMAC system to properly select the dominant controller. When the plant gain is located on a boundary between two plant parameter subspaces, such as $G = G_{j+1}$, the residuals $R_j(K)$ and $R_{j+1}(K)$ should satisfy

$$R_j^2(K) = R_{j+1}^2(K). \quad (25)$$

From (24) and (25),

$$y_{m,j+1}(K) + y_{mj}(K) - 2y(K) = 0. \quad (26)$$

Replacing the values in (26) by their steady-state values for a step input gives

$$G_{m,j+1} = \frac{2(1 + \alpha)}{1 + \alpha_0} G_{j+1} + G_{mj} \quad (j = 1, \dots, N). \quad (27)$$

If it is assumed that $\alpha \cong \alpha_0$, then (27) can be simplified to

$$G_{m,j+1} \cong 2G_{j+1} - G_{mj} \quad (j = 1, \dots, N). \quad (28)$$

Note that G_{m1} should be *a priori* selected such that

$$G_{m1} = \frac{1}{2}(G_1 + G_2). \quad (29)$$

C. Control Algorithm

To achieve desirable system performance and to guarantee patient safety, the control algorithm should converge quickly to the optimal values and should react to time-varying plant characteristics, as well as ensure a reasonable rate of blood pressure change. Thus, the control was computed as a weighted sum of controller bank signals, i.e.,

$$u_c(K) = \sum_{j=1}^N W_j(K) u_j(K) \quad (30)$$

and

N is the number of models,

$u_c(K)$ is the control variable,

$u_j(K)$ are the individual controller outputs,

and

$W_j(K)$ are the weighting factors.

The weights were selected as follows.

1) Recursive update

$$W_j^i(K) = \frac{\exp[-R_j^2(K)/2V^2] W_j^i(K-1)}{\sum_{i=1}^N \exp[-R_i^2(K)/2V^2] W_i^i(K-1)} \quad (j = 1, \dots, N). \quad (31)$$

2) Bounding away from zero

$$W_j(K) = \begin{cases} W_j^i(K) & \text{for } W_j^i(K) > \delta \\ \delta & \text{for } W_j^i(K) \leq \delta. \end{cases} \quad (32)$$

3) Normalization

$$W_j(K) = \frac{[W_j(K)]^2}{\sum_{i=1}^N [W_i(K)]^2} \quad (j = 1, \dots, N) \quad (33)$$

where

$R_j(K)$ are the residuals [e.g., (23)]

V is a parameter controlling the convergence rate of $W_j^i(K)$ with $R_j(K)$

δ is a threshold to limit the importance of past information.

Equations (30) and (31) express the basic relationship between the control, the weighting factors, and the relative residuals. Equation (32) is used to limit the importance of past information so as to enable the adaptive mechanism to react quickly to new information about the plant characteristics. Equation (33) is used to normalize the weighting factors so that their summed squared value is unity.

The parameter V in (31) plays an important role in controlling the convergence rate of $W_j(K)$. To see this, let $R_m(K)$ and $W_m(k)$ represent the residual and the weighting factor corresponding to the matching model, then

$$R_m(K) < R_j(K) \quad (\text{for } j \neq m).$$

From (31) and (33) it can be seen that

$$\frac{W_j(K)}{W_m(K)} = \left\{ \exp \left[-\frac{1}{V^2} (R_j^2 - R_m^2) \right] \right\} \frac{W_j(K-1)}{W_m(K-1)}. \quad (34)$$

Thus, for rapid convergence of $W_j(K)$, a smaller value of V is desired; however, an excessive reduction in V could cause a computer overflow.

In the algorithm, the initial weighting factors $W_j(0)$ and the threshold δ must be determined *a priori*. Since the plant gain may be located in any position in the plant parameter space, the values for $W_j(0)$ were assumed to be uniform, that is,

$$W_j(0) = W_j'(0) = \frac{1}{N} \quad (j = 1, \dots, N). \quad (35)$$

From (31), it is observed that a large value of δ will improve the sensitivity of the algorithm to the new plant information. However, as shown below, an increase in δ will reduce the system phase margin. To see this, use (33) and the converged weighting factors be

$$W_m(K) = W_m \quad (\text{for the main weighting factor})$$

$$W_j(K) = \delta^2 \quad (\text{for } j \neq m).$$

From (10), (18), and (30), the relationship between MIN[PM] and δ can be derived as

$$\text{MIN[PM]} = \frac{\pi}{2} - \frac{(1 + \alpha) T_i \text{MAX}[G_{m+1}]}{2 \tau_o G_{cm} \left[W_m + \delta^2 \sum_{\substack{j=1 \\ j \neq m}}^N \frac{G_{cj}}{G_{cm}} \right]}. \quad (36)$$

Thus, MIN[PM] will be reduced with an increase in δ .

Since the control variable $u_c(K)$ computed by (30) will be in error before the convergence of $W_j(K)$, and this error can cause a large undershoot for high gain plant, the algorithm consisting of (30)–(33) was modified as follows:

$$u_D(K) = \begin{cases} Qu_c(K) & \text{for } K \leq d_m \\ [Q + Q_1(K - d_m)] u_c(K) & d_m < K < (d_m + D_1) \\ u_c(K) & K \geq (d_m + D_1) \end{cases} \quad (37)$$

where Q and Q_1 are coefficients that are less than 1,

$$d_m = \text{INTEGER} [T_m/T_o],$$

$$D_1 = \text{INTEGER} \left[\frac{1 - Q}{Q_1} \right]. \quad (38)$$

Q is used to regulate the initial infusion rate so as to prevent large undershoot. The value of Q should place the initial control variable near the steady-state control input required by the plant with the highest expected gain. Q_1 is then set so that the increment of the initial infusion rate ensures smooth reduction of pressure.

Note that because of this conservative initial control policy, a large error could persist and subsequently cause an undershoot of the system output. To eliminate this behavior, the integral component was decreased during the initial control period as follows:

$$u_j(K) = G_{cj} \left[E(K) + \frac{T_o}{\tau_c} \sum_{i=0}^{K-1} B_j E(i) \right] \quad (j = 1, \dots, N) \quad (39)$$

where B_j are modifying coefficients defined as

$$B_j \leq 1 \quad \text{for } K \leq (d_{m1} + D_1) \\ B_j = 1 \quad \text{for } K > (d_{m1} + D_1). \quad (40)$$

IV. RESULTS

A. System Design

An MMAC system with 8 models was designed to satisfy the requirements of Section I, namely, an undershoot less than 10 mmHg, a settling time less than 300 s, and the limitation condition for the maximum infusion rate given in (1). After summarizing the data given in Section II, the frozen plant parameters were chosen as $\tau = 45$ s, $T_{io} = 40$ s, $T_{co} = 50$ s, and $\alpha = 0.4$. Choosing $T_i = T_{io}$, $\alpha = \alpha_o$, and $C = 0.8$, the tuning parameter λ was found from (16) to be

$$\lambda = -\frac{(1 + 0.4)(300 - 40)}{\ln(1 - 0.8)} = 226.$$

Choosing MIN[PM] = 65° , $T_i = 60$ s and $\alpha = 0.4$ (for the worst possible case), the plant gain partition factor can be determined from (19) to be

$$\frac{G_{j+1}}{G_j} = \frac{(0.5\pi - 1.13)[226 + 1.4 \times 40 + 0.4 \times 50]}{60(1 + 0.4)} = 1.58$$

where $G_1 = G_{\min} = 0.25$.

The controller parameters G_{cj} and τ_{cj} were computed from (17) and (11) after substituting G_j , λ , τ_o , T_{io} , T_{co} , and α_o into the formulas. The resulting values of G_{cj} and τ_{cj} are listed in Table I.

As mentioned in Section III-B, the model parameters τ_{mj} , T_{mcj} , and α_{mj} were chosen as $\tau_{mj} = \tau_o$, $T_{mcj} = T_{co}$, and $\alpha_{mj} = \alpha_o$ (for $j = 1, \dots, N$). The model gains can be found from (28) and (29), and are also listed in Table I.

T_{mj} was selected to be either 60 s (i.e., the maximum of T_i) or 40 s (i.e., the nominal value of T_i).

The coefficient V in (31) was determined by simulation on a PDP-MINC computer. When $V = 0.07$, the compu-

TABLE I
PARAMETERS OF THE SYSTEM WITH 8 MODELS
(a) Coefficients of the control algorithm.

d_m $6t_0$	D1	V	Q	Q1	B1	B2	B3	B4	B5	B6	B7	B8	$W_j(0)$ 1/8	δ .05
	3	0.1	0.4	0.2	0.1	0.3	0.5	0.8	1	1	1	1		

(b) Parameters of controllers and models.

Number	Controller		Model					Plant Gain
	G_c	τ_c	G_m	T_{mi}	T_{me}	τ_m	α_m	
1	0.6		0.32					0.25-0.39
2	0.39		0.46					0.39-0.61
3	0.25		0.76					0.61-0.95
4	0.16	45	1.14	60	50	45	0.4	0.95-1.48
5	0.1		1.82					1.48-2.3
6	0.065		2.8					2.30-3.6
7	0.042		4.4					3.60-5.6
8	0.027		6.8					5.60-9

tation overflowed. When $V = 0.1$ and 0.2 , the settling times were 340 and 460 s, respectively. Thus, V was chosen to be 0.1.

The coefficient δ in (32) can be estimated using (36). To consider the worst possible phase margin, let $\text{MAX}[G_{m+1}] = G_{n+1} = 9$, $\alpha = 0.4$, $T_i = 60$ s, and $\delta = 0.1$ or 0.5 , then

$$\text{MIN[PM]} = 48^\circ \quad \text{for } \delta = 0.1$$

and

$$\text{MIN[PM]} = 60^\circ \quad \text{for } \delta = 0.05.$$

Therefore, δ was chosen to be 0.05.

The initial weighting factors were all assumed to be the same, i.e.,

$$W_j(0) = \frac{1}{8}.$$

Q in (37) was chosen as 0.4 because this value gave an initial infusion rate close to the steady-state control input required by a high-gain plant. Q_1 in (37) should be less than unity in order to limit the increment in the infusion rate. Results obtained by trial and error showed that the undershoot specification can be satisfied when $Q_1 = 0.2$. As stated in Section III-C, modification of B_j is needed only for the control of lower gain plants, so that some components of B_j , such as B_5, \dots, B_8 , corresponding to the controller outputs for high-gain plants, can directly be set to unity. The other components, i.e., B_1, \dots, B_4 , were determined by trial and error. Their values are listed in Table I. A study of the sensitivity to Q , Q_1 , and B_j showed the algorithm to be relatively robust over a wide variation in these parameters.

The parameters U_M and P_L in Fig. 1 can be computed from (1) and (7). As an example, if $W_p = 60$ kg, $i_M = 10$ $\mu\text{g} \cdot \text{kg}^{-1}$, $C_S = 200$ $\mu\text{g}/\text{ml}$, and $P_L = 100$ mmHg, then

$$U_M = 60 \times 60 \times 10 \times 200^{-1} = 180 \text{ ml/h},$$

$$P_L = 100 - 20 = 80 \text{ mmHg}.$$

B. Computer Simulation Studies

Computer simulations were used to evaluate the response of the system design in Section IV-A over a representative plant parameter envelope. Of interest were the responses to a step command in the presence of plant background noise, the adaptation of the algorithm to time-varying plant gains, and the effects of the model delay time on the undershoot. In the simulations, $P_c = 100$ mmHg, $P(0) = 150$ mmHg, $T_0 = 10$ s. The plant background noise $P_n(t)$ was simulated as a white Gaussian noise sequence with standard deviation of 2 mmHg.

The first set of simulations was with the model delay time $T_{mj} = 60$ s and the plant parameters: $\tau = 45$ s, $T_c = 50$ s, $\alpha = 0.4$, as well as for the values of G and T_i given in Table II. Results shown in Table II indicate that the largest undershoot was 12 mmHg (which is close to the undershoot specification of 10 mmHg) and that the longest settling time was 390 s, which is equal to the sum of the desired settling time of 300 s and the initial infusion period ($T_0(d_{m1} + D_1) = 90$ s). Figs. 3-6 show the pressure response, the change in drug infusion rate, and the typical convergence process of the weighting factors. Since the controller gain G_{c_j} corresponding to W_j is greater than $G_{c_{j+1}}$ corresponding to W_{j+1} (see Table I), the convergence sequence of $W_j(K)$ shown in these figures results in the controller gain increasing gradually to its desirable value during the initial control period. Thus, the drug infusion rate and the blood pressure both change in a smooth manner. These responses also show that the MMAC algorithm is robust even in the presence of the plant background noise.

The second set of simulations was made for comparison of system performance under different selections of the plant parameters τ , T_i , T_c , and α . In these simulations, the model delay time T_{mj} was still 60 s, but the plant parameters were chosen as $\tau = 30$ s, $T_i = 20$ s, $T_c = 50$ s, $\alpha = 0$, $G =$ the lower gains of the plant subspaces listed in Table I, or as $\tau = 60$ s, $T_i = 60$ s, $T_c = 75$ s, $\alpha = 0.4$, and $G =$ the higher gains of the plant subspaces in Table

TABLE II

Plant Gain	Settling Time (s)			Undershoot (mmHg)		
	Plant Delay Time (s)			Plant Delay Time (s)		
	20	40	60	20	40	60
0.25	370	370	370	0	0	0
0.32	390	350	320	5.9	4.8	3.5
0.38	350	360	310	8	8.2	8.5
0.39	340	350	310	0	0	2.7
0.59	350	360	280	9.5	12	8
0.62	340	340	290	0	0	0
0.9	320	340	260	9.4	8.9	4.5
1.0	300	310	270	0	0	0
1.4	330	340	240	9.8	11.5	5.4
1.5	310	320	240	0	0	0
2.2	340	350	220	10.5	11.5	3.2
4	310	320	350	0	0	0
5	310	320	200	9	9.7	1.1
3.7	300	300	200	0	0	0
5	340	330	160	8.7	12	0.4
5.8	340	340	390	0	0	0
9	260	270	140	0	0.58	6.5

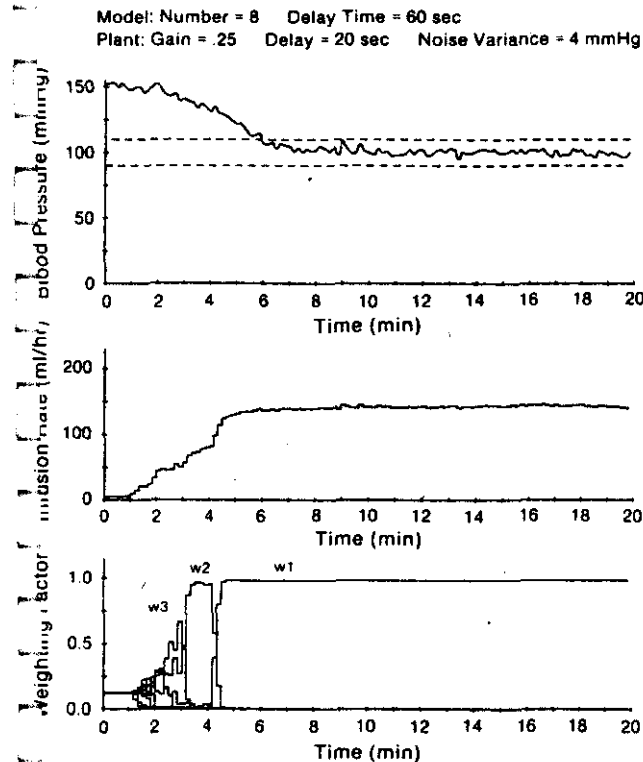


Fig. 3. System simulation.

Results show that except for $G = 0.25$, the largest undershoot and the longest settling time were about 12 mmHg and 390 s, respectively.

In order to show that different model delay times T_{mj} result in different amounts of undershoot, the third simu-

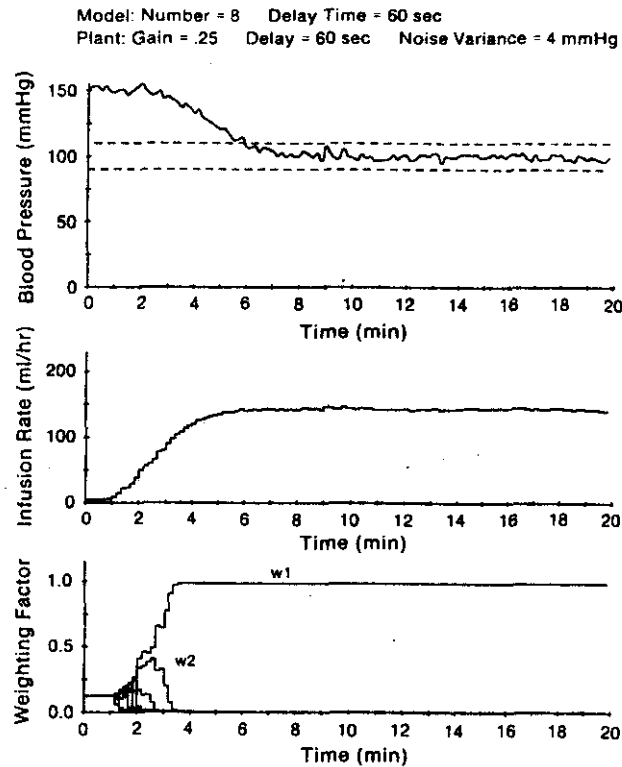


Fig. 4. System simulation.

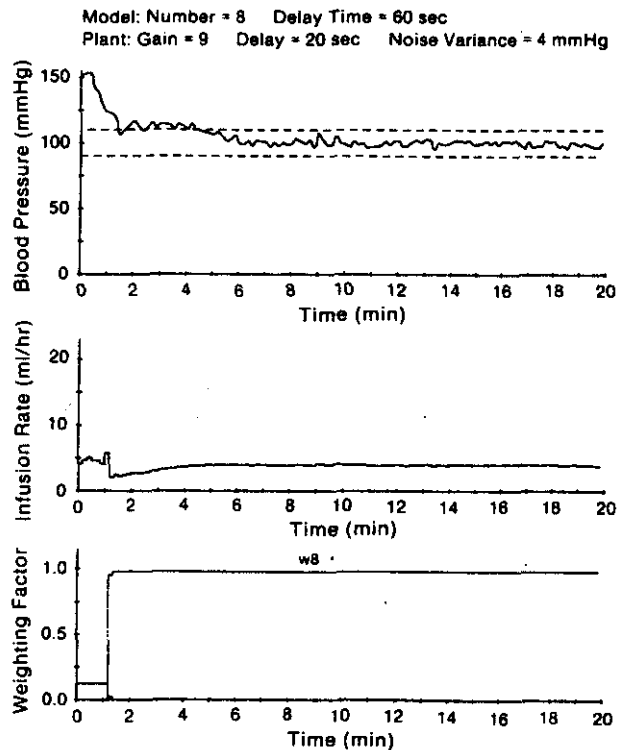


Fig. 5. System simulation.

lation was run for $T_{mj} = 40$ s, and the same plant parameters as in Fig. 6. Comparison of the results in Figs. 6 and 7 indicates an undershoot of 6.5 when $T_{mj} = 60$ s. When $T_{mj} = 60$ s, Fig. 6 shows that the main weighting factor directly converges to W_8 . However, when $T_{mj} = 40$ s, Fig. 7 illustrates that the main weighting factor first converges

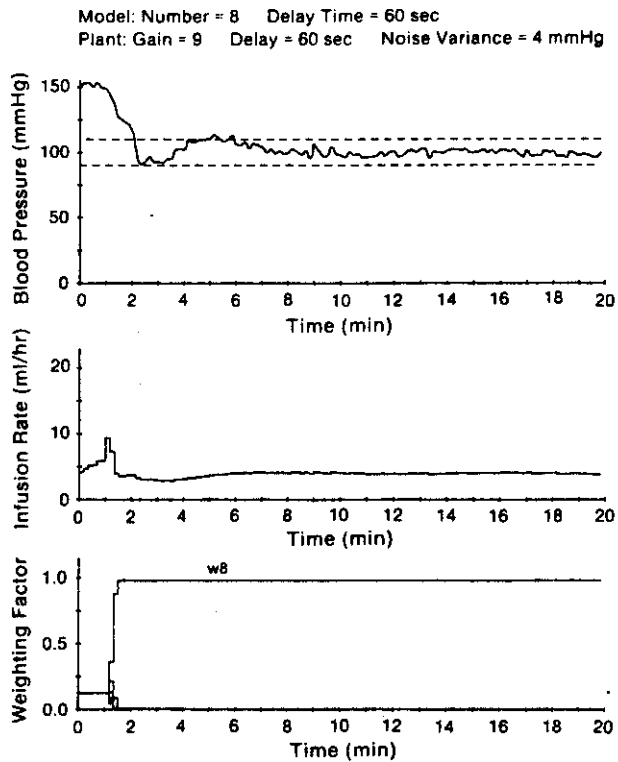


Fig. 6. System simulation.

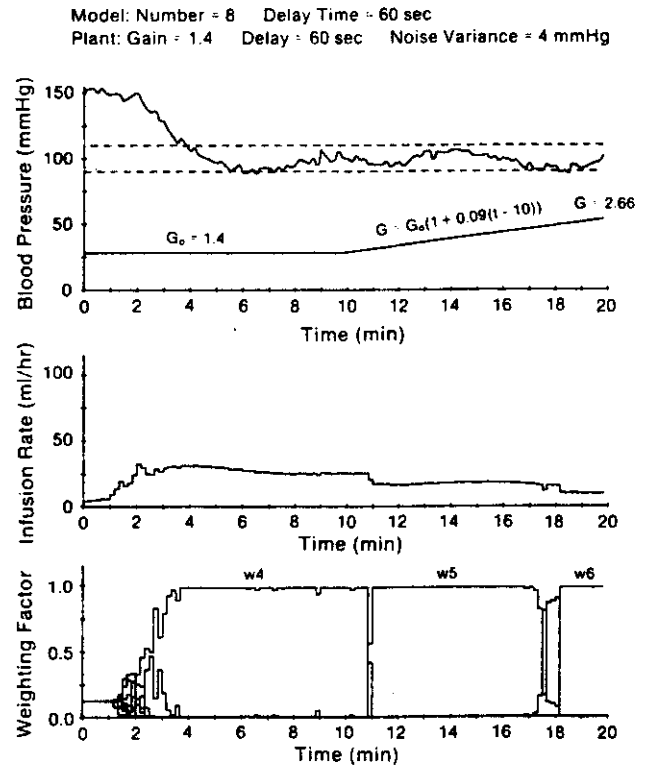


Fig. 8. System simulation.

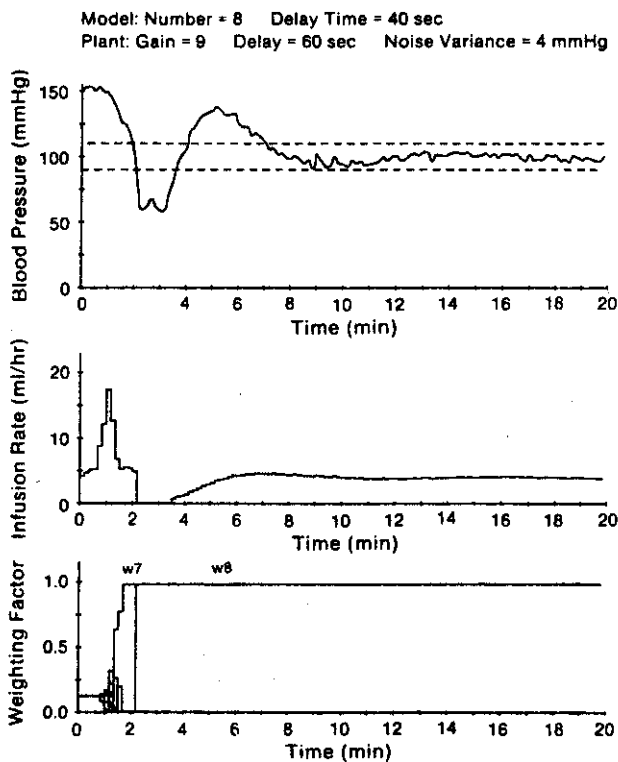


Fig. 7. System simulation.

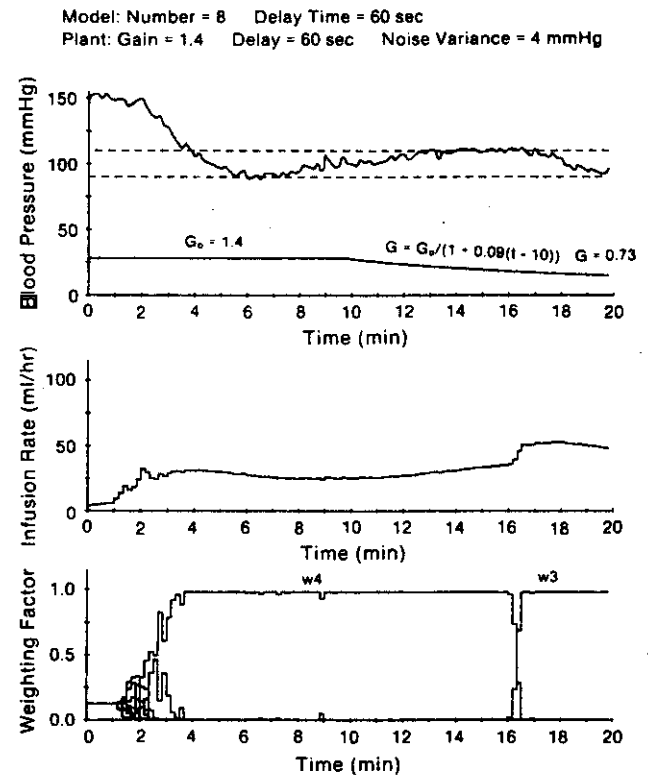


Fig. 9. System simulation.

to W_7 and then to W_8 . Since G_{c7} corresponding to W_7 is greater than G_{c8} corresponding to W_8 , the undershoot results.

The fourth set of simulations considered the system response to a time-varying plant gain. Figs. 8 and 9 show

that the given time-varying plant gains cause the weighting factors to adapt so as to stabilize the pressure within ± 10 mmHg error from the setpoint.

Of interest in all cases is the tendency for one weight to converge to unity and the others to zero.

Dog: 15 kg Nitropruside: 200 mg/l Neosynephrine: 0 ml/hr
 Sampling Time: 10 sec Setpoint: 90 mmHg

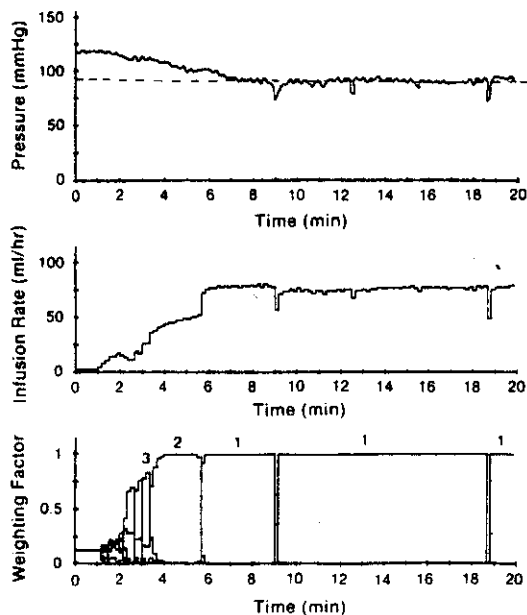


Fig. 10. Results of an animal experiment.

Dog: 26 kg Nitropruside: 200 mg/l Neosynephrine: 100 ml/hr
 Sampling Time: 12 sec Setpoint: 115 mmHg

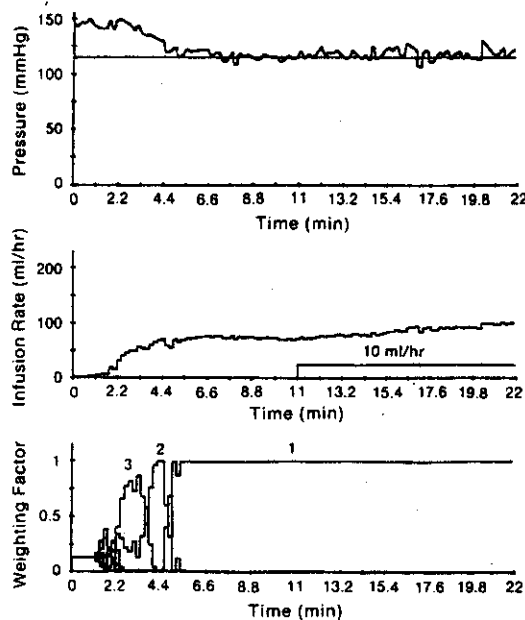


Fig. 12. Results of an animal experiment.

Dog: 15 kg Nitropruside: 200 mg/l Neosynephrine: 15 ml/hr
 Sampling Time: 10 sec Setpoint: 95 mmHg

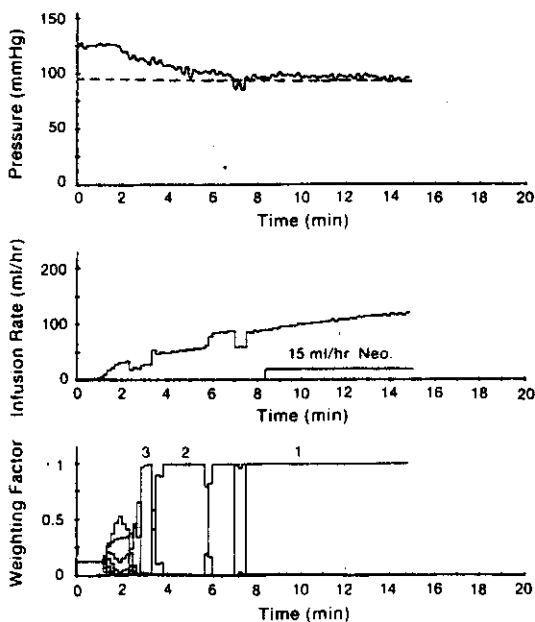


Fig. 11. Results of an animal experiment.

C. Results of Animal Experiments

To further verify the effectiveness of the algorithm and to evaluate the performance of the system design in Section IV-A, animal experiments were carried out on anesthetized mongrel dogs. Arterial pressure was measured through a catheter in the femoral artery by a transducer. The mean pressure signal was obtained by passing the signal through a low-pass filter to remove high-frequency components in the blood pressure signal from the sensor

output. An A/D converter with 12 bits was used for digitization of the mean pressure. Sodium nitropruside with a concentration of 200 mg/l was infused by a Critikon 2100A infusion pump. A PDP MINC-11 computer was used for on-line control. In order to change the plant characteristics, neosynephrine with a concentration of 100 $\mu\text{g}/\text{cc}$ was administered. The sampling period was chosen as 10–15 s. The experiments were run on three dogs.

Fig. 10 shows that the mean arterial pressure (MAP) steadily dropped to within 5 mmHg of the setpoint in 6.5 min and without any undershoot. The mean steady-state error was near zero.

Figs. 11 and 12 show the system responses under neosynephrine infusion on two different dogs. This neosynephrine infusion was such that the anticipated increase in MAP without adaptation would be 30–45 mmHg for Fig. 10 and 20–30 mmHg for Fig. 11. Results indicate that in both cases the system increased the nitropruside infusion rate so as to compensate for the increase in pressure caused by neosynephrine and thus to keep MAP at the given setpoint with a mean error of about 3 mmHg.

Fig. 13 shows the response of the system performed on a third dog with large plant background noise and a higher sensitivity to the drug. The pressure curve shows that the undershoot and the settling time were about 5 mmHg and about 8 min, respectively. The infusion rate and the weighting factors oscillated in the initial control interval, but settled out after 9 min.

V. CONCLUSIONS

The results of both simulations and animal experiments indicate that the MMAC algorithm has the potential for automatically controlling blood pressure over a fairly wide

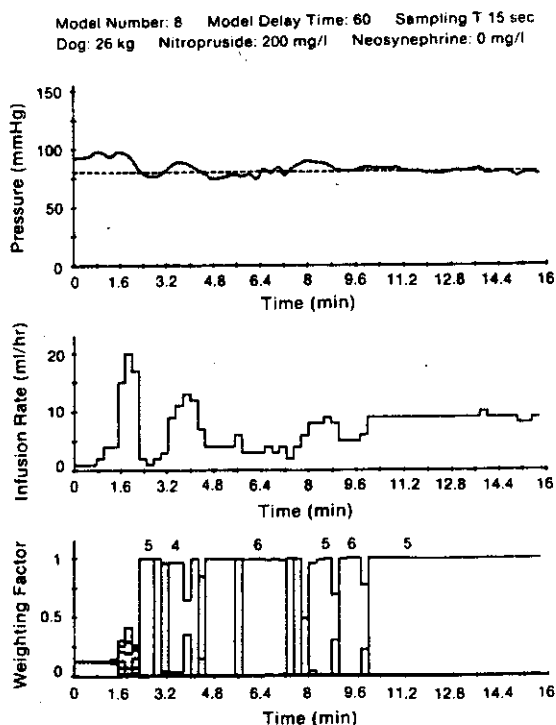


Fig. 13. Results of an animal experiment.

plant parameter envelope, even in the presence of representative background noise.

Further experimentation with animals subjected to significant transfer function variations is recommended prior to clinical usage. Comparative studies with other adaptive algorithms would also be of interest.

ACKNOWLEDGMENT

The authors wish to earnestly thank V. Serna for his valuable help in programming the on-line control system and in running the lab experiments. Special thanks are due to P. Rogers for her invaluable assistance with the animal experiments. Finally, many thanks to M. Mamone for typing the manuscript.

REFERENCES

- [1] J. B. Slate, "Model-based design of a controller for infusing sodium nitroprusside during postsurgical hypertension," Ph.D. dissertation, Univ. Wisconsin-Madison, 1980.
- [2] D. G. Lainiotis, T. N. Upadhyay, and J. G. Deshpande, "A non-linear separation theorem," in *Proc. Symp. Nonlinear Estimation Theory*, San Diego, CA, Sept. 1971, pp. 184-187.
- [3] D. G. Lainiotis *et al.*, "Partitioning: A unifying framework for adaptive systems, II: Control," *Proc. IEEE*, vol. 64, pp. 1182-1198, Aug. 1976.
- [4] G. N. Saridis and T. K. Dao, "A learning approach to the parameter-adaptive self-organizing control problem," *Automatica*, vol. 8, pp. 589-597, Sept. 1972.
- [5] M. Athans *et al.*, "Investigation of the multiple model adaptive control method for flight control systems," NASA Contractor Rep. 3089, May 1979.
- [6] J. B. Slate *et al.*, "A model for design of a blood pressure controller for hypertensive patients," presented at the 5th IFAC Symp. Ident. System Param. Est., Darmstadt, Federal Republic of Germany, Sept. 24-28, 1979.
- [7] H. Kaufman, R. Roy, and X. Xu, "Model reference adaptive control of drug infusion rate," *Automatica*, vol. 20, no. 2, pp. 205-209, 1984.
- [8] J. Martin, Jr., A. B. Corripio, and C. L. Smith, "How to select con-

troller modes and tuning parameters from simple process models," *ISA Trans.*, vol. 15, no. 4, pp. 314-319, 1976.

- [9] G. F. Franklin and J. D. Powell, *Digital Control of Dynamic Systems*. Reading, MA: Addison-Wesley, 1980, p. 119.



W. G. He graduated from the Chongqing University ahead of schedule in 1958 and was trained in the Training Class of Control Theory sponsored by the Institute of Automation in 1960.

He is an Associate Researcher of the Chengdu Institute of Computer Application, Academia Sinica (CICA). He has been with CICA since 1972 and was appointed an Associate Director of the Automatic Control Lab of CICA in 1980. As a visiting scholar, from 1982 to 1984, he has worked in the Electrical, Computer, and Systems Engineering Department of Rensselaer Polytechnic Institute, Troy, NY. From 1958 to 1972 he served as an Assistant Researcher for the Institute of Automation, Academia Sinica. His interests are in computer control, adaptive control, and biomedical control.

Howard Kaufman (S'64-M'66-SM'75) was born in Saratoga Springs, NY, on April 24, 1940. He received the B.E.E., M.E.E., and Ph.D. degrees from the Department of Electrical Engineering, Rensselaer Polytechnic Institute, Troy, NY, in 1962, 1963, and 1965, respectively.



During his undergraduate preparation, he was employed by IBM on a cooperative industrial program, and during his summer vacations as a graduate student he was employed by Saratoga Industries, Saratoga, NY, and by R.P.I. as a Research Assistant. He joined the Computer Research Department of Cornell Aeronautical Laboratory, Buffalo, NY, in 1965, where he was engaged in the development of procedures for applying digital computers to process estimation, identification, and control. In 1968 he joined the General Electric Research and Development Center as a Systems Engineer and developed computer simulations of large-scale industrial processes. Since 1969 he has been a member of the Electrical and Systems Engineering Department of Rensselaer Polytechnic Institute where he is a Professor teaching courses in systems analysis, control theory, and in digital systems. His research interests are in the areas of digital adaptive control, estimation theory, optimal control, and digital signal processing. He has written many papers in these areas and has served as an industrial Consultant in related projects. During the Summer of 1972 he was awarded a NASA Summer Faculty Fellowship at NASA-Langley Research Center where he conducted research in the development of digital adaptive flight control systems. Also during the summer of 1982 he was an NSF Industrial Research participant for General Electric Corporate Research and Development.

Dr. Kaufman is a member of Sigma Xi, Eta Kappa Nu, and Tau Beta Pi honor societies.



Rob Roy (S'56-M'57-SM'73-S'76-A'76-SM'77) received the B.S.E.E. degree from Cooper Union, New York, NY, the M.S.E.E. degree from Columbia University, New York, NY, the D. Eng. Sc. degree from Rensselaer Polytechnic Institute, Troy, NY, and the M.D. degree from Albany Medical College, Albany, NY.

He is currently at Rensselaer Polytechnic Institute and is an Attending Anesthesiologist at Albany Medical Center Hospital. His research interests are in biological signal processing and adaptive cardiorespiratory control systems. He has published extensively in the areas of pattern recognition, control systems, radar signal processing, and process identification.

- [15] D. G. Politte and D. L. Snyder, "A simulated study of design choices in the implementation of time-of-flight reconstruction algorithms," in *Proc. Workshop Time-of-flight Tomogr.*, Washington Univ., St. Louis, MO, May 1982, pp. 130-131, IEEE Comput. Soc. Order No. 448.
- [16] P. Yip and K. R. Rao, "A fast computational algorithm for the discrete sine transform," *IEEE Trans. Commun.*, vol. COM-28, pp. 304-307, Feb. 1980.
- [17] —, "On the computation and the effectiveness of discrete sine transform," *Comput. Elec. Eng.*, vol. 7, no. 1, pp. 45-55, 1980.
- [18] A. V. Oppenheim and R. W. Schaffer, *Digital Signal Processing*. Englewood Cliffs, NJ: Prentice-Hall, 1975.
- [19] W. H. Chen, C. H. Smith, and S. C. Fralick, "A fast computational algorithm for the discrete cosine transform," *IEEE Trans. Commun.*, vol. COM-25, pp. 1004-1009, 1977.

Shirley Nian-Chang Cheng (M'75-S'76-M'80-S'80-M'82) received the B.S. degree in electronics from the Chinese University of Hong Kong in 1974, the M.E. degree in biomedical engineering from the University of Virginia in 1976, and the M.Sc. and D.Sc. degrees in electrical engineering from Washington University, St. Louis, MO, in 1978 and 1982, respectively.

She was a Research Assistant at the Department of Biomedical Engineering, University of Virginia, from January 1975 to May 1976, the Computer System Laboratory, Washington University, from September 1976 to May 1978, and the Biomedical Computer Laboratory, Washington University, from June 1978 to November 1981. From March 1983 to September 1983 she was with Interface Technology Company, St. Louis, MO. She joined the Faculty of Southern Illinois University, Edwardsville, in 1983 as an Assistant Professor of Electrical Engineering. Her primary research interest is in image processing.

Dr. Nian-Chang Cheng is a member of Eta Kappa Nu.

Ref. (13)

The Contribution of Vessel Volume Change and Blood Resistivity Change to the Electrical Impedance Pulse

T. M. RAVI SHANKAR, MEMBER, IEEE, JOHN G. WEBSTER, SENIOR MEMBER, IEEE, AND SHU-YONG SHAO

Abstract—An impedance pulse, recorded noninvasively, has contributions due to both the change in blood volume of the arteries and to the change in the blood resistivity. Other researchers have tried to quantify the relative contributions and have either underestimated or overestimated the contributions since they did not simulate the physiological conditions. We have used an *in vitro* flow circulation system to more closely simulate the physiological conditions and quantify the two contributions. We find that the blood resistivity change contribution is strong enough (21.5 percent of the arterial volume change contribution) to change the morphology of the impedance pulse. There is, however, a phase difference between the two contributions. As a result of this, the blood resistivity change contribution to the height of the impedance pulse will be less than 5.5 percent.

INTRODUCTION

An electrical impedance signal obtained from a limb segment has contribution due to both blood volume change (ΔZ_V) and blood resistivity change (ΔZ_ρ) from arteries, veins,

and smaller blood vessels. Uncertainty exists as to contributions from these two factors. Axial blood resistivity increases about 4 percent as shear rate decreases from 300 to 0 s^{-1} [1]. Other researchers have recorded simultaneously the signals from volume (VPG) and impedance plethysmographs (ZPG) under resting conditions [2], [3]. The systolic upswing of the impedance pulse is typically faster and the diastolic segment differs. Many researchers have tried to explain the differences as due to blood resistivity change (ΔZ_ρ) contribution to the impedance signal. This is clearly possible since ΔZ_ρ peaks with velocity, and hence earlier than ΔZ_V which peaks with pressure. This blood resistivity change contribution, however, has not been well researched.

Using an *in vitro* flow system, a carotid artery, a rigid plastic cylinder, and zero end-diastolic flow [see Fig. 1(a)], Peura *et al.* [3] measured the relative contributions of volume (ΔZ_V) and resistivity (ΔZ_ρ) changes. They found the blood resistivity change contribution to be approximately 10 percent of the total impedance signal. Their *in vitro* flow system did not simulate physiological conditions. Physiologically, there is a minimal transmural pressure of 80 mmHg, the pressure and flow do not peak at the same instant, and the arterial flow typically reverses for short duration during diastole. In their simulation, the pressure and flow peak at the same time. In our study, we will show that the phase difference between pressure and flow indeed plays a major role. They also maintained a minimal transmural pressure of 0 mmHg in the artery. This is an important consideration since the artery is much more

Manuscript received June 23, 1983; revised October 1, 1984. This work was supported by the National Institutes of Health under Grant HL23442.

T. M. Ravi Shankar was with the Department of Electrical and Computer Engineering, University of Wisconsin—Madison, Madison, WI 53706. He is now with the Department of Electrical and Computer Engineering, Florida Atlantic University, Boca Raton, FL 33431.

J. G. Webster is with the Department of Electrical and Computer Engineering, University of Wisconsin—Madison, Madison, WI 53706.

S.-Y. Shao was with the Department of Electrical and Computer Engineering, University of Wisconsin—Madison, Madison, WI 53706. He is now with the Harbin Institute of Technology, Harbin, Heilongjiang Province, People's Republic of China.

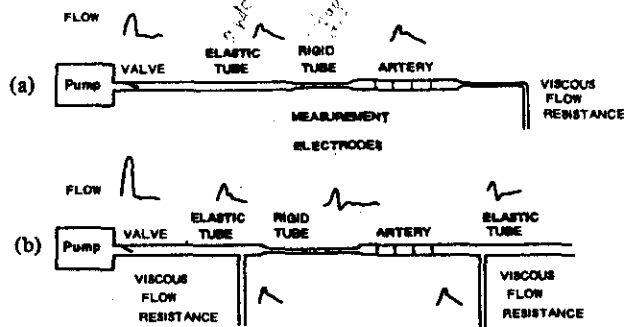


Fig. 1. Experimental methods used to determine the impedance changes caused by the flow (and hence blood resistivity) changes and volume changes in an artery. (a) Method of Peura *et al.* [3]. (b) Our method.

compliant near zero transmural pressure than at high pressures [4]. This would result in an overestimate for the volume change contribution of the impedance pulse. Also, the flow did not reverse in their simulation. Hence, the average flow and the average shear rate were higher, which resulted in an underestimate of the resistivity change contribution.

Sakamoto and Kanai [1] found that for the aorta, the contributions from the volume and resistivity change were about the same order of magnitude. We show later (in the Discussion section) that they overestimated the contribution due to the resistivity change.

The flow circulation system employed is shown in Fig. 1(b) [5]. We use the pressure head and peripheral resistance control to obtain physiological transmural pressures in the artery. We use elastic tubing and a side branch to obtain the proper phase relationship between flow and pressure, and also biphasic arterial flow. This paper presents our experimental data with the flow system.

There are definite contributions from veins and smaller blood vessels to the total impedance signal obtained from a limb segment. We have developed a detailed computer model which quantitates the contributions of all blood vessels in a segment of a leg [6].

METHODS AND MATERIALS

Method Used

Fig. 2 shows the flow model. The blood is in the top reservoir which provides a pressure head. A solenoid valve turns the flow from the reservoir on and off. We change the duty cycle to obtain different pulsatile waveforms. The blood then flows in a pulsatile fashion through elastic tubing (to simulate arteries), a rigid plastic (acrylite) tube of arterial size, and an artery assembled in series with a variable peripheral resistance. The side branches on the *in vivo* system were simulated with a side elastic tube and variable peripheral resistance. The pressure was measured with a side tap and the flow with an extracorporeal electromagnetic flowmeter. We measured the impedance changes on the artery (which is compliant), and this gives the total arterial impedance signal. We also measured the impedance changes on the rigid plastic tube which is noncompliant, and this gives the contribution due to only blood-resistivity changes in vessels of arterial size. We also recorded the volume changes in the artery with an encircling mercury strain gage plethysmograph. Table I provides the pertinent details of the instruments used.

Flow System Details

Rigid Cylinder with Metal Electrodes: A rigid acrylite plastic tube was used to eliminate the component due to volume change. Thus, any measured impedance signal was due to resistivity change only. The electrodes were circular rings of aluminum tubing with a machined collar. The tubing sections were snugly fitted into the collars of the electrodes and glued into place [3]. Compression clamps made connections to the electrodes. The tubing was 7 mm ID and 9 mm OD, with an electrode spacing of 20 mm.

Electrodes for the Artery: To measure the impedance signal from the artery, we used four aluminum electrodes (tape no. 425, 3M Company) 2 mm wide, spaced 15–20 mm apart. They touched roughly two thirds of the circumference of the artery, on the lower side, so that they did not restrain the artery. We have not conducted any study to estimate the error, if any, in not encircling the artery with these tetrapolar electrodes.

Peripheral Resistance Control: The flow was controlled by varying the peripheral resistance, which consisted of a 10 cm long black rubber tubing of 5 mm ID and 18 mm OD. We used compression clamps on two such rubber tubings to independently control the main and side flow.

Tubing Used: Silicone rubber tubing of 7 mm ID and 9 mm OD was used for elastic tubing sections; these were 100 and 50 cm sections, respectively, on the left and right sides of the setup shown in Fig. 2. We used short soft-glass (8 mm ID, 10 mm OD) sections to connect the various parts.

Data Procurement

Blood: Fresh heparinized blood was employed. We always primed the system with saline and obtained recordings for saline before obtaining data for blood. The mixing of saline and blood was kept to a minimum because of the reservoir outlet at the bottom. The blood hematocrit was determined by noting the impedance (with a high constant flow of about 10 ml/s) from the rigid plastic tubing that simulates the artery. We determined the cell constant [8] and from it the hematocrit, to an accuracy of ± 3 percent [9].

Artery: Most arterial sections were obtained from the neck and facial parts of cattle (courtesy of Oscar Mayer and Company). The artery was perfused in Collins solution and refrigerated to maintain it in stable condition for a period of 24–48 h. When we were ready to use it, we injected 0.9 percent cold saline through it and flushed it. We then tested the artery for leaks by forcing saline through one end of the artery while holding the other end of the artery closed. Electrode spacing was 10–20 mm. Tapered tubing was used on both sides to mount the artery in the flow system. We recorded from five arteries. We have provided data for three of them in this paper.

Protocol: We present a detailed protocol elsewhere [10].

RESULTS

Figs. 3–5 show recordings from our flow system experiments. We pumped blood through the system and first recorded the signals shown in Fig. 3 by maintaining a low transmural pressure and then recorded the signals shown in Fig. 4 for a high transmural pressure. Fig. 5 shows the recordings again for a high transmural pressure with 0.9 percent saline in place of

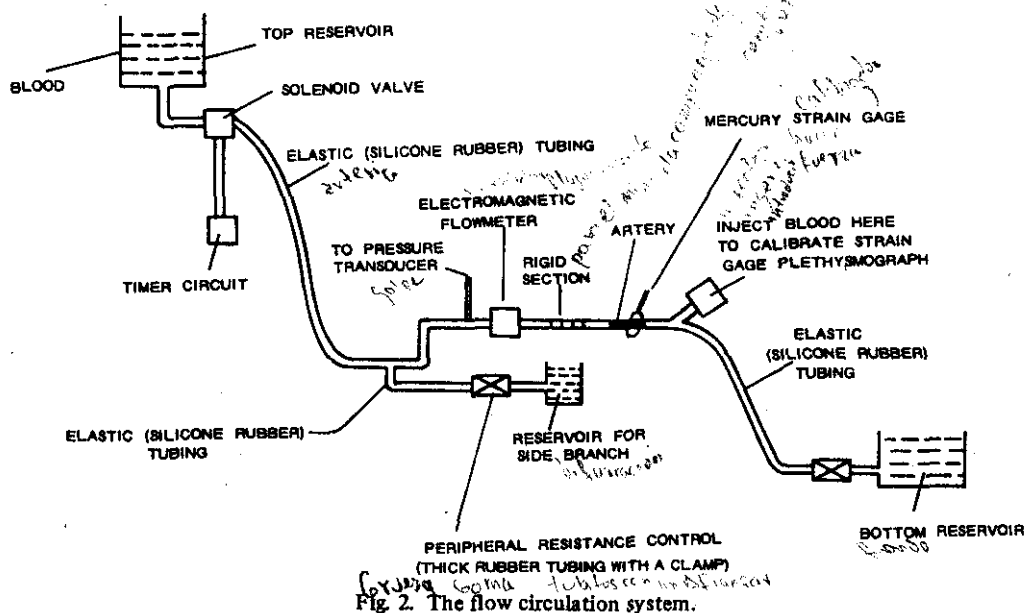


TABLE I
INSTRUMENTS USED IN THE EXPERIMENTAL SETUP AND THEIR CHARACTERISTICS

Instrument Type	Model	Calibration Factor	Noise	Bandwidth
Electromagnetic flowmeter	Statham-Medicon Model K-2000 sine wave type	2.82 (2.46) $\text{ml} \cdot \text{min}^{-1} \text{mV}^{-1}$ for blood (saline)	$2 \text{ ml} \cdot \text{min}^{-1}$	12 Hz
Impedance plethysmographs	Own design [7]	66 $\text{mV}/\text{m}\Omega$	0.33 $\text{m}\Omega$	15 Hz
Pressure transducer	Hewlett-Packard Model 1280	4 $\text{mV} \cdot \text{mm Hg}^{-1}$	—	18 Hz
Strain gage plethysmograph	Own design	Nonlinear: 30 to 100 $\text{mV} \cdot \text{ml}^{-1} \text{a}$	—	18 Hz

^aOnly used for qualitative comparisons.

blood. In Figs. 3-5, plot (a) is the pressure in the artery, plot (b) is the flow, plot (c) is the impedance plethysmograph (ZPG) signal from the artery, plot (d) is the signal from the strain gage plethysmograph (VPG), and plot (e) is the ZPG signal from the rigid section (Fig. 5(e) is not shown, as it was always zero).

Fig. 3(a) shows that the minimal pressure in the artery was low at 20 mmHg. Since the artery was less stretched than when at high transmural pressure, Fig. 3(c) and (d) shows that it was more compliant, and had larger ZPG and VPG signals. Fig. 3(b) shows that the flow reverses for a short duration. If the blood resistivity (and hence shear rate) did not change with flow, the ZPG signal from the rigid section would be zero. However, we do record a signal [see Fig. 3(e)] which peaks with flow, as expected. Notice also that the arterial volume change signal [Fig. 3(d)] peaks with pressure. The ZPG signal from the artery is the sum of the changes due to both volume and resistivity in the artery. Let ΔG_V and ΔG_ρ be the conductance changes corresponding to the impedance changes ΔZ_V and ΔZ_ρ (see (1) below). Since the artery is very compliant at low transmural pressures, ΔG_V is much bigger than ΔG_ρ ,

hence the ZPG signal from the artery looks similar to the VPG signal.

Fig. 4(a) shows the high transmural pressure case where the minimal pressure is 80 mmHg and the arterial compliance is low. Fig. 4(c) shows that the total ZPG signal from the artery looks very much different from the VPG signal shown in Fig. 4(d). Now ΔG_V and ΔG_ρ are of the same order of magnitude. Fig. 4(e) shows that ΔG_ρ peaks with flow [Fig. 4(b)], and hence earlier than ΔG_V which peaks with pressure [Fig. 4(a)]. As a result, the sum of the two signals, i.e., the ZPG signal from the artery [Fig. 4(c)] has a faster rising systolic upswing as compared to the volume change signal [Fig. 4(d)]. Fig. 4(c) shows that the waveform changes in the diastolic part of the ZPG signal from the artery follow the changes in the ZPG signal from the rigid section [Fig. 4(e)]. However, they do not exactly match since the shear rate changes in the rigid section do not exactly match those in the artery (note that axial resistivity decreases 4 percent as shear rate increases from 0 to 300 s^{-1} and remains nearly constant at higher shear rates).

We also conducted the experiment with saline in place of

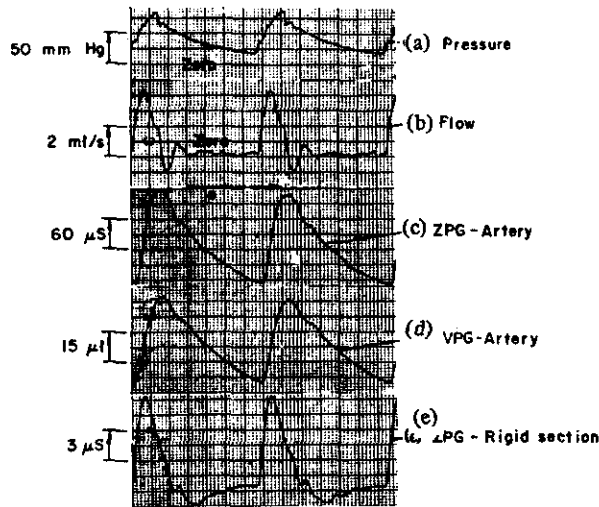


Fig. 3. Flow system recordings for a bovine artery at low transmural pressure, for blood (same artery as in Figs. 4 and 5). Details: (a) pressure: minimum = 20 mmHg, pulse height = 65 mmHg; (b) flow: minimum = -1 ml/s, pulse height = 5.4 ml/s; (c) ZPG-artery: pulse height = $\Delta G_V + \Delta G_\rho = 180 \mu\text{S}$; (d) VPG-artery: used for qualitative comparisons only: the ordinate scale is for average strain; (e) ZPG-rigid section: pulse height = $8.7 \mu\text{S}$, but $\Delta G_\rho = 3.9 \mu\text{S}$.

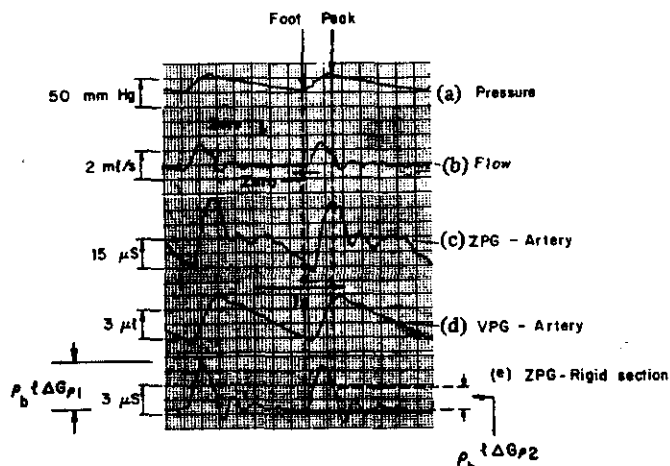


Fig. 4. Flow system recordings for a bovine artery at high transmural pressure for blood (same artery as in Figs. 3 and 5). Details: (a) pressure: minimum = 75 mmHg, pulse height = 30 mmHg; (b) flow: minimum = 0 ml/s, pulse height = 1.8 ml/s; (c) ZPG-artery: pulse height = $\Delta G_V + \Delta G_\rho = 34.5 \mu\text{S}$; (e) ZPG-rigid section: pulse height = $5.1 \mu\text{S}$, but $\Delta G_\rho = 2.1 \mu\text{S}$. $\rho_b \Delta G_{\rho 1}$ is the height of the ZPG signal during its systolic upswing, while $\rho_b \Delta G_{\rho 2}$ is the height of the ZPG signal between the foot and peak of the pressure pulse.

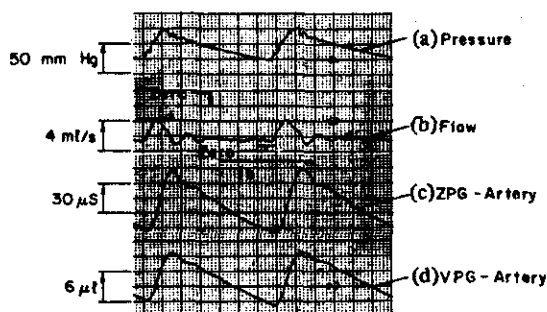


Fig. 5. Flow system recordings for a bovine artery at high transmural pressure for saline (same artery as in Figs. 3 and 4). Details: (a) pressure: minimum = 70 mmHg, pulse height = 50 mmHg; (b) flow: minimum = 0 ml/s, pulse height = 2.8 ml/s; (c) ZPG-artery pulse height = $\Delta G_V = 60 \mu\text{S}$. Note that $\Delta G_\rho = 0$.

blood (see Fig. 5). The pressure is high at 80 mmHg. Since the saline resistivity does not change with shear rate, the ZPG signal from the rigid section is zero (not shown). As a result, the ZPG signal from the artery looks very similar to the VPG signal from the artery [see Fig. 5(c) and (d)]. Since pulse pressures were not the same for Figs. 4 and 5, we first determined the equivalent arterial volume change from the ZPG signal of the artery from the following equation [5]:

$$\Delta V = \rho_b l^2 \Delta G \approx -\rho_b l^2 \Delta R / R^2 \quad \text{for } \Delta R \gg R \quad (1)$$

where

ΔV = arterial volume change in μl

ρ_b = blood resistivity in $\Omega \cdot \text{cm}$

l = length of the arterial section between the voltage electrodes in cm

ΔG = conductance change measured between the voltage electrodes in mS

ΔR = amplitude of the impedance pulse (systolic upswing) in $\text{m}\Omega$ (we ignore the reactive component as it is much smaller than the resistive component)

R = resistance between the voltage electrodes in Ω .

We then divided ΔV by the pulse pressure height to obtain arterial compliance at the transmural pressure. The two values obtained for Figs. 4 and 5 agreed to within 3 percent. This result, surprising at first glance, can be easily understood by referring to the timing relationship between pressure and flow. Note that the flow peaks earlier and decreases considerably by the time pressure peaks. ΔG_ρ peaks with flow and ΔG_V peaks with pressure. Thus, in the net signal (ZPG from the artery), the result is a faster rising systolic upswing, with the foot-to-peak height of ΔG_V affected very little by the presence of the ΔG_ρ signal.

Fig. 6 shows the equivalent arterial volume change as a function of average transmural pressure (determined as the sum of the diastolic pressure and 1/3 of the pulse pressure height) on different arteries. Since the height of the pressure pulse was not the same for different transmural pressures, we normalized the arterial volume changes to a 40 mmHg pulse by multiplying by 40 and dividing by the pulse pressure. Note that with increases in transmural pressure, the compliance decreases [4], and hence the arterial volume decreases. For two of the three arteries represented, there is good agreement for blood and saline over the whole range of transmural pressures. For the third artery, the curves do not agree well at high transmural pressures, with the blood resistivity change contribution being about 10 percent.

Table II tabulates the results for one artery. Column 1 lists the minimal pressure in the artery and column 2 the pulse pressure height. Note that the minimal pressure increased from 0 to 80 mmHg. Column 3 gives the minimal flow and column 4 the flow pulse height. We use the impedance pulse height from the arterial ZPG signal to calculate the equivalent arterial volume change per unit length by modifying (1) as $\rho_b / \Delta G_V$ and list that value in column 5 in units of $\mu\text{l}/\text{cm}$. Column 6 lists the impedance pulse height from the rigid section ZPG signal, $\rho_b \Delta G_{\rho 1}$ in $\mu\text{l}/\text{cm}$ [using (1)], to make it easier to compare it to the ZPG signal from the artery. Column 7 gives the

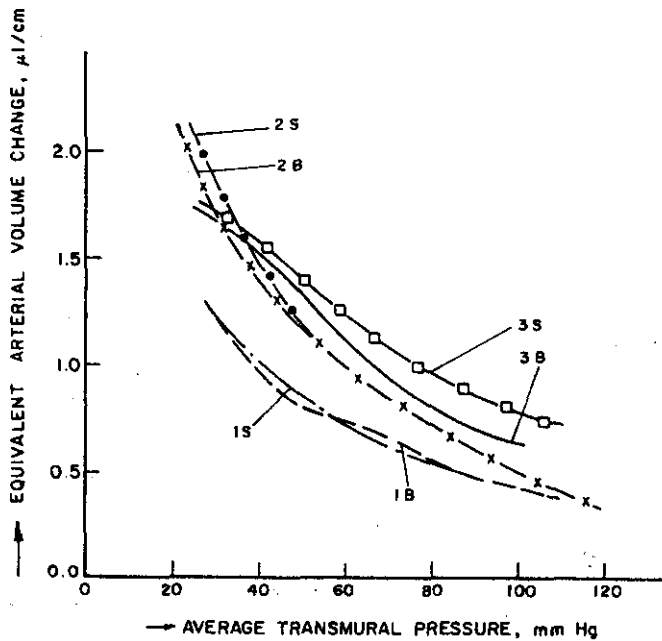


Fig. 6. Equivalent arterial volume change for a 40 mmHg pulse versus average transmural pressure. Labels indicate artery number and S = saline, B = blood.

TABLE II
EXPERIMENTAL DATA FOR ONE ARTERY
(ID = 3 mm, OD = 7 mm (at Zero Transmural Pressure),
 $\rho_h = 158 \Omega \cdot \text{cm}$, $Hct = 45$ Percent)

Case	Pressure		Flow		ZPG-artery	ZPG-rigid section			
	Column 1	2	3	4	5	6	7	8	9
	Minimum mm Hg	Pulse height mm Hg	Minimum ml/s	Pulse height ml/s	$\rho_b \Delta G_V$ $\mu\text{l}/\text{cm}$	$\frac{\rho_b \Delta G_{p,1}}{\rho_b \Delta G_V} \times 100\%$	$\frac{\rho_b \Delta G_{p,2}}{\rho_b \Delta G_V} \times 100\%$	$\frac{\rho_b \Delta G_{p,2}}{\rho_b \Delta G_V} \times 100\%$	$\frac{\rho_b \Delta G_{p,2}}{\rho_b \Delta G_V} \times 100\%$
1	0	65	0.0	8.8	33.7	2.25	6.7	2.25	6.7
2	15	65	0.0	4.4	22.1	1.46	6.6	0.23	1.0
3	15	70	-2.1	6.9	24.5	1.37	5.6	0.23	0.9
4	20	70	-1.1	5.7	23.0	1.64	7.1	0.27	1.2
5	25	65	0.0	4.2	20.0	1.09	5.5	0.00	0.0
6	25	65	-1.5	5.5	23.0	1.73	7.6	0.40	1.8
7	35	60	-0.6	4.6	16.7	1.55	9.3	0.35	2.1
8	40	60	0.0	4.0	14.2	1.00	7.0	0.40	2.8
9	60	45	0.0	2.7	8.7	1.32	15.2	0.00	0.0
10	65	40	0.0	2.5	7.1	1.00	14.1	0.20	2.8
11	80	32	0.0	1.7	4.7	1.00	21.5	0.26	5.5

much less (5.5 percent or less). To make an estimate of the actual contribution, we determined the height of the ZPG signal from the rigid section over the time interval during which the pressure pulse rises from foot to peak amplitude (see Fig. 4). Columns 8 and 9 list this parameter, $\rho_b \Delta G_{p,2}$, as an absolute value in $\mu\text{l}/\text{cm}$ and as a percentage relative to the total ZPG signal from the artery.

For case 1, the pressure and flow peaked at the same time, and the resulting contribution of $\Delta G_{p,2}$ was 6.7 percent. This case is similar to that of Peura *et al.* [3]. However, physiologically, pressure and flow do not peak at the same time, and so we ignore this case in the discussion to follow.

Note the following from Table II.

- 1) With an increase in transmural pressure, arterial compliance decreases, which results in a lower ΔG_V (column 5).
- 2) With flow reversal (nonzero and negative minimal flow cases in Table II), the pulse height of the ZPG signal from the rigid section increases (column 6).
- 3) The percent contribution of the resistivity change decreases with decrease in transmural pressure (see column 9).

Exact quantification is difficult because of the following reasons.

- 1) Our experimental arteries were typically one half as compliant as the arteries found in the human leg. (Estimated h/R_0 ratio (thickness to outer radius ratio) at a transmural pressure of 100 mmHg averaged 0.18 for the arteries.)
- 2) The pulse pressure in our experiments was typically 60 mmHg, while 40 mmHg is a typical physiological value. We had a higher value because of the interaction of flow and pressure controls.
- 3) In our flow system, pressure and flow pulses were interdependent: controls to vary one variable invariably affected the other variable. So flow reversal was typically obtained only at low transmural pressures. Addition of a pulsatile pump to vary the flow independent of the minimal pressure is desirable in a future study.
- 4) The rigid section may not simulate conditions in the artery at all transmural pressures. At low transmural pressures, when the artery is narrower, its shear rates are higher than those in the rigid section, which results in a lower effect of resistivity change in the artery.

DISCUSSION

In this paper, we have presented our experimental data on the relative contributions of arterial volume change and blood resistivity change to the total impedance signal. Other researchers [1], [3] have tried to quantify the relative contributions and have either underestimated or overestimated the contributions since they did not simulate physiological conditions. Our *in vitro* flow circulation system simulates the physiological conditions better than that of Peura *et al.* [3]. We maintained a minimal transmural pressure of 80 mmHg and obtained the proper phase relationship between pressure and flow (see McDonald [11]; the flow peaks earlier than the pressure by about $\frac{1}{8}$ of the cardiac cycle). We could not achieve flow reversal at high transmural pressures because of interaction between flow and pressure controls in the *in vitro* system. We find that the blood resistivity change contribution is strong enough

ratio of column 6 to the arterial ZPG signal in column 5 expressed as a percentage. This is a measure of the relative amplitude of the resistivity change signal to the volume change signal. Note that the resistivity change signal could be as large as 21.5 percent of the volume change signal. However, since the resistivity change and volume change signal do not add in phase, the contribution of the resistivity change signal to the total ZPG signal from the artery is rarely 21.5 percent. Usually, it is

(21.5 percent) to change the morphology of the impedance pulse, but because of the phase difference between the two contributions, it results in less than a 5.5 percent contribution to the height of the impedance pulse.

Sakamoto and Kanai [1] also have studied the relative contributions, and they found that for the aorta, the contributions from the volume and resistivity change were about the same order of magnitude. We computed the average shear rate in their experiment (see [1, p. 694, Fig. 21]) to be 31.5 s^{-1} , while McDonald [11] gives the average shear rate in the aorta as 80 s^{-1} . Thus, they simulated conditions similar to Fig. 15(d) [1, p. 693] in their paper, while Fig. 15(e) represents a more physiological case for normal resting conditions. Hence, Sakamoto and Kanai overestimated the contribution due to the blood resistivity change in the large arteries.

Our paper and those referenced above [1], [3] have addressed the quantification of arterial contributions to the non-invasively measured electrical impedance pulse.

However, an impedance pulse has additional contributions from veins and smaller blood vessels, due both to volume and resistivity changes. To quantitate these contributions, we have modeled the leg circulation in detail, with more than 80 differential equations, to determine the pressure and flow in different sized blood vessels, and hence their contribution to the impedance signal [6]. Our model explains the differences in volume and plethysmographic signals under conditions of rest, reactive hyperemia, atherosclerotic disease, and low transmural pressures (where arterial compliance peaks). See Table III for more details. We concluded that, under resting conditions, the contributions to the impedance pulse from the large arterial volume change and blood resistivity change were, respectively, 77.5 and 3.9 percent with the rest of the contribution (18.6 percent) from the microcirculation ("microcirculation" refers to all the vessels other than the large arteries). We also concluded that the volume plethysmograph was more sensitive to the microcirculatory contributions, which is especially evident in the case of reactive hyperemia.

Atherosclerotic disease was simulated in the computer model. In atherosclerosis, the average flow (hence, the average shear rate) is reduced, and hence the effect of blood resistivity change is increased. Since all the different contributions are more in phase now, the contribution of blood resistivity change is considerably higher at 10.2 percent. Note that the microcirculation contributes 22.5 percent of the total signal. We did not simulate these conditions in the flow circulation system.

Another study was performed on noninvasive determination of arterial compliance using the ZPG [12]. We wrapped a pressure cuff around the lower leg and increased the cuff pressure. Note that as the cuff pressure was increased, the pressure across the arterial wall decreased. Since the artery was less stretched now, its compliance increased [4]. Two circumferential electrodes glued in the middle of the cuff recorded the impedance pulse ΔZ from which we calculated the arterial volume pulse ΔV . We determined the ratio of maximal arterial volume change (recorded near a cuff pressure equal to diastolic pressure) to the blood pressure pulse ΔP as a measure of the maximal compliance. This maximal compliance correlates well with cardiovascular risk factors [13]-[15]. It decreases with age and

TABLE III
RELATIVE CONTRIBUTION TO THE FOOT-TO-PEAK AMPLITUDE (SYSTOLIC UPSWING) OF THE IMPEDANCE SIGNAL FOR A TYPICAL LIMB SECTION

Case	Large Artery		Microcirculation	
	Volume Change (%)	Blood Resistivity Change (%)	Volume Change (%)	Blood Resistivity Change (%)
Normal	77.5	3.9	5.2	13.4
Reactive Hyperemia	82.3	3.3	13.2	1.2
Atherosclerosis	67.3	10.2	8.9	13.7
Peak Compliance	97.7	2.3	0	0

further reduces with hypertension, and still further with peripheral vascular disease. On the other hand, Chinese and subjects who exercised regularly had values well above the average for their age group.

To refine this method in our compliance study, we simulated the condition of peak compliance in both the flow circulation and computer model. Since the average velocity of flow (and hence, average shear rate) is higher now (the volume of flow is about the same as for the normal resting case, but the radius is smaller), the ΔG_p is smaller and ΔG_V is larger because the artery is more compliant now. The contribution from other vessels in the limb section is, however, zero, since they would be collapsed when the cuff pressure is close to the diastolic pressure. Thus, the results show that the impedance can be used to determine the arterial volume change with less than 2.3 percent uncertainty.

CONCLUSIONS

In this paper, we have provided details of an experimental study with a flow circulation system to quantitate the contributions to the arterial impedance signal. We have also conducted a separate modeling study to quantitate the contributions from other blood vessels to a limb impedance signal [6]. We provide here the conclusions of both of our studies.

1) The arterial blood resistivity change contribution is strong enough to change the morphology of the impedance pulse obtained from an artery, but because of the phase difference from the arterial volume change contribution, it results in less than a 5.5 percent contribution to the height of the impedance pulse.

2) There are other contributions to the noninvasively obtained impedance signal from a limb segment. Our computer model estimates that under normal resting conditions, the microcirculatory contribution can be significant, at 18.6 percent of the total impedance signal.

- 3) With reactive hyperemia, the microcirculatory volume change contribution to the impedance signal increases.
- 4) With atherosclerotic disease, there is a significant increase of blood resistivity change contribution to the limb impedance signal.
- 5) At lower transmural pressures, the arterial compliance increases and the maximal arterial volume can be estimated from the limb impedance signal with little uncertainty.

REFERENCES

- [1] K. Sakamoto and H. Kanai, "Electrical characteristics of flowing blood," *IEEE Trans. Biomed. Eng.*, vol. BME-26, pp. 686-695, Dec. 1979.
- [2] J. Nyboer, *Electrical Impedance Plethysmography*, 2nd ed. Springfield, IL: Thomas, 1970.
- [3] R. A. Feura, B. C. Penney, J. Arcuri, F. A. Anderson, Jr., and H. B. Wheeler, "Influence of erythrocyte velocity on impedance plethysmographic measurements," *Med. Biol. Eng. Comput.*, vol. 16, pp. 147-154, Mar. 1978.
- [4] K. Yamakoshi, H. Shimzu, M. Shibata, and A. Kamiya, "New oscillometric method for indirect measurement of systolic and mean arterial pressure in the human finger. Part 1: Model experiment," *Med. Biol. Eng. Comput.*, vol. 20, pp. 307-313, May 1982.
- [5] D. K. Swanson, "Measurement errors and origin of electrical impedance changes in the limbs," Ph.D. dissertation, Dep. Elec. Comput. Eng., Univ. Wisconsin, Madison, 1976.
- [6] T. M. R. Shankar and J. G. Webster, "The contribution of different sized vessels in the extremities to the arterial pulse waveform as recorded by electrical impedance and volume plethysmography," *Med. Biol. Eng. Comput.*, to be published.
- [7] —, "Design of an automatically resetting electrical impedance plethysmograph," in *Proc. IEEE Frontiers Eng. Health Care*, 1980, pp. 346-349.
- [8] D. Dobos, *Electrochemical Data*. New York: Elsevier, 1975, p. 57.
- [9] L. A. Geddes and L. E. Baker, *Principles of Applied Biomedical Instrumentation*, 2nd ed. New York: Wiley, 1975.
- [10] T. M. R. Shankar, "The origin of the impedance pulse in the limbs and arterial compliance studies using impedance plethysmography," Ph.D. dissertation, Dep. Elec. Comput. Eng., Univ. Wisconsin, Madison, 1982.
- [11] D. A. McDonald, *Blood Flow in Arteries*, 2nd ed. Baltimore, MD: Williams and Wilkins, 1974.
- [12] T. M. R. Shankar and J. G. Webster, "Measuring arterial volume-pressure characteristics using impedance plethysmography," in *Proc. 5th Int. Conf. Elec. Bio-Impedance*, 1981, pp. 307-310.
- [13] J. T. Nichol, "The effect of the cholesterol feeding on the distensibility of the isolated thoracic aorta," *Can. J. Biochem. Physiol.*, vol. 33, pp. 507-516, 1955.
- [14] T. I. Pynadath and D. P. Mukherjee, "Dynamic mechanical properties of atherosclerotic aorta, A correlation between the cholesterol ester content and the viscoelastic properties of atherosclerotic aorta," *Atherosclerosis*, vol. 26, pp. 311-318, 1977.
- [15] R. Ross, "The arterial wall and atherosclerosis," *Annu. Rev. Med.*, vol. 30, pp. 1-15, 1980.



T. M. Ravi Shankar (S'76-M'83) received the M.S. and Ph.D. degrees in electrical and computer engineering from the University of Wisconsin, Madison, in 1977 and 1982, respectively.

From 1971 to 1974 he was a Research and Development Engineer with the Computer Division of E.C.I.L., India. At present, he is an Assistant Professor with the Department of Electrical and Computer Engineering, Florida Atlantic University, Boca Raton. His current research interests in biomedical engineering are

in the areas of early and noninvasive detection of atherosclerosis and objective noninvasive determination of blood pressure. He is also active in the areas of VLSI and computer architecture.

Dr. Ravi Shankar is a member of ASEE, AHA, Sigma Xi, and is a Registered Professional Engineer in the State of Florida.



John G. Webster (M'59-SM'69) received the B.E.E. degree from Cornell University, Ithaca, NY, in 1953, and the M.S.E.E. and Ph.D. degrees from the University of Rochester, Rochester, NY, in 1965 and 1967, respectively.

He is a Professor of Electrical and Computer Engineering at the University of Wisconsin, Madison. In the field of medical instrumentation, he teaches undergraduate, graduate, and short courses, and does research on electrodes, biopotential amplifiers, impedance measurements, and tactile vision.

Dr. Webster is Associate Editor, Medical Instrumentation, of the IEEE TRANSACTIONS ON BIOMEDICAL ENGINEERING, and is a member of the IEEE-EMBS Administrative Committee. He is coauthor, with B. Jacobson, of *Medicine and Clinical Engineering* (Englewood Cliffs, NJ: Prentice-Hall, 1977). He is Editor of *Medical Instrumentation: Application and Design* (Boston, MA: Houghton Mifflin, 1978). He is co-editor, with A. M. Cook, of *Clinical Engineering: Principles and Practices* (Englewood Cliffs, NJ: Prentice-Hall, 1979); with W. J. Tompkins, of *Design of Microcomputer-Based Medical Instrumentation* (Englewood Cliffs, NJ: Prentice-Hall, 1981); with A. M. Cook, of *Therapeutic Medical Devices: Application and Design* (Englewood Cliffs, NJ: Prentice-Hall, 1982); and, with A. M. Cook, W. J. Tompkins, and G. C. Vanderheiden, of *Electronic Devices for Rehabilitation* (New York: Wiley, 1984).



Shu-Yong Shao was born in Shanghai, China, on August 4, 1939. He graduated from the Department of Radio Engineering, Beijing Institute of Technology, Beijing, China.

In 1960 he joined the Department of Radio Engineering, Harbin Institute of Technology, Harbin, China, where he is now a Lecturer. He worked in industry for several years, designing a high-frequency phase meter and servosystems. From 1981 to 1983 he was a Visiting Scholar in the Department of Electrical and Computer Engineering, University of Wisconsin, Madison. His present research interests are in medical instrumentation and microprocessor applications.

Mr. Shao is a member of the Chinese Institute of Electronics.

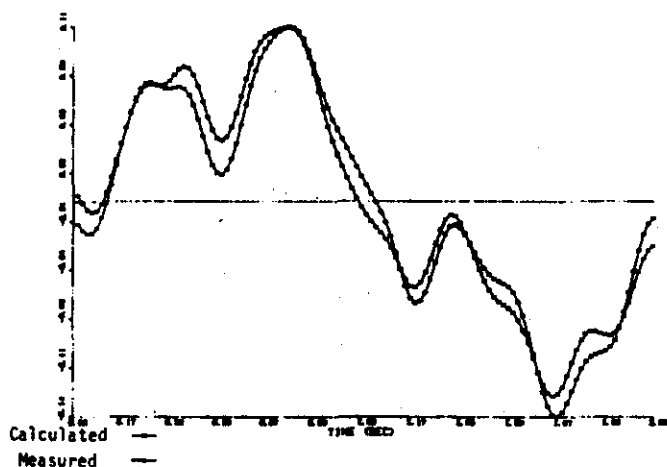


Fig. 4.

as the first model, yet draws from Contini's work to obtain the body segment parameters. The results of this model are seen in Fig. 3. Here again we see a large error in the measured and calculated center of pressure. For the most part, the two results thus far are identical. The explanation probably lies in the fact that the upper body, which is the most massive portion of the body, is modeled identically in both calculations.

Fig. 4 shows results obtained using the general geometric solid model of Hanovan for human body segment parameters. As can be seen, this model provides very good agreement with direct measurement of the center of pressure. The authors believe that these results justify a statistical evaluation of the usefulness of Hanovan's method in quantitative posturography. Such a study is now underway.

REFERENCES

- [1] S. H. Koozekanani, C. W. Stockwell, R. B. McGhee, and F. Firoozmand, "On the role of dynamic models in quantitative posturography," *IEEE Trans. Biomed. Eng.*, vol. BME-27, pp. 605-609, Oct. 1980.
- [2] W. Braune and O. Fisher, *Der Gang der Menschen, Versuche am Unbelasteten und Belasteten Menschen*, Abh. d. Mathem. Phys. Kl. d. K. Sachs. Gesellsch. d. Wissensch. Leipzig, vol. XXI, 1895.
- [3] W. T. Dempster, "Space requirements of the seated operator," Wright Patterson Air Force Base, Dayton, OH, Rep. WADCTR 55-159, 1955.
- [4] R. Contini, "Body segment parameters: Part II," *Artif. Limbs*, vol. 16, no. 1, pp. 1-19, 1972.
- [5] E. P. Hanovan, "A mathematical model of human body," M.S. thesis, USAF Inst. Tech., Wright Patterson Air Force Base, Dayton, OH, 1964.
- [6] M. T. Fatehi, M. T. Balmesada, Jr., and S. H. Koozekanani, from papers presented at the 1984 SCS Simulators Conf., Apr. 1984, Norfolk, VA. (Reprints available from the Simulation Council, Inc., P.O. Box 2228, La Jolla, CA 92038.)

Correlation Between Arterial Blood Pressure Levels and $(dZ/dt)_{\min}$ in Impedance Plethysmography

L. DJORDJEVICH, M. S. SADOVE, J. MAYORAL,
AND A. D. IVANKOVICH

Abstract— $(dZ/dt)_{\min}$, which is the magnitude of the negative peak of the first time derivative of transthoracic electrical impedance Z , plays a key role in impedance plethysmography because it reflects the pumping

Manuscript received November 22, 1983; revised August 30, 1984.
The authors are with the Department of Anesthesiology, Rush Presbyterian St. Luke's Medical Center, Chicago, IL 60612.

action of the heart. Its current applications for measuring stroke volume and quantification of myocardial contractility, however, ignore the possibility that $(dZ/dt)_{\min}$ may be strongly modified by factors that are independent on the heart. Measurements of $(dZ/dt)_{\min}$ on 146 volunteers are statistically correlated with the systolic, diastolic, and mean arterial blood pressure and heart rate. Statistically significant correlations are obtained between the $(dZ/dt)_{\min}$ and blood pressures, but not with heart rate. The correlations indicate that $(dZ/dt)_{\min}$ is expected to decrease as the arterial blood pressure level increases. This relationship is elucidated with the help of a theoretical model which combines the parallel conductor theory with a mechanical model of an elastic artery. The analysis of the model is in agreement with statistical predictions based on measured data, indicating that $(dZ/dt)_{\min}$ explicitly depends on blood pressure level in an inverse manner. It is concluded that the functional dependence of dZ/dt signals on Z and blood pressure levels should be taken into account if valid conclusions from applications of dZ/dt signals are to be drawn. Suggestions are made to use the measured correlations as a means to eliminate Z and blood pressure levels as factors in applications of dZ/dt signals.

I. INTRODUCTION

Impedance plethysmography [1]-[3] continues to attract the attention of many investigators because of its ability to provide in a noninvasive manner valuable information about intravascular and extravascular fluid volume, heart function, and vascular response to the heart function. Since first suggested by Nyboer *et al.* [4] this method has been used with various degrees of success to measure stroke volume and cardiac output [5]-[8] and total peripheral resistance [9] and to quantify myocardial contractility [10]. The recent evaluation by Shimazu *et al.* [11] of the parallel conductor theory, the physical basis of impedance plethysmography, indicates that the error in measuring the blood component of resistivity caused by this modeling is less than ± 2 percent, which shows that the impedance plethysmography signals can be measured with high accuracy.

Ito, Yamakoshi, and Togawa [15]-[17] and Djordjevich *et al.* [12], however, have raised the question of correct application of impedance plethysmography in impedance cardiography and quantification of myocardial contractility; these are based on measurements of $(dZ/dt)_{\min}$, which is the magnitude of the negative peak of the first time derivative of the transthoracic impedance Z . They experimentally demonstrated [12] that this peak is proportional to the time-average value of Z , and suggested that this dependence should be taken into account in all applications where the magnitude of the peak is a major factor, such as in stroke volume measured by impedance cardiography, or in myocardial contractility. In addition, the shape and the amplitude of the dZ/dt signal may be expected to be strongly influenced by the dynamic response of the vascular system to the ejection of blood from the left ventricle, which in turn is the consequence of nonlinear, viscoelastic nature of arterial walls. Thus, dZ/dt should also depend on the rate of ejection, the mean arterial blood pressure, and the modulus of elasticity of arterial walls.

This communication presents the directly measured relationship between the $(dZ/dt)_{\min}$ peaks and arterial blood pressure in normal subjects, and offers an explanation for this relationship.

II. METHODS

Measurements were done on 146 volunteers of both sexes, who had no known cardiovascular disorder other than hypertension. Normal healthy volunteers were used to avoid possible failure of accurate identification of dZ/dt peaks in various pathological cardiovascular states. The transthoracic electrical impedance Z was measured with volunteers in supine position, after 10 min rest in that position, so that a steady-state circula-

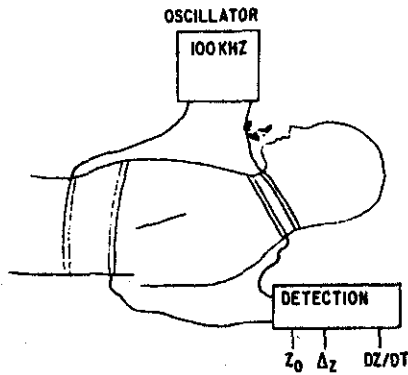


Fig. 1. Electrode attachments for the impedance plethysmograph.

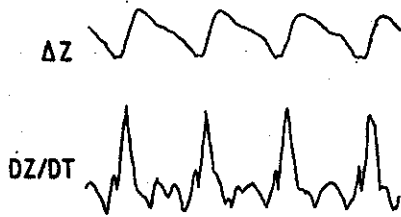


Fig. 2. Recordings of typical signals of Z and dZ/dt .

tion is achieved. Z and dZ/dt were measured with the Impedance Cardiograph, model 200, manufactured by Instrumentation for Medicine. Fig. 1 illustrates electrode attachments. A constant current oscillator produces 4 mA rms current with 100 kHz frequency in the chest region between the two outer electrodes. This combination of current and frequency is considered very safe, with the current level 20 times lower than the threshold of perception. The two inner electrodes serve as measuring electrodes, connected to the detection portion of the impedance meter which measures Z and dZ/dt continuously as functions of time. Typical recordings of the output are shown in Fig. 2.

Z and dZ/dt signals, in the form of voltage, are connected to two input channels of an analog-to-digital converter which is part of a PDP-11/03 minicomputer manufactured by Digital Equipment Corporation. The negative peaks $(dZ/dt)_{\min}$ of the dZ/dt signals are detected in every cardiac cycle by a pattern recognition routine of the computer program, and their magnitudes are stored in an array. Another routine simultaneously samples the values of Z . After 1 min of sampling, the average values of Z and $(dZ/dt)_{\min}$ are calculated and printed.

Simultaneously with impedance measurements, peripheral arterial blood pressures are measured automatically by a Dinamap model 845 (Applied Medical Research Corporation) unit which measures systolic, diastolic, mean arterial blood pressure, and heart rate using a cuff placed on the upper arm. Blood pressure measured in this manner is slightly amplified, but directly proportional to the central arterial pressure.

After each measurement on a volunteer, average values of Z , $(dZ/dt)_{\min}$, systolic, diastolic, mean arterial pressure, and heart rate are stored in a data diskette. When all 146 volunteers were measured, data stored on the diskette were correlated and statistically analyzed by the computer.

III. RESULTS

$(dZ/dt)_{\min}$ represents the average of the absolute values of magnitudes of the negative peaks of the dZ/dt signals, obtained during a 1 min period of measurement on a volunteer (Fig. 2). For each cardiac cycle, there is one such peak corresponding to the maximum rate of change of Z .

The sample size, on the basis of which all correlations below are calculated, is 146. Correlations are obtained by linear regression. The standard deviation around the correlation σ is reported together with the correlation. The statistical signifi-

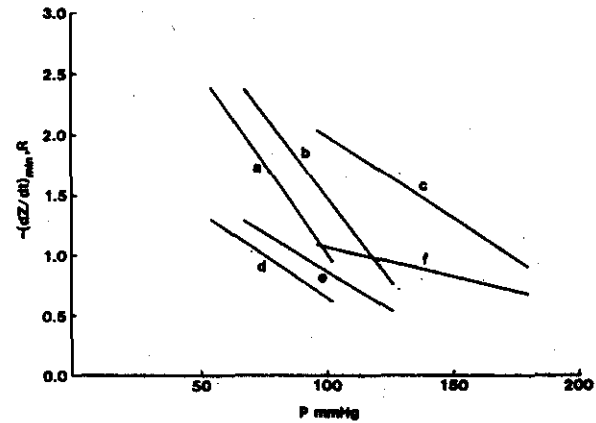


Fig. 3. Correlation of dZ/dt peaks with diastolic pressure a , mean arterial pressure b , and systolic pressure c . Correlation of the ratio R with diastolic pressure d , mean arterial pressure e , and systolic pressure f .

cance of the correlation is determined by calculating the value of p , which represents the probability that the regression coefficients are zero. The significance of correlations is determined by the F test of the null hypothesis that regression coefficients are zero, and that there is no relationship between variables. For values of p which are less than 0.01, the correlation is assumed to be statistically significant because there is a 99 percent probability that there exists a true dependence of $(dZ/dt)_{\min}$ on the independent variable.

In all correlations below, Z is measured in ohms, dZ/dt in ohms/s, blood pressure in millimeters of mercury, and heart rate in beats/min. The mean value of measured $(dZ/dt)_{\min}$ is 1.6325 Ω/s .

$(dZ/dt)_{\min}$ is first correlated to the mean arterial pressure P_m

$$(dZ/dt)_{\min} = 4.220 - 0.02756P_m \quad (1)$$

with $\sigma = 0.5236$, $p < 10^{-5}$. This correlation is valid for the pressure range between 67 and 126 mmHg.

The correlation with systolic pressure P_s in the range from 96 to 180 mmHg is

$$(dZ/dt)_{\min} = 3.3276 - 0.01352P_s \quad (2)$$

with $\sigma = 0.567$ and $p < 10^{-3}$.

The correlation with diastolic pressure P_d in the range from 54 to 102 mmHg is

$$(dZ/dt)_{\min} = 4.0131 - 0.03016P_d \quad (3)$$

with $\sigma = 0.537$, and $p < 10^{-4}$.

The results are graphically represented in Fig. 3, which shows that all three functions are decreasing.

The correlation with heart rate (HR) has $p > 0.5$ indicating the absence of relationship between $(dZ/dt)_{\min}$ and HR in the range from 51 to 117 beats/min.

An earlier study [12] indicated strong correlation between $(dZ/dt)_{\min}$ and Z_0 , which is the time-average value of Z

$$(dZ/dt)_{\min} = 0.0993Z_0 - 0.9038 \quad (4)$$

with $\sigma = 0.2739$ and $p < 10^{-4}$.

Equation (4) is used to eliminate the influence of Z_0 on value of $(dZ/dt)_{\min}$ by forming the ratio

$$R = (dZ/dt)_{\min} / (dZ/dt)_c \quad (5)$$

and the difference

$$D = (dZ/dt)_{\min} - (dZ/dt)_c \quad (6)$$

where $(dZ/dt)_c$ is the predicted value of $(dZ/dt)_{\min}$ calculated from (4), for measured value of Z_0 . R and D are then corre-

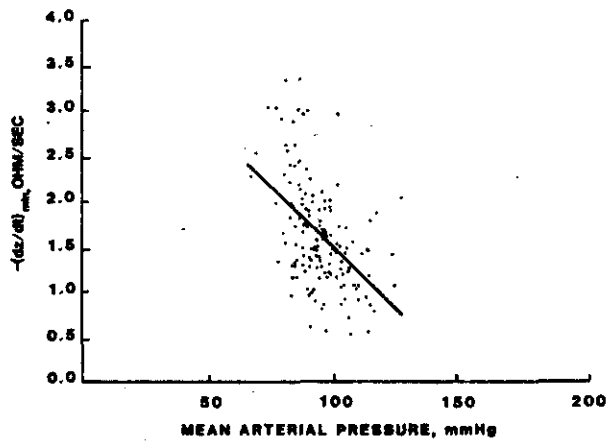


Fig. 4. The distribution of the magnitudes of the dZ/dt peaks (raw data points) as a function of the mean arterial blood pressure (\cdot), and the corresponding linear regression line ($-$).

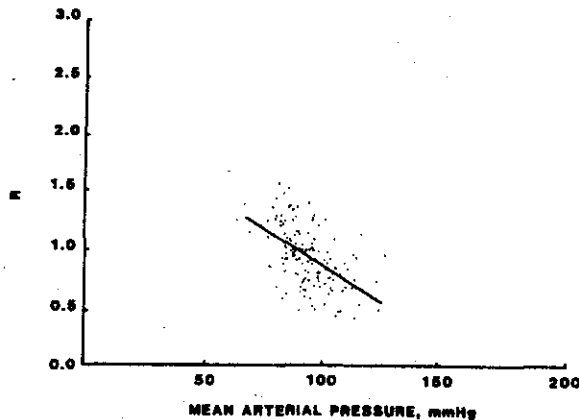


Fig. 5. The distribution of raw data points of the ratio R as a function of the mean arterial blood pressure (\cdot), and the corresponding linear regression line ($-$).

lated with P_m , P_s , P_d , HR, and Z_0

$$R = 2.1312 - 0.01274P_m \quad (7)$$

with $\sigma = 0.2242$ and $p < 10^{-5}$,

$$R = 1.546 - 0.00487P_s \quad (8)$$

with $\sigma = 0.2522$ and $p < 10^{-2}$, and

$$R = 2.0504 - 0.01413P_d \quad (9)$$

with $\sigma = 0.2299$ and $p < 10^{-5}$. All three equations (7)–(9) represent decreasing functions in the respective domains, as seen in Fig. 3. The slopes of all six correlations depend on the physiologic range of respective blood pressures. Hence, the two correlations with P_d (lines a and d in Fig. 3) are the steepest because the range of P_d is the smallest, while lines c and f are considerably less steep because of the large range of P_s . The typical scattergrams, showing all 146 raw data points, are given in Fig. 4 for $(dZ/dt)_{\min}$, and Fig. 5 for the ratio R . Both show the distribution over the range of the mean arterial blood pressure P_m . The scattergrams over the range of P_s and P_d (not shown to avoid crowding of points) are very similar to Figs. 4 and 5 because the ordinates for each point are identical, while only abscissas differ. This is reflected in small differences between the respective standard deviations.

The correlation of R with HR results in $p > 0.05$ while the correlation with Z_0 results in $p > 0.25$. It is therefore concluded that R does not depend on HR and Z_0 . Similarly,

$$D = 2.145 - 0.02408P_m \quad (10)$$

with $\sigma = 0.4048$ and $p < 10^{-5}$,

$$D = 1.2402 - 0.01082P_s \quad (11)$$

with $\sigma = 0.4525$ and $p < 10^{-3}$, and

$$D = 1.931 - 0.02593P_d \quad (12)$$

with $\sigma = 0.4198$ and $p < 10^{-5}$. Again, all three functions (10)–(12) are decreasing in respective domains. Correlation of D with HR gives $p = 0.043$, which is on the borderline of being statistically significant. However, the correlation of R with Z_0 results in $p = 0.88$. Hence, both R and D are independent of Z_0 .

The correlations of Z_0 with P_m , P_s , P_d , and HR all resulted in $p > 0.1$, indicating the absence of a functional relationship.

IV. DISCUSSION

The basic finding of this study, as evidenced by (1)–(3), is that the magnitude of the $(dZ/dt)_{\min}$ peaks is a function of arterial blood pressure, in addition to the dependence on Z_0 , which was reported earlier [12]. Elimination of the influence of Z_0 , using (5) and (6), still leaves the correlation between dZ/dt peaks and blood pressure unchanged, as seen in (7)–(12), indicating that the dependence on blood pressure is direct and not through Z_0 . Thus, dZ/dt peaks depend at least on blood pressure levels, Z_0 [12], [15], [16], and rate of ejection of blood from heart (or aortic flow wave) as pointed out by Ito, Yamakoshi, and Togawa [15], [17]. These relationships can be elucidated by analyzing a simple dynamic model of elastic arterial expansion caused by the variation of blood pressure during the cycle.

Starting with the parallel conductor model of impedance plethysmography [11], we can write

$$1/Z = 1/Z_b + 1/Z_c \quad (13)$$

where Z is the total impedance, Z_b is the impedance contributed by volume of blood, which, according to the basic assumption of impedance plethysmography, contains the only variable component of impedance. Z_c is the constant portion, attributed to the rest of the tissues. The first time derivative of Z is therefore

$$dZ/dt = Z^2/Z_b^2 \times dZ_b/dt. \quad (14)$$

On the other hand, the simple relationship between the cross-sectional area (a) of an elastic artery and blood pressure (P) as derived by Bergel [13], can be written as

$$a = a_0[2P/E(K^2 - 1) + 1]^2 \quad (15)$$

where a_0 is unstretched cross-sectional area, which corresponds to $P = 0$, E is the modulus of elasticity of arterial wall, which is a function of P , and K is the ratio of the outer to the inner diameter of the artery in the unstretched state.

Assuming cylindrical geometry of blood vessels in the region of length L between the measuring electrodes, and that the only variable component of impedance signal comes from blood in the vessels, the relationship between a and Z_b is given by

$$a = \rho L/Z_b \quad (16)$$

so that

$$a_0 = \rho L/Z_{b0} \quad (17)$$

where ρ represents the electrical resistivity of blood.

Differentiating (15) we obtain

$$da/dt = [4a_0/(K^2 - 1)^2][2P + E(K^2 - 1)] \cdot [E - P(dE/dP)]/E^3(dP/dt). \quad (18)$$

Differentiating (16) we obtain

$$da/dt = -(\rho L/Z_b^2)(dZ_b/dt). \quad (19)$$

Combining (14) and (17)-(19)

$$\frac{dZ}{dt} = -(Z^2/Z_{b0})\{4/(K^2 - 1)^2\}[2P + E(K^2 - 1)] \cdot [E - P(dE/dP)]/E^3(dP/dt). \quad (20)$$

The peak of the dZ/dt signal, $(dZ/dt)_{\min}$, occurs when the absolute value of the right side of the equation (20) is at maximum, which timewise closely corresponds to the moment when the rate of ejection of blood from the left ventricle during the cardiac cycle is at maximum, and which in turn causes dP/dt to be at maximum.

In terms of Z_0 , Z can be written as

$$Z = Z_0 + \Delta Z(t) \quad (21)$$

where Z_0 is the time-average value of Z and ΔZ the variable portion of the signal. Typical values of Z_0 are 20-30 Ω , while the maxima of ΔZ are of the order of only 0.1-0.2 Ω . Hence, the predominant portion of signal Z is Z_0 .

It is possible now to offer an explanation for the correlations listed in Section III.

According to (20), $(dZ/dt)_{\min}$ is directly proportional to the Z^2/Z_{b0} factor. Hence, in view of (21), the direct proportionality expressed by (4), which statistically confirms the increase of dZ/dt peaks when Z_0 is increased.

The correlations with blood pressure can be explained using (20), by keeping in mind that the modulus of elasticity E is a monotonically increasing nonlinear function of blood pressure [14]. E can be expressed in terms of P either as a polynomial such as

$$E(P) = A_0 + A_1P + A_2P^2 + \dots \quad (22)$$

of at least second degree, or as an exponential function of P , such as

$$E(P) = B_0 + B_1e^{bP} + B_2e^{cP} + \dots \quad (23)$$

In either case, when (22) or (23) are substituted in (20), the resulting function of P is of the negative net exponent because of the predominance of the E^3 term in the denominator in (20). This, in terms of the mechanics, means that as the average blood pressure increases, then the arteries become more distended and more rigid causing the change of their volume during the cardiac cycle to be less pronounced. Therefore, the dZ/dt peaks tend to decrease when blood pressure increases, as statistically confirmed by correlations in Section III. In this model the presence of mechanical factors, such as vasoconstriction, vasodilatation, and total peripheral resistance, is reflected in the magnitude of P , and the numerical values of coefficients A_1 or B_1 in the expressions (22) or (23) for $E(P)$.

The absence of a conclusive correlation between the dZ/dt peaks and heart rate indicates that the normal physiologic range of heart rates is too narrow, or that the underlying frequencies are too low to significantly induce viscoelastic effects, which otherwise may be expected due to the viscoelastic nature of arterial walls.

V. CONCLUSIONS

It was demonstrated by direct measurement that the magnitudes of the dZ/dt peaks depend on blood pressure levels in an inverse manner. It was further shown that this dependence is retained even when the influence of the base impedance Z_0 is eliminated as a factor through dividing the experimentally measured peaks by calculated peaks obtained from the correlation of $(dZ/dt)_{\min}$ with Z_0 . Similar results were obtained for the differences between the measured and the calculated peaks. It was also demonstrated that Z_0 and blood pressure are mutually independent. It was therefore concluded that the magnitude of dZ/dt peaks, primarily determined by the rate of ejection of blood from the heart (which is reflected in the magnitude of dP/dt), is also significantly modified by the magnitudes of blood pressure level.

This conclusion is consistent with the analysis of a model of elastic arteries having modulus of elasticity which is a nonlinear function of blood pressure.

dZ/dt peaks play a crucial role in current applications of impedance plethysmography, impedance cardiography, and in quantification of myocardial contractility, but in a manner which tends to ignore the discussed factors. This may lead to inaccurate results and erroneous interpretations. Although the measurements of impedance plethysmography signals and the underlying parallel conductor theory are accurate [11], their applications may not be. The correlations suggest that the ratio R or the difference D , as defined in Section III, are better suited than $(dZ/dt)_{\min}$ for applications in impedance cardiography and the analysis of myocardial contractility because they eliminate the influence of Z_0 , which is an artifact in these applications. However, the dependence on blood pressure still remains. It could, perhaps, be eliminated by means of the above reported correlations with blood pressure. In any case, this dependence should be taken into account whenever the dZ/dt signal is a significant factor.

REFERENCES

- [1] S. E. Markovich, Ed., *International Conference of Bioelectrical Impedance*. New York: New York Academy of Sciences, 1970.
- [2] J. Nyboer, *Electrical Impedance Plethysmography*, 2nd ed. Springfield, IL: Thomas, 1970.
- [3] E. F. Bernstein, Ed., *Noninvasive Diagnostic Techniques in Vascular Disease*. St. Louis, MO: Mosby, 1978.
- [4] J. Nyboer, S. Bagno, A. Barnett, and R. H. Halsey, "Radiocardiograms: Electrical impedance changes of the heart in relation to electrocardiograms and heart sounds," *J. Clin. Invest.*, vol. 19, p. 773, 1940.
- [5] W. G. Kubicek, D. A. Witsoe, R. P. Patterson, and A. H. L. From, "Development and evaluation of an impedance cardiographic system to measure cardiac output and other cardiac parameters," Nat. Aeronaut. Space Admin. Manned Spacecraft Center, Houston, TX, 1969, Contract NAS 904500.
- [6] W. L. Cooley, "The calculation of cardiac stroke volume from variations in transthoracic electrical impedance," *Biomed. Eng.*, vol. 7, pp. 316-317, 1972.
- [7] S. Gabriel, H. J. Atterhog, L. Oro, and L. G. Eklund, "Measurements of cardiac output by impedance cardiography in patients with myocardial infarction," *Scand. J. Clin. Lab. Invest.*, vol. 36, no. 1, pp. 29-31, 1976.
- [8] E. K. Lewis, R. A. Peura, and J. B. Singh, "The quantitative effect of the heart on transthoracic impedance measurement," in *Proc. Conf. Eng. Med. Biol.*, Chevy Chase, MD, 1974, vol. 16.
- [9] D. W. Hill and H. J. Lower, "The use of electrical impedance technique for the monitoring of cardiac output and limb blood flow during anesthesia," *Med. Biol. Eng.*, vol. 11, pp. 534-536, 1973.
- [10] J. H. Siegel, J. H. Fabian, C. Lankau, M. Levine, M. Coles, and M. Nahmad, "Clinical and experimental use of thoracic impedance plethysmography in quantifying myocardial contractility," *Surgery*, vol. 67, pp. 907-908, 1970.
- [11] H. Shimazu, K. I. Yamakoshi, T. Togawa, M. Fukuoka, and H. Ito, "Evaluation of the parallel conductor theory for measuring human limb blood flow by electrical admittance plethysmography," *IEEE Trans. Biomed. Eng.*, vol. BME-29, p. 107, Jan. 1982.
- [12] L. Djordjevich and M. S. Sadove, "Experimental study of the relationship between the base impedance and its time derivative in impedance plethysmography," *Med. Phys.*, vol. 8, no. 1, pp. 76-78, 1981.
- [13] D. H. Bergel, "The static elastic properties of the arterial wall," *J. Physiol.*, vol. 156, pp. 445-457, 1961.
- [14] S. Middleman, *Transport Phenomena in the Cardiovascular System*. New York: Wiley-Interscience, 1972, ch. 1, p. 18.
- [15] K. I. Yamakoshi, T. Togawa, and H. Ito, "Evaluation of the theory of cardiac-output computation from transthoracic impedance plethysmogram," *Med. Biol. Eng. Comput.*, vol. 15, pp. 479-488, Sept. 1977.
- [16] H. Ito, K. I. Yamakoshi, and T. Togawa, "Transthoracic admittance plethysmograph for measuring cardiac output," *J. Appl. Physiol.*, vol. 40, no. 3, pp. 451-454, 1976.

Ref. (15)

Measurement of the blood-pressure constant k , over a pressure range in the canine radial artery

M. Voelz

Potter Building, Biomedical Engineering Centre, Purdue University, West Lafayette, Indiana 47907

Abstract—The value of the blood pressure constant k in the now known equation

$$M = D + k(S - D)$$

was measured over a wide pressure range in the canine radial artery. This equation is used to estimate the value of the mean blood pressure from the measured values of the diastolic and systolic blood pressures. It was found that k varies widely. It is concluded that this equation cannot give an accurate estimate of the mean blood pressure from the systolic and diastolic pressure readings.

Keywords—Diastolic blood pressure, Mean blood pressure, Systolic blood pressure

1 Introduction

IN clinical practice, three arterial pressures, systolic, mean and diastolic, are important in the assessment of cardiovascular dynamics. Systolic blood pressure is the maximum and diastolic is the minimum pressure. Mean blood pressure is the average pressure forcing blood through the arteries. Because the blood pressure pulse is not symmetrical, about the time axis, the mean blood pressure is not the average of the systolic and diastolic pressures. The mean pressure is the area under one blood pressure pulse divided by the period of the same pulse (Fig. 1).

Mean blood pressure can be measured directly with a blood-pressure transducer coupled to an artery. The signal from the transducer can be processed using a long rise time constant which dampens out the pulsations of the signal, yielding the mean blood pressure.

Mean blood pressure can be calculated accurately using the following expression

$$M = 1/T \int_0^T \{P(t) dt\} \quad (1)$$

where M is the mean blood pressure, T is the period of one pressure pulse, and the integral of $P(t) dt$ is the area under the pressure pulse.

When the blood pressure is measured indirectly

First received 22nd August and in final form 4th November 1980
0140-0118/050535+03 \$01.50/0
© IFMBE: 1981

[GEDDES, 1970], it is often estimated using the following expression

$$M = D + k(S - D) \quad (2)$$

where M is the mean blood pressure, S and D are the systolic and diastolic blood pressures, respectively, and k is a constant with values ranging from 1/2 to 1/4, depending on the site of measurement. In reality, k represents the fraction of the pulse pressure waveform above diastolic that identifies mean pressure.

If the pulse waveform was a sine wave, the mean value of the pressure pulse would be half way between the peak and the trough of the waveform (Fig. 2). Because the blood pressure waveform is broad at the base and narrow at the top, the mean pressure is

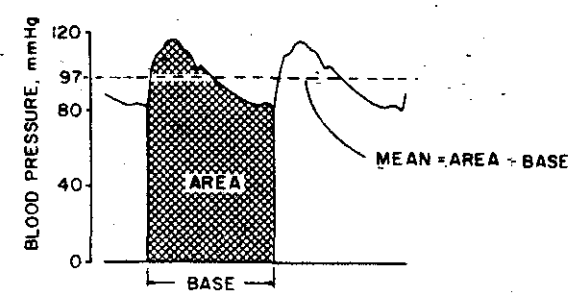


Fig. 1 Mean blood pressure is not the average of the systolic and diastolic blood pressure: it is the area under one blood pressure pulse divided by the base or the period of the pulse

RIGAN, T.
mox. for
3 pH with
matoms. In
Press, New
7) C gen
ing. ech.
xygen and
ors. d. &

expected to be below half way between the peak and the trough of the pulse wave. If the pressure wave becomes more peaked, the mean pressure value moves toward diastolic pressure.

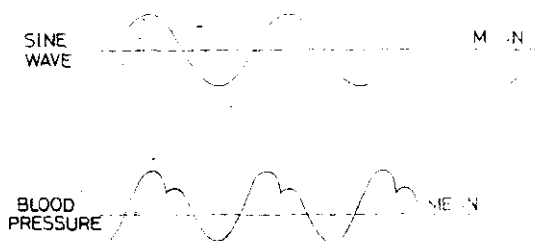


Fig. 2 The mean of a sinewave is the average of its peak and the trough of the waveform. The mean of a blood pressure pulse is less than the average of its waveform peak and trough because of the asymmetry of the waveform.

To date there is very little information on typical values of k . This report presents the values for k measured over a wide pressure range in the canine radial artery.

2 Methods and materials

Ten dogs, ranging in weight from 12 to 22 kg, were anaesthetised with sodium pentobarbital. The right radial artery was cannulated with a stiff-walled catheter, and the blood pressure was recorded using a Microswitch blood pressure transducer (Microswitch Model experimental) which had a uniform frequency response extending from 0 to 150 Hz when coupled to a 0.58 mm internal diameter catheter, 152 mm long. Hypertensive episodes were induced by the controlled

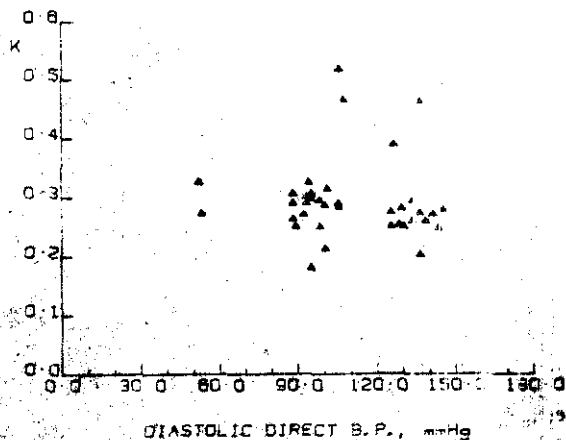


Fig. 3 The value for the blood pressure constant k for one typical dog, varies as the blood pressure changes and is varied at the same pressure.

infusion of a solution of 1.0 g/l of 0.9% B. B. (Bartlett's) saline solution. Hypertensive episodes were induced by the controlled infusion of an 8% solution of sodium chloride (100 mg/ml) at 20 ml/h. The control on the blood pressure was the arterial cannula (epi-aorta) (2 mg pentobarbital/kg body weight) administered intravenously. The mean pressure ranged from 70 to 180 mm Hg.

Diastolic and arterial blood pressure was recorded simultaneously with the mean pressure obtained by processing the pulse pressure signal through a parallel reactive-capacitive circuit with a rise time constant of 82 ms. The reading on the mean pressure manometer was verified by measuring the area under the blood pressure pulse recorded on a high-speed camera.

Blood pressure measurements were made only when the blood pressure was stable. From the recorded systolic, diastolic and mean pressure values, k was calculated using eqn (1).

3 Results

Fig. 3 depicts the relationship between the diastolic blood pressure and k for a typical dog. This graph shows a scattered relationship, which is better visualized by combining the data from all ten dogs as shown in Fig. 4. The mean value of k for the entire pressure range is 0.319 with a standard deviation of 0.09.

It is important to note that the value of k varies widely throughout the pressure. In addition, the data points are fairly uniformly distributed around a mean value throughout the blood pressure range. This suggests that the value of k is not unique, even at the same pressure in the same artery.

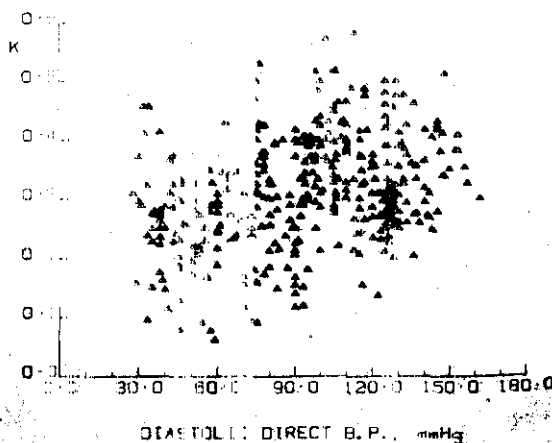


Fig. 4 The large variation in the value of k is independent of the pressure over the range measured. This data is taken from all ten dogs using the same measurement site in the radial artery. The mean value of k is 0.31 with a standard deviation of 0.093 over the entire pressure range.

Fig one st wide value

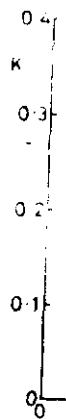


Fig. 5

Fig 5 presents the mean values of k plus and minus one standard deviation for pressure classes 20 mm Hg wide throughout the pressure range. Note that the value of k is not unique over the pressure range.

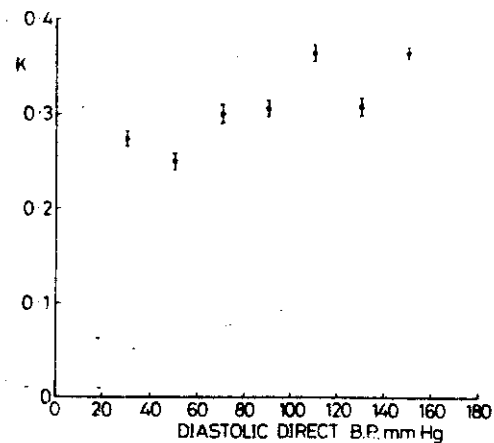


Fig. 5 The data from ten dogs were separated into pressure classes 20 mm Hg wide and the mean and standard deviation of each class is shown. The circles are the mean of each pressure class and the vertical lines are plus and minus one standard deviation of each pressure class

4 Summary

In the dog radial artery, the value for k was measured over a wide blood pressure range. It was found that k does not have a unique value at each pressure. Therefore, it is not possible to obtain an accurate value for the mean blood pressure using the systolic and diastolic pressures and selecting a single value for k .

Acknowledgments—The research was supported by grant HL18947-03 from the US National Heart Lung and Blood Institute, Bethesda, MD. Special thanks are due to Dr. L. A. Geddes, Director of the Biomedical Engineering Centre and to Debra Reiner, Brad Addison, and Connie Combs, undergraduate research assistants.

Reference

GEDDES, L. A. (1970) In *The direct and indirect measurement of blood pressure*, p 70. Year Book Medical Publishers, Inc., Chicago.

CONCLUSIONES

Este trabajo mostró la relación de la presión arterial general del cuerpo humano, con los factores que la regulan, miden y modifican, en un punto de vista no especializado en alto grado de fisiología, ingeniería y patología.

En un enmarcamiento fisiológico (que incluía la anatomía del aparato cardiovascular) las funciones orgánicas y mecanismos que influyen en la presión arterial del aparato vascular en conjunto con órganos como glándulas suprarrenales, cerebro, riñones, etc. se trató.

En el marco ingenieril, se observaron características de la utilización de los diferentes aparatos. Estos destinados al servicio de monitoreo, transducción y medición de los parámetros de la presión (presión sistólica, presión diastólica etc.) Se vio como era ideal la adquisición y transmisión de las diferentes maneras en que se manifestaba el fenómeno involucrado como llegaban a utilizarse las señales obtenidas y su relación con el estado de salud del paciente.

En el marco médico incluimos patologías de la presión arterial tales como son presión alta y presión baja. Junto con los mecanismos que hacen desembocar en estos padecimientos y consecuencias de estas, en diferentes órganos de los pacientes involucrados en estos padecimientos (en casos de inhabilitación de la persona como apoplejías causados por presión alta, o la pérdida de la vida por los peligrosos choques causados por la presión baja ;

Concluimos que este trabajo trató de alcanzar el objetivo para el cual fué elaborado, pero no fué conseguido en su totalidad. En parte por la inexperiencia en dichas ramas de los que participaron en la elaboración de este.

Pero esperamos que si es retomado el tema, a los que lo tomen sirva de auxilio en dicha tarea.

No existe ningún sistema ideal de registro de presión.

Respuesta de frecuencia de los sistemas de registro

Una reproducción de la alta fidelidad de una forma de onda puede ser registrada por medio de un sistema que nos de una respuesta uniforme a la decima armonica de su frecuencia fundamental. Con la frecuencia cardiaca de 240 lat/min., la frecuencia del pulso es de 4/seg. y entonces la decima armonica es de 40 ciclos/seg., necesara para que los cambios más rapidos de la presión durante el pulso sea registrado firmente,

Es mas importante probar la respuesta dinamica del sistema completo, cuando el transductor es conectado con un cateter lleno de liquido, la respuesta de frecuencia del manometro se reduce grandemente para que una masa que debe los cambios de presión y su inercia se reduce y la frecuencia de respuesta del manometro, también.

La masa del liquido puede ser reducida emplando tubos del calibre muy corto, y de aumentar la resistencia friccional al movimiento del liquido, una parte de la energia se disipa en forma de fricción esta es una forma de amortiguación.

Si se iguala con un grado optimo de amortiguacion, mejorara grandemente las características de las repuestas.

Bibliografía:

Cardiología Clínica
Maurice Sokolow
Malcon B. Mc. Irloy

Tratado de Fisiología Médica

A. C. Guyton
Ed. Interamericana

Anatomía y Fisiología
Catherine Parker Anthony
Norma Jene Kolthoff
Ed. Interamericana

Elementos de Anatomía y Fisiología Humana
Orestes Cedrero
Ed. Buenos Aires

Fisiología Humana
Vander

Sistemas Vasculares
Fac. de Medicina de la U.N.A.M.

Pathologic Physiology
Mechanics of Disease
Sodeman and Sodeman
Ed. Saunders Company

Medical and Biological and Computer

Journal Clinical

IEEE Transactions on Biomedical Engineering

Lugares visitados:
Instituto de Cardiología
Facultad de Medicina de la U.N.A.M.